MICROBES IN THE LIMELIGHT: LIMING ALTERS MICROBIAL COMMUNITIES, REDUCING DECOMPOSITION IN NORTHERN HARDWOOD FOREST SOILS

A Dissertation

Presented to the Faculty of the Graduate School

of Cornell University

In Partial Fulfillment of the Requirements for the Degree of

Doctor of Philosophy

by

Bhavya Sridhar

August 2020

MICROBES IN THE LIMELIGHT: LIMING ALTERS MICROBIAL COMMUNITIES, REDUCING DECOMPOSITION IN NORTHERN HARDWOOD FOREST SOILS

Bhavya Sridhar, Ph. D.

Cornell University 2020

Soils hold more carbon (C) than the atmosphere and vegetation combined. This pool of C may be a source or a sink to the atmosphere depending on the microbial mediators of detrital decomposition. However, we are just beginning to discover the identities and ecological functions of the vast majority of uncultivated soil taxa. Edaphic variables like soil pH often govern microbial community composition. In this dissertation, I explore how manipulating soil pH through liming affects microbial community composition and decomposition in acidic northern hardwood forest soils.

In Chapter 1, I investigate changes in decomposition and bacterial and fungal community composition in limed forested subcatchments where soil C stocks had accumulated over two decades. Liming altered bacterial and fungal composition, decreasing the relative abundance of ectomycorrhizal and saprotrophic fungi as well as actinomycetes that were correlated with lignocellulolytic enzyme activity.

In Chapter 2, I compare liming-induced shifts in bacterial and fungal community structure and activity between a short- and long-term liming experiment in northern hardwood forests of the Adirondacks to elucidate the role of pH. Within two years of liming a majority of taxa responded similarly to the long-term site.

Connecting microbial structure and function directly through stable isotope probing in Chapter 3, I prove that limed bacterial and fungal communities metabolize leaf litter C differently than in control acidic soils.

This dissertation bridges scales ranging from ecosystem processes to individual microbial taxon function, connecting the structure of microbial communities to their function in ecosystem C-cycling. The impact of climate change, the most urgent problem of the Anthropocene, will depend heavily on understanding the responses of soil microorganisms.

BIOGRAPHICAL SKETCH

Bhavya Sridhar was born and grew up in Muscat, Oman, with her mother, father, and an older brother. She attended the Indian School Muscat while in Oman and Bethany High School for a year in Bangalore, India. She left for the United States at age 17 to pursue undergraduate studies at the University of Michigan, Ann Arbor. She graduated *magna cum laude* in 2010 as a Bachelor of Science majoring in Economics and Environmental Science and minoring in Environmental Geology. She attended the Yale School of Forestry and Environmental Studies, graduating as a Master of Environmental Science in 2012. She began at Cornell University in 2012 to conduct cross-scale biogeochemistry research to understand the role of microbial communities in soil carbon cycling. While at Cornell, Bhavya was awarded the College of Agriculture and Life Sciences Outstanding Graduate Teaching Assistant Award.

For Mallika and B. Sridhar who taught me resilience

ACKNOWLEDGMENTS

I am grateful to many people who helped me over the course of my time in graduate school. My advisor, Dr. Christine L. Goodale, and committee members, Dr. Daniel H. Buckley and Dr. Timothy J. Fahey, were instrumental in this work, and I thank them wholeheartedly for their encouragement and feedback. I especially enjoyed my time in the field with Dr. Goodale and Dr. Fahey, seeing ecosystem processes through their expert eyes. Special thanks to Dr. Buckley for fostering an ethos of collaboration and open inquiry during my time working in his lab. Dr. Roland C. Wilhelm was a scientific mentor and friend, and our interactions were central to my development as a scientist and human. I thank Dr. Wilhelm, Samuel E. Barnett, Dr. Spencer J. Debenport, Dr. Steven A. Higgins, and past members of the Buckley Lab for their camaraderie and for generously assisting me with microbial lab and bioinformatics work. Thanks to Guinevere Fredriksen, Kimberlee Sparks, Alexis Heinz, Dr. Kevin Panke-Buisse, Dr. Grant Thomspon, Dr. Jed Sparks, Dr. Andre Kessler, and Dr. Ian Hewson, for access to and assistance with lab equipment, and Bridget Darby, Shiyi Li, and Dr. Timothy C. Heath for field assistance.

Funding for this work was provided by the Cornell University Kieckhefer Adirondack Fellowship, the Atkinson Center for Sustainable Future small grants, the U.S. Department of Energy, Office of Biological & Environmental Research Genomic Science Program under award number DE-SC0016364, and the Betty Miller Francis ’47 Fund. I received fellowship support from the New York State Energy Research and Development Authority, Environmental Monitoring, Evaluation, and Protection Program (NYSERDA EMEP 33076). Thanks to the Adirondack League Club and Woods Lake Corp. for site access. Thanks to Dr. Peter M. Groffman and the scientific community at the Advanced Science Research Center at the City University of New

York. I thank the Biogeochemistry, Ecosystem Science, and Sustainability group for providing a vibrant intellectual community across Cornell departments.

Dr. Katherine M. Sirianni and Dr. Allison M. Tracy were sources of friendship and moral support through the rigorous years of graduate school. I would like to express my deepest gratitude to my father, Mr. B. Sridhar, from whom I inherited a thirst for knowledge, and my mother, Mrs. Mallika Sridhar, for her limitless love and support. My life partner and rhetorical sparring mate, Dr. Timothy C. Heath, has been the diamond plate against which I've sharpened my thinking for over a decade.

TABLE OF CONTENTS

LIST OF FIGURES

LIST OF TABLES

CHAPTER 1

LIMING SUPPRESSES DECOMPOSITION IN AN ACID FOREST SOIL BY ALTERING MICROBIAL COMMUNITY COMPOSITION, REDUCING OXIDATIVE ENZYME ACTIVITY

Abstract

Microbial community structure and function often covary with soil pH, yet there are few long-term experimental tests of these relationships in natural ecosystems. We investigated the impacts of experimental liming on microbial community structure and decomposition processes after 25 years at a northern hardwood forest site, where liming produced a unit increase in pH and a doubling of forest floor organic matter. We tested whether liming altered microbial community composition, and whether this change correlated with enzyme activity in the Oe and Oa horizons by assaying seven hydrolytic and two oxidative extracellular enzymes and sequencing bacterial 16S rRNA genes and fungal ITS regions. Twenty-five years later, liming had restructured bacterial and fungal communities. In addition, liming reduced the activities of six extracellular enzymes, indicating a reduced capacity for decomposition. Ligninolytic oxidative enzymes decreased the most, declining 45% in the limed soils. The changes in oxidative enzyme activities correlated with the loss of specific microbial taxa important for lignocellulose decay, including significant reductions in the dominant ectomycorrhizal genera *Russula* and *Cenococcum*, saprotrophs and wood decay fungi, and bacteria related to genus *Actinomadura*. The loss of some of these taxa was

pronounced in the Oa horizon where soil C had accumulated the most. We show that liming can restructure microbial communities and enzyme activities, explaining increased carbon storage in northern hardwood forest floor soils.

Introduction

Understanding how changes in microbial community structure alter carbon (C) and nutrient cycling can reduce uncertainty in carbon-climate feedbacks (Zhou et al. 2011). Given that microbes directly regulate organic matter (OM) turnover, adding 55 Pg C/yr to the atmosphere (Prentice et al. 2001), it is essential to understand factors that regulate microbial decomposition of soil C. The edaphic properties that most strongly influence microbial community structure, like soil pH (Fierer 2017), could have a major impact on soil C storage in certain contexts. Comparisons across sites indicate that soil pH is one of the strongest predictors of variation in microbial community composition across local to continental spatial scales and decadal to millennial temporal scales (Frostegård et al. 1993, Jenkins et al. 2009, Lauber et al. 2009, Baker et al. 2009, Fierer et al. 2012, Tedersoo et al. 2015, Tripathi et al. 2018). In addition, perturbations like deforestation and changes in land use or climate can cause shifts in microbial community composition, which may also be mediated directly or indirectly by soil pH (Crowther et al. 2014, Bell et al. 2014, McGuire et al. 2015). However, soil pH is governed by complex interactions between physicochemical and biological properties that develop in soils over long periods of time, which can obscure the causal relationships between soil pH and microbial community structure and function. There is a compelling need for long-term studies that experimentally manipulate pH to discern causality among the many correlated variables that affect microbial community structure and function (Lauber et al. 2009, Reid and Watmough 2014, Bier et al. 2015).

Clarifying the role of soil pH in regulating microbial community structure and function has both mechanistic and management implications. In Europe, forest managers routinely manipulate soil pH through the application of lime ($CaCO_3$) or wood ash to counteract acid deposition from air pollution, a practice now increasing in acid-sensitive forests of the United States and Canada (Derome et al. 2000, US Forest Service 2011, National Park Service 2015, Long et al. 2015, Hannam et al. 2018, Grüneberg et al. 2019). These manipulations provide opportunities to explore the response of soil processes to altered pH. Application of lime can have divergent effects on forest soil C stocks (Paradelo et al. 2015). In northern forest soils, liming sometimes increases in microbial biomass and respiration, leading to an overall reduction of organic (O) horizon C stocks (Illmer and Schinner 1991, Badalucco et al. 1992, Kreutzer 1995, Nilsson et al. 2001, Andersson and Nilsson 2001, Lundström et al. 2003). In these cases, C loss could result from an increase in microbial activity driven by alleviation of acid stress (Lundström et al. 2003, Malik et al. 2018).

Alternatively, at other sites, liming has increased soil C concentrations and stocks, with proposed mechanisms including increased plant C inputs and a lack of adaptation by the microbial decomposer community to higher pH (Derome 1990, Poulton et al. 2003, Srámek et al. 2012, Melvin et al. 2013, Grüneberg et al. 2019). One liming experiment that produced an especially large increase in soil C is a lime addition in the northern hardwood forest watershed of Woods Lake in the Adirondack Park of New York, resulting in a doubling of O horizon C stocks compared to controls 20 years later (Driscoll et al. 1996, Melvin et al. 2013). Liming did not change litterfall or aboveground biomass, but it did significantly reduce soil basal respiration

rates, suggesting that C accumulated because decomposition slowed and not because plant C inputs increased (Melvin et al. 2013). The variable response of long-term soil C turnover to liming could stem from changes in microbial community structure and function, but the microbial basis for these pH driven changes in soil C stocks remain poorly described (Reid and Watmough 2014).

Northern forest ecosystems with acidic soils usually exhibit well developed surface O horizons that can be differentiated into a fermenting layer (Oe) overlying a more humified layer (Oa). These distinct O horizons differ markedly in specific organic substrates that support differentiable microbial communities (Baldrian et al. 2012). The heavily decomposed Oa horizon, enriched in organic acids and soluble carbon compounds, tends to have more bacteria and mycorrhizae relative to the plant-biomass rich Oe horizon (Baldrian et al. 2012, Baldrian 2017). At Woods Lake, liming had caused a greater accumulation of C in the Oa horizon than in the Oe (Melvin et al. 2013) (Table 1). We expect that differences in C accumulation between these soil horizons occur because the effects of liming interact on microbial community structure and function in the Oe and Oa.

In acidic northern forest soils, fungi typically predominate over bacteria in mediating the breakdown of persistent OM (Fierer et al. 2009, Žifčáková et al. 2017, Bahram et al. 2018). Fungal guilds like ectomycorrhizae and saprotrophs play critical roles in the production of lignocellulolytic enzymes that break down persistent plant biopolymers (Talbot et al. 2008, Baldrian 2017). Over decadal timescales, soil C stocks may be particularly sensitive to changes in OM, which is primarily mediated by oxidative enzymes that breakdown these persistent biopolymers (Sinsabaugh 2010).

Ectomycorrhizal fungi (ECMF) can account for up to a third of fungal biomass in many northern forests, and some major ECMF could be inhibited by an increase in pH (Högberg and Högberg 2002, Carrino-Kyker et al. 2016, Kjøller et al. 2017). Wood decomposing basidiomycete activity may also be disrupted by increasing pH, as late stage oxidative decomposition is typically favored by acidic conditions (Baldrian 2008).

Members of dominant bacterial phylogenetic groups like *Acidobacteria*, *Actinobacteria*, and *Proteobacteria* are also involved in decomposing lignocellulose in forest O horizons (Wilhelm et al. 2019) and may also be sensitive to changes in pH (Wilhelm et al. 2017, Crowther et al. 2019). Global patterns suggest that as soil pH increases, the proportions of *Acidobacteria* and *Alphaproteobacteria* decrease in favor of *Actinobacteria* and *Bacteroidetes* (Lauber et al. 2009, Delgado-Baquerizo et al. 2018). Through pH constraints, we hypothesize that liming-induced changes in the abundance of these key lignocellulolytic bacterial and fungal guilds could explain the accumulation of persistent C in O horizons.

We took advantage of the striking effects of liming on soil C stocks at the Woods Lake watershed to seek a better understanding of the microbial mechanisms driving forest soil C accumulation in acidic northern forest ecosystems. We compared bacterial and fungal community structure and function between the limed and control subcatchments across two O horizons. We hypothesized that by increasing pH, liming fundamentally altered fungal and bacterial community composition, resulting in the suppression of decomposition enzymes. We expected that suppression of oxidative decomposition would be most pronounced in the Oa horizon, where the larger

accumulation of C was observed. Our study is the first to target the underlying microbial mechanisms for liming-induced C storage in forest soil, offering a comprehensive account of changes in microbial function (microbial respiration and a suite of extracellular enzyme activities) and microbial structure (changes in key fungal and bacterial populations).

Methods

Site Description and Field Sampling

The Experimental Watershed Liming Study is set among the subcatchments of Woods Lake in the Adirondack Park in Herkimer County, New York (43°52' N, 74°57' W). The forest is composed of mixed northern hardwood species including beech, maple, birch, and spruce (See (Smallidge and Leopold 1995, Melvin et al. 2013), *Supplementary Methods* for details). In 2009, tree species with ectomycorrhizal associations comprised 60% of the aboveground biomass of focal study plots with a slightly higher proportion of ECM trees in the limed (66%) than the control (53%) subcatchments (Melvin et al. 2013). In October of 1989, a single application of 6.89 tons of $CaCO_3$ ha^{-1} (2.76 t Ca ha^{-1}) was broadcast by helicopter into two ~50 ha subcatchments (Driscoll et al. 1996). Two adjacent subcatchments were maintained as controls. Lime was applied in pellet form with 82% $CaCO_3$, 8% $MgCO_3$, and 4% organic binder, and 6% inorganic salts and silicates (Driscoll et al. 1996). Before lime was added, the forest floor O horizon had a mean soil pH in water of 3.7, which rose to 4.9 and 4.0 in the Oe and Oa horizon respectively two years after liming (Blette and Newton 1996).

Following the studies of short-term responses at Woods Lake, the site was not studied again until twenty years after lime addition in 2009-2010, when Melvin et al. (2013) measured aboveground biomass, litterfall, litter chemistry, soil C and N stocks, nitrification and N mineralization rates, root biomass, and soil basal respiration at five plots in each of the four subcatchments, with plots chosen to capture landscape heterogeneity while minimizing differences in tree composition, slope, and aspect.

For this study, we collected forest floor material in August 2014, 25 years after the lime application from the same plots studied by Melvin et al. (2013). We collected four samples per plot, with each sample composited from three 7 cm diameter cores. We removed the litter (Oi) layer and then sampled to 10 cm depth, separating the underlying forest floor into upper, moderately decomposed (Oe; fermenting layer) and lower, highly decomposed plant material (Oa; humus layer) horizons based on field visual examination (Schoeneberger et al. 2012). This procedure generated 160 samples: 40 samples for each horizon (Oe and Oa) and treatment (Limed and Control) pair. Samples were sieved (4 mm) and stored at 4°C before microbial biomass and respiration measurements, and subsamples for enzyme and microbial community analyses were stored at -80°C.

Physicochemical analyses

Soil pH was measured on a 1:1 soil to deionized water slurry and soil samples were analyzed for concentrations of 27 elements including Ca, Fe, K, Mg, Mn, Mo, Na, P, S, and Zn by ICP-AES. Gravimetric moisture and water holding capacity were assessed (See *Supplementary Methods*) to establish incubation conditions.

Microbial respiration and microbial biomass

We estimated the active microbial biomass carbon (MBC) pool using the substrate induced respiration (SIR) technique (Fierer et al. 2003). Briefly, autolysed yeast extract solution was added to three grams dry weight soil in airtight tubes that were shaken until the microbiological media substrate penetrated the soil matrix. The headspace was then flushed with CO_2-free air and incubated at atmospheric pressure and room temperature for four hours, and the headspace CO_2 was injected into an infrared gas analyzer (LI- 6200, LI-COR, Lincoln, Nebraska, USA). CO_2 flux was calculated per unit dry weight soil and used to estimate microbial biomass carbon (MBC).

Microbial respiration was ascertained using a 60-day incubation, where soils were held at 60% water holding capacity and at 22°C (Bradford et al. 2008). Briefly, another set of three-gram soil microcosms was prepared and soil CO_2 fluxes were sampled on days 1, 4, 10, 20, 30, 45, and 60 (See *Supplementary Methods*). To estimate the cumulative respiration by the microbial biomass in each sample (CR_{mass}), CO_2 flux was calculated per unit SIR-MBC and integrated over 60 days.

Extracellular Enzyme Activity Assays

Potential and biomass-specific activities of extracellular enzymes (EEAs; descriptions in Table S1) were measured as per Panke-Buisse et al. (2015), which is a modified protocol based on Saiya-Cork et al. (2002) and German et al. (2011). Seven hydrolytic enzymes (α-glucosidase (AG), β-xylosidase (BX), β-glucosidase (BG), cellobiohydrolase (CB), N-acetyl glucosaminidase (NAG), leucine aminopeptidase

(LAP), and acid phosphatase (AP)) were measured using fluorescently labeled substrates 4-methylumbelliferone (MUB) and 7-amino-4-methylcoumarin (AMC). Two oxidative enzymes, polyphenol oxidase (POX) and peroxidase (PER), were measured spectrophotometrically using L-3,4-dihydroxyphenylalanine as the substrate (See *Supplementary Methods* for details). Briefly, soil slurries of 2 g fresh soil and pH 5.0 sodium acetate buffer were added to appropriate substrates in 96-well plates. Hydrolytic plates with standard wells and sample + substrate wells were incubated in the dark at 23°C for three hours, and 10 μL of 1.0M NaOH was added to hydrolytic plates to quench the reaction, after which fluorescence was measured on a microplate reader (BioTeK). Oxidative enzyme plates included buffer-, substrate-, and sample-blanks in addition to sample + substrate wells, and absorbance was measured at 460 nm after a four-hour incubation. Potential activity was calculated based on equations from Saiya-Cork et al. (2002) and normalized by MBC (hereby 'biomass-specific enzyme activity') to highlight shifts in microbial allocation strategies.

16S rRNA gene and ITS region amplicon sequencing

Whole DNA was extracted from 0.3 g of each soil sample using the PowerMag Microbiome RNA/DNA Isolation Kit (MO BIO Laboratories, Inc., Carlsbad, CA, USA). DNA quantification, PCR, normalization, purification, and sequencing (MiSeq 2 x 250 bp) are described in detail in *Supplementary Methods*. Briefly, PCR primers targeted the bacterial/archaeal 16S rRNA gene V4 region (515 F / 806 R) and the fungal ITS region (modified nBITS2 F / 58A2 R; (Koechli et al. 2019)). Sequences were demultiplexed, quality processed, and assigned to amplicon sequence variants

(ASVs) using QIIME2 (Bolyen et al. 2018) with the built-in DADA2 pipeline (Callahan et al. 2016). Taxonomic classification was done using the QIIME2 Greengenes database for 16S rRNA genes (DeSantis et al. 2006) and the UNITE database for ITS (Kõljalg et al. 2013). In several cases, the taxonomic classification provided by Greengenes was updated based on the NCBI taxonomy browser. FUNGuild was used to assign ITS ASVs to functional guilds based on taxonomic classification (Nguyen et al. 2016). Following the filtering of contaminants, singletons, and low abundance doubletons, 94.2% of total 16S rRNA gene sequences remained ($n_{filtered}$ = 2,155,006), comprising 2828 bacterial ASVs, and 88.8% of all ITS sequences remained after filtering ($n_{filtered}$ = 1,971,460), comprising 3826 fungal ASVs.

Bioinformatic and Statistical Analysis

Statistics were performed using R v 3.1.0, with general dependencies on the following packages: ggplot2, plyr (Wickham 2009, 2011), and phyloseq (McMurdie and Holmes 2013). The effect of liming on physicochemical properties, MBC, respiration, and EEAs was determined using a mixed effects model (*lme4*; (Bates et al. 2015)) with plot and subcatchment as random effects and elemental variables, MBC, $CR_{mass,}$ and EEAs as fixed effects. Data were log-transformed when necessary to meet conditions of normality, and post-hoc comparisons were carried out with Tukey HSD tests. To compare microbial community composition (i.e. beta-diversity) in limed and control soils, we used Canonical Correspondence Analysis (CCA) and non-metric multidimensional scaling (NMDS) on Bray-Curtis distance matrices. A PERMANOVA test (*adonis*; *vegan*) was used to identify which variables explained

significant proportions of the variation in Bray-Curtis dissimilarities of normalized ASV count data. Environmental variables were fit to community data using *envfit* from the *vegan* package in R (Oksanen et al. 2007), which included soil horizon, pH, $[Ca^{2+}]$, EEAs, MBC, CR_{mass}, and the primary axis from a PCoA of 25 element concentrations. The relative importance of all variables in explaining the primary CCA axis of bacterial and fungal community composition was decomposed using *relaimpo* (Groemping 2006) and corroborated with other methods (*boruta* and *party*).

To understand how variation in each of the nine enzymes was linked to bacterial or fungal community composition, we modeled the relative importance of EEAs exclusively in explaining the first NMDS axis of bacterial and fungal community composition using *relaimpo*. To determine the relationship between overall soil enzyme profiles and microbial composition, we regressed the first NMDS axis of enzyme composition (aggregate EEAs) with the first NMDS axis of fungal and bacterial composition (a measure of beta-diversity) in each sample. Changes in microbial richness were assessed using multiple alpha-diversity metrics including observed species, Chao1, and Shannon's H. Taxa that were strongly associated with either limed or control sample libraries were identified using indicator species analysis (*indicspecies;* (Cáceres and Legendre 2009)) and weighted-linear modeling (*limma* and *voom;* (Ritchie et al. 2015)). P-values were adjusted for false discovery rate according to the Benjamini-Hochberg method. Correlations between enzyme activities and microbial richness were assessed using Pearson's product moment correlation, and P-values were Bonferroni corrected. We identified the ten most abundant bacterial and fungal families in the data set and related them to potential enzyme activities and pH

using Spearman's rank correlation at multiple thresholds of significance ($\alpha = 0.05$, $\alpha = 0.001$, $\alpha = 0.0005$). We report these analyses at the family level under the assumption that majority member ASVs (ranging from 1-4 ASVs per family) share life history strategies and approximate functionally coherent groups (Schimel and Schaeffer 2012). These analyses were also performed at multiple levels (phylum, order, genus, ASV etc.), and we described ASV or genus level associations when they drive patterns in higher taxonomic levels. We used Tukey HSD tests for post-hoc comparisons between relative abundances of ASVs in limed and control soils.

Results

Physicochemical impacts of liming

Twenty-five years after liming, the majority of physicochemical soil properties did not differ significantly from control plots, except for an increase in pH by one unit averaged across both horizons ($F = 58.8$, $P < 0.001$), and the 2.6- and 4.0- fold increases in Ca concentrations in the Oe and Oa horizons, respectively (Table 1). Mg concentrations were 42% higher in the Oa horizon of the limed soils ($P = 0.04$), but no other changes were observed in soil moisture or Al, Cu, Fe, K, Mn, P, Pb, Zn, or the 16 other elemental concentrations analyzed (Table S2). Melvin et al. (2013) previously reported that C and N stocks were higher in O horizons of limed soils relative to control soils (90% and 78% higher respectively), with the greatest accumulations occurring in the Oa horizon (Table 1).

Table 1 Soil microbial and chemical response variables (mean ± standard error) measured in the two forest floor horizons in limed and control watersheds (n = 40). Within horizon P-values significant at α = 0.05 are in bold. Other variables measured are listed in Table S1.

Soil Property	Horizon	Control	Limed	P value
C (Mg/Ha) *	Oe	7.89±1.18	10.4±1.13	**0.01**
	Oa	24.4±4.03	60.6±9.41	**0.001**
N (Mg/Ha) *	Oe	0.38±0.69	0.49±0.69	**0.01**
	Oa	1.08±0.72	2.46±0.76	**0.001**
Microbial biomass C (mg C/g soil)	Oe	439±53.2	718±96.1	**0.013**
	Oa	105±3.5	118±7.8	0.579
pH	Oe	4.62±0.1	5.59±0.1	**<0.001**
	Oa	4.38±0	5.36±0.1	**<0.001**
Ca (mg/kg soil)	Oe	5483±1048	14230±2926	**0.044**
	Oa	3604±734	14502±2279	**<0.001**
Mg (mg/kg soil)	Oe	460±44.9	687±106	0.066
	Oa	333±35.5	475±62.9	**0.045**

* Treatment averages of data from Melvin et al. (2013)

Microbial respiration and extracellular enzyme activity

We observed liming-driven suppression of EEAs and microbial respiration, providing evidence for a reduced capacity for litter and OM decomposition. Liming reduced the biomass-specific activity of certain C-active hydrolytic enzymes involved in cellulose and xylan degradation in the Oe horizon (BG 38% lower, $P = 0.01$; BX 54% lower, $P < 0.001$), but cellobiohydrolase (CB) and α-glucosidase (AG) involved in cellulose and starch degradation were unaffected (Figure 1A). Microbial production of enzymes for nutrient acquisition was also adversely affected by liming. Biomass-specific activities of enzymes used in N and P acquisition were 35% (LAP) and 48% (AP) lower in the limed Oe horizons, respectively ($P < 0.05$) (Figure 1B and 1C). Liming reduced biomass-specific ligninolytic oxidative enzyme activity by an average of 45% ($P < 0.05$) across both horizons. Oxidative enzymes from classes of peroxidases (PER) and phenol oxidases (POX) showed the largest reductions across all the enzymes measured (Figure 1D). PER activity was most diminished in the limed Oa horizon (64% lower; $P = 0.01$) where C accumulation was greatest, while POX activity was most diminished in the limed Oe horizon (35% lower; $P = 0.04$). Overall, biomass-specific EEAs trended higher in the Oa horizon than in the Oe horizon, and liming tended to decrease EEAs. Liming did not alter the cumulative amount of C respired over 60 days, but it did increase the MBC in the Oe horizon ($P = 0.013$; Table 1). As a result, the Oe experienced a 27% reduction in cumulative respiration per gram biomass (CR_{mass}) ($P = 0.004$) (Figure 1E).

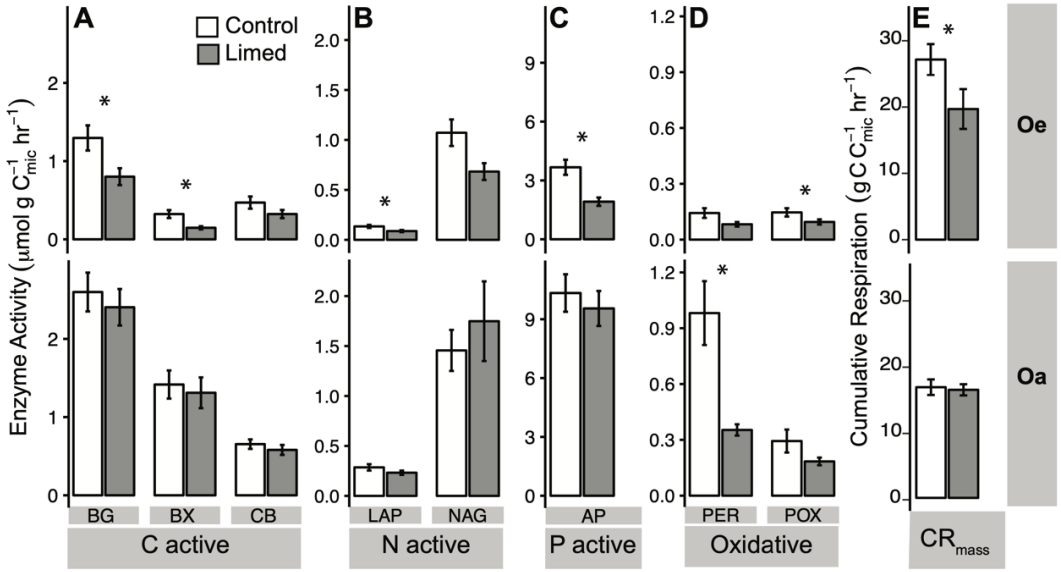

Figure 1 Liming effect on hydrolytic and oxidative enzymes, and microbial respiration in the two organic (O) horizons. Differences between treatment means (±SE) are marked with "*" at significance level $\alpha = 0.05$ ($n_{rep} = 24$). Biomass-specific enzyme activities for (A) C-degrading hydrolases (BG: β-glucosidase, BX: β-Xylosidase, CB: Cellobiohydrolase), (B) N-degrading enzymes (LAP: Leucine aminopeptidase, NAG: N-acetyl glucosaminidase), (C) P-acquiring enzymes (AP: Acid Phosphatase), (D) Oxidative enzymes (PER: Peroxidase, POX: Phenol Oxidase) and (E) Biomass-specific C respired over 60-day incubation (CR_{mass}).

Bacterial and fungal community structure response to liming

The structure of soil bacterial and fungal communities was strongly and consistently different between limed and control soils. Variation in bacterial and fungal community composition (beta-diversity) was primarily attributable to pH and soil horizon, which were strongly correlated with the first and second CCA axes respectively (Figure 2A and 2B). A PERMANOVA (Table S3) showed that horizon and pH explained the greatest variation in bacterial (12% each) and fungal (7-8% each) community composition ($P < 0.001$ *each*). Ca concentration was ranked highly among the explanatory variables of the first CCA axis, but it explained a relatively small percentage of variation in the microbial community (<2%) compared to pH (Figure 2C and 2D). Fungal composition varied significantly at the plot scale ($P < 0.05$), displaying a greater degree of heterogeneity across the landscape than was observed for bacteria (Table S3). A large amount of the variability in bacterial and fungal community structure remained unexplained (60% and 66%, respectively).

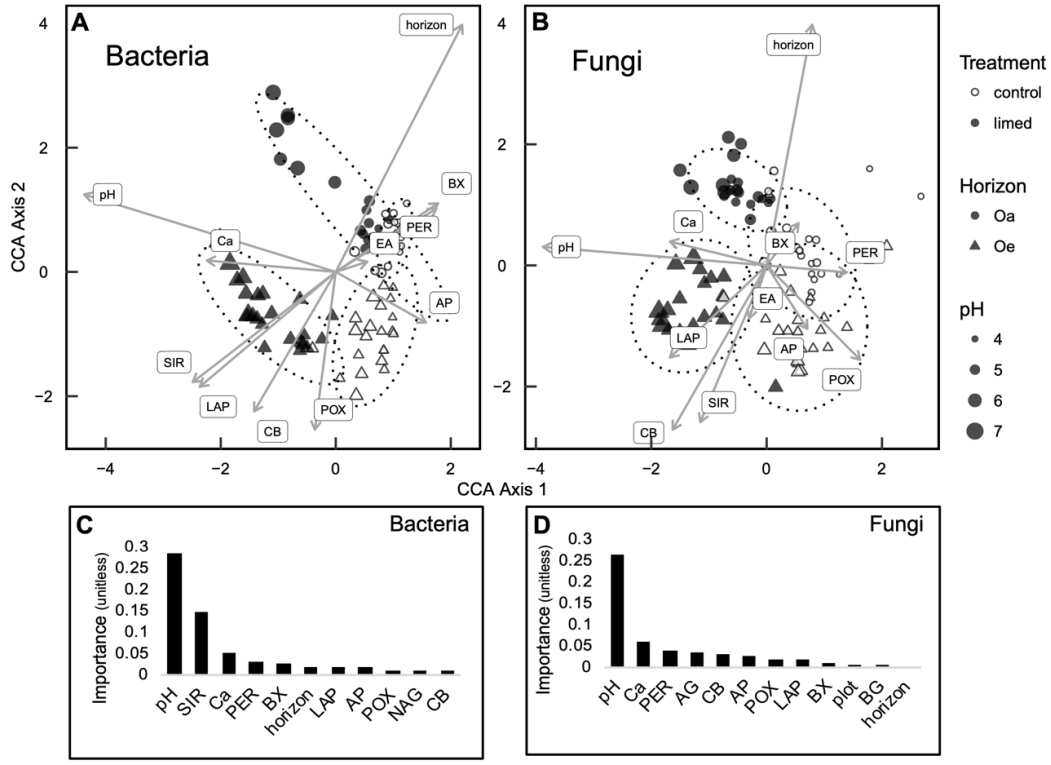

Figure 2 Liming effect on (A) bacterial and (B) fungal community composition in the organic horizons as shown by canonical correspondence analysis of samples from treated and control subcatchments based on Bray-Curtis distances. Variables measured in these samples were fitted to the ordinations with the arrow length proportional to the correlation between the variable and the ordination axes. PERMANOVA test was used to identify variables that explain significant amounts of variation (n_{tot} = 96). For bacteria, pH and horizon were most important (*P < 0.001*), while POX, PER, CB, BX, and SIR were also significant (*P < 0.05*). For fungi, pH and horizon were most important (*P < 0.001*), followed by POX, PER, LAP, BG (*P < 0.05*), and SIR, BX, Ca, and plot (*P < 0.05*). EA, Elemental Axis1; SIR, microbial biomass C; potential enzymes activities (AP, Acid Phosphatase; BX, β-Xylosidase; CB, Cellobiohydrolase; LAP, Leucine aminopeptidase; PER, Peroxidase; POX, Phenol Oxidase). Relative importance of variables in explaining CCA Axis 1 is given for (C) bacteria and (D) fungi.

Potential EEAs were strongly correlated with microbial community composition, more so than soil elemental concentrations. Altogether, potential EEA explained 14% of variation in the fungal community and 12% in the bacterial community across all samples (Table S3). The activities of several lignocellulolytic enzymes (BG, CB, POX, and PER) were significantly associated with fungal (6%) and bacterial (5%) community composition ($P < 0.01$ and $P < 0.05$, respectively). Oxidative enzymes PER and POX had higher explanatory power in fungal than bacterial CCA axis 1, while enzymes involved in N- and P- acquisition and xylan degradation explained more variation in bacterial than fungal CCA axis 1 (Figure 3).

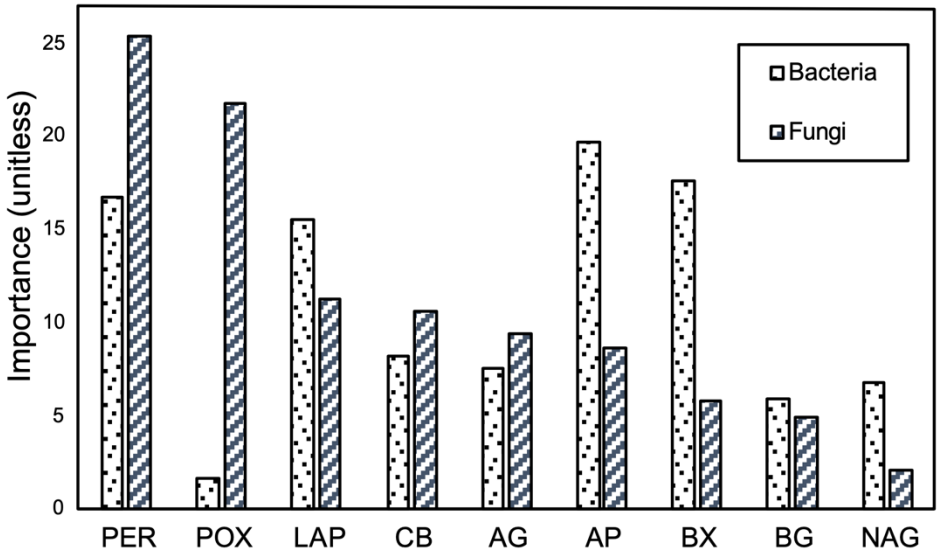

Figure 3 The relative importance of oxidative and hydrolytic enzymes in explaining the variation in fungal and bacterial CCA Axis 1. (AG, α-glucosidase; BG, β-glucosidase; BX, β-Xylosidase; CB, Cellobiohydrolase; LAP, Leucine aminopeptidase; NAG, N-acetyl glucosaminidase; AP, Acid Phosphatase; PER, Peroxidase; POX, Phenol Oxidase).

We determined whether liming-induced variation in fungal and bacterial beta-diversity (as determined by NMDS) correlated with differences in pH, CR_{mass}, and overall EEA. In the Oe horizon, liming-induced changes in fungal beta-diversity correlated strongly with pH and overall EEAs and correlated inversely with CR_{mass} (Figure 4). None of these correlations were observed in conjunction with clear liming-induced shifts in bacterial beta-diversity in either horizon, or with fungal beta-diversity in the Oa horizon.

Fungal alpha-diversity was strongly positively correlated with pH *(observed species*: $\rho = 0.26$, $P = 0.001$; *Shannon's H*: $\rho = 0.23$, $P = 0.005$*)* and limed soils had significantly more observed fungal species than controls ($P = 0.008$). Bacterial alpha-diversity did not correlate with pH or differ significantly by treatment.

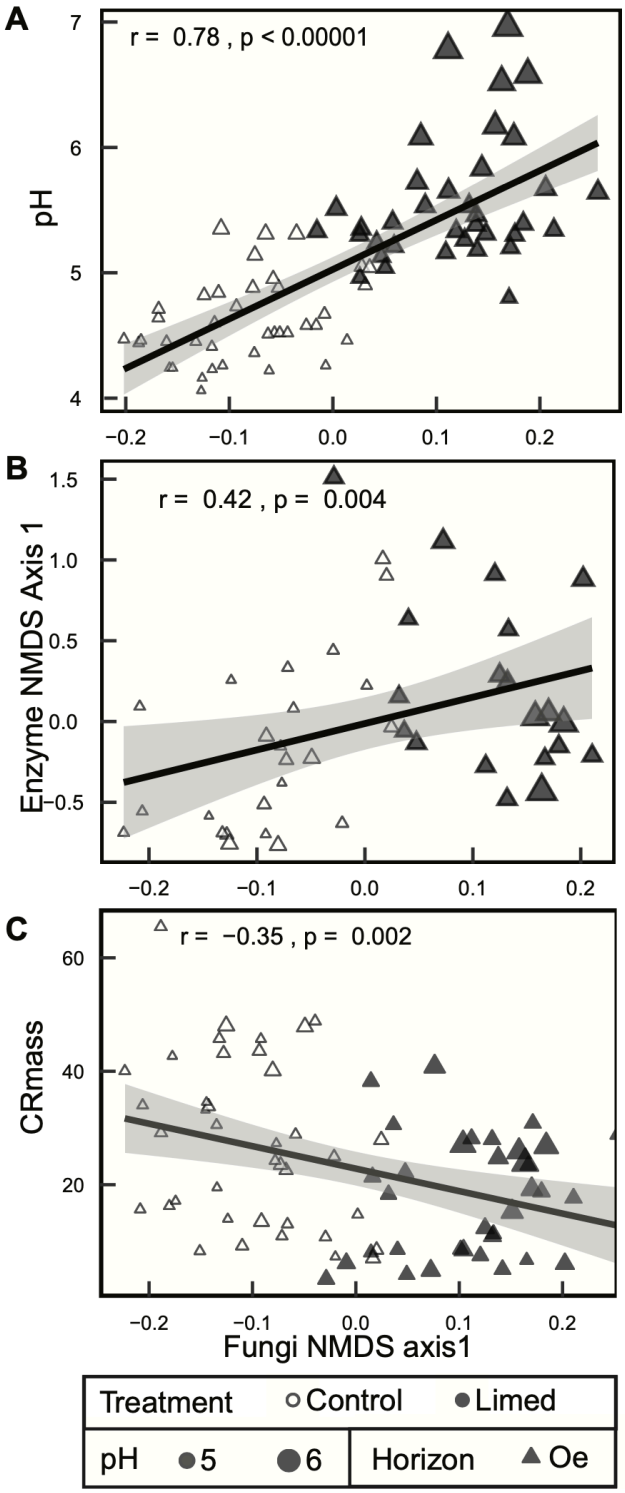

Figure 4 Spearman correlations between Oe horizon fungal community composition and (A) pH, (B) Enzyme composition and (C) Biomass-specific C respired over a 60-day incubation (n_{tot} = 80).

Liming effects on major fungal and bacterial populations

Liming produced long-term changes in fungal functional guilds, particularly ECMF, which made up 41% of ITS reads (Figure 5A). The ECMF guild abundance was significantly lower in the Oe horizon limed soils (*P = 0.03*), and its decrease in relative abundance was correlated with increasing pH (Table S4). The fungal saprotroph guild accounted for 50% of ITS reads and was negatively affected by liming (*P = 0.001*) with a significant reduction in the Oe horizon (Figure 5B; *P = 0.004*). Among saprotrophs, liming reduced abundances of soil saprotrophs overall (26% of ITS reads; *P = 0.02*) and the wood-degrading fungi (4% of total reads) in the Oe horizon (Figure 5C; *P = 0.01*). Many ASVs within fungal functional guilds exhibited contrasting responses, but the overall trend was that ECMF and saprotroph populations were reduced by liming over the long term.

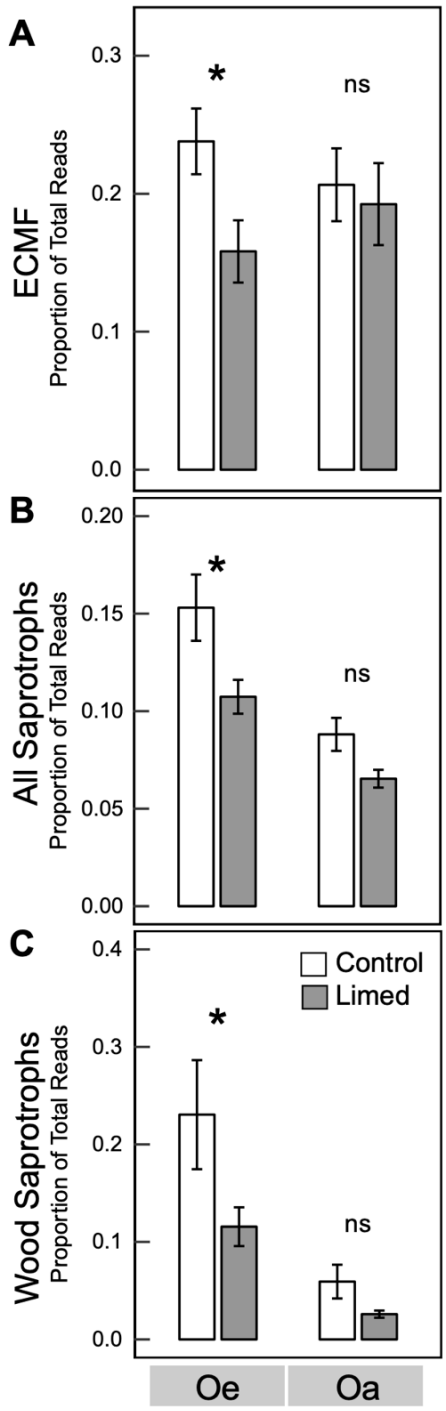

Figure 5 Liming effect on fungal functional groups identified by FUNGuild. (A) ectomycorrhizal (41% of reads), (B) all identifiable saprotroph (50% reads) and (C) wood saprotroph (4% of reads) populations were lower in limed Oe horizons, and similar trends, though non-significant, were observed in the Oa horizon. Relative abundance differences between treatment means (±SE) within horizons significant at $\alpha = 0.05$ are marked with "*" ($n_{rep} = 40$)

Among the major fungal families responding to liming were *Russulaceae*, *Piskurozymyceae*, *Mortierellaceae*, and *Gloniaceae* (Figure S1A; Table S4). The two most abundant responder ASVs in the dataset, classified to *Russula* and *Amanita* (*Basidiomycota*; ECMF species), were greatly reduced in limed soils relative to controls across O horizons (25- and 2- fold lower respectively, $P = 0.0004$; Figure S2A). *Gloniaceae* (*Ascomycota*) populations were also negatively impacted by liming in both horizons, driven by trends in four ASVs (70% of *Gloniaceae* and 2% of ITS reads) classified to the ECMF genus *Cenococcum*. *Cenococcum* ASVs declined by 70% in the Oe horizon and virtually disappeared in the Oa ($P < 0.005$; Figure 6A). This contributed to the phylum level suppression of *Ascomycota* populations in the Oa horizon in response to liming (Figure S3A). In contrast, liming benefitted certain fungi like *Mortierella* ASVs (*Mortierellaceae*; *Zygomycota*) in both horizons (3% of ITS reads; $P < 0.0001$), and a single hyper-abundant ASV classified to *Solicoccozyma* (*Piskurozymaceae*; *Basidiomycota*), a common humus yeast, increased by 280% in the Oa horizon in response to liming (4% of ITS reads; $P = 0.00002$).

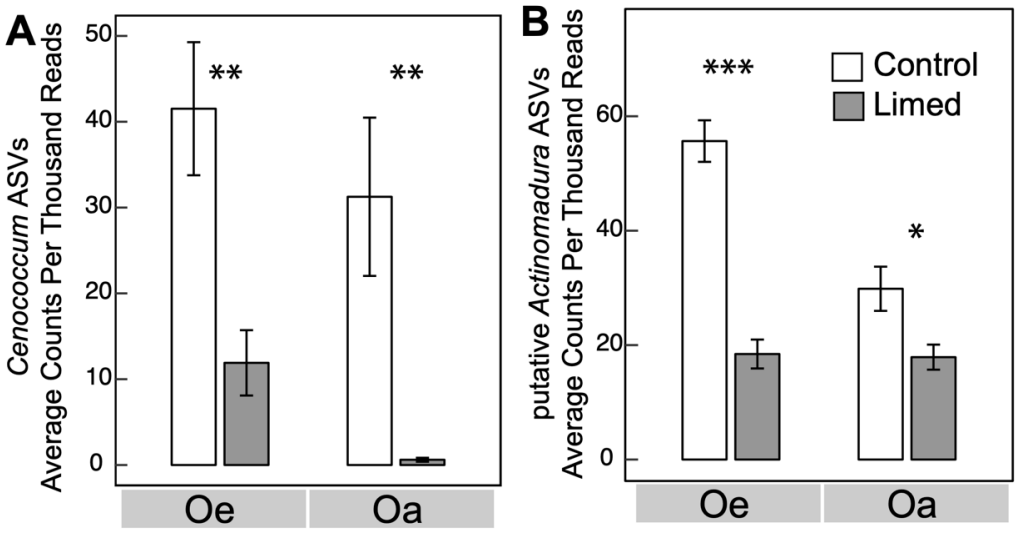

Figure 6 ASVs with high relative abundance that correlated with ligninolytic enzyme activity. (A) putative *Actinomadura* ASVs which accounted for 2.5% of total bacterial reads and correlated with peroxidase activity (R = 0.35, *P < 0.001*). (B) *Cenococcum Geophilum* ASVs, an ectomycorrhizal ascomycete that accounted for 2% of fungal reads and correlated with phenol oxidase activity (R = 0.58, *P < 0.001*). Significant differences at $P < 0.05$ are marked with '*', $P < 0.01$ '**', and $P < 0.001$ '***', ($n_{rep} = 40$).

Among the major bacterial families, members of the *Streptosporangiales* (*Thermomonosporaceae*) and *Methylocystaceae* declined strongly in response to liming, correlating negatively with pH in both horizons (Figure S1B and Table S5). Three closely related ASVs classified to *Streptosporangiales* (2.4% of 16S reads) were 60% less abundant in limed plots ($P < 0.001$; Figure 6B). The closest match for these ASVs was to the genera *Actinoallomurus* and *Actinomadura* (95% similarity NR 044027.1; Figure S4A) and we hereby refer to them as putative *Actinomadura*. These declines contributed to the phylum level negative responses by *Actinobacteria* (Figure S3). High-abundance ASVs related to *Roseiarcus fermentans* (52% of *Methylocystaceae* reads) also declined in relative abundance with liming. Though not among the most abundant bacterial families, members of candidate division *WPS-2* (30% of *WPS-2 reads*) showed some of the sharpest declines in relative abundance in response to liming in both horizons (Figure S2B). At the phylum level, liming benefitted *Proteobacteria* populations (Figure S3B) due to increases in three ASVs most closely related to *Stella vacuolata* (*Rhodospirillaceae*; ~91% similarity) and family level responses in *Hyphomicrobiaceae* and *Bradyrhizobiaceae* (Figure S1B).

Correlations between EEAs and microbial taxa

The relative abundance of major fungal and bacterial families and the most abundant ASVs within them, correlated with EEAs, indicating that changes in community structure likely altered community function by altering extracellular enzyme activities. The decline in the ECMF guild populations was associated with the

decline in N-cycling and oxidative enzyme activity (NAG: $\rho = 0.22$, $P = 0.03$; POX: $\rho = 0.26$, $P = 0.01$). Within the ECMF guild, four *Cenococcum* ASVs (70% of *Gloniaceae*; ~ 2% of fungal reads) were strongly positively correlated with NAG ($\rho = 0.45$, $P < 0.0001$) and POX ($\rho = 0.59$, $P < 0.00001$) and *Russulaceae* correlated with oxidative enzyme activity in the Oa horizon (PER: $\rho = 0.31$, $P = 0.04$; POX: $\rho = 0.3$, $P = 0.04$). Phylum *Ascomycota* abundance was positively correlated with PER activity in the Oa horizon ($\rho = 0.3$, $P = 0.01$). Declines in the wood saprotroph guild were also associated with declines in N-cycling and lignocellulolytic enzymes (LAP: $\rho = 0.56$, $P < 0.0001$; NAG: $\rho = 0.39$, $P < 0.001$; BG: $\rho = 0.24$, $P = 0.03$; POX: $\rho = 0.48$, $P < 0.0001$). Among bacteria, declines in putative *Actinomadura* were significantly correlated with lower PER activity in both horizons ($\rho = 0.33$, $P = 0.001$), and with POX activity ($\rho = 0.45$, $P = 0.002$) in the Oa horizon. Correlations between ASV abundance and EEAs for the most abundant families of bacteria (together 42% of 16S reads) and fungi (together 26% of ITS reads) are summarized in Table S4 and S5.

Discussion

We sought to define the mechanisms by which soil pH can drive soil C dynamics in northern forest soils by examining soil microbial community structure and function in a long-term liming experiment. Twenty-five years after the aerial liming of two forest subcatchments at Woods Lake, an increase of one pH unit has resulted in a striking increase in OM stocks in surface horizons. In support of our hypotheses, microbial community structure differed significantly between control and

limed subcatchments and correlated strongly with key soil enzyme activities and microbial respiration (CR_{mass}), which were much reduced by liming. Moreover, certain microbial guilds and taxa that made up a substantial proportion of the total affected community were strongly associated with lignocellulolytic enzyme activity, and their relative abundance was adversely affected by liming. In particular, declines in the abundance of ECMF, especially family *Russulaceae* and *Cenoccocum* spp., correlated with declines in oxidative enzyme activities. These changes were apparently driven by pH rather than Ca concentration (Table S4). Taken together, these results provide strong evidence that long-term changes in pH altered microbial community structure and function, leading to suppression of decomposition and C accumulation in limed soils at Woods Lake. Similar mechanisms likely control variation of soil C stocks across northern forest ecosystems.

As hypothesized, we observed that liming greatly suppressed oxidative enzyme activity (~45%), which in the long term could explain O horizon C accumulation. Unlike substrate-specific hydrolytic enzymes, oxidative enzyme activities tend to be uncorrelated with substrate availability or microbial nutrient demand (Sinsabaugh et al. 2008, Sinsabaugh 2010). Instead, microbes produce extracellular oxidative enzymes for many purposes, including defense, the synthesis of secondary compounds like melanin, and OM decomposition (Sinsabaugh 2010). However, once in the soil environment, these enzymes oxidize persistent plant and soil C compounds (lignins, tannins, and aromatic compounds) and are thereby a proximate control over the slow pools of C that govern forest floor C storage in the long term. Accumulation of C is often observed when these ligninolytic enzyme activities are diminished, as is

common in N fertilization studies (DeForest et al. 2004, Frey et al. 2004, Waldrop and Zak 2006). Studies measuring oxidative enzymes in limed forest soils are few, but in tundra soils, liming has been shown to lower phenol oxidase activities (Stark et al. 2011). The pH optima of oxidative enzymes typically fall in the acidic range and so an increase in pH can directly inhibit enzyme activity, but oxidative enzyme activity can also decline due to feedbacks from pH constraints on plant symbionts or microbial producers (Sinsabaugh 2010, Frey 2019).

We observed that variation in oxidative enzyme activities were most strongly associated with variation in fungal community composition, while variation in hydrolytic enzyme activities were most strongly associated with variation in bacterial composition. This observation supports the idea that fungi are the principal producers of oxidative enzymes that decompose lignin and persistent plant polymers, while bacteria play a secondary role in their production and metabolize the products of these reactions (Frey et al. 2004, Sinsabaugh 2010, Bugg et al. 2011, Žifčáková et al. 2017).

Taxa and functional groups negatively impacted by liming were clearly associated with oxidative decomposition. The ECMF community at Woods Lake (41% of ITS reads) was dominated by *Russulaceae*, members of which were up to 25-fold less abundant and members of the ECMF species *Cenococcum* were 32-fold less abundant in limed soils at Woods Lake. *Russula* species have previously been reported as pH-sensitive, declining in limed and wood-ash treated soils across Nordic spruce and coniferous forests (Taylor and Finlay 2003, Kjøller et al. 2017). Similarly, *Cenococcum* species markedly declined in limed beech and Norway spruce forests in France (Rineau and Garbaye 2009, Rineau et al. 2010). Both ECMF taxa were

positively correlated with oxidative enzyme activities in our study (*Cenococcum*: POX, *Russulaceae*: POX and PER). *Russula* species are capable of producing cellulases, Mn peroxidases, laccase and polyphenol oxidase (Bödeker et al. 2009, Keskin et al. 2012, Zhu et al. 2013, Voříšková and Baldrian 2013, Kyaschenko et al. 2017). A recent comparative analysis reported that *Cenococcum geophilum* encoded the highest number of genes involved in lignocellulose degradation among ECMF whose genomes have been sequenced (Peter et al., 2016). In addition, *Cenococcum* has been shown to be the main ECM contributor to total root tip enzyme production in beech and Norway spruce forests (Rineau and Garbaye 2009, Rineau et al. 2010). According to our analysis, *Cenococcum*, and its closest sequenced relative (*Glonium stellatum*) encode secretion signal-bearing laccases (see Supplementary Methods).

The importance of ECMF as decomposers in forest soils is highlighted by the fact that declines in N-acquiring and oxidative enzymes correlate with declines in ECMF abundance. In nutrient-limited systems, ECMF fuel the breakdown of persistent OM using host derived sugars (Lindahl and Tunlid 2014). However, this decline in ECMF abundance was not the result of differences in plant host abundance. That is, the biomass of ECM-forming tree species (*Betula*, *Fagus*, and *Picea*) was actually greater in the limed than in the control subcatchments (Melvin et al. 2013). However, it remains unclear whether this response results from direct effects of pH on these fungi or is mediated by responses of their plant hosts. Plants might be expected to reduce C allocation to ECMF in situations where liming increases soil nutrient availability, and nitrification rates in the limed plots exceeded those in the controls (Melvin et al. 2013). Nevertheless, ECMF diversity is often negatively correlated with

pH, and the decrease in pH-sensitive taxa with liming (Kjøller and Clemmensen 2009, Tedersoo et al. 2015) supports our hypothesis about the direct negative impact of increasing pH. These results highlight that losing key ECMF taxa endemic to a particular system can inhibit decomposition of lignin and persistent OM.

Sequences of the saprotroph functional guild (50% of ITS reads) also markedly declined in relative abundance in limed soils. However, the most abundant saprotroph ASVs from *Mortierellaceae* actually benefitted from liming. These fungi are known to be involved in early stages of decay of plant detritus, utilizing more labile organic compounds and are clearly associated with decomposition of fine roots (Li et al. 2015). Most of the fresh detritus in the Oe horizon is derived from fine roots, which were about twice as abundant in the Oe of limed relative to control soils (Melvin et al. 2013). Nevertheless, the saprotroph guild level response originated from the bulk of less abundant wood and soil saprotrophs, suggesting a generalized impairment of detrital decomposition in limed soils. This observation was supported by our finding that the decrease in wood saprotroph relative abundance was correlated with decreases in N-acquiring (LAP, NAG) and lignocellulolytic (POX, PER, BG) enzymes, which is consistent with the well-established role of many white-rot fungi and some brown-rot fungi in producing oxidative enzymes (Baldrian 2008b). Wood saprotroph decline has also been associated with soil C accumulation in N addition experiments (Frey et al. 2004) and is in line with the generalized impairment of saprotrophy and C accumulation seen at Woods Lake. Whether persistence of decaying wood has contributed to the accumulation of OM in the forest floor at Woods Lake deserves further study.

Proteobacteria (especially *Alphaproteobacteria*), *Actinobacteria*, and *Acidobacteria* were the dominant phyla at Woods Lake. While the relative abundances of these phyla trend with pH gradients across ecosystems, individual taxa within them often have contrasting pH preferences (Lauber et al. 2009, Delgado-Baquerizo et al. 2018). *Acidobacteria* declined in response to liming, as expected, largely due to declines in unclassified members of the *Acidobacteriales* like *Ellin6513* and *Koribacteraceae* from *Acidobacteria* subdivision 1, which predominates in acidic environments (Sait et al. 2006). *Alphaproteobacteria*, in particular, tended to increase in limed soils and this result was due to increases in the abundance of unclassified *Rhodospirillaceae ASVs*. *Rhodospirillaceae* are a functionally diverse group and little is known about the ecology of these unclassified ASVs beyond their association with alkaline soils (Delgado-Baquerizo et al. 2018).

Contrary to expectation, *Actinobacteria* as defined at the phylum level did not increase in response to liming. This outcome was a result of major declines in putative *Actinomadura* ASVs in response to liming. These ASVs are closely related to gram-positive mycelia-forming genera *Actinoallomurus* and *Actinomadura,* which grow at moderately acidic pH (4-5.5) (Lee and Hwang 2002, Pozzi et al. 2019). *Actinoallomurus,* known to associate with ectomycorrhizal roots, are a recently classified genus related to *Actinomadura* (Tamura et al. 2009, Sakoda et al. 2019). Frostegård et al. (1993) found that in limed coniferous soils, bacterial communities shifted away from gram-positive taxa towards more gram-negative taxa. Declines in these putative *Actinomadura* correlated with decreases in oxidative enzyme activity across horizons, particularly for peroxidase. *Actinobacteria* are known to be a rich

reservoir of extracellular and lignin peroxidases, and *Actinomycetales* are speculated to oxidize persistent plant polymers, making them plausibly important bacterial decomposers in the system (Kirby 2005, Roes-Hill et al. 2011). *Actinomadura* are capable of decomposing xylan, cellulose, and lignin, like many members of *Actinobacteria* (Mason et al. 1988, Zimmermann and Broda 1989, Holtz et al. 1991, Schellenberger et al. 2009, Verastegui et al. 2014, Yin et al. 2018). We also identified secretion signal-bearing laccase in the majority of publicly available *Actinomadura* genomes (28 / 67 genomes), supporting their capability to catalyze extracellular oxidative processes. Oxidative breakdown of persistent C is thought to be a "narrow" process limited to certain groups of microbes that control the fate of C (McGuire et al. 2010, Schimel and Schaeffer 2012). Our results suggest that liming caused a relative decline in fitness of key decomposer species resulting in C accumulation in O horizon limed soils.

We showed that liming, by modifying pH, caused major shifts in microbial community composition. Soil pH has been identified as a master variable that explains microbial community composition in soils, often having stronger impacts than OM content and quality across many studies (Fierer 2017). The increase in pH had permeated deeper into the Oa horizon after 25 years, and the one-unit pH change was an order of magnitude more influential in altering microbial community composition than the increase in Ca concentrations from liming. The Ca response reflects the effect of detrital recycling of Ca, because any residual lime is now located beneath the forest floor layers that we sampled (R. Newton, personal communication).

At Woods Lake, liming wholly restructured the fungal community, altering beta-diversity between limed and control soils and increasing alpha-diversity. Liming has been reported to shift fungal communities in forest, agricultural, and grassland experiments, though without increasing their species richness (Bååth et al. 1995, Rousk et al. 2010, Cassman et al. 2016, Cruz-Paredes et al. 2017). The observation of an increase in fungal alpha-diversity with pH at Woods Lake was likely an artifact of a change in community evenness, whereby ASVs that were dominant under acidic conditions yielded to a proliferation of neutrophilic species (including yeasts and parasitic fungi) in response to liming. The notable large increase in neutrophilic species of *Solicoccozyma*, a psychrotolerant humus-layer yeast, in the limed Oa could reflect the pH tolerance of these species or a change in substrate availability, since the solubility of DOC increases with pH in acidic O horizons (Evans et al. 2012)

Our expectation that oxidative decomposition would be most suppressed in the Oa horizon was supported, and this suppression likely accounts for much of the doubling of C stocks that occurred in the Oa horizon of limed soils. In this horizon, peroxidase activity decreased 64% in response to liming, which correlated with diminished relative abundances of important groups including wood saprotrophs, *Russulaceae*, and *Streptosporangiales*. However, most other C-cycle responses were limited to the Oe horizon, including increases in MBC and reduction of microbial respiration, glucosidase, xylosidase, and phenol oxidase activity. The tight connection between pH, fungal beta-diversity, CR_{mass}, and EEAs in the Oe horizon suggests that the impacts of liming on fungal community composition was responsible for suppression of decomposition in this plant detritus-enriched horizon. Enzymes

involved in P and N acquisition (AP and LAP) were also diminished in the limed Oe horizons, potentially reflecting a tightening of the N cycle and P limitation in this relatively labile C rich horizon that has been reported in other liming studies (Illmer and Schinner 1991, DeForest et al. 2011, Groffman and Fisk 2011, Carrino-Kyker et al. 2012). The differential impacts of liming on EEAs between horizons may also reflect the quality and quantity of substrates available, but they point overall to impairment of function at many stages of decomposition.

Among ecosystems that have been limed, forest C stocks show especially divergent responses (Paradelo et al. 2015). Soil heterotrophic respiration rates increased at many limed forests, thereby depleting O horizon C stocks (Persson et al. 1995, Andersson and Nilsson 2001, Lundström et al. 2003). In contrast, at Woods Lake no effect on CO_2 efflux was observed one year after application, and a suppression of respiration was observed 20 years later (Yavitt et al. 1995, Melvin et al. 2013), which is in line with the decreased biomass-specific respiration we observed. Accumulation of O horizon C stocks after liming could be explained by changes in microbial community structure and function, or by increased above or belowground C inputs, altered root distribution, and physicochemical stabilization of C though Ca-OM cation bridging (Derome 1990, Park et al. 2008, Mouvenchery et al. 2011, Srámek et al. 2012, Melvin et al. 2013).

Although we cannot discount the possibility that some of these alternate mechanisms contribute to the liming induced suppression of decomposition at Woods Lake, we show a strong correlation between microbial community composition and oxidative enzyme activity and this result suggests that changes in microbial

community structure and function drive C accrual. This study demonstrates one way in which altering a master variable can link microbial structure with ecosystem functions that control the fate of C in longer timescales. We highlight the possibility that pH-sensitive dominant decomposers may be endemic to acidic forest systems, which has implications for the recovery of forests impacted by acid deposition, as well as the effects of land-use and climate change on soil C storage.

REFERENCES

Andersson, S., and S. I. Nilsson. 2001. Influence of pH and temperature on microbial activity, substrate availability of soil-solution bacteria and leaching of dissolved organic carbon in a mor humus. Soil Biology and Biochemistry 33:1181–1191.

Bååth, E., Å. Frostegård, T. Pennanen, and H. Fritze. 1995. Microbial community structure and pH response in relation to soil organic matter quality in wood-ash fertilized, clear-cut or burned coniferous forest soils. Soil Biology and Biochemistry 27:229–240.

Badalucco, L., S. Grego, S. Dell'Orco, and P. Nannipieri. 1992. Effect of liming on some chemical, biochemical, and microbiological properties of acid soils under spruce (Picea abies L.). Biology and Fertility of Soils 14:76–83.

Bahram, M., F. Hildebrand, S. K. Forslund, J. L. Anderson, N. A. Soudzilovskaia, P. M. Bodegom, J. Bengtsson-Palme, S. Anslan, L. P. Coelho, H. Harend, J. Huerta-Cepas, M. H. Medema, M. R. Maltz, S. Mundra, P. A. Olsson, M. Pent, S. Põlme, S. Sunagawa, M. Ryberg, L. Tedersoo, and P. Bork. 2018. Structure and function of the global topsoil microbiome. Nature 560:233–237.

Baker, K. L., S. Langenheder, G. W. Nicol, D. Ricketts, K. Killham, C. D. Campbell, and J. I. Prosser. 2009. Environmental and spatial characterisation of bacterial community composition in soil to inform sampling strategies. Soil Biology and Biochemistry 41:2292–2298.

Baldrian, P. 2008a. British Mycological Society Symposia Series. British Mycological Society Symposia Series 28:19–41.

Baldrian, P. 2008b. Chapter 2 Enzymes of saprotrophic basidiomycetes. Pages 19–41 *in* L. Boddy, Juliet C Frankland, and P. van West, editors. Academic Press.

Baldrian, P. 2017. Forest microbiome: diversity, complexity and dynamics. FEMS Microbiology Reviews 41:fuw040.

Baldrian, P., M. Kolařík, M. Stursová, J. Kopecký, V. Valášková, T. Větrovský, L. Zifčáková, J. Snajdr, J. Rídl, C. Vlček, and J. Voříšková. 2012. Active and total microbial communities in forest soil are largely different and highly stratified during decomposition. The ISME journal 6:248–58.

Bates, D., M. Mächler, B. Bolker, and S. Walker. 2015. Fitting Linear Mixed-Effects Models Using lme4. Journal of Statistical Software 67.

Bell, C. W., D. T. Tissue, M. E. Loik, M. D. Wallenstein, V. A.- Martinez, R. A. Erickson, and J. C. Zak. 2014. Soil microbial and nutrient responses to 7 years of seasonally altered precipitation in a Chihuahuan Desert grassland. Global Change Biology 20:1657–1673.

Bier, R. L., E. S. Bernhardt, C. M. Boot, E. B. Graham, E. K. Hall, J. T. Lennon, D. R. Nemergut, B. B. Osborne, C. Ruiz-González, J. P. Schimel, M. P. Waldrop, and M. D. Wallenstein. 2015. Linking microbial community structure and microbial processes: an empirical and conceptual overview. FEMS Microbiology Ecology 91:fiv113.

Blette, V. L., and R. M. Newton. 1996. Effects of watershed liming on the soil chemistry of Woods Lake, New York. Biogeochemistry 32:175–194.

Bödeker, I. T. M., C. M. R. Nygren, A. F. S. Taylor, Å. Olson, and B. D. Lindahl. 2009. Class II peroxidase-encoding genes are present in a phylogenetically wide range of ectomycorrhizal fungi. The ISME Journal 3:1387–1395.

Bolyen, E., J. R. Rideout, M. R. Dillon, N. A. Bokulich, C. Abnet, G. A. Al-Ghalith, H. Alexander, E. J. Alm, M. Arumugam, F. Asnicar, Y. Bai, J. E. Bisanz, K. Bittinger, A. Brejnrod, C. J. Brislawn, C. T. Brown, B. J. Callahan, A. M. Caraballo-Rodríguez, J. Chase, E. Cope, R. D. Silva, P. C. Dorrestein, G. M. Douglas, D. M. Durall, C. Duvallet, C. F. Edwardson, M. Ernst, M. Estaki, J. Fouquier, J. M. Gauglitz, D. L. Gibson, A. Gonzalez, K. Gorlick, J. Guo, B. Hillmann, S. Holmes, H. Holste, C. Huttenhower, G. Huttley, S. Janssen, A. K. Jarmusch, L. Jiang, B. Kaehler, K. B. Kang, C. R. Keefe, P. Keim, S. T. Kelley, D. Knights, I. Koester, T. Kosciolek, J. Kreps, M. G. Langille, J. Lee, R. Ley, Y.-X. Liu, E. Loftfield, C. Lozupone, M. Maher, C. Marotz, B. D. Martin, D. McDonald, L. J. McIver, A. V. Melnik, J. L. Metcalf, S. C. Morgan, J. Morton, A. T. Naimey, J. A. Navas-Molina, L. F. Nothias, S. B. Orchanian, T. Pearson, S. L. Peoples, D. Petras, M. L. Preuss, E. Pruesse, L. B. Rasmussen, A. Rivers, M. S. R. II, P. Rosenthal, N. Segata, M. Shaffer, A. Shiffer, R. Sinha, S. J. Song, J. R. Spear, A. D. Swafford, L. R. Thompson, P. J. Torres, P. Trinh, A. Tripathi, P. J. Turnbaugh, S. Ul-Hasan, J. J. van der Hooft, F. Vargas, Y. Vázquez-Baeza, E. Vogtmann, M. von Hippel, W. Walters, Y. Wan, M. Wang, J. Warren, K. C. Weber, C. H. Williamson, A. D. Willis, Z. Z. Xu, J. R. Zaneveld, Y. Zhang, Q. Zhu, R. Knight, and J. G. Caporaso. 2018. QIIME 2: Reproducible, interactive, scalable, and extensible microbiome data science. PeerJ Preprints 6:e27295v2.

Bradford, M. A., N. Fierer, and J. F. Reynolds. 2008. Soil carbon stocks in experimental mesocosms are dependent on the rate of labile carbon, nitrogen and phosphorus inputs to soils. Functional Ecology 22:964–974.

Bugg, T. D. H., M. Ahmad, E. M. Hardiman, and R. Rahmanpour. 2011. Pathways for degradation of lignin in bacteria and fungi. Natural product reports 28:1883–96.

Cáceres, M. D., and P. Legendre. 2009. Associations between species and groups of sites: indices and statistical inference. Ecology 90:3566–3574.

Callahan, B. J., P. J. McMurdie, M. J. Rosen, A. W. Han, A. J. A. Johnson, and S. P. Holmes. 2016. DADA2: High-resolution sample inference from Illumina amplicon data. Nature methods 13:581–3.

Carrino-Kyker, S. R., L. A. Kluber, S. M. Petersen, K. P. Coyle, C. R. Hewins, J. L. DeForest, K. A. Smemo, and D. J. Burke. 2016. Mycorrhizal fungal communities respond to experimental elevation of soil pH and P availability in temperate hardwood forests. FEMS Microbiology Ecology 92:fiw024.

Carrino-Kyker, S. R., K. A. Smemo, and D. J. Burke. 2012. The effects of pH change and NO−3 pulse on microbial community structure and function: a vernal pool microcosm study. FEMS Microbiology Ecology 81:660–672.

Cassman, N. A., M. F. A. Leite, Y. Pan, M. de Hollander, J. A. van Veen, and E. E. Kuramae. 2016. Plant and soil fungal but not soil bacterial communities are linked in long-term fertilized grassland. Scientific reports 6:23680.

Crowther, T. W., J. van den Hoogen, J. Wan, M. A. Mayes, A. D. Keiser, L. Mo, C. Averill, and D. S. Maynard. 2019. The global soil community and its influence on biogeochemistry. Science 365:eaav0550.

Crowther, T. W., D. S. Maynard, J. W. Leff, E. E. Oldfield, R. L. McCulley, N. Fierer, and M. A. Bradford. 2014. Predicting the responsiveness of soil biodiversity to deforestation: a cross-biome study. Global change biology 20:2983–94.

Cruz-Paredes, C., H. Wallander, R. Kjøller, and J. Rousk. 2017. Using community trait-distributions to assign microbial responses to pH changes and Cd in forest soils treated with wood ash. Soil Biology and Biochemistry 112:153–164.

DeForest, J. L., K. A. Smemo, D. J. Burke, H. L. Elliott, and J. C. Becker. 2011. Soil microbial responses to elevated phosphorus and pH in acidic temperate deciduous forests. Biogeochemistry 109:189–202.

DeForest, J., D. Pregitzer, K. Burton, and J. Andrew. 2004. Atmospheric nitrate deposition, microbial community composition, and enzyme activity in northern hardwood forests. Soil Science Society of America Journal.

Delgado-Baquerizo, M., A. M. Oliverio, T. E. Brewer, A. Benavent-González, D. J. Eldridge, R. D. Bardgett, F. T. Maestre, B. K. Singh, and N. Fierer. 2018. A global atlas of the dominant bacteria found in soil. Science 359:320–325.

Derome, J. 1990. Effects of forest liming on the nutrient status of podzolic soils in Finland. Water, Air, & Soil Pollution 54:337–350.

Derome, J., M. Kukkola, A. Smolander, and T. Lehto. 2000. Liming of Forest Soils. Pages 328–337.

DeSantis, T. Z., P. Hugenholtz, N. Larsen, M. Rojas, E. L. Brodie, K. Keller, T. Huber, D. Dalevi, P. Hu, and G. L. Andersen. 2006. Greengenes, a Chimera-Checked 16S rRNA Gene Database and Workbench Compatible with ARB. Appl. Environ. Microbiol. 72:5069.

Driscoll, C. T., C. P. Cirmo, T. J. Fahey, V. L. Blette, P. A. Bukaveckas, D. A. Burns, C. P. Gubala, D. J. Leopold, R. M. Newton, D. J. Raynal, C. L. Schofield, J. B. Yavitt, and D. B. Porcella. 1996. The experimental watershed liming study: Comparison of lake and watershed neutralization strategies. Biogeochemistry 32:143–174.

Evans, C. D., T. G. Jones, A. Burden, N. Ostle, P. Zieliński, M. D. A. Cooper, M. Peacock, J. M. Clark, F. Oulehle, D. Cooper, and C. Freeman. 2012. Acidity controls on dissolved organic carbon mobility in organic soils. Global Change Biology 18:3317–3331.

Fierer, N. 2017. Embracing the unknown: disentangling the complexities of the soil microbiome. Nature Reviews Microbiology 15:579–590.

Fierer, N., A. S. Allen, J. P. Schimel, and P. A. Holden. 2003. Controls on microbial CO2 production: a comparison of surface and subsurface soil horizons. Global Change Biology 9:1322–1332.

Fierer, N., J. W. Leff, B. J. Adams, U. N. Nielsen, S. T. Bates, C. L. Lauber, S. Owens, J. A. Gilbert, D. H. Wall, and J. G. Caporaso. 2012. Cross-biome metagenomic analyses of soil microbial communities and their functional attributes. Proceedings of the National Academy of Sciences 109:21390–21395.

Fierer, N., M. S. Strickland, D. Liptzin, M. A. Bradford, and C. C. Cleveland. 2009. Global patterns in belowground communities. Ecology letters 12:1238–49.

Frey, S. D. 2019. Mycorrhizal Fungi as Mediators of Soil Organic Matter Dynamics. Annual Review of Ecology, Evolution, and Systematics 50:237–259.

Frey, S. D., M. Knorr, J. L. Parrent, and R. T. Simpson. 2004. Chronic nitrogen enrichment affects the structure and function of the soil microbial community in temperate hardwood and pine forests. Forest Ecology and Management 196:159–171.

Frostegård, Å., E. Bååth, and A. Tunlid. 1993. Shifts in the structure of soil microbial communities in limed forests as revealed by phospholipid fatty acid analysis. Soil Biology and Biochemistry 25:723–730.

German, D. P., M. N. Weintraub, A. S. Grandy, C. L. Lauber, Z. L. Rinkes, and S. D. Allison. 2011. Optimization of hydrolytic and oxidative enzyme methods for ecosystem studies. Soil Biology and Biochemistry 43:1387–1397.

Groemping, U. 2006. Relative Importance for Linear Regression in R: The Package relaimpo. Journal of Statistical Software; Vol 1, Issue 1 (2007).

Groffman, P. M., and M. C. Fisk. 2011. Calcium constrains plant control over forest ecosystem nitrogen cycling. Ecology 92:2035–2042.

Grüneberg, E., I. Schöning, W. Riek, D. Ziche, and J. Evers. 2019. Carbon Stocks and Carbon Stock Changes in German Forest Soils. Pages 167--198 *in* N. Wellbrock and Andreas Bolte, editors. Status and Dynamics of Forests in Germany: Results of the National Forest Monitoring. Springer International Publishing, Cham.

Hannam, K. D., L. Venier, D. Allen, C. Deschamps, E. Hope, M. Jull, M. Kwiaton, D. McKenney, P. M. Rutherford, and P. W. Hazlett. 2018. Wood ash as a soil amendment in Canadian forests: what are the barriers to utilization? Canadian Journal of Forest Research 48:442–450.

Högberg, M. N., and P. Högberg. 2002. Extramatrical ectomycorrhizal mycelium contributes one-third of microbial biomass and produces, together with associated roots, half the dissolved organic carbon in a forest soil. New Phytologist 154:791–795.

Holtz, C., H. Kaspari, and J.-H. Klemme. 1991. Production and properties of xylanases from thermophilic actinomycetes. Antonie van Leeuwenhoek 59:1–7.

Illmer, P., and F. Schinner. 1991. Effects of lime and nutrient salts on the microbiological activities of forest soils. Biology and Fertility of Soils 11:261–266.

Jenkins, S. N., I. S. Waite, A. Blackburn, R. Husband, S. P. Rushton, D. C. Manning, and A. G. O'Donnell. 2009. Actinobacterial community dynamics in long term managed grasslands. Antonie van Leeuwenhoek 95:319–34.

Keskin, S., N. S. Ertunga, A. Colak, M. Y. Akatin, A. Ozel, and Y. Kolcuoglu. 2012. Characterization of a Polyphenol Oxidase Having Monophenolase and Diphenolase Activities from a Wild Edible Mushroom, Russula delica. Asian Journal of Chemistry 24:1203–1208.

Kirby, R. 2005. Actinomycetes and Lignin Degradation. Pages 125–168 *in* A. I. Laskin, Joan W Bennett, Geoffrey M Gadd, and S. Sariaslani, editors. Academic Press.

Kjøller, R., and K. E. Clemmensen. 2009. Belowground ectomycorrhizal fungal communities respond to liming in three southern Swedish coniferous forest stands. Forest Ecology and Management 257:2217–2225.

Kjøller, R., C. Cruz-Paredes, and K. E. Clemmensen. 2017. Soil Biological Communities and Ecosystem Resilience. Soil Biological Communities and Ecosystem Resilience:223–252.

Koechli, C., A. N. Campbell, C. Pepe-Ranney, and D. H. Buckley. 2019. Assessing fungal contributions to cellulose degradation in soil by using high-throughput stable isotope probing. Soil Biology and Biochemistry 130:150–158.

Kõljalg, U., R. H. Nilsson, K. Abarenkov, L. Tedersoo, A. F. S. Taylor, M. Bahram, S. T. Bates, T. D. Bruns, J. Bengtsson-Palme, T. M. Callaghan, B. Douglas, T. Drenkhan, U. Eberhardt, M. Dueñas, T. Grebenc, G. W. Griffith, M. Hartmann, P. M. Kirk, P. Kohout, E. Larsson, B. D. Lindahl, R. Lücking, M. P. Martín, P. B. Matheny, N. H. Nguyen, T. Niskanen, J. Oja, K. G. Peay, U. Peintner, M. Peterson, K. Põldmaa, L. Saag, I. Saar, A. Schüßler, J. A. Scott, C. Senés, M. E. Smith, A. Suija, D. L. Taylor, M. T. Telleria, M. Weiss, and K.-H. Larsson. 2013. Towards a unified paradigm for sequence-based identification of fungi. Molecular ecology 22:5271–7.

Kreutzer, K. 1995. Effects of forest liming on soil processes. Plant and Soil 168–169:447–470.

Kyaschenko, J., K. E. Clemmensen, A. Hagenbo, E. Karltun, and B. D. Lindahl. 2017. Shift in fungal communities and associated enzyme activities along an age gradient of managed Pinus sylvestris stands. The ISME Journal 11:863–874.

Lauber, C. L., M. Hamady, R. Knight, and N. Fierer. 2009. Pyrosequencing-Based Assessment of Soil pH as a Predictor of Soil Bacterial Community Structure at the Continental Scale. Applied and Environmental Microbiology 75:5111–5120.

Lee, J. Y., and B. K. Hwang. 2002. Diversity of antifungal actinomycetes in various vegetative soils of Korea. Canadian Journal of Microbiology 48:407–417.

Li, A., T. J. Fahey, T. E. Pawlowska, M. C. Fisk, and J. Burtis. 2015. Fine root decomposition, nutrient mobilization and fungal communities in a pine forest ecosystem. Soil Biology and Biochemistry 83:76–83.

Lindahl, B. D., and A. Tunlid. 2014. Ectomycorrhizal fungi - potential organic matter decomposers, yet not saprotrophs. New Phytologist 205:1443–1447.

Long, R. P., S. W. Bailey, S. B. Horsley, T. J. Hall, B. R. Swistock, and D. R. DeWalle. 2015. Long-Term Effects of Forest Liming on Soil, Soil Leachate, and Foliage Chemistry in Northern Pennsylvania. Soil Science Society of America Journal 79:1223–1236.

Lundström, U. S., D. C. Bain, A. F. S. Taylor, and P. A. W. van Hees. 2003. Effects of Acidification and its Mitigation with Lime and Wood Ash on Forest Soil Processes: A Review. Water, Air, and Soil Pollution: Focus 3:5–28.

Malik, A. A., J. Puissant, K. M. Buckeridge, T. Goodall, N. Jehmlich, S. Chowdhury, H. S. Gweon, J. M. Peyton, K. E. Mason, M. van Agtmaal, A. Blaud, I. M. Clark, J. Whitaker, R. F. Pywell, N. Ostle, G. Gleixner, and R. I. Griffiths. 2018. Land use driven change in soil pH affects microbial carbon cycling processes. Nature Communications 9:3591.

Mason, J. C., M. Richards, W. Zimmermann, and P. Broda. 1988. Identification of extracellular proteins from actinomycetes responsible for the solubilisation of lignocellulose. Applied Microbiology and Biotechnology 28:276–280.

McGuire, K. L., E. Bent, J. Borneman, A. Majumder, S. D. Allison, and K. K. Treseder. 2010. Functional diversity in resource use by fungi. Ecology 91:2324–2332.

McGuire, K. L., H. D'Angelo, F. Q. Brearley, S. M. Gedallovich, N. Babar, N. Yang, C. M. Gillikin, R. Gradoville, C. Bateman, B. L. Turner, P. Mansor, J. W. Leff, and N. Fierer. 2015. Responses of soil fungi to logging and oil palm agriculture in Southeast Asian tropical forests. Microbial ecology 69:733–47.

McMurdie, P. J., and S. Holmes. 2013. phyloseq: an R package for reproducible interactive analysis and graphics of microbiome census data. PloS one 8:e61217.

Melvin, A. M., J. W. Lichstein, and C. L. Goodale. 2013. Forest liming increases forest floor carbon and nitrogen stocks in a mixed hardwood forest. Ecological Applications 23:1962–1975.

Mouvenchery, Y. K., J. Kučerík, D. Diehl, and G. E. Schaumann. 2011. Cation-mediated cross-linking in natural organic matter: a review. Reviews in Environmental Science and Bio/Technology 11:41–54.

National Park Service 2015, October 31. Shenandoah National Park, Meadow Run Watershed Restoration Project. https://parkplanning.nps.gov/showFile.cfm?projectID=74048&MIMEType=application%252Fpdf&filename=SHEN%20civic%20engagement%20presentation%2Epdf&sfid=377534.

Nguyen, N. H., Z. Song, S. T. Bates, S. Branco, L. Tedersoo, J. Menke, J. S. Schilling, and P. G. Kennedy. 2016. FUNGuild: An open annotation tool for parsing fungal community datasets by ecological guild. Fungal Ecology 20:241–248.

Nilsson, S. I., S. Andersson, I. Valeur, T. Persson, J. Bergholm, and A. Wirén. 2001. Influence of dolomite lime on leaching and storage of C, N and S in a Spodosol under Norway spruce (Picea abies (L.) Karst.). Forest Ecology and Management 146:55–73.

Oksanen, J., R. Kindt, P. Legendre, B. OHara, and M. H. H. Stevens. 2007. vegan: Community Ecology Package. R package version 1.8-5 10:631–637.

Panke-Buisse, K., A. C. Poole, J. K. Goodrich, R. E. Ley, and J. Kao-Kniffin. 2015. Selection on soil microbiomes reveals reproducible impacts on plant function. The ISME Journal 9:980–989.

Paradelo, R., I. Virto, and C. Chenu. 2015. Net effect of liming on soil organic carbon stocks: A review. Agriculture, Ecosystems & Environment 202:98–107.

Park, B. B., R. D. Yanai, T. J. Fahey, S. W. Bailey, and T. G. Siccama. 2008. Fine Root Dynamics and Forest Production Across a Calcium Gradient in Northern Hardwood and Conifer Ecosystems - Springer. Ecosystems.

Persson, T., A. Rudebeck, and A. Wirén. 1995. Pools and Fluxes of Carbon and Nitrogen in 40-Year-Old Forest Liming Experiments in Southern Sweden. Water, Air and Soil Pollution 85:901–906.

Poulton, P. R., E. Pye, P. R. Hargreaves, and D. S. Jenkinson. 2003. Accumulation of carbon and nitrogen by old arable land reverting to woodland. Global Change Biology 9:942–955.

Pozzi, R., M. Simone, C. Mazzetti, S. Maffioli, P. Monciardini, L. Cavaletti, R. Bamonte, M. Sosio, and S. Donadio. 2019. The genus Actinoallomurus and some of its metabolites. The Journal of antibiotics 64:133–9.

Prentice, I. C., G. D. Farquhar, M. J. R. Fasham, M. L. Goulden, M. Heimann, V. J. Jaramillo, H. S. Kheshgi, C. LeQuéré, R. Scholes, and D. W. R. Wallace. 2001. The carbon cycle and atmospheric carbon dioxide.

Reid, C., and S. A. Watmough. 2014. Evaluating the effects of liming and wood-ash treatment on forest ecosystems through systematic meta-analysis. Canadian Journal of Forest Research 44:867–885.

Rineau, F., and J. Garbaye. 2009. Does forest liming impact the enzymatic profiles of ectomycorrhizal communities through specialized fungal symbionts? Mycorrhiza 19:493–500.

Rineau, F., J. P. Maurice, C. Nys, H Voiry, and J. Garbaye. 2010. Forest liming durably impact the communities of ectomycorrhizas and fungal epigeous fruiting bodies. Annals of Forest Science 67.

Ritchie, M. E., B. Phipson, D. Wu, Y. Hu, C. W. Law, W. Shi, and G. K. Smyth. 2015. limma powers differential expression analyses for RNA-sequencing and microarray studies. Nucleic Acids Research 43:e47–e47.

Roes-Hill, M. le, N. Khan, and S. G. Burton. 2011. Actinobacterial Peroxidases: an Unexplored Resource for Biocatalysis. Applied Biochemistry and Biotechnology 164:681–713.

Rousk, J., E. Bååth, P. C. Brookes, C. L. Lauber, C. Lozupone, J. G. Caporaso, R. Knight, and N. Fierer. 2010. Soil bacterial and fungal communities across a pH gradient in an arable soil. The ISME Journal 4:1340–1351.

Sait, M., K. E. R. Davis, and P. H. Janssen. 2006. Effect of pH on Isolation and Distribution of Members of Subdivision 1 of the Phylum Acidobacteria Occurring in Soil. Applied and Environmental Microbiology 72:1852–1857.

Saiya-Cork, K. R., R. L. Sinsabaugh, and D. R. Zak. 2002. The effects of long term nitrogen deposition on extracellular enzyme activity in an Acer saccharum forest soil. Soil Biology and Biochemistry 34:1309–1315.

Sakoda, S., K. Aisu, H. Imagami, and Y. Matsuda. 2019. Comparison of Actinomycete Community Composition on the Surface and Inside of Japanese Black Pine (Pinus thunbergii) Tree Roots Colonized by the Ectomycorrhizal Fungus Cenococcum geophilum. Microbial Ecology 77:370–379.

Schellenberger, S., S. Kolb, and H. L. Drake. 2009. Metabolic responses of novel cellulolytic and saccharolytic agricultural soil Bacteria to oxygen: Metabolic response of soil cellulose degraders. Environmental Microbiology 12:845–861.

Schimel, J. P., and S. M. Schaeffer. 2012. Microbial control over carbon cycling in soil. Frontiers in microbiology 3:348.

Schoeneberger, P. J., D. A. Wysocki, E. C. Benham, and S. S. Staff. 2012. Field book for describing and sampling soils, Version 3.0. Natural Resources Conservation Service, National Soil Survey Center, Lincoln, NE.

Sinsabaugh, R. L. 2010. Phenol oxidase, peroxidase and organic matter dynamics of soil. Soil Biology and Biochemistry 42:391–404.

Sinsabaugh, R. L., C. L. Lauber, M. N. Weintraub, B. Ahmed, S. D. Allison, C. Crenshaw, A. R. Contosta, D. Cusack, S. Frey, M. E. Gallo, T. B. Gartner, S. E. Hobbie, K. Holland, B. L. Keeler, J. S. Powers, M. Stursova, C. Takacs-Vesbach, M. P. Waldrop, M. D. Wallenstein, D. R. Zak, and L. H. Zeglin. 2008. Stoichiometry of soil enzyme activity at global scale: Stoichiometry of soil enzyme activity. Ecology Letters 11:1252–1264.

Smallidge, P. J., and D. J. Leopold. 1995. Watershed liming and pit and mound topography effects on seed banks in the Adirondacks, New York, USA. Forest Ecology and Management 72:273–285.

Srámek, V., V. Fadrhonsová, L. Vortelová, and B. Lomský. 2012. Development of chemical soil properties in the western Ore Mts. (Czech Republic) 10 years after liming. Journal of Forest Science 58:57–66.

Stark, S., A. Eskelinen, and M. K. Männistö. 2011. Regulation of Microbial Community Composition and Activity by Soil Nutrient Availability, Soil pH, and Herbivory in the Tundra. Ecosystems 15:18–33.

Talbot, J. M., S. D. Allison, and K. K. Treseder. 2008. Decomposers in disguise: mycorrhizal fungi as regulators of soil C dynamics in ecosystems under global change. Functional Ecology 22:955–963.

Tamura, T., Y. Ishida, Y. Nozawa, M. Otoguro, and K. Suzuki. 2009. Transfer of Actinomadura spadix Nonomura and Ohara 1971 to Actinoallomurus spadix gen.

nov., comb. nov., and description of Actinoallomurus amamiensis sp. nov., Actinoallomurus caesius sp. nov., Actinoallomurus coprocola sp. nov., Actinoallomurus fulvus sp. nov., Actinoallomurus iriomotensis sp. nov., Actinoallomurus luridus sp. nov., Actinoallomurus purpureus sp. nov. and Actinoallomurus yoronensis sp. nov. International journal of systematic and evolutionary microbiology 59:1867–74.

Taylor, A. F. S., and R. D. Finlay. 2003. Effects of Liming and Ash Application on Below Ground Ectomycorrhizal Community Structure in Two Norway Spruce Forests. Water, Air, and Soil Pollution: Focus 3:63–76.

Tedersoo, L., M. Bahram, S. Polme, S. Anslan, T. Riit, U. Kõljalg, R. H. Nilsson, F. Hildebrand, and K. Abarenkov. 2015. Global diversity and geography of soil fungi. Science 349:936–936.

Tripathi, B. M., J. C. Stegen, M. Kim, K. Dong, J. M. Adams, and Y. K. Lee. 2018. Soil pH mediates the balance between stochastic and deterministic assembly of bacteria. The ISME Journal 12:1072–1083.

US Forest Service 2011, July 1. Lower Williams Terrestrial Liming Project, Monongahela National Forest. https://www.fs.usda.gov/nfs/11558/www/nepa/42897_FSPLT2_054175.pdf.

Verastegui, Y., J. Cheng, K. Engel, D. Kolczynski, S. Mortimer, J. Lavigne, J. Montalibet, T. Romantsov, M. Hall, B. J. McConkey, D. R. Rose, J. J. Tomashek, B. R. Scott, T. C. Charles, and J. D. Neufeld. 2014. Multisubstrate Isotope Labeling and Metagenomic Analysis of Active Soil Bacterial Communities. mBio 5:e01157-14.

Voříšková, J., and P. Baldrian. 2013. Fungal community on decomposing leaf litter undergoes rapid successional changes. The ISME Journal 7:477–486.

Waldrop, M. P., and D. R. Zak. 2006. Response of Oxidative Enzyme Activities to Nitrogen Deposition Affects Soil Concentrations of Dissolved Organic Carbon. Ecosystems 9:921–933.

Wickham, H. 2009. ggplot2: Elegant Graphics for Data Analysis:216.

Wickham, H. 2011. The split-apply-combine strategy for data analysis. Journal of Statistical Software.

Wilhelm, R. C., E. Cardenas, K. R. Maas, H. Leung, L. McNeil, S. Berch, W. Chapman, G. Hope, J. M. Kranabetter, S. Dubé, M. Busse, R. Fleming, P. Hazlett, K. L. Webster, D. Morris, D. A. Scott, and W. W. Mohn. 2017. Biogeography and organic matter removal shape long-term effects of timber harvesting on forest soil microbial communities. The ISME Journal 11:2552–2568.

Wilhelm, R. C., R. Singh, L. D. Eltis, and W. W. Mohn. 2019. Bacterial contributions to delignification and lignocellulose degradation in forest soils with metagenomic and quantitative stable isotope probing. The ISME Journal 13:413–429.

Yavitt, J. B., T. J. Fahey, and J. A. Simmons. 1995. Methane and Carbon Dioxide Dynamics in a Northern Hardwood Ecosystem. Soil Science Society of America Journal 59:796–804.

Yin, Y.-R., P. Sang, W.-D. Xian, X. Li, J.-Y. Jiao, L. Liu, W. N. Hozzein, M. Xiao, and W.-J. Li. 2018. Expression and Characteristics of Two Glucose-Tolerant GH1 β-glucosidases From Actinomadura amylolytica YIM 77502T for Promoting Cellulose Degradation. Frontiers in Microbiology 9:3149.

Zhou, J., K. Xue, J. Xie, Y. Deng, L. Wu, X. Cheng, S. Fei, S. Deng, Z. He, J. D. V. Nostrand, and Y. Luo. 2011. Microbial mediation of carbon-cycle feedbacks to climate warming. Nature Climate Change 2:106–110.

Zhu, M.-J., F. Du, G.-Q. Zhang, and T.-B. H.-X. and N. Wang. 2013. Purification a laccase exhibiting dye decolorizing ability from an edible mushroom Russula virescens. International Biodeterioration & Biodegradation 82:33–39.

Žifčáková, L., T. Větrovský, V. Lombard, B. Henrissat, A. Howe, and P. Baldrian. 2017. Feed in summer, rest in winter: microbial carbon utilization in forest topsoil. Microbiome 5:122.

Zimmermann, W., and P. Broda. 1989. Utilization of lignocellulose from barley straw by actinomycetes. Applied Microbiology and Biotechnology 30:103–109.

CHAPTER 2

WATERSHED LIMING EXPERIMENTS REVEAL SHORT- AND LONG-TERM PH-DRIVEN CHANGES SOIL MICROBIAL COMMUNITY COMPOSITION AND CARBON CYCLING AFTER 2 AND 25 YEARS

Abstract

Soil pH is one of the best predictors of microbial community structure and function, and large-scale, long-term changes in soil pH resulting from anthropogenic activity are expected to significantly alter ecosystem functions. Here, we characterized the response of the microbial community in northern hardwood forest soils at two watershed-scale liming experiments conducted 2 years (short-term) and 25 years (long-term) earlier. Samples were collected post-liming at the long-term site and both pre- and post-liming at the short-term site, from the Oe and Oa soil horizons in both limed and control plots. Microbial structure was assayed with 16S rRNA gene and ITS region amplicon sequencing, together with measurements of microbial biomass and activity. Liming increased organic horizon pH by one unit at both the short- and long-term sites and reduced microbial biomass-specific respiration by 75% at the short-term site and 28% at the long-term site. In addition, liming was associated with significant accumulation of soil organic carbon, which doubled at the long-term site. Bacterial and fungal community composition changed significantly within two years after liming, and these shifts were amplified over the long-term. The majority of taxa (73%), whose relative abundance was either enhanced or suppressed in response to

liming at the long-term site had a similar response in the short-term. Liming reduced the abundance of dominant ectomycorrhizal fungi including *Amanita*, *Russula,* and *Cenococcum,* suggesting direct pH-driven negative responses. Long-term negative responses to liming were observed in actinomycetes related to *Actinomadura* spp., which taken together with the fungal responses at the long-term site, may have driven forest floor C accumulation. We show that liming can have both rapid and lasting pH-driven effects on microbial community structure, and that these changes are likely to alter community function with respect to the forest soil C cycle.

Introduction

Soil pH is often the principal variable determining the differences in microbial community composition based on observational surveys of bacterial and fungal communities from across the globe and continental gradients spanning multiple ecosystem (Fierer et al. 2012, Bartram et al. 2014, Tedersoo et al. 2015, Delgado-Baquerizo et al. 2018, Tripathi et al. 2018). This influence of soil pH appears to override major differences in other soil physicochemical properties, vegetation, and climate. Similarly, pH is commonly the best predictor of microbial community composition in studies of land use change, despite broad changes in soil properties, including the consequences of deforestation or nitrogen deposition (Fierer et al. 2012a, Crowther et al. 2014, McGuire et al. 2015). Soil pH can directly influence microbial community structure because pH has a direct impact on microbial growth rates, with each species having an optimal pH range. Alternatively, pH may be a variable that summarizes a suite of other variables, that in turn influence microbial community composition (Fierer and Jackson 2006). Experimental manipulations of pH can control for some of the variables that confound gradient studies like ecosystem state factors, including plant species composition or soil age. The direct effects of changing pH include altering the charge, reactivity, and types of bonds formed amongst organic and mineral molecules, nutrient availability, cation exchange capacity, metal toxicity, and other constraints on plant and microbial growth (Deng and Dixon 2018, Rasmussen et al. 2018). Over the long term, these direct changes can drive indirect changes in the microbial community composition through plant-soil feedbacks including changes in

plant species composition, litter chemistry, rooting depth, and belowground C allocation.

Experimental pH manipulations using liming agents have been conducted in temperate forest systems, many of which have a legacy of acid deposition resulting from industrial activities, especially during the 20th century in North America and Europe and early 21st century in east Asia (Vet et al. 2014). However, the effects of these pH manipulations on soil microbial communities, especially across time-scales, remain poorly described (Reid and Watmough 2014). Changes to critical microbially-mediated ecosystem functions like carbon (C) storage may only become apparent at longer time-scales (Schimel and Schaeffer 2012). In one such long-term forest experiment on naturally acidic Spodosols of the Adirondacks, NY, liming radically changed microbial community composition and resulted in large accumulations of forest floor C stocks (Melvin et al. 2013, Sridhar et al. Ch1). After 25 years, liming continues to reduce microbial respiration and extracellular enzyme activities associated with decomposition (Sridhar et al. Ch1). In particular, liming reduced oxidative enzyme activities, which correlated with the loss of dominant ectomycorrhizae (including *Russula* and *Cenococcum*), saprotrophs, wood decay fungi, and bacteria related to genus *Actinomadura* (Sridhar et al. Ch1). These changes in long-term microbial community composition corresponded with pH increase more so than Ca concentration, which also increases with liming (Sridhar et al. Ch1). Discerning the direct influence of pH on microbial communities *in situ* requires an experimental design that is able to distinguish immediate impacts of altering pH from those that might occur after ecosystem feedbacks affecting soil pH.

We studied the effects of raising pH on soil microbial communities at two watershed liming experiments roughly 40 km apart to identify short-term (2 year, Honnedaga Lake) and long-term (25 year, Woods Lake) responses. We assessed changes in microbial respiration and bacterial and fungal community composition at both sites. At Honnedaga Lake, the short-term site, we also measured pre-treatment microbial community composition to assess the impact of liming on microbial shifts against pre-existing differences. Liming raised the pH of forest floor horizons at both short- and long-term experimental sites by one unit on average. We hypothesized that if microbial community composition is largely governed by direct effects of pH on microbial physiology, then changes in microbial composition and activity would be apparent within two years. Alternatively, or in addition, if microbial community composition is governed by indirect pH pathways mediated by plant-soil feedbacks, then we expected to see the magnitude of responses in the microbial community increase over time. We expected that most of the microbial taxa would have a consistent directional response to increasing pH across these studies, and we highlighted such pH-sensitive taxa whose loss might explain reduced microbial activity and the accumulation of soil organic C at the long-term site. Our work contributes understanding to long-term ecological research and to identifying ecological and functional responses of pH-sensitive microbial communities in natural settings in relation to soil C-cycling.

Methods

Site Description and Field Sampling

The two sites in this study are located 38 km apart within the Adirondack Park in Herkimer County, NY (MAT 5.28, MAP 1230 mm) with similar climate, forest composition (mixed northern hardwoods), parent material (hornblende granitic gneiss), and soil order (Orthod Spodosols). At the short-term site, the liming experiment at Honnedaga Lake (43°31' N, 74°51' W), one 30 ha subcatchment was limed by helicopter application of 5 tons ha^{-1} of pelletized $CaCO_3$ (2 t Ca ha^{-1}) in October 2013 following leaf drop. One adjacent subcatchment was maintained as a control. The long-term liming site is located at Woods Lake (43°52' N, 74°57' W), where 6.89 tons of $CaCO_3$ ha^{-1} (2.76 t Ca ha^{-1}) were applied by helicopter to two ~50 ha subcatchments; two additional subcatchments were maintained as controls (Driscoll et al. 1996). At both sites the dominant tree species are American beech (*Fagus grandifolia*), red maple (*Acer rubrum*), and yellow birch (*Betula alleghaniensis*) with some red spruce (*Picea rubens*), sugar maple (*Acer saccharum*), and striped maple (*Acer pensylvanicum*) (Smallidge and Leopold 1995), red spruce being slightly more common at Honnedaga Lake. We hereby refer to Honnedaga Lake as the short-term site and Woods Lake as the long-term site.

At the short-term site, soils were collected immediately prior to liming (October 2013) and two years post liming (October 2015). At the long-term site, soil collection was conducted in August 2014, 25 years after liming. In each of the limed and control subcatchments at both sites, 4-5 composite 7 cm diameter soil cores, spanning two organic horizons, were taken from each of five plots. We first removed

the top litter layer then sampled to a depth of 10 cm, separating the underlying forest floor into upper, moderately decomposed (Oe; fermentation layer) and lower, highly decomposed plant material (Oa; humus layer) horizons based on field visual examination (Schoeneberger et al. 2012). This procedure yielded 160 samples (all post liming) from the long-term site and 200 samples (100 each pre and post liming) from the short-term site. Soils were collected in Ziplock bags and transported on ice back to Cornell University where they were kept at 4°C prior to sieving (4 mm) to remove coarse roots and stones, and immediately assayed for microbial biomass and respiration as described below. Subsamples were stored at -80°C for DNA extraction to assess microbial community composition.

Soil microbial biomass and activity

Soil pH was measured on a 1:1 soil to deionized water slurry following 10 min of equilibration using an Accumet basic AB15 pH meter with a flushable junction soil probe. Gravimetric moisture and water holding capacity were determined on 2 g field-moist subsamples for conversion to dry mass and to control for moisture in the following lab assays.

We assessed microbial respiration relative to the microbial biomass present in each sample as follows. Respiration was measured during a 60-day incubation with samples held at 60% water holding capacity and at 22°C (Bradford et al. 2008). Three grams dry weight soil was measured into 50 ml centrifuge tubes with caps modified to have airtight septum lids. The headspace of each centrifuge tube was flushed with CO_2–free air and incubated for 15 hours at ambient atmospheric pressure and at 22°C.

The concentration of headspace CO_2 was measured after the incubation period by extracting 2 ml from the headspace and analyzing with an infrared gas analyzer (LI-6200, LI-COR, Lincoln, Nebraska, USA). The CO_2 flux was then calculated both per gram dry weight soil per hour and per unit SIR microbial biomass (see below). This procedure was conducted on day 1 of the incubation and repeated on days 5, 10, 20, 30, 45, and 60. Specific CO_2 flux was interpolated between these days and summed to yield the cumulative C respired (CR_{mass}) over the entire 60 day assay by the microbial biomass in each sample.

Microbial biomass C was estimated using the substrate induced respiration (SIR) technique (Fierer et al. 2003). Another set of 50 ml centrifuge microcosms were prepared with 3 g of pre-incubated (at 22°C) dry weight soil. Four milliliters of autolysed yeast extract solution were added to tubes and shaken on a desktop shaker for 2 hours to allow the microbiological media substrate to penetrate the soil matrix and become biologically available. The headspace of each centrifuge tube was then flushed with CO_2-free air and incubated at atmospheric pressure and room temperature for 4 hours. Finally, maximum CO_2 flux was calculated by measuring the CO_2 headspace concentration as described above. Maximum CO_2 flux was converted into microbial biomass C (Anderson and Domsch 1978). Microbial biomass estimates were used to normalize cumulative respiration as described above.

Fungal and Bacterial sequencing

Total DNA was extracted from each soil sample using the 96 well PowerMag Microbiome RNA/DNA Isolation Kit using 0.3 g fresh soil (MO BIO Laboratories, Inc., Carlsbad, CA, USA). DNA quantification was performed with Picogreen as per the manufacturer's protocol (Thermo Fisher Scientific, Inc., Waltham, MA, USA). Amplicon libraries were prepared for the 16S rRNA gene (V4; 515F / 806R) and the internal transcribed spacer (ITS1; nBITSf / 58A2r; (Koechli et al. 2019)) regions. PCR was performed in triplicate using dual-indexed, custom barcoded libraries as described by Kozich et al. (2013). Amplicon libraries were pooled and normalized using SequalPrep Normalization Plates (Applied Biosystems, Norwalk, CT), and sequenced at the Cornell Life Sciences Sequencing Core using an Illumina MiSeq platform (V2; 2 x 250 bp).

Sequence Processing, Bioinformatics, and Statistical Analyses

Amplicon libraries were quality processed using QIIME2 (Bolyen et al. 2018) and assigned to amplicon sequence variants (ASVs) using DADA2 (Callahan et al. 2016). Substitutions and chimeric errors were removed from demultiplexed reads, and exact amplicon sequence variant (ASV) abundances were identified for each sample. Taxonomy was assigned using the RDP naïve Bayesian classifier, and genus-species were assigned using exact sequence matching as per Sridhar et al. (Ch1).

The effect of liming and the effect of sampling time were determined using mixed effects models (R package *lme4*) with plot and subcatchment as random effects and elemental variables, microbial biomass C, and CR_{mass} as fixed effects, which were

log transformed when necessary to address the assumption of normality. To compare short- vs. long-term microbial community responses to liming, we combined 16S and ITS libraries from Honnedaga Lake and Woods Lake. Indicator species analysis (R package *indicspecies*) was used to identify statistically significant responder ASVs, and linear modeling (R packages *limma*, *voom*, and *edgeR*) was used to identify the direction of response. ASVs that had a response ratio >10 were considered to be "strong" responders. False discovery rate adjustment was done using the Benjamini-Hochberg method. To test the effect of liming on community composition, we modeled Bray-Curtis distance matrices as a function of treatment, horizon, plot, and subcatchment using PERMANOVA in *vegan* (adonis) (Oksanen et al. 2007). Non-metric multidimensional scaling (NMDS) ordinations and diversity metrics were calculated using *phyloseq* (McMurdie and Holmes 2013). To assess whether the effect of liming was stronger at the short-term site or the long-term site in each horizon, we compared R statistics in an Analysis of Similarities (ANOSIM). FUNGuild was used to assign functional guilds based on fungal taxonomic classification (Nguyen et al. 2016). All ASV counts were normalized to counts per thousand reads, except for calculations of richness, where samples were rarefied to the smallest sample.

Results

Soil pH and microbial activity

Prior to liming forest floor pH did not differ between the control and limed subcatchments at the short-term (2-year) site ($P \geq 0.1$) (Figure 1A). After liming, pH increased by one unit on average across horizons with marked increases relative to

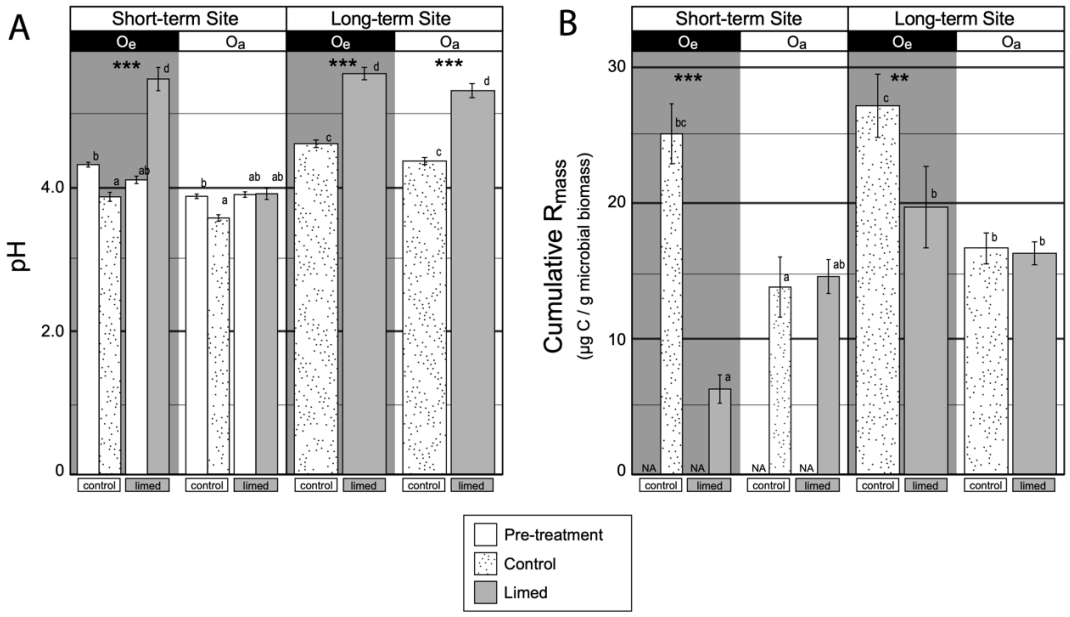

Figure 1 Mean ± SE (A) pH and (B) Cumulative biomass-specific respiration over 60 days from short-term site (pre-treatment and 2 years after liming) and long-term site (25 years after liming) summarized by horizon. Significant pairwise differences within time-scale and horizon groupings are denoted by lettering (Tukey HSD; '*' $P_{adj} \leq 0.05$, '**' $P_{adj} \leq 0.01$, '***' $P_{adj} \leq 0.001$).

control plots in the Oe horizon (3.9 to 5.5, $P < 0.0001$) and modest increases in the Oa horizon (3.6 to 3.9, $P = 0.011$) (Figure 1A). At the long-term (25-year) site, soil pH was also one unit higher in limed soils on average, although the response occurred more uniformly in both horizons (both $P < 0.0001$, Figure 1A). Extractable Ca concentration at the long-term site was approximately 3 times higher in limed soils than controls, primarily due to plant recycling of added Ca through detrital pathways (Sridhar et al. Ch1). Microbial biomass C at the short-term site was substantially larger in the limed Oe horizon relative to controls ($P < 0.0001$) (Figure S1), yet cumulative C respired by the microbial biomass (CR_{mass}) was 75% lower in limed plots ($P < 0.0001$) (Figure 1B). This pattern also occurred at the long-term site where CR_{mass} was 28% lower in limed Oe soils relative to controls ($P = 0.029$). Changes in microbial biomass and C mineralization were not observed in any of the Oa horizons, indicating that microbial biomass and respiration in this well decomposed organic horizon were insensitive to the modest increases in pH.

The effects of liming on microbial community composition and diversity

Prior treatment, spatial heterogeneity caused differences in microbial community composition between control and limed subcatchments at the short-term site (Table S1), but no pre-treatment differences in Shannon diversity were observed. At the short-term site, bacterial communities increased in Shannon diversity when sampled again after treatment in both the control and limed plots, indicating temporal heterogeneity ($P < 0.001$). In contrast, fungal Shannon diversity did not vary across sampling time points at the short-term site. Despite the spatial and temporal

heterogeneity, statistical models controlling for variation due to sampling time and pre-treatment community composition detected large and significant changes in community composition due to liming at the short-term site, as described in the paragraph below.

Liming caused an early and persistent restructuring of bacterial and fungal communities in the short- and long-term (Figure 2). At the short-term site, a significant proportion of variation in community composition was attributed to liming, while the effect of pH on microbial community composition was larger at the long-term site (Table S2). In the Oe horizon, differences in microbial community composition between limed and control soils were greater at the long-term site than at the short-term site for both fungi ($R_{ANOSIM} = 0.16$ vs. $R_{ANOSIM} = 0.75$) and bacteria ($R_{ANOSIM} = 0.07$ vs. $R_{ANOSIM} = 0.22$; Table S3). Liming-induced differences in community composition were absent in the Oa horizon at the short-term site but were well developed at the long-term site (Table S3). At the long-term site, limed communities were as different from control communities as Oe horizon communities were from Oa horizon (Table S2). However, no liming-induced differences in diversity (Shannon) for bacterial or fungal communities were observed at either site.

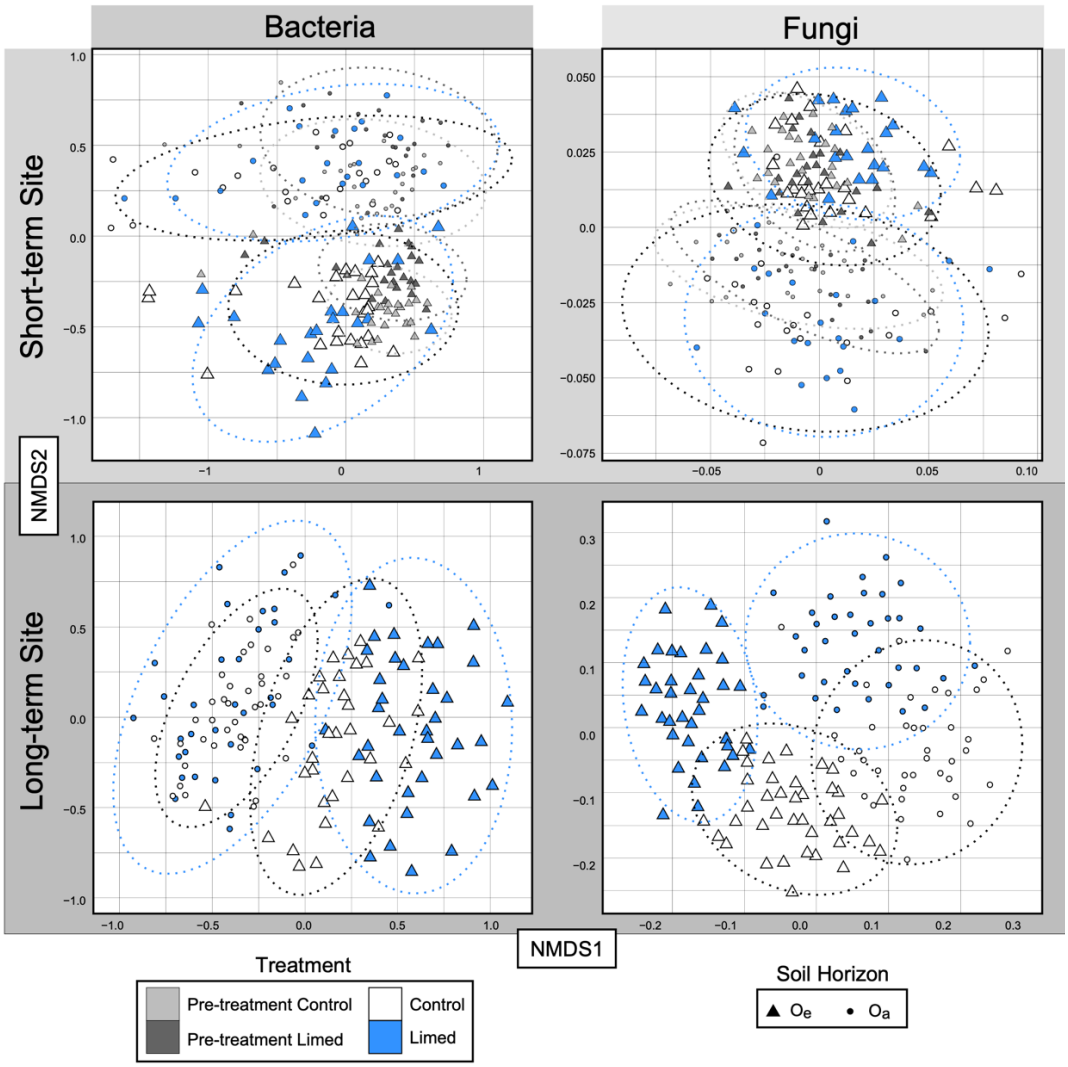

Figure 2 NMDS ordinations based on Bray-Curtis distances of bacterial and fungal composition in short-term (2 years after liming) and long-term (25 years after liming) sites. Ellipses represent 95% confidence that samples from the respective treatments fall within that region. Sample points are fractions coded by treatment and horizon, with pre-treatment samples in grey.

A total of 554 bacterial and 515 fungal ASVs were identified as significantly responding either positively or negatively to liming at both sites, based on their relative abundance in limed versus control soils (strong responders summarized in Table S4). Among bacteria, the responses to liming were often phylogenetically conserved (Figure 3). A higher proportion of all ASVs responded to liming at the short-term site (70%) than at the long-term site (30%), indicating that liming induces rapid changes in community composition (Figure 4A). However, while fewer ASVs responded at the long-term site, those that did responded much more strongly, suggesting enrichment over time (Figure 4B). Fewer ASVs responded to liming in the Oa horizon relative to the Oe horizon at both sites.

Short- vs. long-term ecological response by microbial community

Liming reduced the relative abundance of taxa associated with acidic environments, such as members of *Acidobacteria* and *WPS-2* in both the short- and long-term, indicating a direct pH effect (Figure S2). Of ASVs that responded strongly at the long-term site, 73% also responded similarly at the short-term site. Among these, ectomycorrhizal fungi (ECMF) were the most abundant and functionally important group to exhibit an immediate and sustained negative response to liming with previously dominant ASVs *Amanita*, *Russula*, and *Cenococcum* reduced in relative abundance (Figure 4C and Figure S3). As a phylum, *Ascomycota* responded negatively to liming in both the short- and long-term, particularly in the Oa horizon (Figure S4). Members of the *Rhizobiales* were generally favored by liming in the Oe horizon, particularly a single *Bradyrhizobium* phylotype at the long-term site, as well

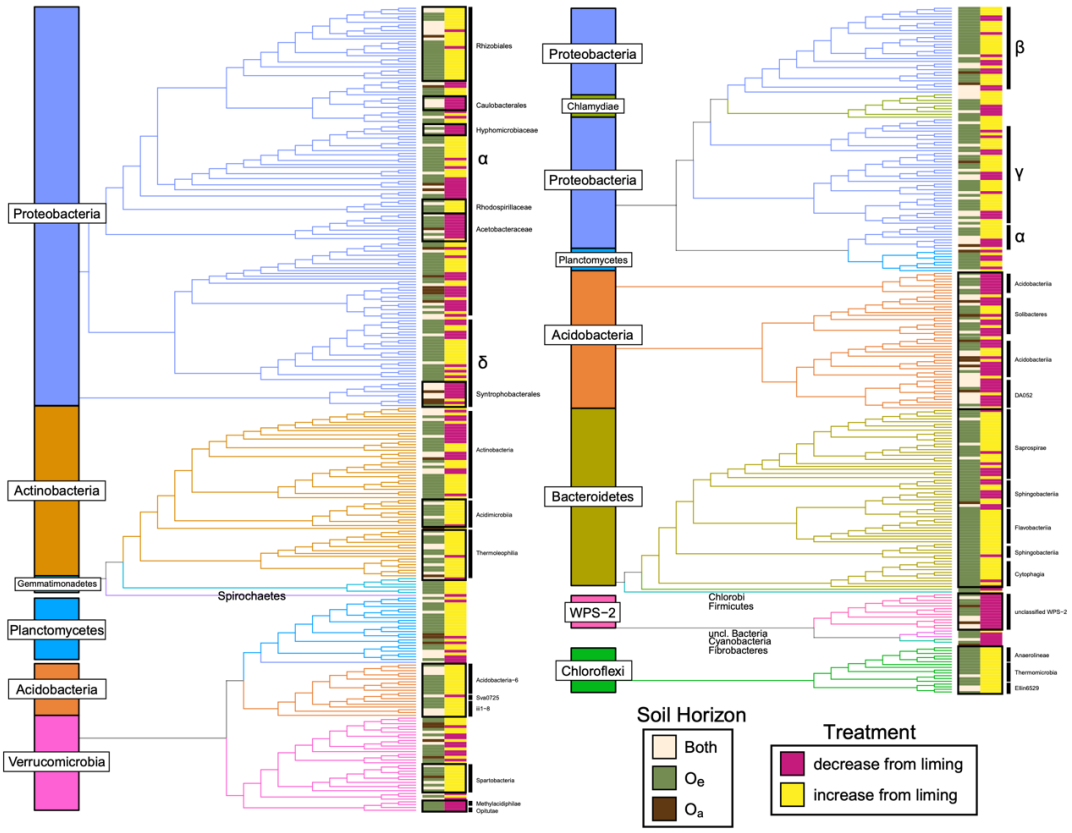

Figure 3 Phylogenetic distribution of bacterial responders to liming revealing clades that increased (yellow) or decreased (pink) in limed soils relative to controls across organic soil horizons.

as ASVs of *Labrys*, *Devosia*, and *Mesorhizobium* (Figure S5). Some members of *Bacteroidetes*, *Planctomycetes*, and *Proteobacteria* were favored by liming at the short- and long-term sites (Figure S6). While the most prevalent actinobacterial taxa (putative *Actinomadura* spp.; see below) decreased in relative abundance in limed soils over the long-term, certain other *Actinobacteria* were positively affected in the short- and long-term, namely *Micromonosporaceae*, *Streptosporangiaceae*, *Frankiaceae*, *Kineosporiaceae,* and *Nocardioidaceae*.

Transient responses of some fungi were also observed; for example, certain ECMF ASVs, like *Laccaria and Tuber* (Figure S3), and several members of *Sordariales* from well-known families of decomposers (*Lasiosphaeriaceae* and *Chaetomiaceae*) (Figure 4D) all benefitted from liming at the short-term site, but not at the long-term site. The greatest effect of liming on individual populations occurred only over the long-term, as populations of unclassified *Methylocystaceae* and *Actinomycetales*, were reduced from ~4% and ~20% of total sequences in control plots to ~1% and ~12% in limed soils, respectively (Figure 4EF). The closest documented relatives to the unclassified *Methylocystaceae* were mainly *Roseiarcus fermentans* (97-99% similar to type strain; NR_134158.1) and *Methylovirgula ligni* (100%; NR_044611.1), and for *Actinomycetales* the best matches were to *Actinoallomurus vinaceus* (96%; NR_113559.1) and *Actinomadura cellulosilytica* (95%; NR_136828.2). We hereby refer to these *Actinomycetales* ASVs as putative *Actinomadura*.

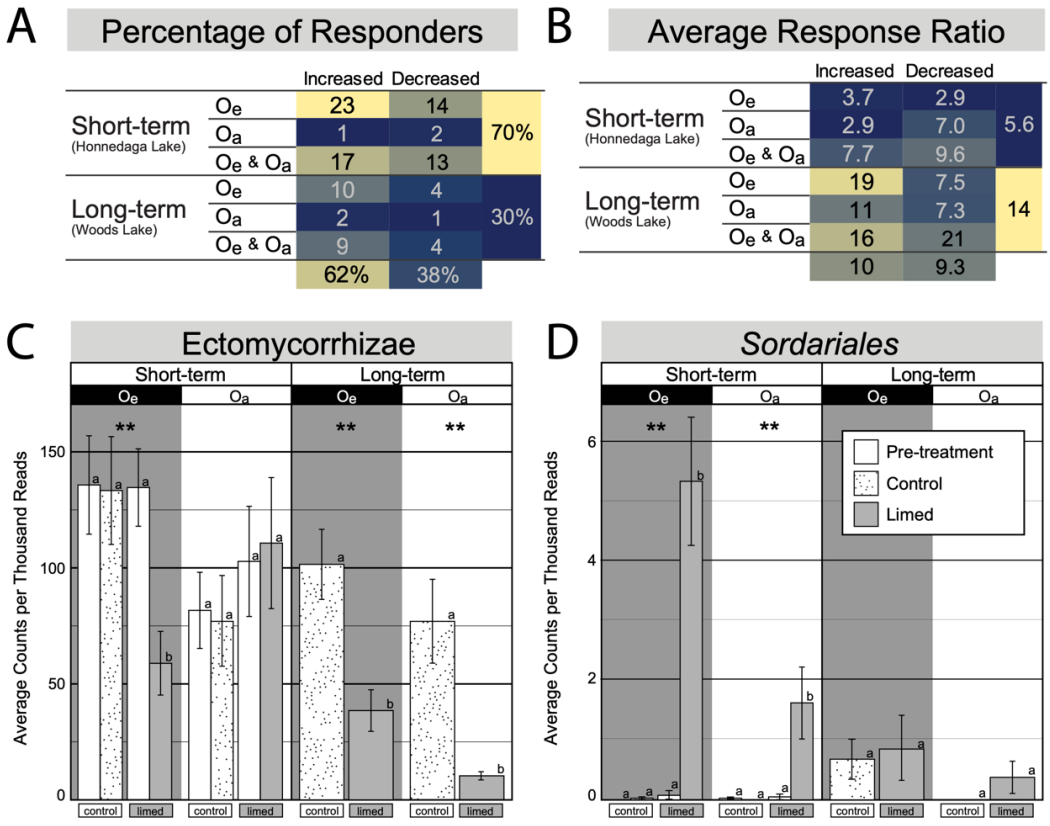

Figure 4 Summary of (A) the percentage of microbial responders to liming by horizon and site and (B) the magnitude of their response given by response ratio. (C) Ectomycorrhizal populations (classified as using FUNGuild) decreased with liming in both short-term (2 years) and long-term (25 years) sites, while others showed responses that were either transient (D) or took decades to manifest (E and F). Significant pairwise differences within time-scale and horizon groupings are denoted by lettering (Tukey HSD; '*' $P_{adj} \leq 0.05$, '**' $P_{adj} \leq 0.01$, '***' $P_{adj} \leq 0.001$).

Figure 4 (Continued)

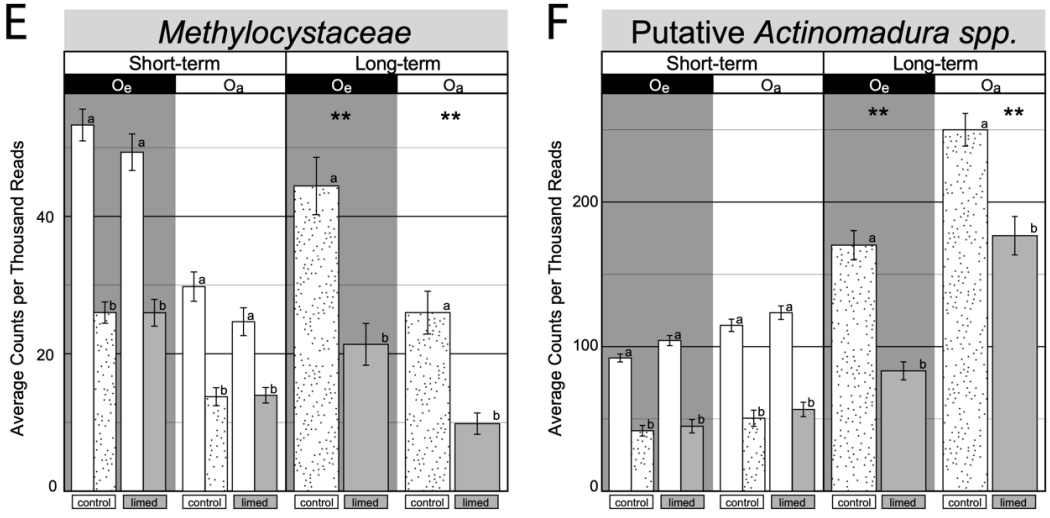

Discussion

Twenty-five years after liming at Woods Lake, soil C accumulation was associated with the loss of potentially important decomposers and marked shifts in bacterial and fungal communities, primarily driven by changes in pH (Sridhar et al. Ch1). These findings led us to question whether the microbial responses were due to a direct effect of pH or indirect plant-soil feedbacks to increasing pH that manifested over time. Here, we compared pre- and two years post-liming measurements at a short-term liming experiment to reveal similar microbial responses in many decomposer taxa seen at the long-term site. Major changes in microbial community composition and activity were apparent within two years after liming, supporting our hypothesis that microbial community composition is largely governed by the direct effects of pH on microbial physiology. Overall shifts in microbial community composition at the short-term site occurred in the limed Oe horizon, and no such shifts were observed in the Oa horizon where liming had only a limited impact on soil pH. In addition, we also demonstrated that the magnitude of microbial shifts and responses to liming increased over time, supporting the role of indirect pH effects. Evidence for this observation came from the larger aggregate shifts in microbial community composition and the 2.5-fold higher average response ratio of responder ASVs at the long-term site compared to the short-term site. The majority of taxa affected by liming at the long-term site had the same directional response at the short-term site. Bacterial and fungal populations that were affected either positively or negatively at the long-term site, like ectomycorrhizae, *Ascomycota*, *WPS-2*, certain members of *Rhizobiales*, *Bacteroidetes,* and *Protobacteria*, which exhibited a similar response at the short-term

site, indicated that they are likely governed by the direct effects of pH. In addition, we showed that in bacteria responses to changing pH are often phylogenetically conserved. However, a few important long-term responders, such as members of *Methylocystaceae* and *Actinomycetales*, did not respond in the short-term, indicating that they responded to ecosystem feedbacks of increasing pH rather than direct pH effects.

Here we also showed that limed microbial communities respire less C per gram microbial biomass in the short-term and long-term, though the effect was greater in the short-term, indicating a pulsed response of microbial activity (Figure 1). The increased pH in limed soils typically increases microbial biomass, and similar increases have been observed as soon as two years after liming in German forests (Bååth and Arnebrant 1994, Persson et al. 1995, Anderson 1998, Nilsson et al. 2001, Lundström et al. 2003). Contrary to our results, liming also typically increases microbial respiration in other liming studies (Lundström et al. 2003). However, the short- and long-term responses of microbial respiration in our study are concordant with other findings at the long-term site where lower rates of soil basal respiration and extracellular enzyme activities were observed, (Melvin et al. 2013, Sridhar et al. Ch1). This suggests that in the long run, a liming-induced restructuring of the community might exclude important decomposers in these naturally acidic Adirondack soils.

Liming produced pH-driven changes in several fungal groups that have ecosystem functions relating to C cycling**.** Guild-level long- and short-term effects were observed for ectomycorrhizal fungi, which can decompose organic matter while mining for nutrients (Lindahl and Tunlid 2014). *Russula* (*Basidiomycota*) is the most

abundant ectomycorrhizal fungal responder in these forest soils, and their reduction in the short-term parallels observations at the long-term site where a dominant *Russula* ASV was ~25 times less abundant in limed soils (Sridhar et al. Ch1). These reductions were strongly correlated with reductions in phenol oxidase and peroxidase enzyme activities (Sridhar et al. Ch1). Since *Russula* spp. are capable of producing cellulases and Mn peroxidases (Bödeker et al. 2009, Voříšková and Baldrian 2013, Kyaschenko et al. 2017), they are likely important degraders of persistent organic matter in these forests. Furthermore, the magnitude of change in the ectomycorrhizal genus *Cenococcum* at the short-term site was mirrored at the long-term site, where some *Cenococcum* ASVs were 32 times less abundant (Sridhar et al. Ch1). *Cenococcum* spp. are some of the most commonly encountered tree root symbionts, and members are capable of producing a wide range of lignocellulolytic enzymes (Peter et al. 2016). *Cenococcum* population reductions also correlated with decreases in phenol oxidase activity at the long-term site (Sridhar et al. Ch1). *Russula* and *Cenococcum* also decreased with liming in beech and Norway spruce forests in France, Germany, and Sweden (Agerer et al. 1998, Rineau and Garbaye 2009, Kjøller and Clemmensen 2009, Rineau et al. 2010). Changes in ectomycorrhizal host abundance likely did not explain these reductions in ECMF, since at the long-term site, the combined aboveground biomass of ECM tree species (*Betula*, *Fagus*, and *Picea*) was higher in limed plots relative to controls (Melvin et al. 2013). This observation, in combination with the short-term ectomycorrhizal fungal response reveals that pH directly impacts the prevalence of ectomycorrhizal fungi. While hosts can alter their C allocation to mycorrhizae in less than a year (Juice et al. 2006), we did not observe short-term

changes in ectomycorrhizal relative abundances in the Oa horizon after two years, and this suggests that these fungi respond directly to a change in pH rather than indirectly to changes in stand-scale belowground C allocation. The phylum-level fungal responses we observed at the short- and long-term sites appear to signal broad shifts in ecosystem function. The reduction in abundance of *Ascomycota,* whose members often dominate the utilization of plant biomass in the early stages of litter decomposition (Voříšková and Baldrian 2013, López-Mondéjar et al. 2018), could ultimately alter the fate of soil organic C in these forests.

Liming also produced pH-driven changes in several bacterial groups involved in soil C cycling. The putative *Actinomadura* spp. were among the strongest responders in the dataset. However, their negative response to liming did not develop in the short-term site, which suggests that pH affects their populations indirectly. Cultivated relatives *Actinoallomurus* and *Actinomadura* spp. are gram-positive and form branched mycelia (Pozzi et al. 2019). *Actinoallomurus,* known to associate with ectomycorrhizal roots, are a recently classified genus related to *Actinomadura* (Tamura et al. 2009, Sakoda et al. 2019). *Actinomadura* are capable of decomposing xylan, cellulose, and lignin, like many members of *Actinobacteria* (Mason et al. 1988, Zimmermann and Broda 1989, Holtz et al. 1991, Schellenberger et al. 2009, Verastegui et al. 2014, Yin et al. 2018). The abundance of these putative *Actinomadura* ASVs at the long-term site are positively correlated with oxidative enzyme activity (Sridhar et al. Ch1), further linking them to the fate of organic C in these forest soils. *Methylovirgula* spp., which are aerobic, acidophilic, gram-negative bacteria from family *Methylocystaceae* (Vorob'ev et al. 2009) and capable of

methylotrophy, were also strongly negatively impacted by liming in the long-term. More direct pH-driven changes were observed in members of *Bacteroidetes*, *Planctomycetes,* and *Deltaproteobacteria*, which responded positively to liming and are relatively more abundant in the Oe horizon. These ASVs were shown to be assimilators of xylan, lignin, and cellulose in stable isotope probing experiments (Eichorst and Kuske 2012, Wilhelm et al. 2019). We show that exact sequence matches for these ASVs were associated with cellulose and xylose degradation in data from a stable isotope probing experiment in soils from Chazy, NY (Koechli et al. in prep) (Figure S6). Taken together these results suggest a large-scale restructuring of the composition and function of the soil community in response to liming. The net effect on soil organic C stocks at the short-term site remains to be seen, though the loss of the important decomposers described above would predict a buildup of C stocks as was observed at the long-term site.

We expected species richness and diversity to increase after liming as the microbial community is released from the strong selective pressure of highly acidic conditions. However, liming-induced pH increases in this study did not boost richness or diversity as is commonly observed in pH gradient studies (Fierer and Jackson 2006, Lauber et al. 2009, Rousk et al. 2010, Tedersoo et al. 2015). Malik et al. (2018) found that acid stress-alleviation was observed when soils were limed past a threshold of pH 6.2, but when acidic soils were limed to below this threshold, stress protein indicators were higher in the limed soils. In this study, which falls into the latter category of pH change, the lack of response in diversity may be explained in part by a largely acid-adapted community being constrained by the increased pH.

The increased number of responder taxa two years after liming indicates that liming altered microbial community assembly. Acidic soils are characterized by deterministic (selective) processes of community assembly, at least for bacteria (Tripathi et al. 2018). With reduced acidity, stochastic processes could be resurgent, producing a larger number of positive responders to liming in the short term than in the long term. The transient positive response of *Sordariales*, which are saprobic coprophilous microfungi that thrive in alkaline environments (Huhndorf et al. 2004, Zhang et al. 2016), and *Laccaria*, which are pioneer ECMF following disturbance (Mason et al. 1983, Nara et al. 2003, Ishida et al. 2008), at the short-term site offers evidence of this.

Several taxa responding to liming in our study have previously been identified as strongly positively correlated with soil pH, including *Nitrospirae*, *Saprospirae*, *Flavobacteriia*, *Planctomycetales*, *Acidobacteria* grp. 6 (iii1-15), *Solirubrobacterales*, *Gaiellaceae*, *Methylibium*, *Steroidobacter*, *Sphingomonas*, and *Nocardioides* and negatively correlated with increasing pH like Candidatus *Solibacter* and *Actinomadura* (Zhalnina et al. 2014, Delgado-Baquerizo et al. 2018). This result suggests that these taxa have traits that cause them to favor acidic or alkaline soils. These pH tolerance traits might be phylogenetically conserved, like the phylum-wide negative responses of *WPS-2* to liming in our study. *WPS-2* is clearly associated with acidic environments like acid mine drainage, high latitude peatlands, and tundra ecosystems, which can be sphagnum dominated environments (Friedman et al. 2013, Gittel et al. 2014, Lipson et al. 2015, Holland-Moritz et al. 2018), and its response in this study reflects a selection pressure by pH that magnifies over time.

Our results from these pH manipulation experiments support the idea that soil pH is a master variable that structures microbial communities through direct constraints on microbial physiology, though ecosystem feedbacks to changing pH undoubtedly continue to influence and shape microbial community composition. In this study we assumed that calcium availability was not responsible for short-term responses because it was not an important factor explaining community variation at the long-term site (Sridhar et al. Ch1); however, further work is required to disentangle the pH effect of liming from the calcium effect on the microbial community and decomposability of soil organic carbon (Paradelo et al. 2015). Nonetheless, our study adds evidence that certain groups are highly sensitive to disturbances in pH, information which allows for a more trait-based understanding of soil bacterial and fungal communities. This may be critical to forecasting the ecological consequences of pH altering global change factors on carbon and nutrient cycling.

REFERENCES

Agerer, R., A. F. S. Taylor, and R. Treu. 1998. Effects of acid irrigation and liming on the production of fruit bodies by ectomycorrhizal fungi. Plant and Soil 199:83–89.

Anderson, J. P. E., and K. H. Domsch. 1978. A physiological method for the quantitative measurement of microbial biomass in soils. Soil Biology and Biochemistry 10:215–221.

Anderson, T.-H. 1998. The influence of acid irrigation and liming on the soil microbial biomass in a Norway spruce (Picea abies [L.] K.) stand. Plant and Soil 199:117–122.

Bååth, E., and K. Arnebrant. 1994. Growth-rate and response of bacterial communities to pH in limed and ash treated forest soils. Soil Biology and Biochemistry 26:995-1001.

Bartram, A. K., X. Jiang, M. D. J. Lynch, A. P. Masella, G. W. Nicol, J. Dushoff, and J. D. Neufeld. 2014. Exploring links between pH and bacterial community composition in soils from the Craibstone Experimental Farm. FEMS Microbiology Ecology 87:403–415.

Bödeker, I. T. M., C. M. R. Nygren, A. F. S. Taylor, Å. Olson, and B. D. Lindahl. 2009. ClassII peroxidase-encoding genes are present in a phylogenetically wide range of ectomycorrhizal fungi. The ISME Journal 3:1387–1395.

Bolyen, E., J. R. Rideout, M. R. Dillon, N. A. Bokulich, C. Abnet, G. A. Al-Ghalith, H. Alexander, E. J. Alm, M. Arumugam, F. Asnicar, Y. Bai, J. E. Bisanz, K. Bittinger, A. Brejnrod, C. J. Brislawn, C. T. Brown, B. J. Callahan, A. M. Caraballo-Rodríguez, J. Chase, E. Cope, R. D. Silva, P. C. Dorrestein, G. M. Douglas, D. M. Durall, C. Duvallet, C. F. Edwardson, M. Ernst, M. Estaki, J. Fouquier, J. M. Gauglitz, D. L. Gibson, A. Gonzalez, K. Gorlick, J. Guo, B. Hillmann, S. Holmes, H. Holste, C. Huttenhower, G. Huttley, S. Janssen, A. K. Jarmusch, L. Jiang, B. Kaehler, K. B. Kang, C. R. Keefe, P. Keim, S. T. Kelley, D. Knights, I. Koester, T. Kosciolek, J. Kreps, M. G. Langille, J. Lee, R. Ley, Y.-X. Liu, E. Loftfield, C. Lozupone, M. Maher, C. Marotz, B. D. Martin, D. McDonald, L. J. McIver, A. V. Melnik, J. L. Metcalf, S. C. Morgan, J. Morton, A. T. Naimey, J. A. Navas-Molina, L. F. Nothias, S. B. Orchanian, T. Pearson, S. L. Peoples, D. Petras, M. L. Preuss, E. Pruesse, L. B. Rasmussen, A. Rivers, M. S. R. II, P. Rosenthal, N. Segata, M. Shaffer, A. Shiffer, R. Sinha, S. J. Song, J. R. Spear, A. D. Swafford, L. R. Thompson, P. J. Torres, P. Trinh, A. Tripathi, P. J. Turnbaugh,

S. Ul-Hasan, J. J. van der Hooft, F. Vargas, Y. Vázquez-Baeza, E. Vogtmann, M. von Hippel, W. Walters, Y. Wan, M. Wang, J. Warren, K. C. Weber, C. H. Williamson, A. D. Willis, Z. Z. Xu, J. R. Zaneveld, Y. Zhang, Q. Zhu, R. Knight, and J. G. Caporaso. 2018. QIIME 2: Reproducible, interactive, scalable, and extensible microbiome data science. PeerJ Preprints 6:e27295v2.

Bradford, M. A., N. Fierer, and J. F. Reynolds. 2008. Soil carbon stocks in experimental mesocosms are dependent on the rate of labile carbon, nitrogen and phosphorus inputs to soils. Functional Ecology 22:964–974.

Callahan, B. J., P. J. McMurdie, M. J. Rosen, A. W. Han, A. J. A. Johnson, and S. P. Holmes. 2016. DADA2: High-resolution sample inference from Illumina amplicon data. Nature methods 13:581–3.

Crowther, T. W., D. S. Maynard, J. W. Leff, E. E. Oldfield, R. L. McCulley, N. Fierer, and M. A. Bradford. 2014. Predicting the responsiveness of soil biodiversity to deforestation: a cross-biome study. Global change biology 20:2983–94.

Delgado-Baquerizo, M., A. M. Oliverio, T. E. Brewer, A. Benavent-González, D. J. Eldridge, R. D. Bardgett, F. T. Maestre, B. K. Singh, and N. Fierer. 2018. A global atlas of the dominant bacteria found in soil. Science 359:320–325.

Deng, Y., and J. B. Dixon. 2018. Soil Organic Matter and Organic-Mineral Interactions. Pages 69–107 Soil Mineralogy with Environmental Applications. John Wiley & Sons, Ltd.

Driscoll, C. T., C. P. Cirmo, T. J. Fahey, V. L. Blette, P. A. Bukaveckas, D. A. Burns, C. P. Gubala, D. J. Leopold, R. M. Newton, D. J. Raynal, C. L. Schofield, J. B. Yavitt, and D. B. Porcella. 1996. The experimental watershed liming study: Comparison of lake and watershed neutralization strategies. Biogeochemistry 32:143–174.

Eichorst, S. A., and C. R. Kuske. 2012. Identification of cellulose-responsive bacterial and fungal communities in geographically and edaphically different soils by using stable isotope probing. Applied and environmental microbiology 78:2316–27.

Fierer, N., A. S. Allen, J. P. Schimel, and P. A. Holden. 2003. Controls on microbial CO2 production: a comparison of surface and subsurface soil horizons. Global Change Biology 9:1322–1332.

Fierer, N., and R. B. Jackson. 2006. The diversity and biogeography of soil bacterial communities. Proceedings of the National Academy of Sciences 103:626–631.

Fierer, N., C. L. Lauber, K. S. Ramirez, J. Zaneveld, M. A. Bradford, and R. Knight. 2012a. Comparative metagenomic, phylogenetic and physiological analyses of soil microbial communities across nitrogen gradients. The ISME journal 6:1007–17.

Fierer, N., J. W. Leff, B. J. Adams, U. N. Nielsen, S. T. Bates, C. L. Lauber, S. Owens, J. A. Gilbert, D. H. Wall, and J. G. Caporaso. 2012b. Cross-biome metagenomic analyses of soil microbial communities and their functional attributes. Proceedings of the National Academy of Sciences 109:21390–21395.

Friedman, E. S., K. E. Miller, D. A. Lipson, and L. T. Angenent. 2013. Potentiostatically Poised Electrodes Mimic Iron Oxide and Interact with Soil Microbial Communities to Alter the Biogeochemistry of Arctic Peat Soils. Minerals 3:318–336.

Gittel, A., J. Bárta, I. Kohoutová, J. Schnecker, B. Wild, P. Čapek, C. Kaiser, V. L. Torsvik, A. Richter, C. Schleper, and T. Urich. 2014. Site- and horizon-specific patterns of microbial community structure and enzyme activities in permafrost-affected soils of Greenland. Frontiers in Microbiology 5:541.

Holland-Moritz, H., J. Stuart, L. R. Lewis, S. Miller, M. C. Mack, S. F. McDaniel, and N. Fierer. 2018. Novel bacterial lineages associated with boreal moss species. Environmental Microbiology 20:2625–2638.

Holtz, C., H. Kaspari, and J.-H. Klemme. 1991. Production and properties of xylanases from thermophilic actinomycetes. Antonie van Leeuwenhoek 59:1–7.

Huhndorf, S. M., A. N. Miller, and F. A. Fernández. 2004. Molecular systematics of the Sordariales: the order and the family Lasiosphaeriaceae redefined. Mycologia 96:368–387.

Ishida, T. A., K. Nara, M. Tanaka, A. Kinoshita, and T. Hogetsu. 2008. Germination and infectivity of ectomycorrhizal fungal spores in relation to their ecological traits during primary succession. New Phytologist 180:491–500.

Juice, S. M., T. J. Fahey, T. G. Siccama, C. T. Driscoll, E. G. Denny, C. Eagar, N. L. Cleavitt, R. Minocha, and A. D. Richardson. 2006. Response of sugar maple to calcium addition to northern hardwood forest. Ecology 87:1267–1280.

Kjøller, R., and K. E. Clemmensen. 2009. Belowground ectomycorrhizal fungal communities respond to liming in three southern Swedish coniferous forest stands. Forest Ecology and Management 257:2217–2225.

Koechli, C., A. N. Campbell, C. Pepe-Ranney, and D. H. Buckley. 2019. Assessing fungal contributions to cellulose degradation in soil by using high-throughput stable isotope probing. Soil Biology and Biochemistry 130:150–158.

Kozich, J. J., S. L. Westcott, N. T. Baxter, S. K. Highlander, and P. D. Schloss. 2013. Development of a dual-index sequencing strategy and curation pipeline for analyzing amplicon sequence data on the MiSeq Illumina sequencing platform. Applied and environmental microbiology 79:5112–20.

Kyaschenko, J., K. E. Clemmensen, A. Hagenbo, E. Karltun, and B. D. Lindahl. 2017. Shift in fungal communities and associated enzyme activities along an age gradient of managed Pinus sylvestris stands. The ISME Journal 11:863–874.

Lauber, C. L., M. Hamady, R. Knight, and N. Fierer. 2009. Pyrosequencing-Based Assessment of Soil pH as a Predictor of Soil Bacterial Community Structure at the Continental Scale. Applied and Environmental Microbiology 75:5111–5120.

Lindahl, B. D., and A. Tunlid. 2014. Ectomycorrhizal fungi - potential organic matter decomposers, yet not saprotrophs. New Phytologist 205:1443–1447.

Lipson, D. A., T. K. Raab, M. Parker, S. T. Kelley, C. J. Brislawn, and J. Jansson. 2015. Changes in microbial communities along redox gradients in polygonized Arctic wet tundra soils. Environmental Microbiology Reports 7:649–657.

López-Mondéjar, R., V. Brabcová, M. Štursová, A. Davidová, J. Jansa, T. Cajthaml, and P. Baldrian. 2018. Decomposer food web in a deciduous forest shows high share of generalist microorganisms and importance of microbial biomass recycling. The ISME journal 12:1768–1778.

Lundström, U. S., D. C. Bain, A. F. S. Taylor, and P. A. W. van Hees. 2003. Effects of Acidification and its Mitigation with Lime and Wood Ash on Forest Soil Processes: A Review. Water, Air, and Soil Pollution: Focus 3:5–28.

Malik, A. A., J. Puissant, K. M. Buckeridge, T. Goodall, N. Jehmlich, S. Chowdhury, H. S. Gweon, J. M. Peyton, K. E. Mason, M. van Agtmaal, A. Blaud, I. M. Clark, J. Whitaker, R. F. Pywell, N. Ostle, G. Gleixner, and R. I. Griffiths. 2018. Land use driven change in soil pH affects microbial carbon cycling processes. Nature Communications 9:3591.

Mason, J. C., M. Richards, W. Zimmermann, and P. Broda. 1988. Identification of extracellular proteins from actinomycetes responsible for the solubilisation of lignocellulose. Applied Microbiology and Biotechnology 28:276–280.

Mason, P. A., J. Wilson, F. T. Last, and C. Walker. 1983. The concept of succession in relation to the spread of sheathing mycorrhizal fungi on inoculated tree seedlings growing in unsterile soils. Plant and Soil 71:247–256.

McGuire, K. L., H. D'Angelo, F. Q. Brearley, S. M. Gedallovich, N. Babar, N. Yang, C. M. Gillikin, R. Gradoville, C. Bateman, B. L. Turner, P. Mansor, J. W. Leff, and N. Fierer. 2015. Responses of soil fungi to logging and oil palm agriculture in Southeast Asian tropical forests. Microbial ecology 69:733–47.

McMurdie, P. J., and S. Holmes. 2013. phyloseq: an R package for reproducible interactive analysis and graphics of microbiome census data. PloS one 8:e61217.

Melvin, A. M., J. W. Lichstein, and C. L. Goodale. 2013. Forest liming increases forest floor carbon and nitrogen stocks in a mixed hardwood forest. Ecological Applications 23:1962–1975.

Nara, K., H. Nakaya, and T. Hogetsu. 2003. Ectomycorrhizal sporocarp succession and production during early primary succession on Mount Fuji. New Phytologist 158:193–206.

Nguyen, N. H., Z. Song, S. T. Bates, S. Branco, L. Tedersoo, J. Menke, J. S. Schilling, and P. G. Kennedy. 2016. FUNGuild: An open annotation tool for parsing fungal community datasets by ecological guild. Fungal Ecology 20:241–248.

Nilsson, S. I., S. Andersson, I. Valeur, T. Persson, J. Bergholm, and A. Wirén. 2001. Influence of dolomite lime on leaching and storage of C, N and S in a Spodosol under Norway spruce (Picea abies (L.) Karst.). Forest Ecology and Management 146:55–73.

Oksanen, J., R. Kindt, P. Legendre, B. OHara, and M. H. H. Stevens. 2007. vegan : Community Ecology Package. R package version 1.8-5 10:631–637.

Paradelo, R., I. Virto, and C. Chenu. 2015. Net effect of liming on soil organic carbon stocks: A review. Agriculture, Ecosystems & Environment 202:98–107.

Persson, T., A. Rudebeck, and A. Wirén. 1995. Pools and Fluxes of Carbon and Nitrogen in 40-Year-Old Forest Liming Experiments in Southern Sweden. Water, Air and Soil Pollution 85:901–906.

Peter, M., A. Kohler, R. A. Ohm, A. Kuo, J. Krützmann, E. Morin, M. Arend, K. W. Barry, M. Binder, C. Choi, A. Clum, A. Copeland, N. Grisel, S. Haridas, T. Kipfer, K. LaButti, E. Lindquist, A. Lipzen, R. Maire, B. Meier, S. Mihaltcheva, V. Molinier, C. Murat, S. Pöggeler, C. A. Quandt, C. Sperisen, A. Tritt, E. Tisserant, P. W. Crous, B. Henrissat, U. Nehls, S. Egli, J. W. Spatafora, I. V. Grigoriev, and F. M. Martin. 2016. Ectomycorrhizal ecology is imprinted in the genome of the dominant symbiotic fungus Cenococcum geophilum. Nature communications 7:12662.

Pozzi, R., M. Simone, C. Mazzetti, S. Maffioli, P. Monciardini, L. Cavaletti, R. Bamonte, M. Sosio, and S. Donadio. 2019. The genus Actinoallomurus and some of its metabolites. The Journal of antibiotics 64:133–9.

Rasmussen, C., K. Heckman, W. R. Wieder, M. Keiluweit, C. R. Lawrence, A. A. Berhe, J. C. Blankinship, S. E. Crow, J. L. Druhan, C. E. H. Pries, E. Marin-Spiotta, A. F. Plante, C. Schädel, J. P. Schimel, C. A. Sierra, A. Thompson, and R. Wagai. 2018. Beyond clay: towards an improved set of variables for predicting soil organic matter content. Biogeochemistry 137:297–306.

Reid, C., and S. A. Watmough. 2014. Evaluating the effects of liming and wood-ash treatment on forest ecosystems through systematic meta-analysis. Canadian Journal of Forest Research 44:867–885.

Rineau, F., and J. Garbaye. 2009. Does forest liming impact the enzymatic profiles of ectomycorrhizal communities through specialized fungal symbionts? Mycorrhiza 19:493–500.

Rineau, F., J. P. Maurice, C. Nys, H Voiry, and J. Garbaye. 2010. Forest liming durably impact the communities of ectomycorrhizas and fungal epigeous fruiting bodies. Annals of Forest Science 67.

Rousk, J., E. Bååth, P. C. Brookes, C. L. Lauber, C. Lozupone, J. G. Caporaso, R. Knight, and N. Fierer. 2010. Soil bacterial and fungal communities across a pH gradient in an arable soil. The ISME Journal 4:1340–1351.

Sakoda, S., K. Aisu, H. Imagami, and Y. Matsuda. 2019. Comparison of Actinomycete Community Composition on the Surface and Inside of Japanese Black Pine (Pinus thunbergii) Tree Roots Colonized by the Ectomycorrhizal Fungus Cenococcum geophilum. Microbial Ecology 77:370–379.

Schellenberger, S., S. Kolb, and H. L. Drake. 2009. Metabolic responses of novel cellulolytic and saccharolytic agricultural soil Bacteria to oxygen: Metabolic response of soil cellulose degraders. Environmental Microbiology 12:845–861.

Schimel, J. P., and S. M. Schaeffer. 2012. Microbial control over carbon cycling in soil. Frontiers in microbiology 3:348.

Schoeneberger, P. J., D. A. Wysocki, E. C. Benham, and S. S. Staff. 2012. Field book for describing and sampling soils, Version 3.0. Natural Resources Conservation Service, National Soil Survey Center, Lincoln, NE.

Smallidge, P. J., and D. J. Leopold. 1995. Watershed liming and pit and mound topography effects on seed banks in the Adirondacks, New York, USA. Forest Ecology and Management 72:273–285.

Tamura, T., Y. Ishida, Y. Nozawa, M. Otoguro, and K. Suzuki. 2009. Transfer of Actinomadura spadix Nonomura and Ohara 1971 to Actinoallomurus spadix gen. nov., comb. nov., and description of Actinoallomurus amamiensis sp. nov., Actinoallomurus caesius sp. nov., Actinoallomurus coprocola sp. nov., Actinoallomurus fulvus sp. nov., Actinoallomurus iriomotensis sp. nov., Actinoallomurus luridus sp. nov., Actinoallomurus purpureus sp. nov. and Actinoallomurus yoronensis sp. nov. International journal of systematic and evolutionary microbiology 59:1867–74.

Tedersoo, L., M. Bahram, S. Polme, S. Anslan, T. Riit, U. Koljalg, R. H. Nilsson, F. Hildebrand, and K. Abarenkov. 2015. Global diversity and geography of soil fungi. Science 349:936–936.

Tripathi, B. M., J. C. Stegen, M. Kim, K. Dong, J. M. Adams, and Y. K. Lee. 2018. Soil pH mediates the balance between stochastic and deterministic assembly of bacteria. The ISME Journal 12:1072–1083.

Verastegui, Y., J. Cheng, K. Engel, D. Kolczynski, S. Mortimer, J. Lavigne, J. Montalibet, T. Romantsov, M. Hall, B. J. McConkey, D. R. Rose, J. J. Tomashek, B. R. Scott, T. C. Charles, and J. D. Neufeld. 2014. Multisubstrate Isotope Labeling and Metagenomic Analysis of Active Soil Bacterial Communities. mBio 5:e01157-14.

Vet, R., R. S. Artz, S. Carou, M. Shaw, C.-U. Ro, W. Aas, A. Baker, V. C. Bowersox, F. Dentener, C. Galy-Lacaux, A. Hou, J. J. Pienaar, R. Gillett, M. C. Forti, S. Gromov, H. Hara, T. Khodzher, N. M. Mahowald, S. Nickovic, P. S. P. Rao, and N. W. Reid. 2014. A global assessment of precipitation chemistry and deposition of sulfur, nitrogen, sea salt, base cations, organic acids, acidity and pH, and phosphorus. Atmospheric Environment 93:3–100.

Voříšková, J., and P. Baldrian. 2013. Fungal community on decomposing leaf litter undergoes rapid successional changes. The ISME Journal 7:477–486.

Vorob'ev, A. V., W. de Boer, L. B. Folman, P. L. E. Bodelier, N. V. Doronina, N. E. Suzina, Y. A. Trotsenko, and S. N. Dedysh. 2009. Methylovirgula ligni gen. nov., sp. nov., an obligately acidophilic, facultatively methylotrophic bacterium with a highly divergent mxaF gene. International Journal of Systematic and Evolutionary Microbiology 59:2538–2545.

Wilhelm, R. C., R. Singh, L. D. Eltis, and W. W. Mohn. 2019. Bacterial contributions to delignification and lignocellulose degradation in forest soils with metagenomic and quantitative stable isotope probing. The ISME Journal 13:413–429.

Yin, Y.-R., P. Sang, W.-D. Xian, X. Li, J.-Y. Jiao, L. Liu, W. N. Hozzein, M. Xiao, and W.-J. Li. 2018. Expression and Characteristics of Two Glucose-Tolerant GH1 β-glucosidases From Actinomadura amylolytica YIM 77502T for Promoting Cellulose Degradation. Frontiers in Microbiology 9:3149.

Zhalnina, K., R. Dias, P. D. de Quadros, A. Davis-Richardson, F. A. O. Camargo, I. M. Clark, S. P. McGrath, P. R. Hirsch, and E. W. Triplett. 2014. Soil pH Determines Microbial Diversity and Composition in the Park Grass Experiment. Microbial Ecology 69:395–406.

Zhang, T., N.-F. Wang, H.-Y. Liu, Y.-Q. Zhang, and L.-Y. Yu. 2016. Soil pH is a Key Determinant of Soil Fungal Community Composition in the Ny-Ålesund Region, Svalbard (High Arctic). Frontiers in Microbiology 7:227.

Zimmermann, W., and P. Broda. 1989. Utilization of lignocellulose from barley straw by actinomycetes. Applied Microbiology and Biotechnology 30:103–109.

CHAPTER 3

DNA STABLE ISOTOPE PROBING REVEALS THAT FOREST LIMING ALTERS LEAF LITTER CARBON ASSIMILATION BY SOIL BACTERIAL AND FUNGAL COMMUNITIES

Abstract

Liming of northern hardwood forest soils can alter microbial community composition and C cycling, however the mechanistic link between changes in structure and decomposer function that lead to soil C sequestration is unclear. We tracked the flow of leaf ^{13}C into bacterial and fungal communities in limed and control soils from Woods Lake, NY, where liming doubled organic horizon C stocks after 20 years. We hypothesized that microbial ^{13}C assimilation would differ between limed and control soil microbial communities, consistent with field observations of microbial community shifts from an earlier study. We addressed this hypothesis using Multiple Window High Resolution DNA stable isotope probing (MW-HR-SIP) with ^{13}C labeled oak leaves in soil microcosms. Liming significantly altered bacterial and fungal communities that actively assimilated leaf litter C, with ≤ 20% overlap between the leaf incorporator ASVs in limed and control soils. In limed soils, the number of bacterial ASVs that incorporated ^{13}C into their DNA was 4-fold higher and amplified over 40 days, while the number of fungal ^{13}C incorporators increased to a lesser extent and only during the initial stages of incubation. We validated the ecosystem relevance of our microcosm experiment by assessing whether these C assimilating microbial

groups were present in the field and if their directional response to liming matched. We identified several such groups of prominent (>13% relative abundance), phylogenetically related ^{13}C incorporators, many of which were negatively impacted by liming, including fungal phylogroups belonging to *Ascomycota*, and bacterial phylogroups belonging to *Actinobacteria* and *Proteobacteria*. We show that liming has fundamentally altered how the microbial community metabolizes litter C, thus linking changes in structure to changes in function.

Introduction

The pool of carbon (C) stored in forest soils represents the balance between plant production and microbial decomposition, and augmenting this terrestrial reservoir has the potential to help mitigate climate change. Decomposition in forest soils is carried out by a wide range of microorganisms, however the vast majority of soil organic matter decomposers remain uncultured and their physiology and ecology uncharacterized. In particular, it is uncertain how decomposer community structure and function respond to changes in fundamental characteristics of forest soil, such as pH. Furthermore, forest soils across Europe and eastern North America incurred acidification through decades of anthropogenic air pollution and several managed forests have been limed to counteract this acidification (Lundström et al. 2003, Reid and Watmough 2014). The addition of liming agents like calcium carbonate to forest soils has been shown to alter microbial community composition and carbon (C) cycling, in some cases leading to accumulation of C stocks in organic horizons over the long term (Derome 1990, Bååth et al. 1995, Melvin et al. 2013), while in other cases to decreases (Lundström et al. 2003).

In an experimental watershed liming study at Woods Lake, NY, a dose of 6.9 tons ha^{-1} of limestone added to a northern mixed hardwood forest watershed doubled C stocks in the forest floor 20 years later (Driscoll et al. 1996, Melvin et al. 2013). This C accumulation in limed soils probably resulted primarily from suppressed microbial mineralization of organic matter, as no differences were observed in plant litter inputs (Melvin et al. 2013). Limed forest floor soils increased in pH (by one unit to 5.5), had lower extracellular enzyme activity, and their fungal and bacterial communities

differed relative to un-limed control soils (Sridhar et al. Ch1). Liming suppressed dominant ectomycorrhizae, wood saprotrophs, and bacteria related to genus *Actinomadura*, whose change in abundance corresponded with decreased activity of oxidative enzymes central to lignocellulose degradation (Sridhar et al. Ch1). These results demonstrate that liming altered microbial community structure and function resulting in an increase in soil carbon stocks, though these responses were correlative and the mechanism for this increase remains unclear.

Altering microbial community structure can have quantitative impacts on the decomposition of plant detritus, C mineralization, and soil C sequestration, as demonstrated in reciprocal transplant or selective inoculation experiments (Schimel 1995, Strickland et al. 2009, Wagg et al. 2014). By altering the microbial community, liming may regulate the processing of SOM and lead to C accumulation through a variety of mechanisms that are not mutually exclusive. On one hand, pH could directly constrain microbial growth and define the environmental niche of microbial groups involved in C cycling, which could alter the turnover of SOM. For example, increasing pH can favor bacterial growth over fungal growth or increase microbial turnover rates as physiological stress from soil acidity is relaxed (Rousk et al. 2009, Malik et al. 2018). Carbon can accumulate over the long term if this larger pool of microbial necromass is stabilized through aggregation or mineral interactions that inhibit its recycling (Cotrufo et al. 2013, Geyer et al. 2016). On the other hand, liming may have induced constraints on C mineralization by suppressing microbial guilds involved in litter degradation or by disrupting plant-microbe interactions.

Microbial community composition changes during litter decomposition as components of plant biomass (hemicellulose, cellulose and lignin) are degraded at different stages (Snajdr et al. 2010). Fungi are thought to carry out the majority share of litter degradation, producing extracellular enzymes that breakdown persistent plant polymers in litter. This is evidenced by the fungal share of hydrolase proteins and transcription of lignocellulolytic enzymes in litter (Schneider et al. 2012, Žifčáková et al. 2017). *Ascomycota* dominate early in decomposition, but they gradually give way to saprotrophic *Basidiomycota* that specialize in producing ligninolytic enzymes later in decomposition (Sethuraman et al. 1998, Baldrian 2008, Voříšková and Baldrian 2013, Purahong et al. 2016). Bacteria also contribute significantly to litter decomposition, composing 30% of microbial transcripts in litter, and exhibit the ability to assimilate carbon from hemicellulose, cellulose, and lignin into their biomass (Štursová et al. 2012, López-Mondéjar et al. 2016, Žifčáková et al. 2017, Wilhelm et al. 2019). Bacterial colonization of litter increases through recruitment from soil bacterial populations, leading to growth in litter bacterial biomass over time (Voříšková and Baldrian 2013, Tláskal et al. 2016, Baldrian 2017). Several major phyla, including *Proteobacteria*, *Actinobacteria*, *Bacteroidetes*, and *Acidobacteria* are common during litter decomposition, with the relative abundance of certain *Actinobacteria* like *Streptomyces* increasing over time (Snajdr et al. 2010, Tláskal et al. 2016, Purahong et al. 2016). Suppression of members of the microbial community involved in particular stages of litter degradation could lead to changes in the fate of soil C.

Plant-microbe interactions could also be disrupted by liming, which can increase the availability of nutrients like N and P to plants, altering their relationship with mycorrhizal fungi (Groffman and Fisk 2011, Carrino-Kyker et al. 2016). In previous work at this and other sites, liming negatively impacted the abundance and activity of certain ectomycorrhizal (ECM) fungi like *Russula* or *Cenococcum* spp., which could cause a reduction in decomposition rates (Sridhar et al. Ch1, Rineau and Garbaye 2009, Kjøller and Clemmensen 2009, Rineau et al. 2010, Lindahl and Tunlid 2014).

While the various microbial mechanisms by which liming alters decomposition are difficult to disentangle, tracking the fate of plant C through microbial food webs is one way to test whether C is being processed differently by microbial communities in limed soils. Such food web mapping can provide insight into the mechanisms underlying the accumulation of forest floor C stocks at Woods Lake. Nucleic acid stable isotope probing (SIP), where soil microbes are allowed to incorporate isotopically labeled substrates into their biomass, enables the tracking of the metabolic activity of microbes in environmentally relevant settings (Pepe-Ranney et al. 2016, Barnett et al. 2019, Koechli et al. 2019). When coupled with advances in high throughput sequencing (HTS), SIP has the potential to link thousands of microbial taxa to their metabolic activity. Advances in statistical methods to support inference on large HTS-SIP datasets have increased the sensitivity and specificity of detecting the enrichment of metabolically active taxa (Pepe-Ranney et al. 2016, Youngblut et al. 2018, Barnett et al. 2019). SIP has illuminated the flow of C through soil bacterial and fungal communities, allowing the identification of taxa associated with the

assimilation of specific litter-analogous purified substrates like hemicellulose, cellulose, and lignin (Šturšová et al. 2012, Leung et al. 2015, Pepe-Ranney et al. 2016, Koechli et al. 2019, Wilhelm et al. 2019). However, SIP experiments that use more complex substrates have the potential to access a larger proportion of the metabolically active microbial community. For example, Kramer et al. (2016) found when using a range of substrates from glucose to plant biomass, that increasing substrate complexity increased successional labeling of the microbial food web.

We conducted a SIP experiment to track the flow of leaf litter C through microbial communities of limed and control soils, to determine whether liming changed microbial assimilation of litter C, and to identify differences in community function with respect to liming. We used oak leaves, an ecologically relevant source of C in temperate forest soils, tracking ^{13}C from labeled leaves into bacterial and fungal DNA to identify which microbes actively assimilated added C. Lab microcosms with soil from limed and control subcatchments from two organic horizons (Oe and Oa) were incubated with ^{13}C labeled- or ^{12}C control- oak leaves, and were sampled after 15 and 40 days to capture the metabolically active bacterial and fungal community over time. In addition, we validated the ecosystem-level relevance of our findings, by tracking the response of those microbial taxa that assimilated C in the DNA-SIP experiment, in the field.

Methods

Site description and soil sampling

The Experimental Watershed Liming Study at Woods Lake was initiated by Driscoll et al in 1989. Woods Lake is located in the Adirondack Park, Herkimer County, NY, USA (43°52' N, 74°57' W). Its forested watershed consists of northern mixed hardwood forests, dominated by American beech, red maple, and yellow birch and soils are predominantly Typic Haplorthords derived from glacial till. To replenish acid-deposition induced loss of base cations, $CaCO_3$ was applied at the rate of 6.9 tons ha^{-1} to two 50 ha subcatchments, with two adjacent subcatchments maintained as references (see for details: Sridhar et al. Ch 1, Driscoll et al. 1996, Melvin et al. 2013). Liming immediately increased soil pH from 3.7 to 4.4 on average in the organic horizons (Blette and Newton 1996). The site was revisited in 2010, and ecosystem measures of C and N cycling were measured by Melvin et al. (2013). Notably, by this time large differences in soil Ca reflect higher calcium concentrations in plant litter as any residual added lime is now deep in the soil (R. Newton, personal communication). In 2014 samples were collected from the same plots from the Melvin et al. (2013) study to assess microbial function and community composition (microbial biomass, C mineralization, pH, elemental analysis, 16S rRNA gene and ITS1 sequencing) (Sridhar et al. Ch 1).

For this study, fresh soils were collected in November 2016 from plots within one set of limed and control subcatchments. A composite sample of four O horizon (>20-30% SOC) cores in each plot was collected with a tulip bulb corer 10 cm past the top (Oi) layer and separated into upper (Oe) and lower (Oa) organic horizons by field examination (Schoeneberger et al. 2012). This yielded four samples (Limed Oe, Limed Oa, Control Oe, Control Oa) that were transported back to Cornell University on ice and stored at 4°C. Following this moisture content was determined, and soils were sieved to 4 mm.

Microcosm experiment

A microcosm experiment was set up as per (Pepe-Ranney et al. 2016, Koechli et al. 2019) and oak leaves were added as the C substrate. Briefly, microcosms were prepared by adding 10 g dry weight (d.w.) sieved soil to 250 ml Erlenmeyer flasks. Microcosms were then pre-incubated for 2 weeks until CO_2 flux stabilized and were maintained at 60% water holding capacity by weight at room temperature without exposure to light throughout the experiment. To simulate leaf litter inputs in natural systems, we added *Quercus robur* leaves to the top of soils in microcosms, in C concentrations reflecting fresh C in soil during the early stages of decomposition. Leaves were freeze-dried and either unlabeled or >97 atom%-enriched and uniformly labeled with ^{13}C (U-64001, IsoLife, Wageningen, Netherlands). We added 6 mg leaf mass or ~3 mg C g soil $^{-1}$ d.w. (i.e. assuming 50% C in litter), an amount high enough to ensure detection, but low enough to discourage waste respiration from excess C

(Schneckenberger et al. 2008). Whole leaves were shredded to between 2 mm to 4 mm to simulate litter fragmentation and facilitate substrate solubilization and colonization by microbial decomposers.

Microcosm flasks were capped with butyl rubber stoppers and headspace CO_2 was sampled at 12 time points, including prior to and during the experiment via GCMS (Shimadzu GCMS-QP2010). Flasks were briefly vented after each measurement. After 15 and 40 days, microcosms were destructively harvested to capture the temporal dynamics of C incorporation. SIP was conducted on 16 microcosms with one replicate per combination of subcatchment (C, L), horizon (Oe, Oa), C isotope (^{12}C, ^{13}C), and time point (15 days, 40 days). Respiration was measured on these 16 representative samples. Respiration was also measured on an additional set of 16 samples from the second pair of limed and control subcatchments of Woods Lake that were collected, processed and incubated in the same manner. Substrate control microcosms, which consisted of ^{12}C and ^{13}C leaf fragments only (i.e. no soil), were also maintained and sequenced alongside sample microcosms to identify and account for the native microbial community present on the oak leaves.

DNA extraction and centrifugation

DNA was extracted from 2 g soil per sample using the 96-well DNeasy PowerSoil Kit (Qiagen, Hilden, Germany) as per the manufacturer's protocol and using multiple extractions until 2-5 μg DNA was available from each of the 16 microcosm samples. DNA was quantified with Quant-iT PicoGreen fluorescent dye using a λ DNA standard curve according to the manufacturer's protocol (Thermo

Fischer Scientific, Waltham, MA). Cesium chloride gradient formation and fractionation was conducted as previously described with minor modifications (Pepe-Ranney et al. 2016, Koechli et al. 2019). Briefly 1.945 μg DNA was added to a 4.7 ml CsCl gradient of 1.69 g ml^{-1} average density (1.68 g ml^{-1} CsCl in 0.15mM Tris-HCl, 15mM EDTA, and 15mM KCl) and spun at 55,000 x g for 66 hrs at 20°C. After centrifugation, 30 fractions of 100 μl were collected by displacement using a syringe pump. Fraction buoyant density was determined using a Reichert AR200 handheld digital refractometer. DNA was desalted by superparamagnetic bead purification and resuspended in 50 μL TE. Fractions between 1.7 g ml^{-1} and 1.77 g ml^{-1} were retained to be used in multiple window high resolution SIP (MW-HR-SIP) analysis (Youngblut et al. 2018). These fractions were pooled to create 9 fractions per sample before downstream PCR.

Sequence preparation

We extracted DNA from the 16 sample microcosms and sequenced pre-fractionated DNA from each sample and 9 gradient fractions per sample (total 144). Dual-indexed custom barcoded PCR primers targeted the bacterial/archaeal 16S rRNA gene V4 region (515 F / 806 R), and the fungal internal transcribed spacer ITS1 region (nBITSf / 58A2r), which are described in (Kozich et al. 2013, Pepe-Ranney et al. 2016, Koechli et al. 2019). Each 25 μL PCR reaction contained 12.5 μL Q5 High Fidelity PCR Master Mix (New England Biolabs), 2.5 μL primers, and 5 μL template DNA. PCR amplifications were performed in triplicate for ITS1 and 16S rRNA and then pooled, followed by gel electrophoresis to confirm amplification. The amplicon

libraries were then purified and normalized using a SequalPrep normalization kit (Thermo Fischer Scientific, Waltham, MA) following manufacturer's protocols. Samples were concentrated down to 5 ng μL^{-1} by vacuum centrifugation at 20°C, and sent to the Cornell Core Facility in Ithaca, NY for Illumina MiSeq sequencing, using the V2 chemistry with 2 × 250 bp read length.

Bioinformatic pre-processing

Sequences were demultiplexed using deML (default settings), assembled with PEAR (-p 0.001 –q 30), followed by Illumina adapter contamination and primer sequence removal using Cutadapt (-n 2 -O 5 --match-read-wildcards). Sequences were quality-filtered (--fastq_maxee 0.25 --fastq_minlen 50 --fastq_maxns 0 --fasta_width 0) and dereplicated using VSEARCH, followed by amplicon sequence variant (ASV) assignment using UNOISE3 (-minsize 9 option). Taxonomic classification was performed using the Bayesian-based lowest common ancestor classifier tool (BLCA) against the 16S rRNA gene database from NCBI (-n 100 -j 50 -d 0.1 -e 0.01 -b 100 -c 0.9 --iset 90). ASVs affiliated with taxonomic assignments pertaining to chloroplast of mitochondrial sequences were removed from the data set. Processing of fungal ITS1 sequences followed a similar protocol, except that after quality-filtering and dereplication, fungal ITS1 sequences were identified and extracted with ITSx (-E 0.01 –heuristics –t F) and padded with "N" characters to the maximum ITS1 sequence length prior to ASV identification using UNOISE3. After removal of "N" characters from the ITS1 ASVs, the taxonomy of fungal ITS1 sequences were assigned with the UNITE database (version no. 7.2, release date 2017-20-10) using BLCA. Fungal ITS1

ASV sequences were subsequently post-clustered at 96% nucleotide identity using LULU, a methodology that uses pairwise ASV nucleotide identity and co-occurrence to correctly delineate species hypotheses with ITS marker sequences in ecological data sets (Frøslev et al. 2017). Analysis of LULU output using multiple, decreasing nucleotide identity cutoffs revealed a plateau in ASV decline at nucleotide identities below 96%, the output of which was selected for further analysis. A total of 31 fungal ITS1 ASVs were merged into existing ASVs at the 96% identity cutoff used.

HRSIP Analysis

To assess the ^{13}C labeling of DNA, we used multiple window high resolution stable isotope probing (MW-HR-SIP), which identifies ASVs that had significant $\log_2$ fold change in relative abundance in multiple ^{13}C heavy fractions over corresponding ^{12}C controls (hereafter termed "incorporators"). We identified incorporators of ^{13}C leaf substrate using MW-HR-SIP in *HTSSIP* (R package) as described in (Youngblut et al. 2018). Briefly, ASVs that were statistically more abundant in the ^{13}C heavy fractions relative to corresponding ^{12}C control heavy fractions were determined as ^{13}C incorporators for downstream analysis using DESeq2 (Love et al. 2014). We included 9 gradient fractions from multiple overlapping windows of buoyant density (1.70 - 1.73 g mL^{-1}; 1.72 - 1.75 g mL^{-1}; 1.74 - 1.77 g mL^{-1}). Read count distribution was similar for bacteria and fungi as well as across all samples and for leaf ^{13}C incorporators in particular, which supports the comparison of labeled and unlabeled community dynamics.

Bioinformatic and Statistical Analysis

We used $\log_2$ fold change (LFC) in abundance of ^{13}C fractions over ^{12}C fractions for each ASV as a proxy for the degree of ^{13}C incorporation or enrichment, where significant. P-values from a one-sided z-test for differential abundance were considered significant ($\alpha < 0.05$) after a Benjamini-Hochberg false discovery rate adjustment (FDR of 0.01). ASVs were filtered to those that had reads > 500 per sample. Pre-fractionated samples had an average of 16,366 16S sequences and 21,769 ITS sequences per sample after filtering low abundance taxa removed < 0.1% of 16S and ITS reads. The sequencing depth was adequate to ensure a high degree of sensitivity (i.e. ability to detect true positives) using the MW-HR-SIP pipeline (Youngblut et al. 2018). Pre-fractionated samples contained 3574 of the total 4055 bacterial ASVs and 709 of the total 796 fungal ASVs in the sequencing effort across all fractions. ASV counts were normalized to total counts per thousand reads.

Differences in ASV composition among experimental design groups was assessed using Canonical Correspondence Analysis (CCA) on a Bray-Curtis dissimilarity matrix, and statistical significance was tested using PERMANOVA (adonis) in *vegan* (Oksanen et al. 2007). ASVs with positive LFC values in limed relative to control soils were denoted as "responders" to liming. Strong responders to liming were defined as those with LFC ≥ 1, while poor responders to liming had LFC ≤ -1. Because of the small number of replicates per treatment (n = 4), effect sizes (LFC) were estimated with *apeglm* which reduces variance, while preserving the true large effect sizes (Zhu et al. 2019). Functional classifications for fungi were

ascertained using FUNGuild, which yielded classifications for 89% of fungal ASVs in the dataset (Nguyen et al. 2016). We limited our analysis to those classifications that were deemed "Probable" and "Highly Probable" and kept ASVs that were only assigned to a single guild. We treated isotopically different microcosms as additional replicates in our experimental design and drew conclusions about the effects of liming by studying the number of incorporators present in different treatments and their relative abundance and diversity in pre-fractionated DNA samples.

We compared microcosm responses to the responses in a larger field survey of the microbial community in limed and control subcatchments (Sridhar et al. Ch1). Sequences representing ASVs from this study were aligned to ASVs identified in the field survey using a threshold ≥ 99% alignment identity and ≥ 95% query coverage to ensure robust ASV assignment between studies. For 16S ASVs with taxonomic assignments at the order rank, we observed monophyletic clades of incorporator ASVs responding to liming (suggesting a phylogenetically conserved response) and hereafter describe them as phylogroups throughout the text (e.g. Figure S7). Phylogenetic estimation was performed as follows. A phylogenetic tree of 16S ASVs was produced by aligning 16S rRNA gene sequences using mafft (default settings) and tree reconstruction using FastTree2 (-nt -gtr -slow -gamma -bionj -spr 4 -mlacc 2 –slownni). Since insertions and deletions are common within fungal ITS regions, we constrained phylogenetic analyses of these sequences to ASVs classified at the genus level. Hence, monophyletic sets of fungal ASVs at the genus rank sharing a conserved response of incorporation were described as phylogroups throughout the text. Phylogroups created this way suggest an evolutionary conservation of ^{13}C incorporator

responses. The relative abundances of incorporator phylogroups detected in our SIP study were investigated in the field study to validate their ecological relevance.

Results

^{13}C assimilation into bacterial and fungal taxa

Over 40 days, labeled and unlabeled leaf litter decomposed in the microcosms (Figure S1), and approximately 29% of added leaf C was respired by day 27, at which point cumulative respiration plateaued (Figure S2). Significant differences in taxonomic composition between ^{13}C gradient fractions and corresponding ^{12}C fractions (Figure S3 and Table S1) demonstrate successful incorporation of ^{13}C label into fungal and bacterial DNA. Leaf C amendments decomposed and were incorporated into actively respiring microorganisms, confirmed by detection of $^{13}CO_2$ respired from microcosms (Figure S2) and the significant enrichment of ^{13}C relative to ^{12}C DNA in heavy fractions for 630 ASVs (496 bacteria and 134 fungi).

Incorporators accounted for 14% of all bacterial ASVs found in limed soils and 17% of incorporators in control soils. Fungal incorporators accounted for 23% of all fungal ASVs in both limed and control soils. Bacterial and fungal incorporators were prominent among all ASVs that responded strongly to liming (Figure S4). The unlabeled responders to liming likely changed in abundance by metabolizing native SOC more in one than the other treatment. We focus the following analysis on ASVs that incorporated ^{13}C into their biomass.

Lime effects on bacterial and fungal ^{13}C incorporator community composition

Bacterial and fungal taxa incorporating ^{13}C from ^{13}C-oak litter differed between limed and control soils. Liming treatment explained 18% of the variation in bacterial incorporator composition and 23% of fungal incorporator composition (PERMANOVA $p = 0.001$; Figure 1, Table S2). Treatment explained a similar amount of the variation in bacterial and fungal incorporation as soil horizon did (Figure 1; Table S2). Contrary to expectations of community shifts during different stages of litter decomposition, bacterial and fungal incorporator composition did not change between the two time points of the experiment.

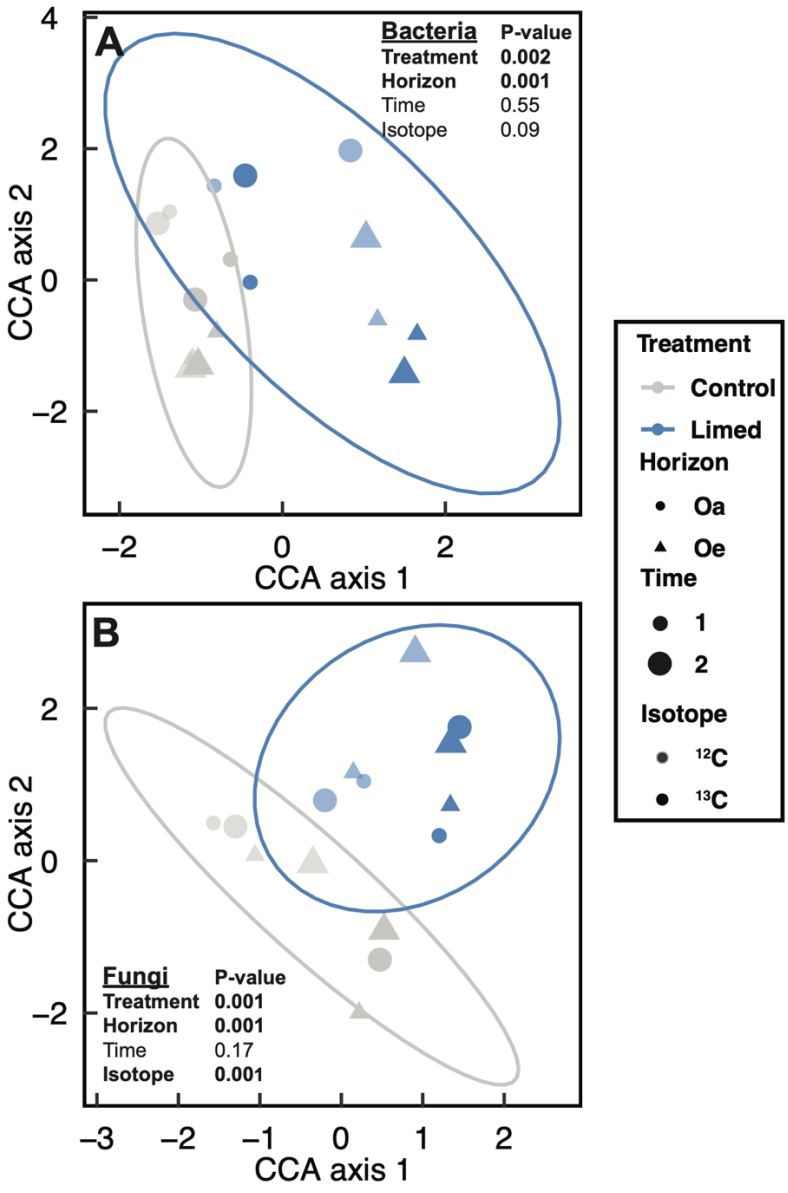

Figure 1 Canonical correspondence analysis ordinations of (A) bacterial (16S) and (B) fungal (ITS) DNA sequence composition of incorporators in pre-fractionated soil from 16 microcosms. Ellipses represent 95% confidence that samples from the respective treatments fall within that region. Dissimilarity in sequence composition was quantified using the Bray-Curtis metric. Sample points are fractions coded by treatment, horizon, time, and isotope. The significance of each factor as a predictor of community composition from a PERMANOVA model is inset.

As expected, isotope treatment had no impact on the pre-fractionated bacterial community members that were determined to be incorporators, indicating incubation with isotopically different substrates introduced no bias. However, this was not the case for fungal communities; as fungal incorporators differed between ^{13}C and ^{12}C litter. This artifact potentially limits the sensitivity of SIP in detecting uptake of label among fungi in our study (Youngblut 2018b). The lower sensitivity of MW-HR-SIP in this situation was shown to be primarily driven by differences in the number of shared taxa rather than differences in their distribution within the samples (Youngblut 2018b). Pre-fractionated ^{12}C and ^{13}C samples shared 76% of their fungal taxa, which could lower the sensitivity of our methods in detecting label uptake from 0.9 when 100% of taxa are shared, to ~0.7, where sensitivity is the fraction of labeled taxa (true positives) identified correctly (Youngblut 2018b). Thus, we expect that our method failed to detect approximately 30% of fungal incorporators present. Nevertheless, the high degree of specificity of MW-HR-SIP ensures a low false positive rate of those fungal ASVs that were detected as incorporators in our study.

Lime effects on bacterial and fungal ^{13}C incorporator richness

Liming increased the phylotype richness of the microbial incorporators, with greater increases in bacteria than in fungi. The number of bacterial ASVs incorporating ^{13}C in limed soils over controls increased ~4 fold ($P < 0.001$), and their median degree of enrichment increased up to 11% (e.g. Oe horizon day 15; Figure 2 and Figure S5A). Of the 496 bacterial ^{13}C incorporator ASVs, 77% were active only in limed soils, while 10% were active only in control soils, and the rest, only 13% were

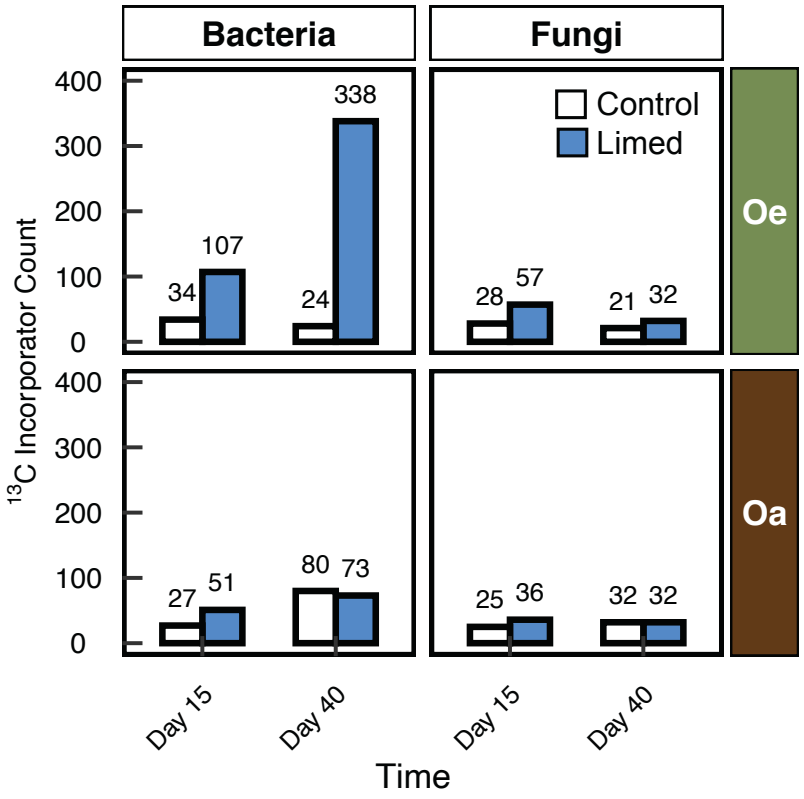

Figure 2 The number of bacterial and fungal ASVs that incorporated ^{13}C from ^{13}C-labeled leaf in each treatment over two time points and across each organic horizon.

active in both (Figure S5A). Meanwhile, there were ~1.5 times as many fungal ASVs that incorporated ^{13}C in limed soils compared to controls ($P < 0.001$), and these fungi saw significant increases in their median degree of enrichment of up to 12% in certain conditions (Oe horizon day 15; Figure 2 and Figure S5B). Of the 134 fungal incorporators, 53% were active only in limed soils vs 27% only in control soils; the remaining 20% were active in both (Figure S5B). Over incubation time, liming amplified the increase in bacterial incorporators, while the number of fungal incorporators in limed soils decreased by day 40. The stimulation of bacterial and fungal incorporation of leaf C in limed soils primarily occurred in the Oe horizon, which is composed of partially decomposed plant litter, while Oa horizon (humus) incorporators typically did not respond significantly to liming in degree or number (Figure 2 and Figure S5).

Identities of bacterial ^{13}C incorporators and their response to liming

^{13}C leaf litter assimilation among bacteria was phylogenetically broader in limed than control soils, with incorporators observed across 17 classes from 8 different phyla, whereas control soils had incorporators across 12 classes and only 3 phyla (Figure S6A, Table S3).

Phylum *Actinobacteria* represented 35% of bacterial incorporators. In class *Actinobacteria*, liming increased the number of incorporators from 30 to 111 but decreased their aggregate relative abundance by 18% (Figure 3). ASVs constituting two major phylogroups PG1 and PG2 from *Streptosporangiales* were responsible for class level declines in relative abundance of incorporators. Incorporation in PG1,

which comprised 20% of 16S incorporator reads, declined 11% in limed soils (Figure 4A). PG1 contained seven *Actinoallomurus* ASVs and six other closely related unidentified ASVs (Figure S7). Incorporation in PG2, which comprised 3.6% of 16S incorporator reads declined 57% with liming (Figure 4A). PG2 contained seven as yet unclassified ASVs closely related to *Actinomadura* (Figure S7).

In phylum *Proteobacteria* (49% of incorporator reads), liming benefitted some classes and not others. Liming roughly doubled and quadrupled the number of *Betaproteobacteria* and *Gammaproteobacteria* incorporators, respectively, while also increasing their relative abundance in the community (Figure 3). A group of six ASVs most closely related to *Paraburkholderia caffeinilytica/madseniana* constituted phylogroup PG3 (Figure S8). PG3 accounted for 13% of incorporator reads and had a relative abundance that was 3.4-fold larger in the limed soils (Figure S8). *Alphaproteobacteria* were the most abundant class within *Proteobacteria*, and while the number of incorporators more than quadrupled, their relative abundance declined in limed soils by 11% (Figure 3). Much of this decline was due to PG4, nine unclassified *Rhizhobiales* ASVs that comprised 15% of 16S incorporators (Figure S9). PG4 ASVs were a 97.95% identity match to *Rhodoplanes roseus* and were 19% less abundant in limed soils (Figure 4C, Figure S9).

Figure 3 Normalized counts of ^{13}C-labeled ASVs or 'incorporators' across treatments in pre-fractionated samples ($n_{rep} = 8$) organized by taxonomic class. Six classes that had highest relative abundance among bacteria and fungi are presented here. ASVs are sorted by relative abundance within their genus where available.

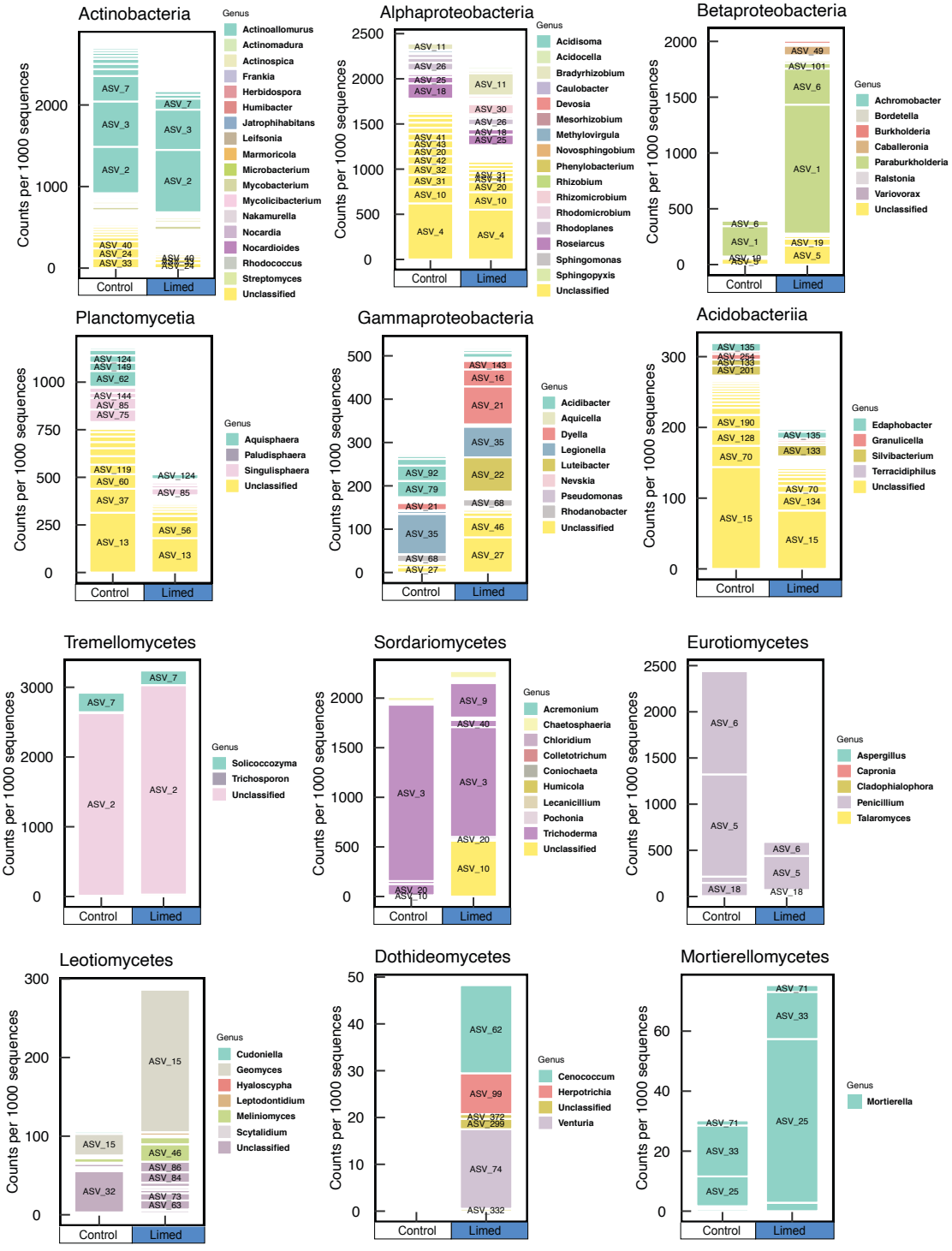
Actinobacteria
Counts per 1000 sequences
Control
Limed
Genus
Actinoallomurus
Actinomadura
Actinospica
Frankia
Herbidospora
Humibacter
Jatrophihabitans
Leifsonia
Marmoricola
Microbacterium
Mycobacterium
Mycolicibacterium
Nakamurella
Nocardia
Nocardioides
Rhodococcus
Streptomyces
Unclassified
Alphaproteobacteria
Acidisoma
Acidocella
Bradyrhizobium
Caulobacter
Devosia
Mesorhizobium
Methylovirgula
Novosphingobium
Phenylobacterium
Rhizobium
Rhizomicrobium
Rhodomicrobium
Rhodoplanes
Roseiarcus
Sphingomonas
Sphingopyxis
Unclassified
Betaproteobacteria
Achromobacter
Bordetella
Burkholderia
Caballeronia
Paraburkholderia
Ralstonia
Variovorax
Unclassified
Planctomycetia
Aquisphaera
Paludisphaera
Singulisphaera
Unclassified
Gammaproteobacteria
Acidibacter
Aquicella
Dyella
Legionella
Luteibacter
Nevskia
Pseudomonas
Rhodanobacter
Unclassified
Acidobacteriia
Edaphobacter
Granulicella
Silvibacterium
Terracidiphilus
Unclassified
Tremellomycetes
Solicoccozyma
Trichosporon
Unclassified
Sordariomycetes
Acremonium
Chaetosphaeria
Chloridium
Colletotrichum
Coniochaeta
Humicola
Lecanicillium
Pochonia
Trichoderma
Unclassified
Eurotiomycetes
Aspergillus
Capronia
Cladophialophora
Penicillium
Talaromyces
Leotiomycetes
Cudoniella
Geomyces
Hyaloscypha
Leptodontidium
Meliniomyces
Scytalidium
Unclassified
Dothideomycetes
Cenococcum
Herpotrichia
Unclassified
Venturia
Mortierellomycetes
Mortierella

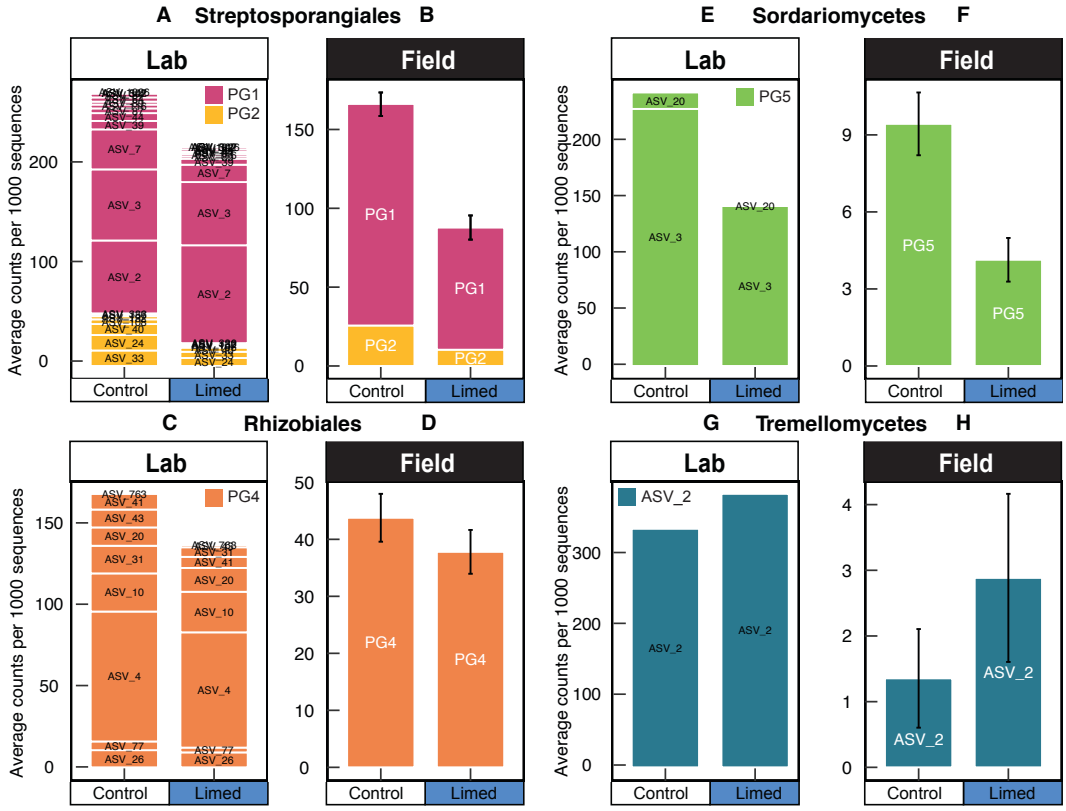

Figure 4 Comparison of selected major bacterial and fungal phylogroup (monophyletic clades of ^{13}C incorporator ASVs) responses to liming shown by their relative abundance when amended with oak leaf fragments (Lab) and their relative abundance in field samples collected in Sridhar et al. Ch1 (Field). Error bars in field data reflect replication across multiple treated subcatchments. ASVs that comprise each phylogroup are displayed in 'Lab' bar plots. Relative abundances are combined across horizon and time points.

Identities of fungal ^{13}C incorporators and their response to liming

Incorporation was heavily skewed in fungi, with just 7 ASVs out of the 134 incorporators accounting for over 80% of the fungal incorporator community. Fungal incorporators of ^{13}C leaves in limed soils spanned 11 classes from 5 phyla, while incorporators in control soils spanned 10 classes from 4 phyla (Figure S6B, Table S4). Incorporators in the study were dominated by phylum *Ascomycota*, on which liming had the effect of decreasing their relative abundance by 24%, despite a 70% increase in the number of incorporators. Most of the increase in the number of incorporators was due to class *Sordariomycetes* (27% of ITS reads), in which twice as many ASVs incorporated label in the limed soils relative to controls. The relative abundance of *Sordariomycetes* increased 12% with liming, despite a decrease for two of its ASVs, ASV_3 and ASV_20, which we denote as PG5 (Figure 3, Figure 4E). The two ASVs in PG5 matched to *Trichoderma theobromicola* and made up 18% of ITS reads (Figure S10). In the limed soils, PG5 gave way to other *Sordariomycetes* including other *Trichoderma* ASVs that thrived at the higher pH (ASV_10, ASV_9, ASV_40; together 6% of ITS reads) (Figure 3). The second most abundant class in *Ascomycota*, *Eurotiomycetes* (19% of ITS reads), had marginally more incorporator numbers but much lower abundance in limed soils. This was due to a 4.5-fold decline in limed soils of three closely related ASVs from genus *Penicillium* (PG6: ASV_6, ASV_5, and ASV_18; together 18% of ITS reads (Figure 3). An ASV from genus *Cenococcum,* which is typically ectomycorrhizal, was abundant in the field, but represented a small proportion of the SIP communities (0.1%). Nevertheless, this *Cenococcum* ASV incorporated ^{13}C-labeled litter and was 4.5-fold more abundant in the limed soils than

control, the exact opposite of its pattern in the field (Figure S11A). *Basidiomycota* were dominated by class *Tremellomycetes* (39% of ITS reads; Figure 3), which increased 15% in abundance in limed soils due to a single unclassified ASV (ASV_2, 35% of ITS reads) most closely related (97.69% identity match) to *Saitozyma podzolica* (Figure 4G, Figure S12).

Functional guild assignments were available for 48 ASVs through FUNGuild. Soil saprotrophs made up 61% of these fungal incorporator sequence counts, though their abundance as a guild was not affected by treatment. ASVs classified as purely 'Ectomycorrhizal' constituted ~2% of the fungal incorporators and were more abundant in the limed soils, largely due to *Cenococcum* spp. mentioned earlier ($P = 0.004$; Figure S13). No other guilds as a whole responded significantly to treatment.

Presence of incorporators in larger field survey

To validate the relevance of our SIP experiment, we compared the SIP community responses to the response of microbial communities from 160 field samples collected from limed and control subcatchments in a previous study (Sridhar et al. Ch 1). Bacterial and fungal incorporators in our lab SIP microcosms (hereafter "lab incorporators") were readily identified in the field with 85% of bacterial and 100% of fungal lab ASVs matching to ASVs present in the field (hereafter "field incorporators"; see Methods). Field and lab incorporator communities were dominated by the same bacterial and fungal classes: *Actinobacteria* (51% of 16S reads in field and 31% in the lab) and *Alphaproteobacteria* (37% of 16S reads in the field and 29% in the lab) among bacteria and *Tremellomycetes* (27% of ITS reads in the field and

39% in the lab) and *Sordariomycetes* (20% of ITS reads in field and 27% in the lab) among fungi. The responses of lab and field incorporator phylogroups/ASVs most often matched in direction and sometimes in magnitude (Figure 4). Notably, PG1 and PG2 *Actinoallomurus*/*Actinomadura* were similarly abundant in lab and field and responded in the same way to liming. On the other hand, PG3 *Paraburkholderia* and PG6 *Penicillium*, were both far less abundant in the field. Overall, while fungi that made up the majority of SIP incorporators (PG5, ASV_2: together 53% of lab incorporators) were present in the field and had similar responses to liming, they comprised a very small proportion of the field community.

Discussion

We tested whether forest liming impacts microbial community structure-function relationships by examining microbial community assimilation of leaf litter C in soils from a northern hardwood forest where liming raised pH by one unit and doubled forest floor C stocks. We found significant differences between limed and control microbial communities assimilating leaf litter C in both bacteria and fungi, supporting our main hypothesis. The magnitude of this shift in composition parallels the differences between microbial communities assimilating C in the Oe horizon versus the Oa horizon. In previous work at Woods Lake, we showed that bacterial and fungal communities in limed soils differed from controls (Sridhar et al. Ch1). In this study, we prove that liming has fundamentally altered how this new microbial community metabolizes litter C, thus linking changes in structure to changes in function. Overall, liming greatly increased the diversity of the active microbial

decomposer community; hence, it appears that low-diversity, acid-tolerant microbial communities enable more complete decomposition of detritus in these northern hardwood forest ecosystems.

Liming affected the number and relative abundance of leaf litter C incorporators, affecting several phylogroups implicated in the decomposition of plant biopolymers. Some of these phylogroup responses to liming matched those of the same organisms found in a previous field study (Sridhar et al. Ch1). Differences in the response of phylogroups between lab and field may be artifacts of our lab microcosms or reveal differences between active and dormant populations within each group (e.g. PG3, PG6, ASV_62).

High throughput stable isotope probing of microbial DNA using complex C substrates is a powerful tool that allowed the identification of 496 bacteria and 134 fungi that assimilated ^{13}C from in ^{13}C oak leaves. By using leaf fragments rather than a single substrate like cellulose, it is likely that a wider range of plant C degraders, secondary, and tertiary consumers in the microbial food web became labeled. Single substrates like cellulose may only be assimilated by 1-10% of the bacterial and fungal taxa present in soils (Koechli et al. 2019) whereas by using whole leaf fragments, we recruited 17% and 23% of bacterial and fungal taxa present respectively.

Over the 40 day incubation, cumulative respiration from pre-fragmented *Q.robur* leaves added to microcosms plateaued by day 15, indicating that litter degradation had progressed past the initial rapid decomposition of cell solubles, into the early or intermediate phase where persistent biopolymers were being decomposed (Snajdr et al. 2010). Contrary to our expectation that microbial community

composition would shift concurrently with anticipated changes in litter chemistry between day 15 and day 40 of the experiment, we found no significant differences in overall composition between time points. Given that respiration had already begun to level off by day 15, it is possible that both time points captured the same phase of decomposition.

While incorporator community composition did not change over time, liming influenced the richness of ^{13}C incorporators over time. In control soils, a similar number of bacterial and fungal incorporators had accessed leaf litter C by day 15 and 40 but liming markedly accelerated the number of bacterial incorporators over time, while the number of fungal incorporators was largely unchanged. Bacterial phylotype richness tends to increase in neutral soils relative to acidic soils, potentially due to a release of physiological constraints on intracellular pH in bacteria (Lauber et al. 2009, Bahram et al. 2018). The boost in richness of bacteria participating in decomposition in limed soils could indicate a change in competitive dynamics between bacteria and fungi. Declines in fungal:bacterial growth and fungal:bacterial biomass at higher pH suggest that bacterial contributions to decomposition are greater at neutral pH than acidic pH (Bååth et al. 1995, Rousk et al. 2009). We did not detect differences between cumulative C respired from limed and control soils in the first 30 days after adding leaf litter C. However, previous studies at Woods Lake suggest that C mineralization in the field is affected over the long term as evidenced by decreases in ligninolytic enzyme activity and soil basal respiration in response to liming, consistent with accumulating C stocks (Melvin et al. 2013, Sridhar et al. Ch1). Because fungi are considered primary decomposers of leaf litter (Tláskal et al. 2016, López-Mondéjar et

al. 2018), the boost to bacterial incorporator richness may signify that bacterial secondary and tertiary consumers benefit from liming. Fungal mycelial biomass that pervades litter is an important pool of C for bacteria (Tláskal et al. 2016, López-Mondéjar et al. 2018), and other SIP studies support the idea that fungi may be the first to access litter C, which subsequently moves through bacterial communities (Koechli et al. 2019).

Liming altered the relative abundance of microbial groups associated with multiple stages of decomposition. *Ascomycota* are presumed to be early stage litter degraders that dominate the utilization of plant biomass (Voříšková and Baldrian 2013, López-Mondéjar et al. 2018). We found that *Ascomycota* were key mediators of leaf litter degradation in the microcosms and were 24% less abundant in limed soil relative to control. In particular, PG5, a phylogroup within the genus *Trichoderma* contributed to this decline in early stage degraders. This *Trichoderma* phylogroup was lower in relative abundance in limed soils in both lab microcosm and field settings. Other members of genus *Trichoderma* have been reported as acidophilic, able to produce lignocellulolytic enzymes including endoglucanases and laccases, and have been associated with litter and fungal mycelium decomposition (Chakroun et al. 2010, Steyaert et al. 2010, Peterson and Nevalainen 2012, Brabcová et al. 2017). *Trichoderma theobromicola* was originally isolated as a leaf endosymbiont, and its presence on oak leaves in this experiment demonstrate its importance as a phyllosphere fungal decomposer (Samuels et al. 2006). As may be expected, several bacteria and fungi present on the *Q. robur* leaves incubated without soil were detected as ^{13}C incorporators in our study, corroborating the participation of phyllosphere

communities in the early litter decomposition (Unterseher et al. 2013, Voříšková and Baldrian 2013). As litter decomposition progresses towards later stages, increases have been observed in the relative abundance of *Basidiomycota*, and in particular basidiomycetous yeasts (Voříšková and Baldrian 2013). In our study one of the dominant incorporators was a basidiomycetous yeast most closely related to *Saitozyma podzolica* that benefitted from liming in lab and field settings. Known to be cellulose decomposers, *Saitozyma podzolica* are abundant and ubiquitous basidiomycetes in forest soils (Štursová et al. 2012, Mašínová et al. 2016). This suggests that liming may alter the roles that fungal saprotrophs typically play in successive litter decomposition and consequently, the flow of C though the detritusphere.

Liming also altered C flow through major bacterial channels. *Rhizhobiales* phylogroup 4, comprising taxa related to *Rhodoplanes* spp., were less abundant in limed soils in lab and field settings. *Rhodoplanes* is a genus of facultative photoheterotrophic bacteria, commonly abundant in the DNA of forest soils, and is an indicator of advanced stages of wood decomposition requiring low pH (Tláskal et al. 2017). They take up simple organic carbon substrates in aerobic conditions, which explains their assimilation of leaf C and prominent role in decomposition in these soils (Hiraishi and Ueda 1994). We also found that *Actinobacteria* that assimilate ^{13}C from ^{13}C-oak leaves, were lower in abundance in limed soils compared to controls in both lab and field settings. In other SIP studies, *Actinobacteria* frequently emerge as some of the dominant degraders of plant-derived C among bacteria (Ai et al. 2015, Gschwendtner et al. 2016). *Actinobacteria* phylogroups 1 and 2, which are yet to be classified, accounted for almost a quarter of the bacterial community assimilating ^{13}C

in the lab microcosms and a fifth of the soil bacterial community in field soils (Sridhar et al. Ch1). The relative abundance of these phylogroups was markedly lower in limed soils at both time points in the incubation, and the direction and magnitude of their response were consistent in both lab and field settings. *Actinoallomurus* and *Actinomadura* spp. are cultivated close relatives of phylogroups 1 and 2 and are gram-positive, mycelia-forming taxa that show a growth preference for acidic pH (4-5.5) (Lee and Hwang 2002, Pozzi et al. 2019). Like many members of *Actinobacteria*, *Actinomadura* are capable of decomposing xylan, cellulose, and lignin (Mason et al. 1988, Zimmermann and Broda 1989, Holtz et al. 1991, Schellenberger et al. 2009, Verastegui et al. 2014, Yin et al. 2018). *Actinoallomurus* is a relatively new genus from *Actinomadura* that are known to associate with ectomycorrhizal roots (Tamura et al. 2009, Sakoda et al. 2019), and their decline could be related to the guild level declines in ectomycorrhizae seen previously at Woods Lake (Sridhar et al. Ch1). In previous work at this site, the relative abundance of these *Actinobacteria* ASVs were connected to ligninolytic enzyme activity, making it plausible that these phylogroups are important among the microbial community for the decomposition of complex plant biopolymers (Roes-Hill et al. 2011, Sridhar et al. Ch1). We show that these *Actinobacteria* play a significant role in C degradation in lab and field settings and are negatively impacted by liming, making them prime candidates for further study of the causes of C accumulation in the limed subcatchments of Woods Lake.

While disruption to plant-microbe interactions is one mechanism by which liming may alter decomposition dynamics in the field, we did not expect to see responses among mycorrhizal fungi due to the absence of plant roots in our

microcosms. For example, the ectomycorrhizal genus *Russula* was among the most abundant fungal responders in field soils and notably diminished in limed soils but were absent from the community of leaf C incorporators in lab microcosms (Sridhar et al. Ch1). However, contrary to expectations, a few uncharacterized taxa from typically ectomycorrhizal genera such as *Chloridium* and *Cenococcum* became strongly labeled in our experiment in the limed soils, confirming their assimilation of added leaf C. Putatively ECM fungi have been known to assimilate C in SIP experiments, and the existence of divergent pseudomycorrhizal lineages within these two genera could explain this phenomenon (Wang and Wilcox 1985, Štursová et al. 2012, Obase et al. 2016). *Cenococcum geophilum* forms a mantle and Hartig net with melanized hyphae and is one of the most commonly encountered and globally abundant ECM fungi (Smith and Read 2008, Tedersoo et al. 2010, Spatafora et al. 2017). *C. geophilum*'s genome contains a large number of genes involved in plant cell wall degradation having recently diverged from saprotrophs (Peter et al. 2016). As such *Cenococcum* spp. may have coincidentally assimilated C while mining for N or have switched to saprotrophy in the absence of photosynthate supply through plant roots, a scenario often deemed unlikely (Talbot et al. 2008, Lindahl and Tunlid 2014, Zak et al. 2019). Whether ectomycorrhizae are considered mutualists or facultative saprotrophs alters predictions of ecosystem function in plant-soil coupled C-cycle models (Moore et al. 2015). The fact that liming had contrasting effects on *Cenococcum* spp. incorporators in the lab microcosms compared with their populations in the field underscores the role of plant feedbacks to liming in soil C storage at this site. Nevertheless, in combination with other changes in C flow through fungi and bacteria produced by

liming, we show that plant roots are not required to produce differences in function between limed and control microbial communities.

We show that differences in soil C stocks caused by liming at Woods Lake correspond with changes in microbial community structure and function that alter C allocation within the microbial food web. Our results identify fungal and bacterial phylogroups that mediate litter decomposition, and that were negatively impacted by liming. In particular, we observed that liming suppressed the involvement of ascomycete taxa early in decomposition and increased bacterial access to litter C later in decomposition. Over time, accumulation of C stocks could be due to suppression of decomposition, or alteration of the microbial loop resulting in enhanced protection of microbial products within the soil matrix. Over decadal timescales, such mechanisms could generate the large differences in C stocks observed at Woods Lake.

REFERENCES

Ai, C., G. Liang, J. Sun, X. Wang, P. He, W. Zhou, and X. He. 2015. Reduced dependence of rhizosphere microbiome on plant-derived carbon in 32-year long-term inorganic and organic fertilized soils. Soil Biology and Biochemistry 80:70–78.

Bååth, E., Å. Frostegård, T. Pennanen, and H. Fritze. 1995. Microbial community structure and pH response in relation to soil organic matter quality in wood-ash fertilized, clear-cut or burned coniferous forest soils. Soil Biology and Biochemistry 27:229–240.

Bahram, M., F. Hildebrand, S. K. Forslund, J. L. Anderson, N. A. Soudzilovskaia, P. M. Bodegom, J. Bengtsson-Palme, S. Anslan, L. P. Coelho, H. Harend, J. Huerta-Cepas, M. H. Medema, M. R. Maltz, S. Mundra, P. A. Olsson, M. Pent, S. Põlme, S. Sunagawa, M. Ryberg, L. Tedersoo, and P. Bork. 2018. Structure and function of the global topsoil microbiome. Nature 560:233–237.

Baldrian, P. 2008. Chapter 2 Enzymes of saprotrophic basidiomycetes. Pages 19–41 *in* L. Boddy, Juliet C Frankland, and P. van West, editors. Academic Press.

Baldrian, P. 2017. Forest microbiome: diversity, complexity and dynamics. FEMS Microbiology Reviews 41:fuw040.

Barnett, S. E., N. D. Youngblut, and D. H. Buckley. 2019. Data Analysis for DNA Stable Isotope Probing Experiments Using Multiple Window High-Resolution SIP. Methods in molecular biology (Clifton, N.J.) 2046:109–128.

Blette, V. L., and R. M. Newton. 1996. Effects of watershed liming on the soil chemistry of Woods Lake, New York. Biogeochemistry 32:175–194.

Brabcová, V., M. Štursová, and P. Baldrian. 2017. Nutrient content affects the turnover of fungal biomass in forest topsoil and the composition of associated microbial communities. Soil Biology and Biochemistry 118:187–198.

Carrino-Kyker, S. R., L. A. Kluber, S. M. Petersen, K. P. Coyle, C. R. Hewins, J. L. DeForest, K. A. Smemo, and D. J. Burke. 2016. Mycorrhizal fungal communities respond to experimental elevation of soil pH and P availability in temperate hardwood forests. FEMS Microbiology Ecology 92:fiw024.

Chakroun, H., T. Mechichi, M. J. Martinez, A. Dhouib, and S. Sayadi. 2010. Purification and characterization of a novel laccase from the ascomycete Trichoderma atroviride: Application on bioremediation of phenolic compounds. Process Biochemistry 45:507–513.

Cotrufo, M. F., M. D. Wallenstein, C. M. Boot, K. Denef, and E. Paul. 2013. The Microbial Efficiency-Matrix Stabilization (MEMS) framework integrates plant litter decomposition with soil organic matter stabilization: do labile plant inputs form stable soil organic matter? Global Change Biology 19:988–995.

Derome, J. 1990. Effects of forest liming on the nutrient status of podzolic soils in Finland. Water, Air, & Soil Pollution 54:337–350.

Driscoll, C. T., C. P. Cirmo, T. J. Fahey, V. L. Blette, P. A. Bukaveckas, D. A. Burns, C. P. Gubala, D. J. Leopold, R. M. Newton, D. J. Raynal, C. L. Schofield, J. B. Yavitt, and D. B. Porcella. 1996. The experimental watershed liming study: Comparison of lake and watershed neutralization strategies. Biogeochemistry 32:143–174.

Frøslev, T. G., R. Kjøller, H. H. Bruun, R. Ejrnæs, A. K. Brunbjerg, C. Pietroni, and A. J. Hansen. 2017. Algorithm for post-clustering curation of DNA amplicon data yields reliable biodiversity estimates. Nature communications 8:1188.

Geyer, K. M., E. Kyker-Snowman, A. S. Grandy, and S. D. Frey. 2016. Microbial carbon use efficiency: accounting for population, community, and ecosystem-scale controls over the fate of metabolized organic matter. Biogeochemistry 127:173–188.

Groffman, P. M., and M. C. Fisk. 2011. Calcium constrains plant control over forest ecosystem nitrogen cycling. Ecology 92:2035–2042.

Gschwendtner, S., M. Engel, T. Lueders, F. Buegger, and M. Schloter. 2016. Nitrogen fertilization affects bacteria utilizing plant-derived carbon in the rhizosphere of beech seedlings. Plant and Soil 407:203–215.

Hiraishi, A., and Y. Ueda. 1994. Rhodoplanes gen. nov., a New Genus of Phototrophic Bacteria Including Rhodopseudomonas rosea as Rhodoplanes roseus comb. nov. and Rhodoplanes elegans sp. nov. International Journal of Systematic Bacteriology 44:665–673.

Holtz, C., H. Kaspari, and J.-H. Klemme. 1991. Production and properties of xylanases from thermophilic actinomycetes. Antonie van Leeuwenhoek 59:1–7.

Kjøller, R., and K. E. Clemmensen. 2009. Belowground ectomycorrhizal fungal communities respond to liming in three southern Swedish coniferous forest stands. Forest Ecology and Management 257:2217–2225.

Koechli, C., A. N. Campbell, C. Pepe-Ranney, and D. H. Buckley. 2019. Assessing fungal contributions to cellulose degradation in soil by using high-throughput stable isotope probing. Soil Biology and Biochemistry 130:150–158.

Kozich, J. J., S. L. Westcott, N. T. Baxter, S. K. Highlander, and P. D. Schloss. 2013. Development of a dual-index sequencing strategy and curation pipeline for analyzing amplicon sequence data on the MiSeq Illumina sequencing platform. Applied and environmental microbiology 79:5112–20.

Kramer, S., D. Dibbern, J. Moll, M. Huenninghaus, R. Koller, D. Krueger, S. Marhan, T. Urich, T. Wubet, M. Bonkowski, F. Buscot, T. Lueders, and E. Kandeler. 2016. Resource Partitioning between Bacteria, Fungi, and Protists in the Detritusphere of an Agricultural Soil. Frontiers in Microbiology 7:1524.

Lauber, C. L., M. Hamady, R. Knight, and N. Fierer. 2009. Pyrosequencing-Based Assessment of Soil pH as a Predictor of Soil Bacterial Community Structure at the Continental Scale. Applied and Environmental Microbiology 75:5111–5120.

Lee, J. Y., and B. K. Hwang. 2002. Diversity of antifungal actinomycetes in various vegetative soils of Korea. Canadian Journal of Microbiology 48:407–417.

Leung, H. T. C., K. R. Maas, R. C. Wilhelm, and W. W. Mohn. 2015. Long-term effects of timber harvesting on hemicellulolytic microbial populations in coniferous forest soils. The ISME journal 10:363–75.

Lindahl, B. D., and A. Tunlid. 2014. Ectomycorrhizal fungi - potential organic matter decomposers, yet not saprotrophs. New Phytologist 205:1443–1447.

López-Mondéjar, R., V. Brabcová, M. Štursová, A. Davidová, J. Jansa, T. Cajthaml, and P. Baldrian. 2018. Decomposer food web in a deciduous forest shows high share of generalist microorganisms and importance of microbial biomass recycling. The ISME journal 12:1768–1778.

López-Mondéjar, R., D. Zühlke, D. Becher, K. Riedel, and P. Baldrian. 2016. Cellulose and hemicellulose decomposition by forest soil bacteria proceeds by the action of structurally variable enzymatic systems. Scientific Reports 6:25279.

Love, M. I., W. Huber, and S. Anders. 2014. Moderated estimation of fold change and dispersion for RNA-seq data with DESeq2. Genome Biology 15:550.

Lundström, U. S., D. C. Bain, A. F. S. Taylor, and P. A. W. van Hees. 2003. Effects of Acidification and its Mitigation with Lime and Wood Ash on Forest Soil Processes: A Review. Water, Air, and Soil Pollution: Focus 3:5–28.

Malik, A. A., J. Puissant, K. M. Buckeridge, T. Goodall, N. Jehmlich, S. Chowdhury, H. S. Gweon, J. M. Peyton, K. E. Mason, M. van Agtmaal, A. Blaud, I. M. Clark, J. Whitaker, R. F. Pywell, N. Ostle, G. Gleixner, and R. I. Griffiths. 2018. Land use driven change in soil pH affects microbial carbon cycling processes. Nature Communications 9:3591.

Mašínová, T., B. D. Bahnmann, T. Větrovský, M. Tomšovský, K. Merunková, and P. Baldrian. 2016. Drivers of yeast community composition in the litter and soil of a temperate forest. FEMS Microbiology Ecology 93:fiw223.

Mason, J. C., M. Richards, W. Zimmermann, and P. Broda. 1988. Identification of extracellular proteins from actinomycetes responsible for the solubilisation of lignocellulose. Applied Microbiology and Biotechnology 28:276–280.

Melvin, A. M., J. W. Lichstein, and C. L. Goodale. 2013. Forest liming increases forest floor carbon and nitrogen stocks in a mixed hardwood forest. Ecological Applications 23:1962–1975.

Moore, J. A. M., J. Jiang, W. M. Post, and A. T. Classen. 2015. Decomposition by ectomycorrhizal fungi alters soil carbon storage in a simulation model. Ecosphere 6(3):29.

Nguyen, N. H., Z. Song, S. T. Bates, S. Branco, L. Tedersoo, J. Menke, J. S. Schilling, and P. G. Kennedy. 2016. FUNGuild: An open annotation tool for parsing fungal community datasets by ecological guild. Fungal Ecology 20:241–248.

Obase, K., G. W. Douhan, Y. Matsuda, and M. E. Smith. 2016. Revisiting phylogenetic diversity and cryptic species of Cenococcum geophilum sensu lato. Mycorrhiza 26:529–540.

Oksanen, J., R. Kindt, P. Legendre, B. OHara, and M. H. H. Stevens. 2007. vegan : Community Ecology Package. R package version 1.8-5 10:631–637.

Pepe-Ranney, C., A. N. Campbell, C. N. Koechli, S. Berthrong, and D. H. Buckley. 2016. Unearthing the Ecology of Soil Microorganisms Using a High Resolution DNA-SIP Approach to Explore Cellulose and Xylose Metabolism in Soil. Frontiers in Microbiology 7:703.

Peter, M., A. Kohler, R. A. Ohm, A. Kuo, J. Krützmann, E. Morin, M. Arend, K. W. Barry, M. Binder, C. Choi, A. Clum, A. Copeland, N. Grisel, S. Haridas, T. Kipfer, K. LaButti, E. Lindquist, A. Lipzen, R. Maire, B. Meier, S. Mihaltcheva, V. Molinier, C. Murat, S. Pöggeler, C. A. Quandt, C. Sperisen, A. Tritt, E. Tisserant, P. W. Crous, B. Henrissat, U. Nehls, S. Egli, J. W. Spatafora, I. V. Grigoriev, and F. M. Martin. 2016. Ectomycorrhizal ecology is imprinted in the genome of the dominant symbiotic fungus Cenococcum geophilum. Nature communications 7:12662.

Peterson, R., and H. Nevalainen. 2012. Trichoderma reesei RUT-C30 – thirty years of strain improvement. Microbiology 158:58–68.

Pozzi, R., M. Simone, C. Mazzetti, S. Maffioli, P. Monciardini, L. Cavaletti, R. Bamonte, M. Sosio, and S. Donadio. 2019. The genus Actinoallomurus and some of its metabolites. The Journal of antibiotics 64:133–9.

Purahong, W., T. Wubet, G. Lentendu, M. Schloter, M. J. Pecyna, D. Kapturska, M. Hofrichter, D. Krüger, and F. Buscot. 2016. Life in leaf litter: novel insights into community dynamics of bacteria and fungi during litter decomposition. Molecular ecology 25:4059–74.

Reid, C., and S. A. Watmough. 2014. Evaluating the effects of liming and wood-ash treatment on forest ecosystems through systematic meta-analysis. Canadian Journal of Forest Research 44:867–885.

Rineau, F., and J. Garbaye. 2009. Does forest liming impact the enzymatic profiles of ectomycorrhizal communities through specialized fungal symbionts? Mycorrhiza 19:493–500.

Rineau, F., J. P. Maurice, C. Nys, H Voiry, and J. Garbaye. 2010. Forest liming durably impact the communities of ectomycorrhizas and fungal epigeous fruiting bodies. Annals of Forest Science 67.

Roes-Hill, M. le, N. Khan, and S. G. Burton. 2011. Actinobacterial Peroxidases: an Unexplored Resource for Biocatalysis. Applied Biochemistry and Biotechnology 164:681–713.

Rousk, J., P. C. Brookes, and E. Bååth. 2009. Contrasting Soil pH Effects on Fungal and Bacterial Growth Suggest Functional Redundancy in Carbon Mineralization. Applied and Environmental Microbiology 75:1589–1596.

Sakoda, S., K. Aisu, H. Imagami, and Y. Matsuda. 2019. Comparison of Actinomycete Community Composition on the Surface and Inside of Japanese Black Pine (Pinus thunbergii) Tree Roots Colonized by the Ectomycorrhizal Fungus Cenococcum geophilum. Microbial Ecology 77:370–379.

Samuels, G. J., C. Suarez, K. Solis, K. A. Holmes, S. E. Thomas, A. Ismaiel, and H. C. Evans. 2006. Trichoderma theobromicola and T-paucisporum: two new species isolated from cacao in South America. Mycological Research 110:381-392.

Schellenberger, S., S. Kolb, and H. L. Drake. 2009. Metabolic responses of novel cellulolytic and saccharolytic agricultural soil Bacteria to oxygen: Metabolic response of soil cellulose degraders. Environmental Microbiology 12:845–861.

Schimel, J. 1995. Ecosystem Consequences of Microbial Diversity and Community Structure. Arctic and Alpine Biodiversity: Patterns, Causes and Ecosystem Consequences:239–254.

Schneckenberger, K., D. Demin, K. Stahr, and Y. Kuzyakov. 2008. Microbial utilization and mineralization of [14C] glucose added in six orders of concentration to soil. Soil Biology and Biochemistry 40:1981–1988.

Schneider, T., K. M. Keiblinger, E. Schmid, K. Sterflinger-Gleixner, G. Ellersdorfer, B. Roschitzki, A. Richter, L. Eberl, S. Zechmeister-Boltenstern, and K. Riedel. 2012. Who is who in litter decomposition? Metaproteomics reveals major microbial players and their biogeochemical functions. The ISME Journal 6:1749–1762.

Schoeneberger, P. J., D. A. Wysocki, E. C. Benham, and S. S. Staff. 2012. Field book for describing and sampling soils, Version 3.0. Natural Resources Conservation Service, National Soil Survey Center, Lincoln, NE.

Sethuraman, A., D. E. Akin, and K.-E. L. Eriksson. 1998. Plant-Cell-Wall-Degrading Enzymes Produced by the White-Rot Fungus Ceriporiopsis Subvermispora. Biotechnology and Applied Biochemistry 27:37–47.

Smith, S. E., and D. Read. 2008. 6 - Structure and development of ectomycorrhizal roots. Pages 191–X *in* S. E. Smith and D. Read, editors. Academic Press.

Snajdr, J., T. Cajthaml, V. Valášková, V. Merhautová, M. Petránková, P. Spetz, K. Leppänen, and P. Baldrian. 2010. Transformation of Quercus petraea litter: successive changes in litter chemistry are reflected in differential enzyme activity and changes in the microbial community composition. FEMS microbiology ecology 75:291–303.

Spatafora, J. W., C. A. Owensby, G. W. Douhan, E. W. A. Boehm, and C. L. Schoch. 2017. Phylogenetic placement of the ectomycorrhizal genus Cenococcum in Gloniaceae (Dothideomycetes). Mycologia 104:758–765.

Steyaert, J. M., R. J. Weld, and A. Stewart. 2010. Ambient pH intrinsically influences Trichoderma conidiation and colony morphology. Fungal Biology 114:198-208.

Strickland, M. S., C. Lauber, N. Fierer, and M. A. Bradford. 2009. Testing the functional significance of microbial community composition. Ecology 90:441–451.

Štursová, M., L. Žifčáková, M. B. Leigh, R. Burgess, and P. Baldrian. 2012. Cellulose utilization in forest litter and soil: identification of bacterial and fungal decomposers. FEMS Microbiology Ecology 80:735–746.

Talbot, J. M., S. D. Allison, and K. K. Treseder. 2008. Decomposers in disguise: mycorrhizal fungi as regulators of soil C dynamics in ecosystems under global change. Functional Ecology 22:955–963.

Tamura, T., Y. Ishida, Y. Nozawa, M. Otoguro, and K. Suzuki. 2009. Transfer of Actinomadura spadix Nonomura and Ohara 1971 to Actinoallomurus spadix gen. nov., comb. nov., and description of Actinoallomurus amamiensis sp. nov., Actinoallomurus caesius sp. nov., Actinoallomurus coprocola sp. nov.,

Actinoallomurus fulvus sp. nov., Actinoallomurus iriomotensis sp. nov., Actinoallomurus luridus sp. nov., Actinoallomurus purpureus sp. nov. and Actinoallomurus yoronensis sp. nov. International journal of systematic and evolutionary microbiology 59:1867–74.

Tedersoo, L., T. W. May, and M. E. Smith. 2010. Ectomycorrhizal lifestyle in fungi: global diversity, distribution, and evolution of phylogenetic lineages. Mycorrhiza 20:217–263.

Tláskal, V., J. Voříšková, and P. Baldrian. 2016. Bacterial succession on decomposing leaf litter exhibits a specific occurrence pattern of cellulolytic taxa and potential decomposers of fungal mycelia. FEMS microbiology ecology 92:fiw177.

Tláskal, V., P. Zrůstová, T. Vrška, and P. Baldrian. 2017. Bacteria associated with decomposing dead wood in a natural temperate forest. FEMS Microbiology Ecology 93:143.

Unterseher, M., D. Peršoh, and M. Schnittler. 2013. Leaf-inhabiting endophytic fungi of European Beech (Fagus sylvatica L.) co-occur in leaf litter but are rare on decaying wood of the same host. Fungal Diversity 60:43–54.

Verastegui, Y., J. Cheng, K. Engel, D. Kolczynski, S. Mortimer, J. Lavigne, J. Montalibet, T. Romantsov, M. Hall, B. J. McConkey, D. R. Rose, J. J. Tomashek, B. R. Scott, T. C. Charles, and J. D. Neufeld. 2014. Multisubstrate Isotope Labeling and Metagenomic Analysis of Active Soil Bacterial Communities. mBio 5:e01157-14.

Voříšková, J., and P. Baldrian. 2013. Fungal community on decomposing leaf litter undergoes rapid successional changes. The ISME Journal 7:477–486.

Wagg, C., S. F. Bender, F. Widmer, and M. G. A. van der Heijden. 2014. Soil biodiversity and soil community composition determine ecosystem multifunctionality. Proceedings of the National Academy of Sciences 111:5266–5270.

Wang, C. J. K., and H. E. Wilcox. 1985. New Species of Ectendomycorrhizal and Pseudomycorrhizal Fungi: Phialophora finlandia, Chloridium paucisporum, and Phialocephala fortinii. Mycologia 77:951–958.

Wilhelm, R. C., R. Singh, L. D. Eltis, and W. W. Mohn. 2019. Bacterial contributions to delignification and lignocellulose degradation in forest soils with metagenomic and quantitative stable isotope probing. The ISME Journal 13:413–429.

Yin, Y.-R., P. Sang, W.-D. Xian, X. Li, J.-Y. Jiao, L. Liu, W. N. Hozzein, M. Xiao, and W.-J. Li. 2018. Expression and Characteristics of Two Glucose-Tolerant GH1 β-glucosidases From Actinomadura amylolytica YIM 77502T for Promoting Cellulose Degradation. Frontiers in Microbiology 9:3149.

Youngblut, N. D., S. E. Barnett, and D. H. Buckley. 2018. HTSSIP: An R package for analysis of high throughput sequencing data from nucleic acid stable isotope probing (SIP) experiments. PLOS ONE 13:e0189616.

Zak, D. R., P. T. Pellitier, W. Argiroff, B. Castillo, T. Y. James, L. E. Nave, C. Averill, K. V. Beidler, J. Bhatnagar, J. Blesh, A. T. Classen, M. Craig, C. W. Fernandez, P. Gundersen, R. Johansen, R. T. Koide, E. A. Lilleskov, B. D. Lindahl, K. J. Nadelhoffer, R. P. Phillips, and A. Tunlid. 2019. Exploring the role of ectomycorrhizal fungi in soil carbon dynamics. The New phytologist 223:33–39.

Zhu, A., J. G. Ibrahim, and M. I. Love. 2019. Heavy-tailed prior distributions for sequence count data: removing the noise and preserving large differences. Bioinformatics (Oxford, England) 35:2084–2092.

Žifčáková, L., T. Větrovský, V. Lombard, B. Henrissat, A. Howe, and P. Baldrian. 2017. Feed in summer, rest in winter: microbial carbon utilization in forest topsoil. Microbiome 5:122.

Zimmermann, W., and P. Broda. 1989. Utilization of lignocellulose from barley straw by actinomycetes. Applied Microbiology and Biotechnology 30:103–109.

APPENDIX

CHAPTER 1

SUPPLEMENTARY MATERIAL

Supplementary Methods

Site Information and Field Sampling

The climate is characterized as temperate with a mean annual temperature of 5.28°C and a mean annual precipitation of 1230 mm [1]. The forest is composed of American beech (*Fagus grandifolia*), red maple (*Acer rubrum*), and yellow birch (*Betula alleghaniensis*) dominating the canopy and a lesser amount of red spruce (*Picea rubens*), sugar maple (*Acer saccharum*), and striped maple (*Acer pensylvanicum*) [2]. The soils are classified as Spodosols overlaying glacial sandy till with a bedrock of hornblende granitic gneiss. Before liming Ca^{2+} was the dominant base cation in the O horizon (>20-30% SOC), and after liming, calcium availability also rose from 8.5 to 35 $cmol_c\ kg^{-1}$ and from 6 to 10 $cmol_c\ kg^{-1}$ in the Oe and Oa horizons respectively [3].

After sampling, we placed samples into plastic bags and transported them on ice back to Cornell University, storing them at 4°C for two days prior to sieving. Following a 4 mm sieving to remove coarse roots and stones, we assayed samples for microbial biomass and C mineralization rates. We stored subsamples for enzyme and microbial community analyses at -80°C [4].

Physicochemical analyses

Soil pH was measured on a 1:1 soil / deionized water slurry following 10 min of equilibration using an Accumet basic AB15 pH meter with a flushable junction soil probe. Soil samples were analyzed for concentrations of 27 elements including Modified Morgan, Morgan, Mehlich I, or Mehlich III extractable Ca, Fe, K, Mg, Mn, Mo, Na, P, S, and Zn by ICP-AES at the Cornell Nutrient Analysis Laboratory (Ithaca, NY). Gravimetric moisture was assessed for each sample by calculating the difference in weight between 1 g of fresh material and its weight after drying at 105°C for 24 hours. Water holding capacity of the organic soils was ascertained by comparing the difference in soil weights when they were saturated with DI water and when they were dried at 105°C for 24 hours.

Microbial respiration and microbial biomass

We estimated the active microbial biomass carbon (MBC) pool using the substrate induced respiration (SIR) technique as per Fierer et al. (2003) [5]. Three grams dry weight soil were measured into 50 ml centrifuge tubes with caps made with airtight septa. Next, four milliliters of autolysed yeast extract solution (12 g/L) was added and tubes were shaken on a desktop shaker for 2 hours to allow the microbiological media substrate to penetrate the soil matrix. The headspace was then flushed with CO_2-free air and incubated at atmospheric pressure and room temperature for 4 hours, after which 2 ml of the headspace was extracted with a syringe and injected into an infrared gas analyzer (LI- 6200, LI-COR, Lincoln, Nebraska, USA) for measurements of CO_2 concentrations. CO_2 flux was calculated per unit dry weight

soil and used to estimate microbial biomass C (MBC) as per Anderson and Domsch (1978) [6].

Microbial respiration was ascertained as per Bradford et al. (2008) [7] using a 60-day incubation where soils were held at 60% water holding capacity and at 22°C. Another set of three-gram soil microcosms were prepared in 50 ml centrifuge tubes with caps made using airtight septa. Soil CO_2 fluxes were sampled on days 1, 4, 10, 20, 30, 45, and 60. At each timepoint, we flushed the headspace with CO_2–free air and incubated the tubes at atmospheric pressure and room temperature for 15 hours. After this, 2-ml of the headspace was extracted with a syringe and injected into an infrared gas analyzer (LI- 6200, LI-COR, Lincoln, Nebraska, USA) for measurements of CO_2 concentrations. CO_2 flux was calculated per unit dry weight soil and per unit SIR MBC to estimate the biomass specific mineralization rates for each sample. Specific CO_2 flux was integrated over 60 days to estimate the cumulative amount of C respired by the microbial biomass in each sample (CR_{mass}).

Extracellular Enzyme Activity Assays

Potential and microbial biomass-specific activities of extracellular enzymes (descriptions in Table S1) were measured as per Panke-Buisse et al. (2015) [8], which is a modified protocol based on Saiya-Cork et al. (2002) [9] and German et al. (2011) [10]. Potential and microbial biomass-specific activities of seven hydrolytic and two oxidative enzymes were measured for seven hydrolytic enzymes, (α-glucosidase (AG), β-xylosidase (BX), β-glucosidase (BG), cellobiohydrolase (CB), N-acetyl glucosaminidase (NAG), leucine aminopeptidase (LAP), acid phosphatase (AP)), and

two oxidative enzymes, polyphenol oxidase (POX), and peroxidase (PER) (descriptions in Table S1). The hydrolytic enzyme activities were measured using fluorescently labeled substrates 4-methylumbelliferone (MUB) and 7-amino-4-methylcoumarin (AMC) at 200 μM. The oxidative enzyme activities were measured spectrophotometrically using L-3,4-dihydroxyphenylalanine (25 mM) as the substrate. Soil slurries were prepared by blending 2 g fresh soil with 100 ml of pH 5.0 sodium acetate buffer (50mM) for 1 min. Sample plates were prepared by adding 200 μL of soil slurry and 50 μL of appropriate substrates into wells of white or transparent-bottom 96-well plates for either fluorimetric or absorbance based assays, respectively. Standards were prepared by adding 200 μL of soil slurry with either 50 μL of MUB or 50 μL AMC standards (at 0, 2.5, 5, 10, 15, 25, 50, and 100 µM). Plates were incubated in the dark at 23°C for 3 hours, and 10 µL of 1.0M NaOH was added to hydrolytic plates to quench the reaction. Fluorescence was measured on a microplate reader (BioTeK) with excitation wavelength at 365 nm and emission wavelength at 450 nm. Oxidative enzyme plates consisted of a blank (250 µL buffer), an L-3,4-dihydroxyphenylalanine blank (200 µL buffer + 50 µL L-3,4-dihydroxyphenylalanine), a sample blank (200 µL soil slurry + 50 µL buffer), and the sample wells (200 µL soil slurry + 50 µl L-3,4-dihydroxyphenylalanine). Peroxidase incubations received 10 μL of 0.3% H_2O_2 solution. Absorbance was measured at 460 nm with the BioTek microplate reader after a 4-hr incubation. Potential activity was calculated based on equations from Saiya-Cork et al. (2002) and normalized by MBC to highlight shifts in microbial allocation strategies.

16S rRNA gene and ITS region amplicon sequencing

Whole DNA was extracted from 0.3 g of each soil sample using the 96-well PowerMag Microbiome RNA/DNA Isolation Kit (MO BIO Laboratories, Inc., Carlsbad, CA, USA) according to the manufacturer's protocol. DNA was quantified with Picogreen fluorescent dye using a λ DNA standard curve according to the manufacturer's protocol (Thermo Fisher Scientific, Inc., Waltham, MA, USA). All pipetting for DNA extraction and normalization was conducted with a Hamilton STARlet Liquid Handling System robot (Hamilton Robotics, Reno, USA). Triplicate polymerase chain reactions (PCR) were used to amplify the 16S rRNA gene (bacteria) and hypervariable internal transcribed region (ITS) of the 18S rRNA gene (fungi) from soil DNA extracts. Dual-indexed, custom barcoded amplicon libraries were generated for bacteria and fungi according to methods by Kozich et al. (2013) [11] and Koechli et al. (2019) [12] respectively. PCR primers targeted the bacterial/archaeal 16S rRNA gene V4 region (515 F / 806 R) and the fungal ITS region (modified nBITS2 F / 58A2 R; see Koechli et al. 2019). Triplicate amplified samples were pooled, normalized, and purified using SequalPrep Normalization Plates (Applied Biosystems, Norwalk, CT). Multiplexed samples were combined and sequenced at the Cornell Life Sciences Sequencing Core on a single lane of Illumina using the MiSeq (2 x 250 bp) platform. Sequences were demultiplexed, quality processed, and assigned to amplicon sequence variants (ASVs) using QIIME2 [13] with the built-in DADA2 pipeline [14]. A no-template control was processed identically, and all ASVs present in this control were removed as contaminants. Taxonomic classification was performed using the Naive Bayes classifiers ('q2-feature-classifier') packaged with QIIME2 Greengenes database

for 16S rRNA genes ([15]; version: gg_13_8_99) and the UNITE database for ITS [16]; version: unite_ver7.99_20.11.2016). FUNGuild was used to assign ITS ASVs to functional guilds based on taxonomic classification [17]. Following the filtering of contaminants, singletons, and low abundance doubletons, 94.2% of total 16S rRNA gene sequences remained ($n_{filtered}$ = 2,155,006), comprising 2828 bacterial ASVs, and 88.8% of all ITS sequences remained after filtering ($n_{filtered}$ = 1,971,460), comprising 3826 fungal ASVs.

Identification of secretion signal-bearing oxidases in genomes of major taxa

All publicly available genomes were downloaded (on July 1st, 2020) for the genera *Solicoccozyma* (NCBI TaxID: 1851575; n = 3), *Actinomadura* (ID: 1988; n = 67), and *Cenococcum* (5569; n = 1). The closest relative of *Cenococcum* with an available genome, *Glonium stellatum* (574774; n = 1), was included to increase the sample size. Open-reading frames were predicted with Prodigal (v2.6.2) [18]. Lignin-degrading oxidative enzymes were annotated with hmmsearch [19] using Hidden Markov models supplied by Wilhelm et al. (2019) [20] for laccases, aryl alcohol oxidases and dye-decoloring peroxidases. Secreted proteins were identified based on signal peptide sequence predictions from SignalP-5.0 [21] with a threshold of $p_{other} < 0.05$. For fungal genomes, Prodigal is only capable of predicting single-exon genes and, thus, there is a degree of uncertainty in our annotations of fungal genomes [22] (Table S6).

REFERENCES

1. Yavitt, J. B., Fahey, T. J. & Simmons, J. A. Methane and Carbon Dioxide Dynamics in a Northern Hardwood Ecosystem. *Soil Sci Soc Am J* **59**, 796–804 (1995).

2. Smallidge, P. J. & Leopold, D. J. Watershed liming and pit and mound topography effects on seed banks in the Adirondacks, New York, USA. *Forest Ecology and Management* **72**, 273–285 (1995).

3. Blette, V. L. & Newton, R. M. Effects of watershed liming on the soil chemistry of Woods Lake, New York. *Biogeochemistry* **32**, 175–194 (1996).

4. Darby, B. A. *et al.* Depth patterns and connections between gross nitrogen cycling and soil exoenzyme activities in three northern hardwood forests. *Soil Biology Biochem* **147**, 107836 (2020).

5. Fierer, N., Allen, A. S., Schimel, J. P. & Holden, P. A. Controls on microbial CO2 production: a comparison of surface and subsurface soil horizons. *Global Change Biol* **9**, 1322–1332 (2003).

6. Anderson, J. P. E. & Domsch, K. H. A physiological method for the quantitative measurement of microbial biomass in soils. *Soil Biology Biochem* **10**, 215–221 (1978).

7. Bradford, M. A., Fierer, N. & Reynolds, J. F. Soil carbon stocks in experimental mesocosms are dependent on the rate of labile carbon, nitrogen and phosphorus inputs to soils. *Funct Ecol* **22**, 964–974 (2008).

8. Panke-Buisse, K., Poole, A. C., Goodrich, J. K., Ley, R. E. & Kao-Kniffin, J. Selection on soil microbiomes reveals reproducible impacts on plant function. *Isme J* **9**, 980–989 (2015).

9. Saiya-Cork, K. R., Sinsabaugh, R. L. & Zak, D. R. The effects of long term nitrogen deposition on extracellular enzyme activity in an Acer saccharum forest soil. *Soil Biology and Biochemistry* **34**, 1309–1315 (2002).

10. German, D. P. *et al.* Optimization of hydrolytic and oxidative enzyme methods for ecosystem studies. *Soil Biology Biochem* **43**, 1387–1397 (2011).

11. Kozich, J. J., Westcott, S. L., Baxter, N. T., Highlander, S. K. & Schloss, P. D. Development of a dual-index sequencing strategy and curation pipeline for analyzing amplicon sequence data on the MiSeq Illumina sequencing platform. *Appl Environ Microb* **79**, 5112–20 (2013).

12. Koechli, C., Campbell, A. N., Pepe-Ranney, C. & Buckley, D. H. Assessing fungal contributions to cellulose degradation in soil by using high-throughput stable isotope probing. *Soil Biology Biochem* **130**, 150–158 (2019).

13. Bolyen, E. *et al.* QIIME 2: Reproducible, interactive, scalable, and extensible microbiome data science. *Peerj Prepr* **6**, e27295v2 (2018).

14. Callahan, B. J. *et al.* DADA2: High-resolution sample inference from Illumina amplicon data. *Nat Methods* **13**, 581–3 (2016).

15. DeSantis, T. Z. *et al.* Greengenes, a Chimera-Checked 16S rRNA Gene Database and Workbench Compatible with ARB. *Appl. Environ. Microbiol.* **72**, 5069 (2006).

16. Kõljalg, U. *et al.* Towards a unified paradigm for sequence-based identification of fungi. *Mol Ecol* **22**, 5271–7 (2013).

17. Nguyen, N. H. *et al.* FUNGuild: An open annotation tool for parsing fungal community datasets by ecological guild. *Fungal Ecology* **20**, 241–248 (2016).

18. Hyatt, D. *et al.* Prodigal: prokaryotic gene recognition and translation initiation site identification. *Bmc Bioinformatics* **11**, 119 (2010).

19. Eddy, S. R. Profile hidden Markov models. *Bioinformatics* **14**, 755–763 (1998).

20. Wilhelm, R. C., Singh, R., Eltis, L. D. & Mohn, W. W. Bacterial contributions to delignification and lignocellulose degradation in forest soils with metagenomic and quantitative stable isotope probing. *Isme J* **13**, 413–429 (2019).

21. Armenteros, J. J. A. *et al.* SignalP 5.0 improves signal peptide predictions using deep neural networks. *Nat Biotechnol* **37**, 420–423 (2019).

22. Brian J. Haas, Qiandong Zeng, Matthew D. Pearson, Christina A. Cuomo & Jennifer R. Wortman. Approaches to Fungal Genome Annotation. *Mycology* **2**, 118–141 (2011).

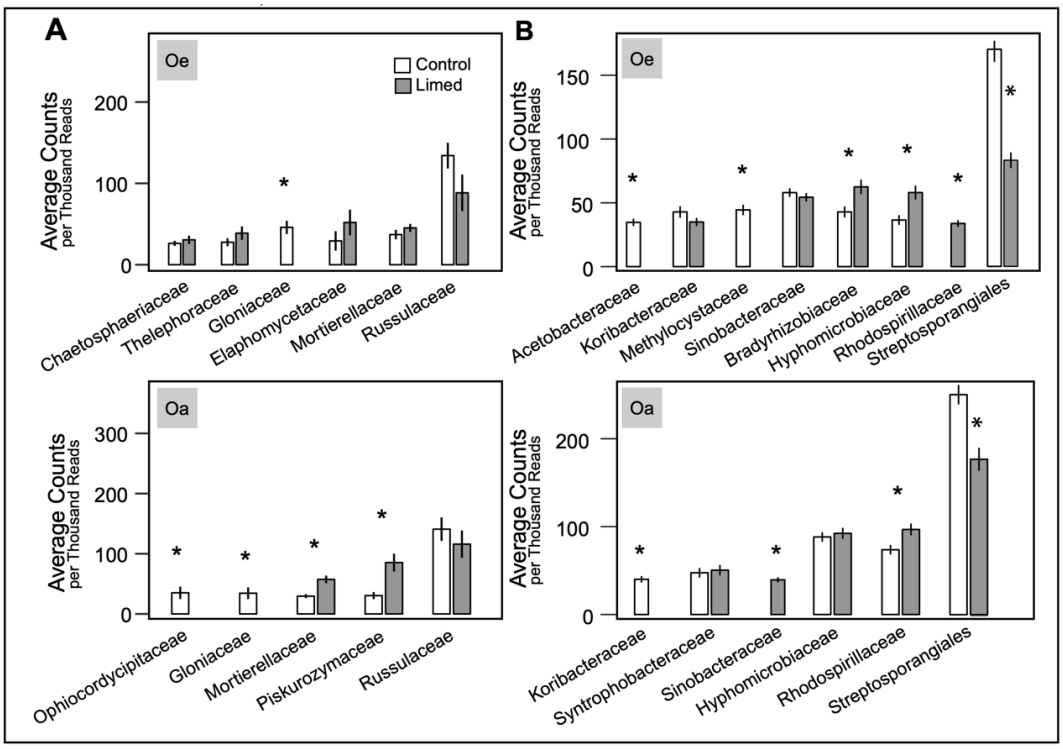

Figure S1 Relative abundances of high abundance (A) fungal and (B) bacterial at the family level where available, in limed and control soils in the two horizons. Differences between treatment means (±SE) within horizons significant at $\alpha = 0.05$ are marked with "*" ($n_{rep} = 40$).

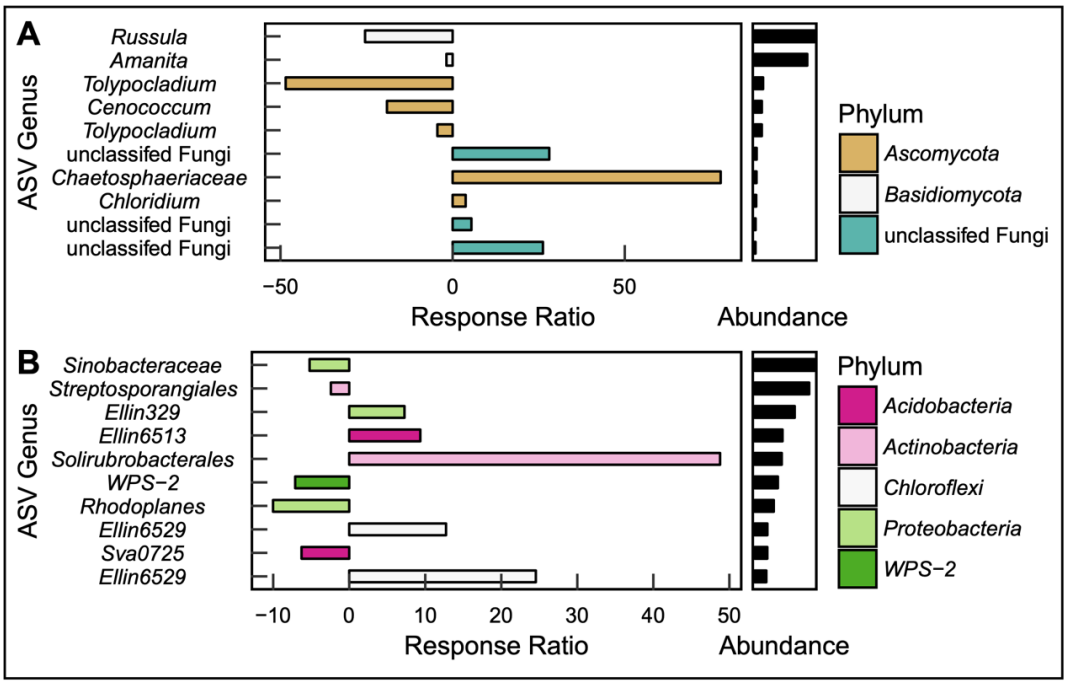

Figure S2 (A) Fungal and (B) bacterial genera containing ASVs that responded strongly to liming, ranked by their abundance. The response ratio is negative when average abundances in limed soils is smaller than in the control soils and positive otherwise and the magnitude is the ratio of the average relative abundances. Only the ten most abundant responder ASVs are shown here, colored by the phylum they belong to.

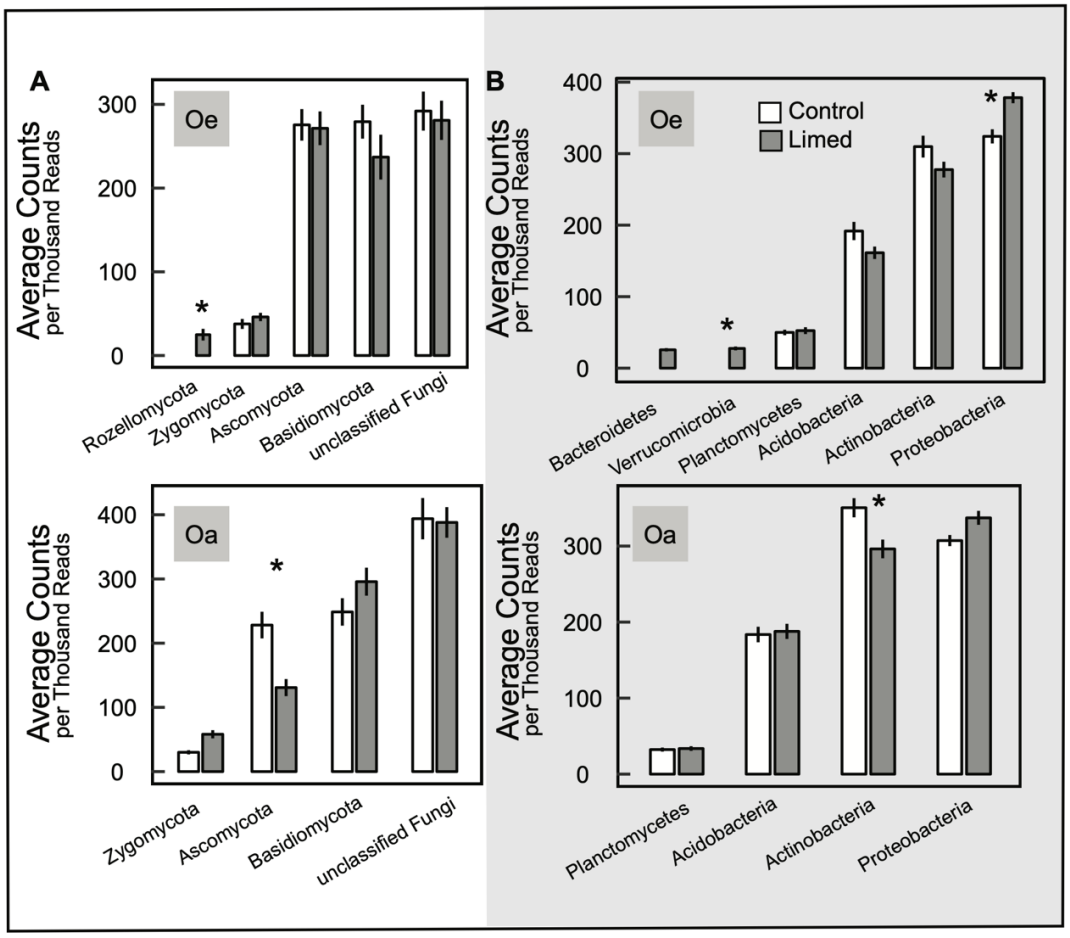

Figure S3 Relative abundances of (A) fungi and (B) bacteria among treatments at the phylum level. Differences between treatment means (±SE) within horizons significant at $\alpha = 0.05$ are marked with "*" ($n_{rep} = 40$).

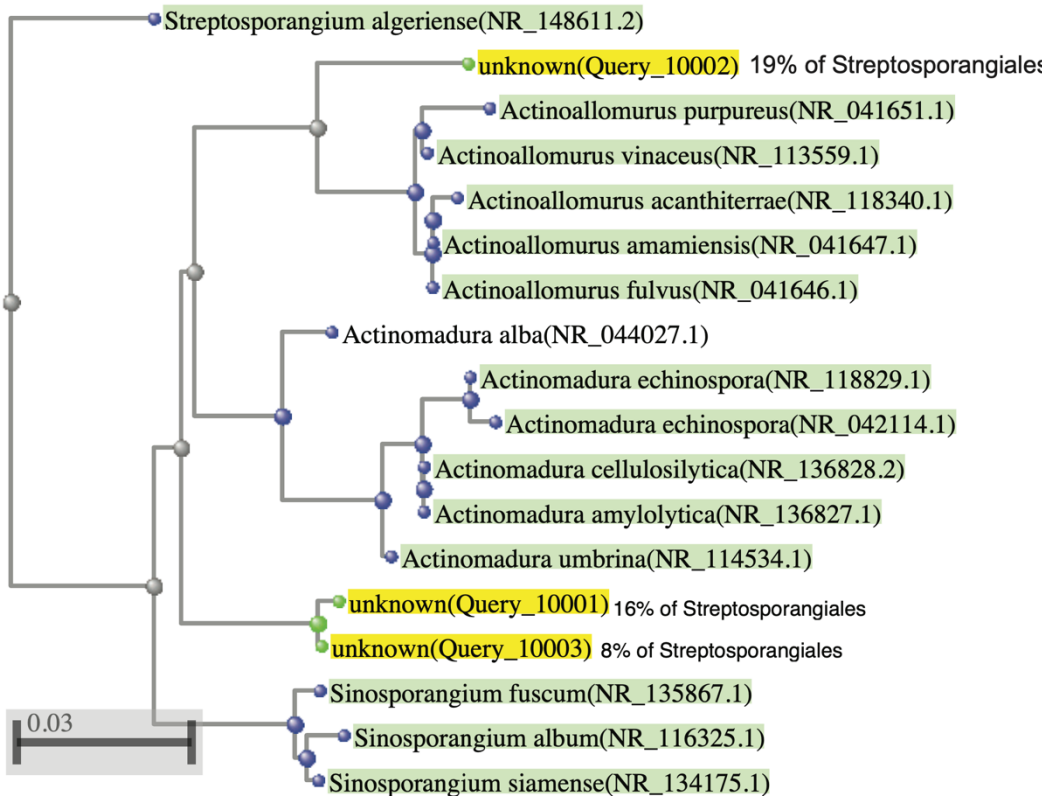

Figure S4 Distance tree for *Streptosporangiales* ASVs that respond negatively to liming and increasing pH**.**

Table S1 Description of enzymes assayed adapted from German et al. (2011)

Enzyme	Purpose	Laboratory substrate
a-glucosidase (AG)	Breaks down starch catalyzing the hydrolysis of terminal, non-reducing 1,4-linked a-D-glucose residues, releasing a-D-glucose	4-methylumbelliferyl-α-d-glucoside
Acid phosphatase (AP)	Mineralizes organic P into phosphate by hydrolyzing phosphoric (mono) ester bonds	4- methylumbelliferyl - phosphate
β-glucosidase (BG)	Catalyzes the hydrolysis of terminal 1,4-linked b-D-glucose residues from b-D-glucosides, including short chain cellulose oligomers	4- methylumbelliferyl - b-D-glucopyranoside
Cellobiohydrolase (CB)	Catalyzes the hydrolysis of 1,4-b-D-glucosidic linkages in cellulose and cellotetraose, releasing cellobiose	4- methylumbelliferyl - b-D-cellobioside
β-Xylosidase (BX)	Releases xylose from short xylan chains	4- methylumbelliferyl - b-D-xylopyranoside

Table S1 (Continued)

N-acetyl glucosaminidase (NAG)	Catalyzes the hydrolysis of terminal 1,4 linked N-acetyl-beta-D-glucosaminide residues in chitin derived oligomers	4- methylumbelliferyl - N-acetyl-b-D-glucosaminide
Leucine aminopeptidase (LAP)	Catalyzes the hydrolysis of leucine and other amino acid residues from the N-terminus of peptides. Amino acid amides and methyl esters are also readily hydrolyzed by this enzyme.	L-Leucine-7-amido-4-methylcoumarin hydrochloride
Phenol Oxidase (POX)	Oxidizes benzenediols to semiquinones with O2	3, 4 – Dihydroxy-L-phenylalanine and 2,2'-azino-bis (3-ethylbenzothiazoline-6-sulphonic acid)
Peroxidase (PER)	Catalyzes oxidation of lignin substrates via the reduction of H2O2.	3, 4 – Dihydroxy-L-phenylalanine and 2,2'-azino-bis (3-ethylbenzothiazoline-6-sulphonic acid)

Table S2 Soil elemental variables (mean ± standard error) measured in the two forest floor horizons in limed and control watersheds (n = 40). Within horizon test were carried out at $\alpha = 0.05$.

Soil Property		Control	Limed	P value
Soil moisture (g/g soil)				
	Oe	3.51±0.1	3.59±0.1	0.816
	Oa	2.31±0.2	2.75±0.2	0.152
Cu (mg/kg soil)				
	Oe	37.1±2.9	37.7±2.3	0.631
	Oa	30.2±2.3	26.4±1.8	0.342
Fe (mg/kg soil)				
	Oe	4541±788	5016±1249	0.503
	Oa	5260±819	4968±568	0.447
K (mg/kg soil)				
	Oe	455±17.8	505±23	0.211
	Oa	358±17.2	352±22.6	0.667
Mn (mg/kg soil)				
	Oe	463±72.8	544±103	0.66
	Oa	264±89.7	432±149	0.15
P (mg/kg soil)				
	Oe	977±56.3	979±63.7	0.995
	Oa	786±56	796±63.2	0.92
Pb (mg/kg soil)				
	Oe	71±9.7	69.5±8.7	0.917
	Oa	70.3±6	88.1±6.2	0.172
Zn (mg/kg soil)				
	Oe	79.2±10.4	118±18.8	0.064
	Oa	65.8±7.5	86.1±15.9	0.252

Table S3 Statistical testing of differences in bacterial (A) and fungal (B) community composition according to experimental variables with PERMANOVA based on Bray-Curtis dissimilarities (nperm = 999). EA.axis1 represents the first PCoA axis of 25 elemental concentrations.

A: PERMANOVA FOR BACTERIA

Variables	Df	SumsOfSqs	MeanSqs	F.Model	R2	P value
horizon	1	3.395	3.395	15.277	0.124	**0.001**
pH	1	3.236	3.236	14.565	0.118	**0.001**
SIR	1	0.413	0.413	1.860	0.015	**0.039**
plot	1	0.326	0.326	1.468	0.012	0.111
AG	1	0.266	0.266	1.196	0.010	0.232
AP	1	0.334	0.334	1.502	0.012	0.093
BG	1	0.300	0.300	1.351	0.011	0.146
BX	1	0.434	0.434	1.954	0.016	**0.029**
CB	1	0.434	0.434	1.955	0.016	**0.030**
LAP	1	0.290	0.290	1.306	0.011	0.157
NAG	1	0.348	0.348	1.565	0.013	0.065
POX	1	0.394	0.394	1.771	0.014	**0.040**
PER	1	0.443	0.443	1.994	0.016	**0.029**
Ca	1	0.352	0.352	1.584	0.013	0.069
EA.axis1	1	0.240	0.240	1.082	0.009	0.297
Residuals	73	16.221	0.222		0.591	
Total	88	27.426			1.000	

Table S3 (Continued)

B: PERMANOVA FOR FUNGI

Variables	Df	SumsOfSqs	MeanSqs	F.Model	R2	P value
horizon	1	2.305	2.305	8.666	0.079	**0.001**
plot	1	0.437	0.437	1.643	0.015	**0.040**
pH	1	2.073	2.073	7.796	0.071	**0.001**
SIR	1	0.449	0.449	1.687	0.015	**0.021**
AG	1	0.301	0.301	1.133	0.010	0.272
AP	1	0.244	0.244	0.918	0.008	0.573
BG	1	0.548	0.548	2.059	0.019	**0.006**
BX	1	0.407	0.407	1.529	0.014	**0.043**
CB	1	0.313	0.313	1.176	0.011	0.240
LAP	1	0.597	0.597	2.246	0.020	**0.004**
NAG	1	0.367	0.367	1.381	0.013	0.090
POX	1	0.615	0.615	2.313	0.021	**0.003**
PER	1	0.610	0.610	2.293	0.021	**0.002**
Ca	1	0.466	0.466	1.752	0.016	**0.019**
EA.axis1	1	0.348	0.347	1.307	0.012	0.152
Residuals	72	19.149	0.266		0.655	
Total	87	29.228			1.000	

Table S4 Correlations between ASV abundance and EEA for the most abundant fungi (and % relative abundance) at the taxonomic level of family and by functional guild. Significant spearman correlation coefficients (ρ) are in bold. Values in green indicate positive correlations and values in red indicate negative correlations. Increasing color intensity corresponds to the level of significance ($\alpha = 0.05$, $\alpha = 0.001$, $\alpha = 0.0005$). AG, a-glucosidase; AP, Acid Phosphatase; BG, β-glucosidase; BX, β-Xylosidase; CB, Cellobiohydrolase; NAG, N-acetyl glucosaminidase; LAP, Leucine aminopeptidase; PER, Peroxidase; POX, Phenol Oxidase; CRmass, Cumulative C respired in a 60d incubation.

Fungal families

Oe	AG	BG	BX	CB	AP	LAP	NAG	PER	POX	CRmass	pH
Ophiocordycipitaceae (1%)	**-0.32**	0.13	0.16	0.04	0.27	-0.05	-0.1	0.1	-0.12	-0.18	**-0.29**
Chaetosphaeriaceae (1%)	**0.44**	**0.34**	0.25	**0.34**	-0.05	-0.13	0.01	0.18	-0.19	-0.17	0
Thelephoraceae (2%)	-0.18	-0.09	0.12	-0.09	-0.02	-0.17	-0.21	0.15	-0.09	**0.28**	-0.01
Gloniaceae (2%)	-0.17	-0.16	0.15	-0.29	**0.44**	-0.11	**0.33**	-0.15	**0.34**	**0.36**	**-0.5**
Elaphomycetaceae (2%)	-0.17	-0.2	-0.11	-0.24	-0.12	-0.13	0.04	-0.03	**0.39**	0.03	-0.04
Piskurozymaceae (3%)	0.13	-0.2	-0.06	-0.14	**-0.36**	-0.09	-0.15	0.21	-0.11	0	0.15
Mortierellaceae (3%)	-0.02	-0.16	-0.12	-0.08	**-0.39**	-0.11	-0.12	0.14	-0.11	-0.01	**0.3**
Russulaceae (12%)	**-0.42**	-0.07	0.21	-0.15	**0.36**	0.05	0.08	-0.13	0.21	0.21	**-0.4**
Functional guilds											
Ectomycorrhizae (ECM)	**-0.38**	0.03	0.23	-0.06	**0.39**	0.04	**0.3**	-0.22	0.16	0.22	**-0.25**
Arbuscular mycorrhizae (AM)	0.01	-0.1	0.04	-0.07	0.07	0.05	-0.08	0.03	-0.07	-0.02	**-0.32**
Wood Saprotrophs	0.13	-0.05	-0.21	0.06	0.08	0.15	0.09	0.03	0.15	0.16	0.04
All Saprotrophs	-0.01	-0.04	-0.16	0.02	0.19	0.17	0.13	-0.17	0.07	0.07	-0.08

Table S4 (Continued)

Oa	AG	BG	BX	CB	AP	LAP	NAG	PER	POX	CRmass	pH
Ophiocordycipitaceae (1%)	0.01	0.13	0.05	0.16	-0.08	0.17	-0.05	**0.48**	-0.09	0.06	-0.18
Chaetosphaeriaceae (1%)	-0.31	-0.25	-0.27	**-0.33**	-0.1	-0.13	**-0.33**	0.17	-0.24	-0.19	0.03
Thelephoraceae (2%)	0.02	0.05	0.05	-0.14	0.16	-0.2	-0.07	0.24	0.11	0.07	-0.12
Gloniaceae (2%)	0.02	0.02	-0.07	0.02	0.11	-0.13	0.18	0.16	**0.51**	0.21	**-0.62**
Elaphomycetaceae (2%)	-0.04	-0.03	-0.08	-0.06	0.07	-0.08	0.06	0.28	**0.46**	**0.27**	**-0.31**
Piskurozymaceae (3%)	0.29	-0.22	-0.15	-0.24	-0.24	0.16	-0.16	**-0.48**	**-0.33**	-0.01	**0.5**
Mortierellaceae (3%)	0.1	-0.1	**-0.36**	-0.09	-0.27	**0.31**	-0.11	**-0.34**	-0.16	0.15	**0.51**
Russulaceae (12%)	-0.15	0.15	0.16	0.2	0.03	0.12	0.01	**0.31**	**0.3**	0.06	**-0.24**
Functional guilds											
Ectomycorrhizae (ECM)	0.01	0.02	-0.04	0.06	-0.04	0.06	0.01	0.25	0.25	-0.07	-0.18
Arbuscular mycorrhizae (AM)	0.29	-0.18	0.05	-0.13	-0.03	-0.02	-0.01	-0.08	0.16	**-0.25**	-0.01
Wood Saprotrophs	0.08	-0.09	**-0.37**	0.02	-0.28	**0.32**	-0.19	**0.38**	0.05	-0.03	**-0.3**
All Saprotrophs	0.08	-0.18	-0.25	0.02	-0.29	0.23	-0.17	0.19	0.05	-0.01	-0.2

Table S5 Correlations between ASV abundance and EEA for the most abundant bacteria (and % relative abundance) at the taxonomic level of family, where available. Significant spearman correlation coefficients (ρ) are in bold. Values in green indicate positive correlations and values in red indicate negative correlations. Increasing color intensity corresponds to the level of significance ($\alpha = 0.05$, $\alpha = 0.001$, $\alpha = 0.0005$). AG, a-glucosidase; AP, Acid Phosphatase; BG, β-glucosidase; BX, β-Xylosidase; CB, Cellobiohydrolase; NAG, N-acetyl glucosaminidase; LAP, Leucine aminopeptidase; PER, Peroxidase; POX, Phenol Oxidase; CRmass, Cumulative C respired in a 60d incubation.

Oe	AG	BG	BX	CB	AP	LAP	NAG	PER	POX	CRmass	pH
Methylocystaceae (1%)	0.21	0.07	0.27	0.06	**0.31**	-0.2	-0.01	-0.07	-0.09	0.04	**-0.42**
Syntrophobacteraceae (2%)	-0.19	-0.22	-0.06	**-0.33**	0.05	-0.28	-0.25	0.04	0.16	0	**-0.42**
Bradyrhizobiaceae (3%)	0.07	0.03	-0.16	0.05	-0.12	0.08	0.11	0.2	0.06	0.23	**0.53**
Koribacteraceae (3%)	-0.23	-0.13	0.06	-0.11	0.17	0.11	-0.02	-0.27	0.25	-0.07	-0.12
Sinobacteraceae (4%)	0	**0.32**	0.23	0.19	**0.36**	-0.1	-0.05	0.02	-0.09	-0.04	-0.19
Rhodospirillaceae (5%)	-0.15	-0.2	-0.28	0.01	-0.21	0.25	-0.11	-0.08	0	-0.02	**0.41**
Hyphomicrobiaceae (7%)	-0.05	0.19	0.1	0.22	-0.16	0.15	-0.07	0.01	-0.07	**-0.27**	**0.34**
Streptosporangiales_f (17%)	-0.28	-0.16	0.15	-0.29	0.24	**-0.36**	-0.13	0.01	0.07	0.12	**-0.74**

Table S5 (Continued)

Oa	AG	BG	BX	CB	AP	LAP	NAG	PER	POX	CRmass	pH
Methylocystaceae (1%)	0	0.04	-0.02	0.11	-0.01	-0.15	-0.12	**0.44**	0.21	**0.26**	**-0.49**
Syntrophobacteraceae (2%)	0.06	-0.07	**0.34**	-0.25	**0.34**	**-0.62**	0.15	-0.14	0.23	0.05	**-0.32**
Bradyrhizobiaceae (3%)	-0.23	0.05	-0.24	0.18	-0.08	0.25	0.03	0.12	0.04	0.23	0.09
Koribacteraceae (3%)	-0.15	-0.06	-0.08	0.12	-0.14	**0.31**	-0.13	0.25	0.11	-0.02	-0.11
Sinobacteraceae (4%)	0.16	0.28	-0.09	**0.37**	-0.04	**0.36**	0.26	-0.17	**-0.38**	0.22	**0.41**
Rhodospirillaceae (5%)	-0.13	-0.24	0.01	-0.25	-0.09	-0.12	-0.17	0.03	0.16	**-0.32**	0.11
Hyphomicrobiaceae (7%)	-0.28	0.08	-0.21	0.01	-0.16	0.1	-0.05	**0.3**	0	0.15	0.04
Streptosporangiales_f (17%)	-0.2	-0.08	**0.3**	-0.03	0.18	**-0.3**	-0.1	0.29	**0.45**	0.05	**-0.57**

Table S6 Secretion-signal bearing oxidases in genomes of major taxa

Domain	Species	# of secretion-signal bearing oxidases	NCBI Assembly Accession
Bacteria	Actinomadura rifamycini	3	GCF_000425065.1
Bacteria	Actinomadura oligospora	3	GCF_000518265.1
Bacteria	Actinomadura sp. NEAU-G17	3	GCF_003428695.1
Bacteria	Actinomadura sp. WAC 06369	3	GCF_003947565.1
Bacteria	Actinomadura montaniterrae	3	GCF_008923365.1
Bacteria	Actinomadura fibrosa	3	GCF_900659615.1
Bacteria	Actinomadura kijaniata	2	GCF_001552175.1
Bacteria	Actinomadura rubrobrunea	2	GCF_001552235.1
Bacteria	Actinomadura viridilutea	2	GCF_003001795.1
Bacteria	Actinomadura umbrina	2	GCF_003386555.1
Bacteria	Actinomadura amylolytica	2	GCF_003589885.1
Bacteria	Actinomadura sp. NEAU-Ht49	2	GCF_003696215.1
Bacteria	Actinomadura sp. NEAU-AAG5	2	GCF_009733595.1
Bacteria	Actinomadura sp. J1-007	2	GCF_009793335.1
Bacteria	Actinomadura verrucosospora	2	GCF_013211575.1
Bacteria	Actinomadura madurae	1	GCA_000715965.1
Bacteria	Actinomadura parvosata	1	GCA_900323885.1
Bacteria	Actinomadura formosensis	1	GCF_001552155.1
Bacteria	Actinomadura sp. 7K534	1	GCF_004348575.1
Bacteria	Actinomadura geliboluensis	1	GCF_005889745.1
Bacteria	Actinomadura rudentiformis	1	GCF_008923185.1

Table S6 (Continued)

Bacteria	Actinomadura sp. LD22	1	GCF_008923205.1
Bacteria	Actinomadura sp. LD22	1	GCF_008923205.2
Bacteria	Actinomadura sp. RB68	1	GCF_009604375.1
Bacteria	Actinomadura bangladeshensis	1	GCF_010548065.1
Bacteria	Actinomadura echinospora	1	GCF_900108175.1
Bacteria	Actinomadura formosensis	1	GCF_900659625.1
Bacteria	Actinomadura roseirufa	1	GCF_900659635.1
Bacteria	Actinomadura citrea	0	GCA_013409045.1
Bacteria	Actinomadura luteofluorescens	0	GCA_013409365.1
Bacteria	Actinomadura flavalba	0	GCF_000374305.1
Bacteria	Actinomadura atramentaria	0	GCF_000381885.1
Bacteria	Actinomadura madurae	0	GCF_000468475.2
Bacteria	Actinomadura chibensis	0	GCF_001552135.1
Bacteria	Actinomadura latina	0	GCF_001552195.1
Bacteria	Actinomadura macra	0	GCF_001552215.1
Bacteria	Actinomadura hibisca	0	GCF_001552635.1
Bacteria	Actinomadura sp. CNU-125	0	GCF_001942465.1
Bacteria	Actinomadura sp. RB29	0	GCF_002911665.1
Bacteria	Actinomadura sp. LHW63021	0	GCF_003289645.1
Bacteria	Actinomadura sp. LHW52907	0	GCF_003432485.1
Bacteria	Actinomadura pelletieri	0	GCF_003634705.1
Bacteria	Actinomadura bangladeshensis	0	GCF_004348335.1
Bacteria	Actinomadura sp. 7K507	0	GCF_004348425.1
Bacteria	Actinomadura sp. KC345	0	GCF_004348515.1
Bacteria	Actinomadura sp. KC216	0	GCF_004348535.1

Table S6 (Continued)

Bacteria	Actinomadura sp. GC306	0	GCF_004348665.1
Bacteria	Actinomadura sp. KC06	0	GCF_004348735.1
Bacteria	Actinomadura sp. H3C3	0	GCF_004349215.1
Bacteria	Actinomadura darangshiensis	0	GCF_004349235.1
Bacteria	Actinomadura sp. 6K520	0	GCF_004349245.1
Bacteria	Actinomadura sp. 14C53	0	GCF_005889715.1
Bacteria	Actinomadura sp. WMMA1423	0	GCF_006547145.1
Bacteria	Actinomadura hallensis	0	GCF_006716765.1
Bacteria	Actinomadura chibensis	0	GCF_008085895.1
Bacteria	Actinomadura syzygii	0	GCF_008085905.1
Bacteria	Actinomadura sp. CYP1-5	0	GCF_008121305.1
Bacteria	Actinomadura sp. K4S16	0	GCF_008327685.1
Bacteria	Actinomadura rayongensis	0	GCF_009831215.1
Bacteria	Actinomadura sp. DSM 109109	0	GCF_010491635.1
Bacteria	Actinomadura latina	0	GCF_012396395.1
Bacteria	Actinomadura sp. NAK00032	0	GCF_013364275.1
Bacteria	Actinomadura sp. BRA 177	0	GCF_013372625.1
Bacteria	Actinomadura madurae	0	GCF_900115095.1
Bacteria	Actinomadura mexicana	0	GCF_900188105.1
Bacteria	Actinomadura meyerae	0	GCF_900188445.1
Bacteria	Actinomadura madurae	0	GCF_900445005.1
Fungi	Cenococcum geophilum	1	GCA_001692895.1
Fungi	Glonium stellatum	1	GCA_001692915.1
Fungi	Solicoccozyma phenolica	0	GCA_001600015.1
Fungi	Solicoccozyma terricola	0	GCA_001600875.1
Fungi	Solicoccozyma terricola	0	GCA_001712455.1

CHAPTER 2

SUPPLEMENTARY MATERIAL

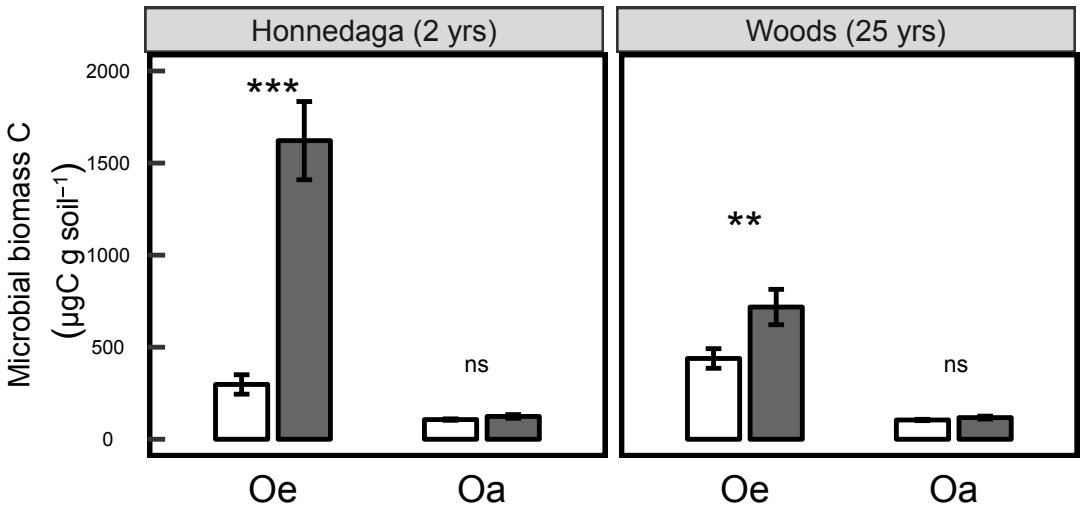

Figure S1 Mean ± SE SIR microbial biomass C at the short-term site (pre-treatment and 2 years after liming) and long-term site (25 years after liming) summarized by horizon. Significant pairwise differences within time-scale and horizon groupings are denoted by lettering (Tukey HSD; '*' $P_{adj} \leq 0.05$, '**' $P_{adj} \leq 0.01$, '***' $P_{adj} \leq 0.001$).

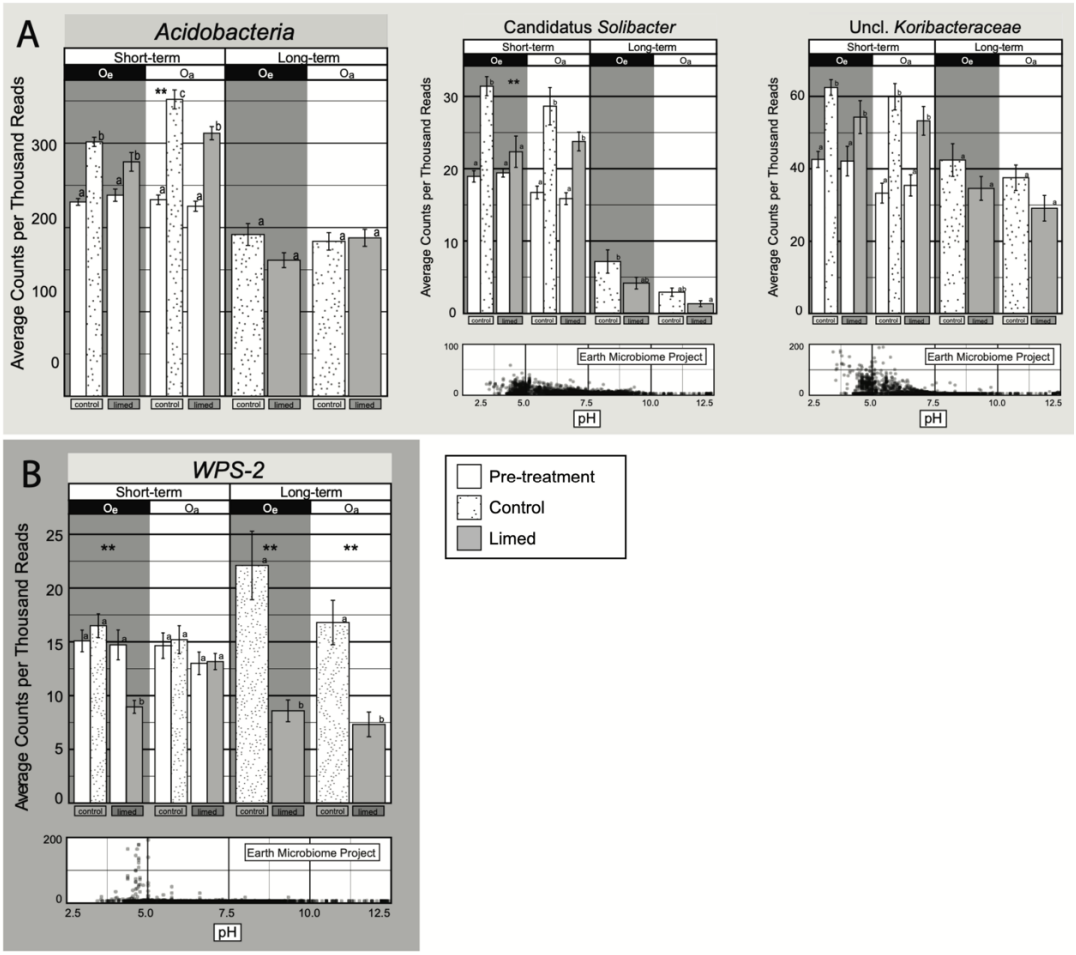

Figure S2 Acidophilic bacteria were negatively impacted by liming in short-term (2 years) and long-term (25 years). Panel below shows the pH at which ASVs found in this study are found globally. Data on global soil sample pH are from the Earth Microbiome Project database. Significant pairwise differences within time-scale and horizon groupings are denoted by lettering (Tukey HSD; '*' $P_{adj} \leq 0.05$, '**' $P_{adj} \leq 0.01$, '***' $P_{adj} \leq 0.001$).

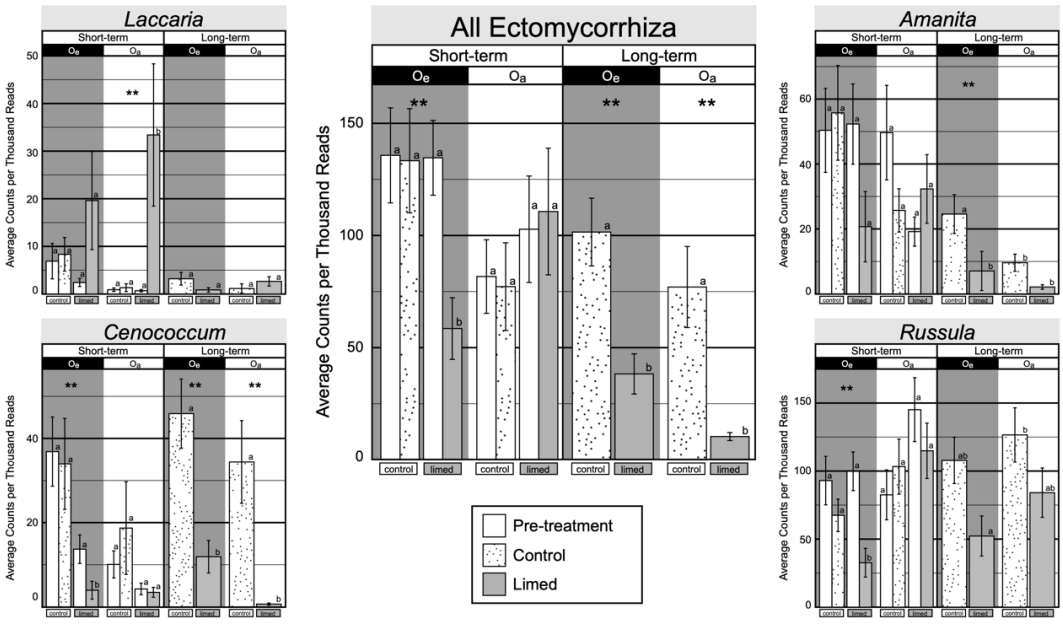

Figure S3 Ectomycorrhizal populations including *Amanita*, *Russula*, and *Cenococcum* were negatively impacted by liming in the short- (2 years) and long-term (25 years), while *Laccaria* populations increased at the short-term site. Significant pairwise differences within time-scale and horizon groupings are denoted by lettering (Tukey HSD; '*' $P_{adj} \leq 0.05$, '**' $P_{adj} \leq 0.01$, '***' $P_{adj} \leq 0.001$).

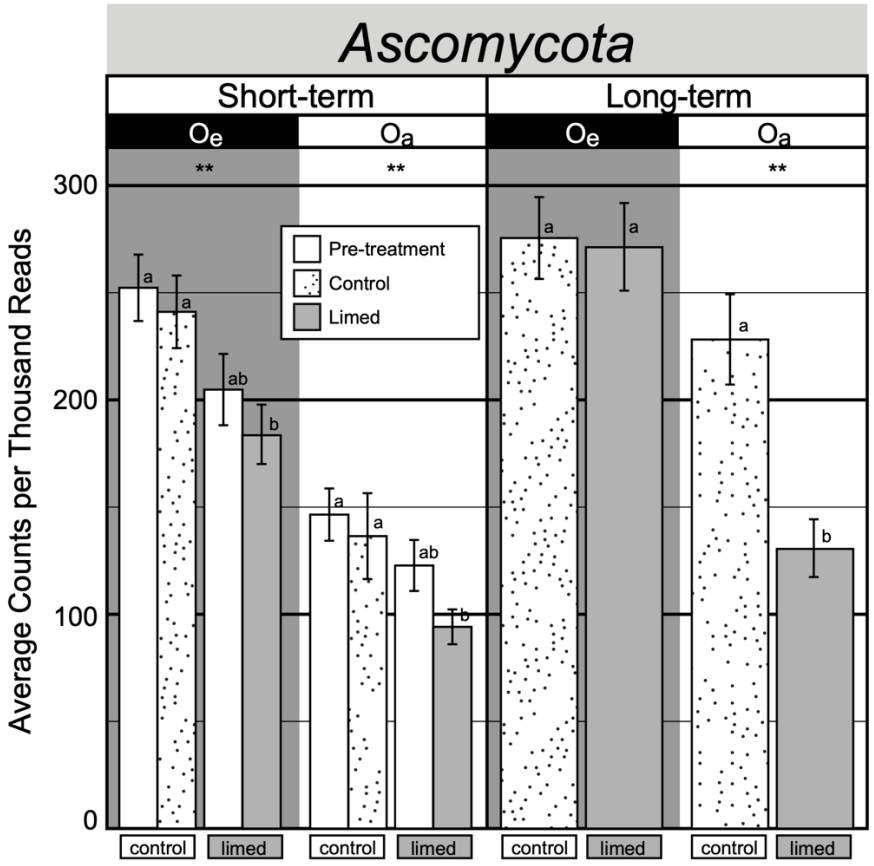

Figure S4 The relative abundance of phylum *Ascomycota* was lower in limed soils at both short-term (2 years) and long-term (25 years) sites. Significant pairwise differences within time-scale and horizon groupings are denoted by lettering (Tukey HSD; '*' $P_{adj} \leq 0.05$, '**' $P_{adj} \leq 0.01$, '***' $P_{adj} \leq 0.001$).

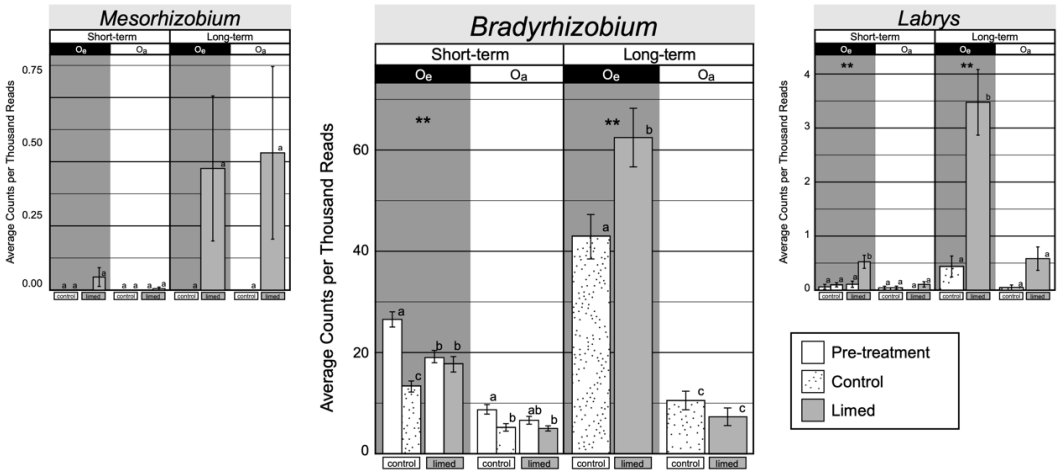

Figure S5 Members of *Rhizobiales* were relatively more abundant in limed soils in the short-term (2 years) and long-term (25 year) sites. Significant pairwise differences within time-scale and horizon groupings are denoted by lettering (Tukey HSD; '*' $P_{adj} \leq 0.05$, '**' $P_{adj} \leq 0.01$, '***' $P_{adj} \leq 0.001$).

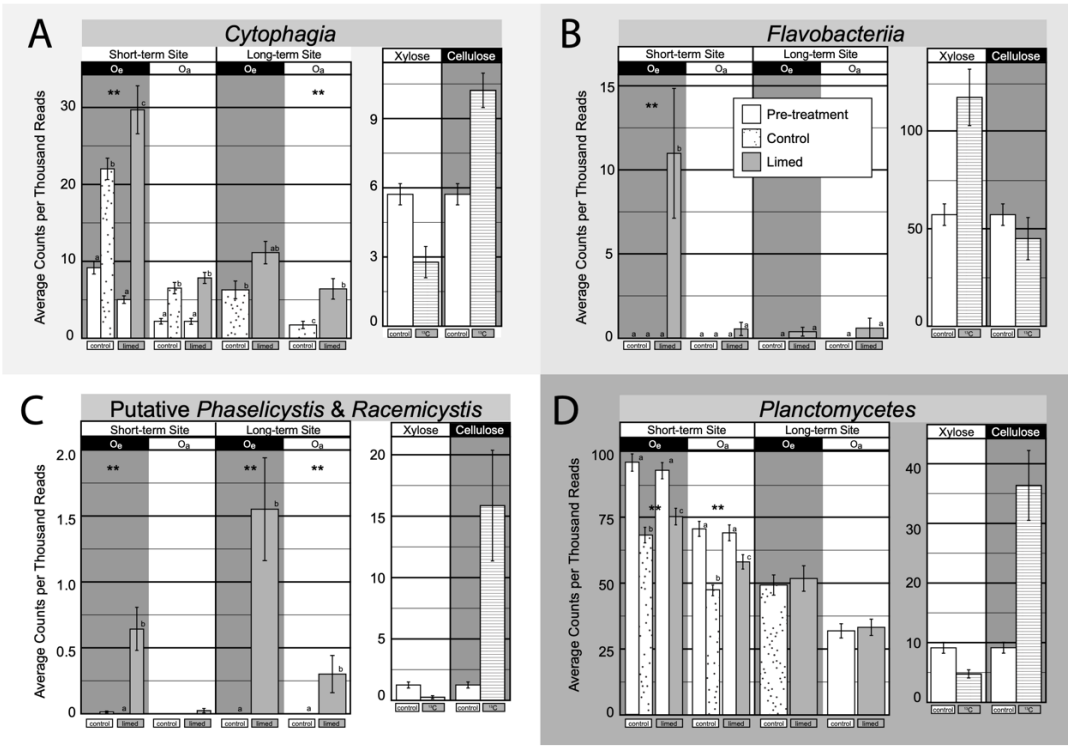

Figure S6 Members of *Bacteroidetes* (AB), *Proteobacteria* (C), and *Planctomycetes* (D) that were favored by liming in short-term (2 years) and long-term (25 years). These bacteria were associated with cellulose and xylose degradation in stable isotope probing experiments (Data from Koechli et al. *in prep*). Significant pairwise differences within time-scale and horizon groupings are denoted by lettering (Tukey HSD; '*' $P_{adj} \leq 0.05$, '**' $P_{adj} \leq 0.01$, '***' $P_{adj} \leq 0.001$).

Table S1 Statistical testing of pre-treatment differences in sample community composition between to-be-limed and control subcatchments at the short-term site with PERMANOVA based on Bray-Curtis dissimilarities (nperm = 999).

A: Pre-treatment PERMANOVA for Fungi at Short-term site

Variable	**Df**	**SumsOfSqs**	**MeanSqs**	**F.Model**	**R2**	**P**	**Sig.**
treatment	1	0.893	0.89333	2.8885	0.027	0.0009	***
plot	4	3.59	0.89744	2.9017	0.108	0.0009	***
horizon	1	1.561	1.56086	5.0468	0.047	0.0009	***
Residuals	87	26.907	0.30928	0.81658			
Total	93	32.951	1				

B: Pre-treatment PERMANOVA for Bacteria at Short-term site

Variable	**Df**	**SumsOfSqs**	**MeanSqs**	**F.Model**	**R2**	**P**	**Sig.**
treatment	1	0.3744	0.3744	2.874	0.021	0.0059	**
plot	4	0.953	0.2383	1.828	0.055	0.0049	**
horizon	1	4.3204	4.3204	33.156	0.252	0.0009	***
Residuals	88	11.4669	0.1303	0.67			
Total	94	17.1148	1				
Significance codes	'***'	0.001	'**'	0.01	'*'	0.05	'.'

Table S2 Statistical testing of treatment differences in sample community composition between limed and control subcatchments at the short-term and long-term site with PERMANOVA based on Bray-Curtis dissimilarities (nperm = 999).

A: Post-treatment PERMANOVA for Fungi at Short-term site

Variable	Df	SumsOfSqs	MeanSqs	F.Model	R2	P	Sig.
treatment	1	1.211	1.21068	3.555	0.034	0.0009	***
plot	4	3.319	0.82984	2.4367	0.094	0.0009	***
horizon	1	1.308	1.30757	3.8395	0.037	0.0009	***
Residuals	86	29.288	0.34056	0.83381			
Total	92	35.126	1				

B: Post-treatment PERMANOVA for Bacteria at Short-term site

Variable	Df	SumsOfSqs	MeanSqs	F.Model	R2	P	Sig.
treatment	1	0.515	0.515	2.8288	0.024	0.0019	**
plot	4	1.3961	0.349	1.9171	0.065	0.0009	***
horizon	1	3.4562	3.4562	18.9846	0.162	0.0009	***
Residuals	87	15.8388	0.1821	0.7469			
Total	93	21.2061	1				

Table S2 (Continued)

C: Post-treatment PERMANOVA for Fungi at Long-term site

Variable	Df	SumsOfSqs	MeanSqs	F.Model	R2	P	Sig.
treatment	1	1.863	1.8628	5.1647	0.03	0.0009	***
watershed	2	1.874	0.9372	2.5984	0.03	0.0009	***
plot	4	2.581	0.6451	1.7887	0.04	0.0009	***
horizon	1	3.512	3.5125	9.7383	0.05	0.0009	***
Residuals	142	51.217	0.3607	0.83897			
Total	150	61.047	1				

D: Post-treatment PERMANOVA for Bacteria at Long-term site

Variable	Df	SumsOfSqs	MeanSqs	F.Model	R2	P	Sig.
treatment	1	2.083	2.0829	8.22	0.04	0.0009	***
watershed	2	1.186	0.5932	2.3	0.02	0.0019	**
plot	4	1.423	0.3558	1.406	0.03	0.0179	*
horizon	1	6.98	6.9801	27.58	0.15	0.0009	***
Residuals	135	34.166	0.2531	0.745			
Total	143	45.839	1				
Significance codes	'***'	0.001	'**'	0.01	'*'	0.05	'.'

Table S3 Analysis of Similarity (ANOSIM) of microbial community composition between limed and control subcatchments at the short- and long-term site (nperm = 999).

Post-treatment short-term site | Oa | Fungi						
ANOSIM R:	-0.0011	Significance:	0.402			
Upper quantiles of permutations (null model):						
90%	95%	97.50%	99%			
0.0371	0.0559	0.076	0.0922			
Dissimilarity ranks between and within classes:						
	0%	25%	50%	75%	100%	N
Between	1	237.5	451	680.75	903	462
control_post	5	231.5	507	733	902	231
limed_post	4	197.5	404.5	620.25	899	210

Post-treatment short-term site | Oe | Fungi						
ANOSIM R:	0.1598	Significance:	0.002	**		
Upper quantiles of permutations (null model):						
90%	95%	97.50%	99%			
0.0379	0.0569	0.0795	0.104			
Dissimilarity ranks between and within classes:						
	0%	25%	50%	75%	100%	N
Between	1	360	614	814.5	1081	550
control_post	3	182	450	874.25	1077	300
limed_post	2	210.5	421	762	1064	231

Table S3 (Continued)

Post-treatment short-term site | Oa | Bacteria						
ANOSIM R:	-0.0246	Significance:	0.856			
Upper quantiles of permutations (null model):						
90%	95%	97.50%	99%			
0.0326	0.05	0.0655	0.0836			
Dissimilarity ranks between and within classes:						
	0%	25%	50%	75%	100%	N
Between	1	254.5	510.5	774.25	1033	528
control_post	4	267.5	571.5	836.5	1035	276
limed_post	5	266.5	487	712	1008	231

Post-treatment short-term site | Oe | Bacteria						
ANOSIM R:	0.06799	Significance:	0.02	*		
Upper quantiles of permutations (null model):						
90%	95%	97.50%	99%			
0.0333	0.0464	0.0633	0.0823			
Dissimilarity ranks between and within classes:						
	0%	25%	50%	75%	100%	N
Between	4	319.5	604	835	1128	575
control_post	1	182.75	412	840.5	1120	300
limed_post	5	355	633	867	1121	253

Table S3 (Continued)

Post-treatment long-term site | Oa | Fungi						
ANOSIM R:	0.5576	Significance:	0.001	***		
Upper quantiles of permutations (null model):						
90%	95%	97.50%	99%			
0.0251	0.0363	0.0499	0.0622			
Dissimilarity ranks between and within classes:						
	0%	25%	50%	75%	100%	N
Between	8	1291	1975	2440.5	2850	1443
control	1	423	908	1527	2818	741
limed	7	443.75	952	1511.25	2668	666
Post-treatment long-term site | Oe | Fungi						
ANOSIM R:	0.7502	Significance:	0.001	***		
Upper quantiles of permutations (null model):						
90%	95%	97.50%	99%			
0.0253	0.0378	0.0505	0.0667			
Dissimilarity ranks between and within classes:						
	0%	25%	50%	75%	100%	N
Between	2	1513.5	2034.5	2419.25	2775	1404
control	1	385	806	1250	2192	741
limed	3	371.75	782.5	1291.75	2573	630

Table S3 (Continued)

Post-treatment long-term site | Oa | Bacteria						
ANOSIM R:	0.03782	Significance:	0.055			
Upper quantiles of permutations (null model):						
90%	95%	97.50%	99%			
0.0275	0.0392	0.0528	0.0683			
Dissimilarity ranks between and within classes:						
	0%	25%	50%	75%	100%	N
Between	2	722	1399	2055	2700	1365
control	1	500	1069	1717	2683	741
limed	12	889.5	1687	2293.5	2701	595
Post-treatment long-term site | Oe | Bacteria						
ANOSIM R:	0.2233	Significance:	0.001	***		
Upper quantiles of permutations (null model):						
90%	95%	97.50%	99%			
0.027	0.041	0.0544	0.0707			
Dissimilarity ranks between and within classes:						
	0%	25%	50%	75%	100%	N
Between	1	779	1398	1937	2415	1221
control	2	408.5	927.5	1574.75	2385	528
limed	3	532.25	1081	1665.5	2409	666

Table S3 (Continued)

Pre-treatment short-term site | Oa | Fungi						
ANOSIM R:	-0.0217	Significance:	0.761			
Upper quantiles of permutations (null model):						
90%	95%	97.50%	99%			
0.0406	0.0619	0.0797	0.107			
Dissimilarity ranks between and within classes:						
	0%	25%	50%	75%	100%	N
Between	1	271.25	529.5	797.75	1080	550
control_pre	5	284.75	569.5	839.5	1081	300
limed_pre	2	262.5	534	789	1075	231

Pre-treatment short-term site | Oe | Fungi						
ANOSIM R:	-0.0137	Significance:	0.655			
Upper quantiles of permutations (null model):						
90%	95%	97.50%	99%			
0.0335	0.0505	0.0664	0.0852			
Dissimilarity ranks between and within classes:						
	0%	25%	50%	75%	100%	N
Between	1	260.25	538.5	801.25	1080	552
control_pre	2	271.25	506.5	790	1077	276
limed_pre	8	298	571	843	1081	253

Table S3 (Continued)

Pre-treatment short-term site | Oa | Bacteria						
ANOSIM R:	0.08225	Significance:	0.012	*		
Upper quantiles of permutations (null model):						
90%	95%	97.50%	99%			
0.0338	0.0482	0.0649	0.0846			
Dissimilarity ranks between and within classes:						
	0%	25%	50%	75%	100%	N
Between	4	318.25	578.5	818.75	1081	550
control_pre	2	214.5	445.5	789.25	1079	300
limed_pre	1	278	563	802	1055	231

Pre-treatment short-term site | Oe | Bacteria						
ANOSIM R:	0.2156	Significance:	0.001	***		
Upper quantiles of permutations (null model):						
90%	95%	97.50%	99%			
0.032	0.0465	0.058	0.0694			
Dissimilarity ranks between and within classes:						
	0%	25%	50%	75%	100%	N
Between	2	384.5	661	878.5	1127	575
control_pre	1	196.75	433	721.5	1128	300
limed_pre	5	229	487	848	1098	253

Table S4: Strong responders (response ratio >10) to liming common to multiple methods of analysis (indicspeceis and limma), and their taxonomic classification. All strong responders were u_ at the rank of species. Prefix p_ stands for "putative", u_ for "unclassified", c_ for "Candidatus", and suffix _is for "Incertae_sedis"

Response to liming	Site	Soil Horizon	Domain	Phylum	Class	Order	Family	Genus	Oa Abundance	Oe Abundance	Statistic	Adjusted p-value	Response Ratio
Increased	Both	Oe	Bacteria	Proteobacteria	Deltaproteobacteria	Myxococcales	u_BIrii41	u_BIrii41	0.002	0.267	41.28	0	271.3
Increased	Woods	both	Fungi	Basidiomycota	Agaricomycetes	Sebacinales	Sebacinaceae	Sebacina	1.347	0.864	19.38	0.0075	264
Increased	Both	Oe	Bacteria	Proteobacteria	Alphaproteobacteria	Rhizobiales	Rhizobiaceae	Rhizobium	0.094	0.249	20.94	0.0012	253.5
Increased	Both	Oe	Bacteria	Proteobacteria	Alphaproteobacteria	Caulobacterales	Caulobacteraceae	Phenylobacterium	0.04	0.142	24.46	0.0003	219.5
Increased	Both	Oe	Bacteria	Proteobacteria	Alphaproteobacteria	Ellin329	u_Ellin329	u_Ellin329	0	0.346	15.05	0.0082	217.9
Decreased	Both	both	Fungi	Ascomycota	Dothideomycetes	Hysteriales	Gloniaceae	Cenococcum	0.681	0.576	17.84	0.0037	202.1
Decreased	Both	both	p_Fungi	p_Basidiomycota	p_Agaricomycetes	p_Boletales	u_p_Boletales	u_p_Boletales	0.236	0.178	23.22	0.0007	159.4
Decreased	Both	Oe	Bacteria	Bacteroidetes	Cytophagia	Cytophagales	Cytophagaceae	Cytophaga	0.003	0.074	26.7	0.0002	119.4
Increased	Both	Oe	Bacteria	Proteobacteria	Alphaproteobacteria	Rhizobiales	Rhizobiaceae	Rhizobium	0.004	0.483	16.71	0.0049	114.3
Increased	Honnedaga	both	Fungi	u_Fungi	u_Fungi	u_Fungi	u_Fungi	u_Fungi	0.055	0.104	19.59	0.0047	107.2
Increased	Woods	both	Fungi	Basidiomycota	Agaricomycetes	Thelephorales	Thelephoraceae	Tomentella	0.269	2.137	26.06	0.0011	100.8
Decreased	Woods	both	Fungi	u_Fungi	u_Fungi	u_Fungi	u_Fungi	u_Fungi	0.108	0.318	15.16	0.0066	100
Increased	Both	both	Bacteria	Chlamydiae	Chlamydiia	Chlamydiales	Parachlamydiaceae	c_protochlamydia	0.032	0.053	21.05	0.0012	89.9
Increased	Both	Oe	Bacteria	Proteobacteria	Deltaproteobacteria	Myxococcales	u_BIrii41	u_BIrii41	0.003	0.086	16.77	0.0049	85
Decreased	Both	both	Fungi	u_Fungi	u_Fungi	u_Fungi	u_Fungi	u_Fungi	0.223	0.234	20.52	0.0015	82.1
Decreased	Honnedaga	Oe	Fungi	Basidiomycota	Tremellomycetes	Cystofilobasidiales	Cystofilobasidiaceae	Guehomyces	3.475	1.147	17.23	0.0054	79.5
Increased	Both	both	Fungi	Ascomycota	Sordariomycetes	Chaetosphaeriales	Chaetosphaeriaceae	u_Chaetosphaeriaceae	0.098	1.187	16.05	0.0054	77.9
Increased	Both	both	Fungi	u_Fungi	u_Fungi	u_Fungi	u_Fungi	u_Fungi	0.198	0.102	16.06	0.0054	73.7
Decreased	Woods	Oe	Bacteria	Actinobacteria	Actinobacteria	Actinomycetales	u_Actinomycetales	u_Actinomycetales	0.006	0.726	0.52	0.0169	73.6
Increased	Honnedaga	Oe	Fungi	Zygomycota	Mortierellomycotina_cls_is	Mortierellales	Mortierellaceae	Mortierella	0.03	0.135	17.78	0.0052	72.5
Increased	Woods	Oa	Fungi	Ascomycota	Sordariomycetes	Hypocreales	Clavicipitaceae	Metarhizium	0.136	0.213	21.28	0.0061	68.5
Decreased	Honnedaga	both	Fungi	u_Fungi	u_Fungi	u_Fungi	u_Fungi	u_Fungi	0.054	0.06	0.35	0.0424	61.7
Decreased	Honnedaga	both	Fungi	Basidiomycota	Tremellomycetes	Cystofilobasidiales	Cystofilobasidiaceae	Guehomyces	3.154	0.263	19.59	0.0006	58.6
Increased	Both	both	Bacteria	Proteobacteria	Alphaproteobacteria	Rhodospirillales	Rhodospirillaceae	u_Rhodospirillaceae	0.179	0.57	15.53	0.0043	51.6
Increased	Both	both	Bacteria	Actinobacteria	Thermoleophilia	Solirubrobacterales	u_Solirubrobacterales	u_Solirubrobacterales	0.844	2.439	58.94	0	48.8
Decreased	Woods	both	Fungi	Ascomycota	Sordariomycetes	Hypocreales	Ophiocordycipitaceae	Tolypocladium	3.491	2.143	20.03	0.0046	48.5
Increased	Woods	both	Fungi	u_Fungi	u_Fungi	u_Fungi	u_Fungi	u_Fungi	0.003	0.053	0.38	0.0271	48.2
Increased	Honnedaga	both	Protista	Cercozoa	unidentified	unidentified	unidentified	unidentified	0.078	0.133	58.21	0	48
Increased	Woods	both	Fungi	Ascomycota	Sordariomycetes	Hypocreomycetidae_ord_is	Plectosphaerellaceae	Verticillium	0	0.115	0.33	0.0424	46.5
Increased	Honnedaga	both	Fungi	u_Fungi	u_Fungi	u_Fungi	u_Fungi	u_Fungi	0.019	0.09	19.62	0.0006	46.2
Increased	Honnedaga	both	Fungi	u_Fungi	u_Fungi	u_Fungi	u_Fungi	u_Fungi	1.468	0.886	19.06	0.0049	44.6
Increased	Woods	both	Bacteria	Proteobacteria	Gammaproteobacteria	Xanthomonadales	Sinobacteraceae	u_Sinobacteraceae	0.643	0.406	20.45	0.0021	44.2
Decreased	Honnedaga	Oe	Fungi	Basidiomycota	Tremellomycetes	Cystofilobasidiales	Cystofilobasidiaceae	Guehomyces	1.89	0.607	17.23	0.0054	42.9
Increased	Honnedaga	Oe	Fungi	Basidiomycota	Agaricomycetes	Agaricales	Clavariaceae	unidentified	0.005	0.252	26.59	0.0006	42.7
Increased	Both	both	Bacteria	Proteobacteria	Alphaproteobacteria	Rhizobiales	Hyphomicrobiaceae	Devosia	0.106	1.554	53.09	0	41.7
Increased	Both	Oe	Bacteria	Planctomycetes	Planctomycetia	Planctomycetales	Planctomycetaceae	Planctomyces	0.048	0.407	16.74	0.0049	40.5
Increased	Honnedaga	both	Fungi	Basidiomycota	Agaricomycetes	Russulales	Russulaceae	Russula	1.697	0.384	15.88	0.0022	39.4
Decreased	Both	both	p_Fungi	p_Ascomycota	p_Leotiomycetes	u_p_Leotiomycetes	u_p_Leotiomycetes	u_p_Leotiomycetes	0.14	0.18	16.31	0.0052	38.5
Increased	Both	Oe	Bacteria	Actinobacteria	Actinobacteria	Actinomycetales	Micromonosporaceae	Dactylosporangium	0.034	0.504	24.71	0.0003	38
Increased	Both	both	Bacteria	Proteobacteria	Deltaproteobacteria	Myxococcales	Haliangiaceae	u_Haliangiaceae	0.367	1.042	27.62	0.0001	35.3
Increased	Both	both	Fungi	u_Fungi	u_Fungi	u_Fungi	u_Fungi	u_Fungi	0.02	0.068	0.32	0.0424	35
Decreased	Honnedaga	Oe	Fungi	Basidiomycota	Tremellomycetes	Cystofilobasidiales	Cystofilobasidiaceae	Guehomyces	1.516	0.476	17.15	0.0054	34.2
Increased	Honnedaga	Oe	Bacteria	Proteobacteria	Alphaproteobacteria	Rhodospirillales	Rhodospirillaceae	u_Rhodospirillaceae	0.028	0.192	40.94	0	34
Decreased	Honnedaga	Oe	Bacteria	Proteobacteria	Alphaproteobacteria	Ellin329	u_Ellin329	u_Ellin329	0.004	0.046	20.22	0.0007	33.8
Increased	Honnedaga	both	Fungi	u_Fungi	u_Fungi	u_Fungi	u_Fungi	u_Fungi	0.909	0.872	18.32	0.0009	33.8
Increased	Honnedaga	both	Fungi	u_Fungi	u_Fungi	u_Fungi	u_Fungi	u_Fungi	1.09	0.647	32.24	0	32.9
Increased	Both	Oe	Bacteria	Actinobacteria	Thermoleophilia	Gaiellales	Gaiellaceae	u_Gaiellaceae	0.136	1.5	42.65	0	32.2
Increased	Honnedaga	both	Fungi	u_Fungi	u_Fungi	u_Fungi	u_Fungi	u_Fungi	0.987	0.665	19.04	0.0049	31.3
Decreased	Both	both	Fungi	Ascomycota	u_Ascomycota	u_Ascomycota	u_Ascomycota	u_Ascomycota	0.034	0.115	15.61	0.0062	30.1
Decreased	Honnedaga	Oe	Fungi	u_Fungi	u_Fungi	u_Fungi	u_Fungi	u_Fungi	0.004	0.156	15.6	0.0072	30
Decreased	Both	Oe	Fungi	Zygomycota	Mortierellomycotina_cls_is	Mortierellales	Mortierellaceae	Mortierella	0.104	0.429	20.62	0.0065	30
Increased	Both	both	Fungi	u_Fungi	u_Fungi	u_Fungi	u_Fungi	u_Fungi	0.091	0.132	17.59	0.004	29.1
Increased	Both	Oe	Bacteria	Proteobacteria	Alphaproteobacteria	Rhizobiales	Hyphomicrobiaceae	Rhodoplanes	0	1.453	39.7	0	29.1
Increased	Both	Oe	Bacteria	Actinobacteria	Actinobacteria	Actinomycetales	Nocardioidaceae	Nocardioides	0.139	1.439	67.54	0	28.8
Increased	Woods	Oa	Bacteria	Proteobacteria	Gammaproteobacteria	Pseudomonadales	Moraxellaceae	u_Moraxellaceae	0.077	0.063	0.41	0.0488	28.6
Increased	Woods	Oe	Fungi	u_Fungi	u_Fungi	u_Fungi	u_Fungi	u_Fungi	0.008	0.453	0.7	0.0169	28.5
Increased	Both	both	Fungi	u_Fungi	u_Fungi	u_Fungi	u_Fungi	u_Fungi	0.325	1.059	23.33	0.0007	28.1

Decreased	Both	both	Fungi	u_ Fungi	u_ Fungi	u_ Fungi	u_ Fungi	u_ Fungi	0.305	0.13	18.32	0.0031	28
Increased	Woods	Oe	Bacteria	Proteobacteria	Gammaproteobacteria	Xanthomonadales	Sinobacteraceae	u_ Sinobacteraceae	0.006	0.669	27.54	0.0002	27.6
Increased	Woods	both	Fungi	u_ Fungi	u_ Fungi	u_ Fungi	u_ Fungi	u_ Fungi	0.099	0.12	20.43	0.0061	27.6
Increased	Honnedaga	Oe	Fungi	Ascomycota	Sordariomycetes	Hypocreales	Nectriaceae	Volutella	0.02	0.061	22.55	0.0021	27.3
Increased	Both	both	Bacteria	Actinobacteria	Thermoleophilia	Gaiellales	u_ Gaiellales	u_ Gaiellales	1.049	1.606	55.94	0	27.3
Decreased	Honnedaga	both	Fungi	Basidiomycota	Tremellomycetes	Cystofilobasidiales	Cystofilobasidiaceae	Guehomyces	1.454	0.122	19.05	0.0007	27
Increased	Both	Oe	Bacteria	Actinobacteria	Actinobacteria	Actinomycetales	Mycobacteriaceae	Mycobacterium	0	1.323	37.69	0	26.5
Increased	Both	both	Fungi	u_ Fungi	u_ Fungi	u_ Fungi	u_ Fungi	u_ Fungi	0.291	0.349	16.12	0.0053	26.2
Decreased	Both	Oe	Bacteria	Acidobacteria	Acidobacteriia	Acidobacteriales	Acidobacteriaceae	u_ Acidobacteriaceae	0.017	0.179	15.64	0.0066	26
Increased	Woods	both	Fungi	Basidiomycota	Agaricomycetes	Thelephorales	Thelephoraceae	u_ Thelephoraceae	0.001	0.175	0.32	0.0271	25.6
Decreased	Woods	both	Fungi	Basidiomycota	Agaricomycetes	Russulales	Russulaceae	Russula	13.303	26.352	27.04	0.0008	25.4
Increased	Woods	Oe	Fungi	u_ Fungi	u_ Fungi	u_ Fungi	u_ Fungi	u_ Fungi	0.017	0.137	0.46	0.0354	25.3
Increased	Both	both	Fungi	Zygomycota	Mortierellomycotina_cls_is	Mortierellales	Mortierellaceae	Mortierella	0.032	0.652	20.49	0.0065	25
Increased	Woods	Oe	Fungi	Ascomycota	u_ Ascomycota	u_ Ascomycota	u_ Ascomycota	u_ Ascomycota	0.006	0.96	17.94	0.0076	24.7
Increased	Both	both	Bacteria	Chloroflexi	Ellin6529	u_ Ellin6529	u_ Ellin6529	u_ Ellin6529	1.161	0.26	28.48	0.0005	24.5
Decreased	Both	Oa	Bacteria	Proteobacteria	Alphaproteobacteria	Rhizobiales	Methylocystaceae	u_ Methylocystaceae	1.292	0.062	41.38	0	24.5
Increased	Both	Oe	Bacteria	Actinobacteria	Thermoleophilia	Gaiellales	u_ Gaiellales	u_ Gaiellales	0.002	0.727	30.95	0	23.9
Decreased	Honnedaga	both	Fungi	u_ Fungi	u_ Fungi	u_ Fungi	u_ Fungi	u_ Fungi	1.006	0.379	26.01	0.0001	23.8
Decreased	Honnedaga	both	Bacteria	Proteobacteria	Betaproteobacteria	Burkholderiales	Oxalobacteraceae	u_ Oxalobacteraceae	0.052	0.028	0.37	0.0169	23.4
Increased	Both	both	Fungi	u_ Fungi	u_ Fungi	u_ Fungi	u_ Fungi	u_ Fungi	0.126	0.672	17.3	0.0044	22.6
Decreased	Honnedaga	both	Fungi	Basidiomycota	Tremellomycetes	Cystofilobasidiales	Cystofilobasidiaceae	Guehomyces	1.206	0.108	19.05	0.0007	22.5
Increased	Both	both	Protista	Cercozoa	unidentified	unidentified	unidentified	unidentified	0.063	0.045	15.13	0.0074	22
Increased	Both	Oe	Bacteria	Actinobacteria	Thermoleophilia	Gaiellales	u_ Gaiellales	u_ Gaiellales	0.007	1.077	16.7	0.0049	22
Increased	Honnedaga	both	Fungi	u_ Fungi	u_ Fungi	u_ Fungi	u_ Fungi	u_ Fungi	0.02	0.031	17.09	0.0014	21.9
Decreased	Woods	both	Bacteria	Proteobacteria	Alphaproteobacteria	Rhizobiales	Hyphomicrobiaceae	Rhodoplanes	0.634	0.107	19.26	0.0011	20.3
Increased	Honnedaga	Oe	Bacteria	Bacteroidetes	Sphingobacteriia	Sphingobacteriales	Sphingobacteriaceae	u_ Sphingobacteriaceae	0.005	0.145	31.95	0	20.2
Increased	Honnedaga	both	Fungi	u_ Fungi	u_ Fungi	u_ Fungi	u_ Fungi	u_ Fungi	0.516	0.534	18.37	0.0009	20
Decreased	Honnedaga	both	Fungi	u_ Fungi	u_ Fungi	u_ Fungi	u_ Fungi	u_ Fungi	0.966	0.192	25.07	0.0001	19.9
Increased	Both	Oe	Bacteria	Actinobacteria	Thermoleophilia	Solirubrobacterales	u_ Solirubrobacterales	u_ Solirubrobacterales	0.142	0.989	56.22	0	19.8
Increased	Both	Oe	Fungi	Ascomycota	Eurotiomycetes	Chaetothyriales	Herpotrichiellaceae	Cladophialophora	0.021	0.479	20.02	0.0076	19.5
Increased	Both	Oe	Bacteria	Actinobacteria	Actinobacteria	Actinomycetales	Streptosporangiaceae	Streptosporangium	0.051	0.356	16.2	0.0056	19.5
Increased	Woods	both	Bacteria	Proteobacteria	Alphaproteobacteria	Rhodospirillales	Rhodospirillaceae	u_ Rhodospirillaceae	1.073	0.346	0.4	0.0169	19.3
Decreased	Both	both	Fungi	Ascomycota	Dothideomycetes	Hysteriales	Gloniaceae	Cenococcum	2.147	2.666	33.59	0.0001	19.1
Increased	Woods	Oa	Bacteria	Actinobacteria	MB-A2-108	0319-7L14	u_ 0319-7L14	u_ 0319-7L14	0.82	0	23.07	0.0023	19
Decreased	Honnedaga	both	Fungi	Ascomycota	u_ Ascomycota	u_ Ascomycota	u_ Ascomycota	u_ Ascomycota	0.3	0.059	15.06	0.0084	19
Decreased	Honnedaga	both	Fungi	u_ Fungi	u_ Fungi	u_ Fungi	u_ Fungi	u_ Fungi	0.747	0.355	29.83	0	19
Decreased	Both	Oe	Bacteria	Bacteroidetes	Cytophagia	Cytophagales	Cytophagaceae	Sporocytophaga	0.004	0.038	16.75	0.0049	18.7
Increased	Honnedaga	Oe	p_ Bacteria	p_proteobacteria	p_ Betaproteobacteria	p_ Burkholderiales	p_ Comamonadaceae	p_ Variovorax	0.008	0.21	44.06	0	18.6
Increased	Honnedaga	both	Fungi	u_ Fungi	u_ Fungi	u_ Fungi	u_ Fungi	u_ Fungi	0.584	0.387	32	0	18.4
Increased	Woods	both	Fungi	u_ Fungi	u_ Fungi	u_ Fungi	u_ Fungi	u_ Fungi	0	0.04	0.34	0.0424	18.3
Increased	Woods	both	Bacteria	Acidobacteria	Acidobacteria-6	iii1-15	u_ iii1-15	u_ iii1-15	0.433	0.419	20.97	0.0006	17.5
Increased	Woods	both	Fungi	u_ Fungi	u_ Fungi	u_ Fungi	u_ Fungi	u_ Fungi	0.056	0.153	0.46	0.0169	17.5
Increased	Woods	Oe	Bacteria	Proteobacteria	Gammaproteobacteria	Xanthomonadales	Sinobacteraceae	u_ Sinobacteraceae	0	0.428	19.86	0.0025	17.3
Increased	Woods	both	Fungi	Ascomycota	u_ Ascomycota	u_ Ascomycota	u_ Ascomycota	u_ Ascomycota	0.06	0.033	0.44	0.0271	17
Increased	Both	Oe	p_ Bacteria	p_ Actinobacteria	p_ Actinobacteria	p_ Actinomycetales	p_ Microbacteriaceae	p_ Salinibacterium	0	0.848	42.92	0	17
Decreased	Both	both	p_ Fungi	p_ Ascomycota	p_ Leotiomycetes	p_ Helotiales	u_p_ Helotiales	u_p_ Helotiales	0.128	0.221	20.63	0.0015	16.9
Increased	Honnedaga	both	Fungi	u_ Fungi	u_ Fungi	u_ Fungi	u_ Fungi	u_ Fungi	0.027	0.007	18.28	0.001	16.7
Increased	Honnedaga	Oe	Fungi	Ascomycota	Leotiomycetes	Leotiomycetes_ord_is	u_ Leotiomycetes_ord_is	u_ Leotiomycetes_ord_is	0.009	0.064	0.49	0.0169	16.6
Increased	Honnedaga	both	Fungi	u_ Fungi	u_ Fungi	u_ Fungi	u_ Fungi	u_ Fungi	0.555	0.313	18.19	0.001	16.5
Increased	Honnedaga	both	Fungi	u_ Fungi	u_ Fungi	u_ Fungi	u_ Fungi	u_ Fungi	0.562	0.302	17.95	0.0011	16.4
Decreased	Honnedaga	both	Fungi	Ascomycota	u_ Ascomycota	u_ Ascomycota	u_ Ascomycota	u_ Ascomycota	0.162	0.044	19.49	0.0006	16.3
Increased	Both	Oe	Bacteria	Acidobacteria	Acidobacteria-6	iii1-15	u_ iii1-15	u_ iii1-15	0.042	1.298	25.1	0.0003	16.2
Increased	Honnedaga	both	Fungi	u_ Fungi	u_ Fungi	u_ Fungi	u_ Fungi	u_ Fungi	0.39	0.456	18.38	0.0049	16.1
Decreased	Honnedaga	both	Fungi	u_ Fungi	u_ Fungi	u_ Fungi	u_ Fungi	u_ Fungi	0.634	0.292	19.33	0.0007	15.9
Increased	Both	Oe	Bacteria	Actinobacteria	Thermoleophilia	Solirubrobacterales	u_ Solirubrobacterales	u_ Solirubrobacterales	0.028	0.79	45.75	0	15.8
Decreased	Honnedaga	both	Fungi	u_ Fungi	u_ Fungi	u_ Fungi	u_ Fungi	u_ Fungi	0.201	0.693	18.49	0.0009	15.5
Increased	Woods	Oe	Fungi	Basidiomycota	Agaricomycetes	Agaricales	Clavariaceae	Clavaria	0.036	0.037	0.41	0.0488	15.4
Increased	Honnedaga	Oe	Fungi	u_ Fungi	u_ Fungi	u_ Fungi	u_ Fungi	u_ Fungi	0.392	0.415	18.28	0.0049	15.3
Increased	Honnedaga	Oe	Bacteria	Proteobacteria	Alphaproteobacteria	Ellin329	u_ Ellin329	u_ Ellin329	0	0.065	18.92	0.0012	15.2
Decreased	Woods	both	Fungi	Ascomycota	Dothideomycetes	Hysteriales	Gloniaceae	Cenococcum	3.465	4.365	20.93	0.0034	15.2
Increased	Honnedaga	both	Fungi	u_ Fungi	u_ Fungi	u_ Fungi	u_ Fungi	u_ Fungi	0.338	0.459	18.32	0.0009	15.2
Decreased	Both	Oe	Bacteria	Verrucomicrobia	Pedosphaerae	Pedosphaerales	auto67_4W	u_ auto67_4W	0.037	0.183	0.35	0.0354	14.9
Increased	Woods	Oa	Fungi	u_ Fungi	u_ Fungi	u_ Fungi	u_ Fungi	u_ Fungi	0.14	0.021	0.49	0.0271	14.7
Increased	Honnedaga	both	Fungi	u_ Fungi	u_ Fungi	u_ Fungi	u_ Fungi	u_ Fungi	0.482	0.279	18.06	0.001	14.4
Decreased	Woods	both	Bacteria	Actinobacteria	Actinobacteria	Actinomycetales	u_ Actinomycetales	u_ Actinomycetales	0.381	0.644	26.43	0.0001	14.4

Decreased	Both	Oe	Bacteria	Proteobacteria	Alphaproteobacteria	Caulobacterales	Caulobacteraceae	Asticcacaulis	0.008	0.064	0.37	0.0271	14.3
Increased	Woods	Oe	Fungi	u_ Fungi	u_ Fungi	u_ Fungi	u_ Fungi	u_ Fungi	0.048	0.375	0.51	0.0424	14.2
Increased	Honnedaga	both	Fungi	u_ Fungi	u_ Fungi	u_ Fungi	u_ Fungi	u_ Fungi	0.474	0.27	18.09	0.001	14.1
Increased	Both	Oe	Bacteria	Proteobacteria	Alphaproteobacteria	Rhizobiales	Xanthobacteraceae	Labrys	0.003	0.437	15.52	0.0069	14.1
Increased	Woods	both	Bacteria	Acidobacteria	Acidobacteriia	Acidobacteriales	Koribacteraceae	u_ Koribacteraceae	0.126	1.161	20.89	0.0019	14
Decreased	Both	Oe	Bacteria	Chlamydiae	Chlamydiia	Chlamydiales	Rhabdochlamydiaceae	c_ Rhabdochlamydia	0.037	0.087	16.88	0.0048	14
Decreased	Honnedaga	Oe	Fungi	u_ Fungi	u_ Fungi	u_ Fungi	u_ Fungi	u_ Fungi	0.633	0.168	16.47	0.0058	13.8
Increased	Woods	Oe	Bacteria	Actinobacteria	Thermoleophilia	Solirubrobacterales	u_ Solirubrobacterales	u_ Solirubrobacterales	0.006	0.36	15.43	0.0099	13.5
Increased	Woods	Oe	Bacteria	Verrucomicrobia	Methylacidiphilae	Methylacidiphilales	u_ Methylacidiphilales	u_ Methylacidiphilales	0.385	0.565	17.28	0.0055	13.5
Decreased	Honnedaga	both	Bacteria	Acidobacteria	Acidobacteriia	Acidobacteriales	Koribacteraceae	c_ Koribacter	0.041	0	0.39	0.0169	13.4
Decreased	Both	Oe	Fungi	u_ Fungi	u_ Fungi	u_ Fungi	u_ Fungi	u_ Fungi	0.045	0.219	18.97	0.0095	13.4
Decreased	Honnedaga	both	Fungi	u_ Fungi	u_ Fungi	u_ Fungi	u_ Fungi	u_ Fungi	0.377	0.395	27.77	0	13.3
Increased	Both	Oe	p_ Fungi	p_ Ascomycota	p_ Leotiomycetes	p_ Helotiales	u_p_ Helotiales	u_p_ Helotiales	0.004	0.049	0.35	0.0169	13.3
Increased	Woods	Oe	Fungi	Zygomycota	Mortierellomycotina_cls_is	Mortierellales	Mortierellaceae	Mortierella	0.018	0.481	17.49	0.0087	13.2
Increased	Both	Oe	Bacteria	Proteobacteria	Gammaproteobacteria	Xanthomonadales	Xanthomonadaceae	Dokdonella	0.079	0.653	30.72	0	13.1
Increased	Both	Oa	Fungi	u_ Fungi	u_ Fungi	u_ Fungi	u_ Fungi	u_ Fungi	0.619	0.005	38.09	0	13
Increased	Honnedaga	both	Fungi	Ascomycota	Pezizomycetes	Pezizales	Tuberaceae	Tuber	0.043	0.039	18.92	0.0008	12.9
Decreased	Honnedaga	Oe	Fungi	u_ Fungi	u_ Fungi	u_ Fungi	u_ Fungi	u_ Fungi	0.462	0.284	16.38	0.006	12.8
Increased	Both	both	Bacteria	Chloroflexi	Ellin6529	u_ Ellin6529	u_ Ellin6529	u_ Ellin6529	0.633	0.914	19.13	0.0025	12.7
Decreased	Honnedaga	Oe	Fungi	Ascomycota	Leotiomycetes	Helotiales	Helotiales_fam_is	Leptodontidium	0.084	0.338	26.29	0.0006	12.4
Increased	Honnedaga	both	Fungi	u_ Fungi	u_ Fungi	u_ Fungi	u_ Fungi	u_ Fungi	0.384	0.263	26.27	0.0001	12.3
Increased	Woods	both	Fungi	Ascomycota	Sordariomycetes	Chaetosphaeriales	Chaetosphaeriaceae	Chloridium	0.552	1.702	22.32	0.0024	12.3
Increased	Honnedaga	Oe	Fungi	u_ Fungi	u_ Fungi	u_ Fungi	u_ Fungi	u_ Fungi	0.07	0.564	16.86	0.0054	12.1
Increased	Both	Oe	Bacteria	Acidobacteria	Acidobacteriia	Acidobacteriales	Koribacteraceae	u_ Koribacteraceae	0	0.603	25.04	0.0003	12.1
Decreased	Honnedaga	both	Fungi	u_ Fungi	u_ Fungi	u_ Fungi	u_ Fungi	u_ Fungi	0.45	0.245	18.82	0.0008	12
Increased	Both	both	Bacteria	Actinobacteria	Thermoleophilia	Solirubrobacterales	u_ Solirubrobacterales	u_ Solirubrobacterales	0.984	0.177	15.96	0.0038	12
Increased	Both	Oe	Bacteria	Bacteroidetes	Cytophagia	Cytophagales	Cytophagaceae	u_ Cytophagaceae	0.099	0.093	15.51	0.0069	11.9
Increased	Both	Oe	Bacteria	Chloroflexi	Ktedonobacteria	JG30-KF-AS9	u_ JG30-KF-AS9	u_ JG30-KF-AS9	0.014	0.377	18.81	0.0027	11.8
Decreased	Honnedaga	Oe	Bacteria	Proteobacteria	Alphaproteobacteria	Rhodospirillales	Rhodospirillaceae	u_ Rhodospirillaceae	0.023	0.028	22.5	0.0003	11.6
Decreased	Both	both	Fungi	u_ Fungi	u_ Fungi	u_ Fungi	u_ Fungi	u_ Fungi	1.054	3.015	19.43	0.0089	11.4
Decreased	Honnedaga	both	Fungi	u_ Fungi	u_ Fungi	u_ Fungi	u_ Fungi	u_ Fungi	0.137	0.522	18.43	0.0009	11.4
Decreased	Honnedaga	both	Fungi	u_ Fungi	u_ Fungi	u_ Fungi	u_ Fungi	u_ Fungi	0.542	0.122	19.99	0.0005	11.4
Increased	Honnedaga	Oe	Bacteria	Proteobacteria	Betaproteobacteria	Burkholderiales	Oxalobacteraceae	Janthinobacterium	0.034	0.095	27.75	0.0001	11.3
Decreased	Woods	both	Fungi	u_ Fungi	u_ Fungi	u_ Fungi	u_ Fungi	u_ Fungi	0.732	0.285	22.96	0.0043	10.8
Increased	Honnedaga	Oe	Fungi	u_ Fungi	u_ Fungi	u_ Fungi	u_ Fungi	u_ Fungi	0.138	0.431	18.41	0.0049	10.8
Increased	Woods	Oe	Bacteria	Proteobacteria	Betaproteobacteria	u_ Betaproteobacteria	u_ Betaproteobacteria	u_ Betaproteobacteria	0.03	0.286	20.42	0.0021	10.8
Decreased	Both	both	Fungi	Ascomycota	Eurotiomycetes	Eurotiales	Trichocomaceae	Paecilomyces	0.305	0.887	24.53	0.0022	10.8
Increased	Woods	Oe	Bacteria	Acidobacteria	Acidobacteria-6	iii1-15	u_ iii1-15	u_ iii1-15	0.825	0.75	17.72	0.005	10.7
Increased	Honnedaga	both	Fungi	u_ Fungi	u_ Fungi	u_ Fungi	u_ Fungi	u_ Fungi	0.002	0.033	0.35	0.0354	10.7
Decreased	Honnedaga	both	Bacteria	Acidobacteria	Solibacteres	Solibacterales	u_ Solibacterales	u_ Solibacterales	0.013	0.169	0.36	0.0488	10.6
Increased	Honnedaga	Oe	Bacteria	Proteobacteria	Alphaproteobacteria	Rhizobiales	Phyllobacteriaceae	u_phyllobacteriaceae	0.004	0.169	16.75	0.0025	10.5
Decreased	Honnedaga	Oe	Bacteria	Bacteroidetes	Saprospirae	Saprospirales	Chitinophagaceae	u_ Chitinophagaceae	0.069	0.303	17.73	0.0018	10.5
Decreased	Woods	both	Bacteria	Actinobacteria	Actinobacteria	Actinomycetales	Mycobacteriaceae	Mycobacterium	0.411	0.754	25.83	0.0001	10.4
Increased	Both	Oe	Bacteria	Actinobacteria	Thermoleophilia	Solirubrobacterales	u_ Solirubrobacterales	u_ Solirubrobacterales	0.005	1.561	18	0.0033	10.3
Increased	Woods	Oe	Bacteria	Proteobacteria	Alphaproteobacteria	Rhodospirillales	Rhodospirillaceae	u_ Rhodospirillaceae	0.269	0.292	26.83	0.0003	10.2
Increased	Both	both	Fungi	Zygomycota	Mortierellomycotina_cls_is	Mortierellales	Mortierellaceae	Mortierella	0.108	0.294	33.3	0.0001	10.1
Increased	Both	both	Bacteria	Bacteroidetes	Saprospirae	Saprospirales	Chitinophagaceae	u_ Chitinophagaceae	0.183	0.507	46.27	0	10.1
Decreased	Honnedaga	Oe	Fungi	u_ Fungi	u_ Fungi	u_ Fungi	u_ Fungi	u_ Fungi	0	0.056	0.54	0.0354	10.1
Decreased	Both	both	Bacteria	WPS-2	u_ WPS-2	u_ WPS-2	u_ WPS-2	u_ WPS-2	0.094	0.411	17.45	0.0022	10.1
Decreased	Honnedaga	both	Bacteria	Proteobacteria	Gammaproteobacteria	Xanthomonadales	Sinobacteraceae	u_ Sinobacteraceae	0.011	0.076	0.42	0.0169	10.1
Decreased	Woods	both	Bacteria	Proteobacteria	Alphaproteobacteria	Rhizobiales	Hyphomicrobiaceae	Rhodoplanes	1.379	0.94	19.61	0.0026	10

CHAPTER 3

SUPPLEMENTARY MATERIAL

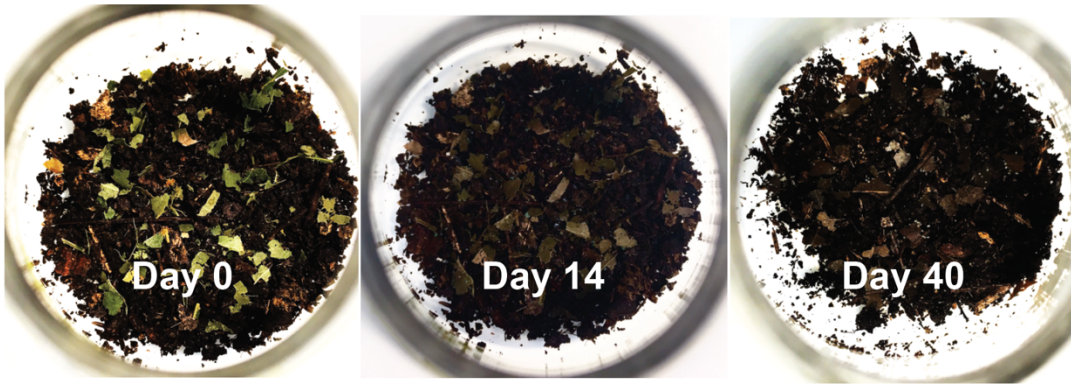

Figure S1 Photographs showing leaf substrates decomposing in one microcosm containing Oe horizon control soils over 40 days of incubation.

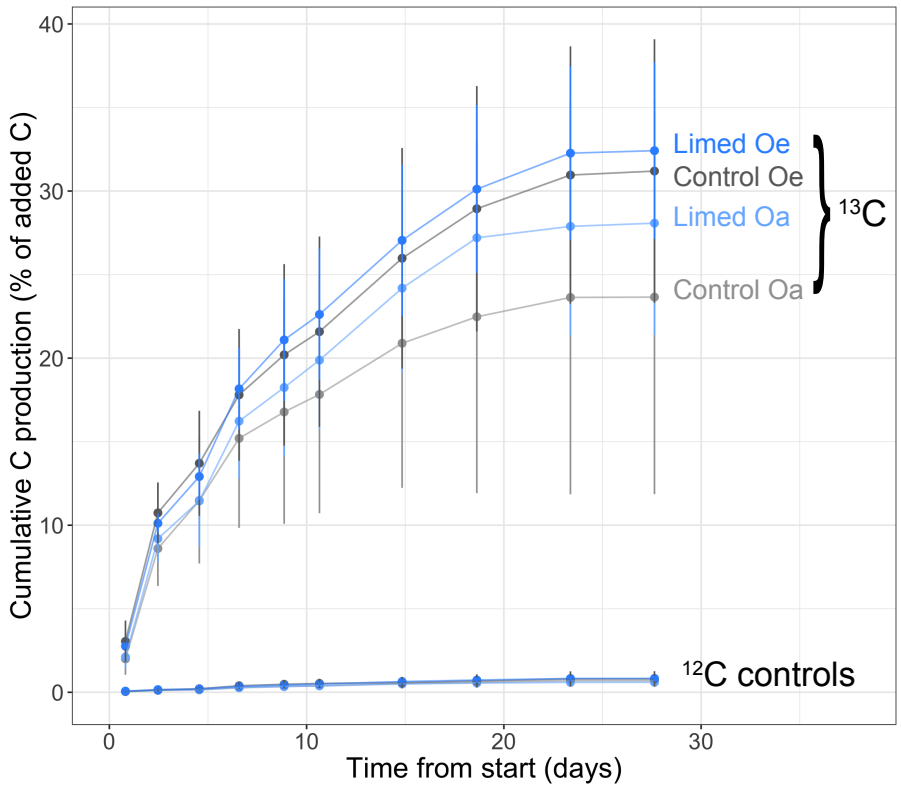

Figure S2 Cumulative ^{13}C respiration from microcosms as a percent of added labeled and unlabeled leaf C over 27 days. Mean and standard deviation are shown with $n_{rep} = 4$ for the first 14 days, and $n_{rep} = 2$ for the final three time points after half the samples were destructively harvested. Each microcosm received 6 g leaf fragments per gram dry wt. soil.

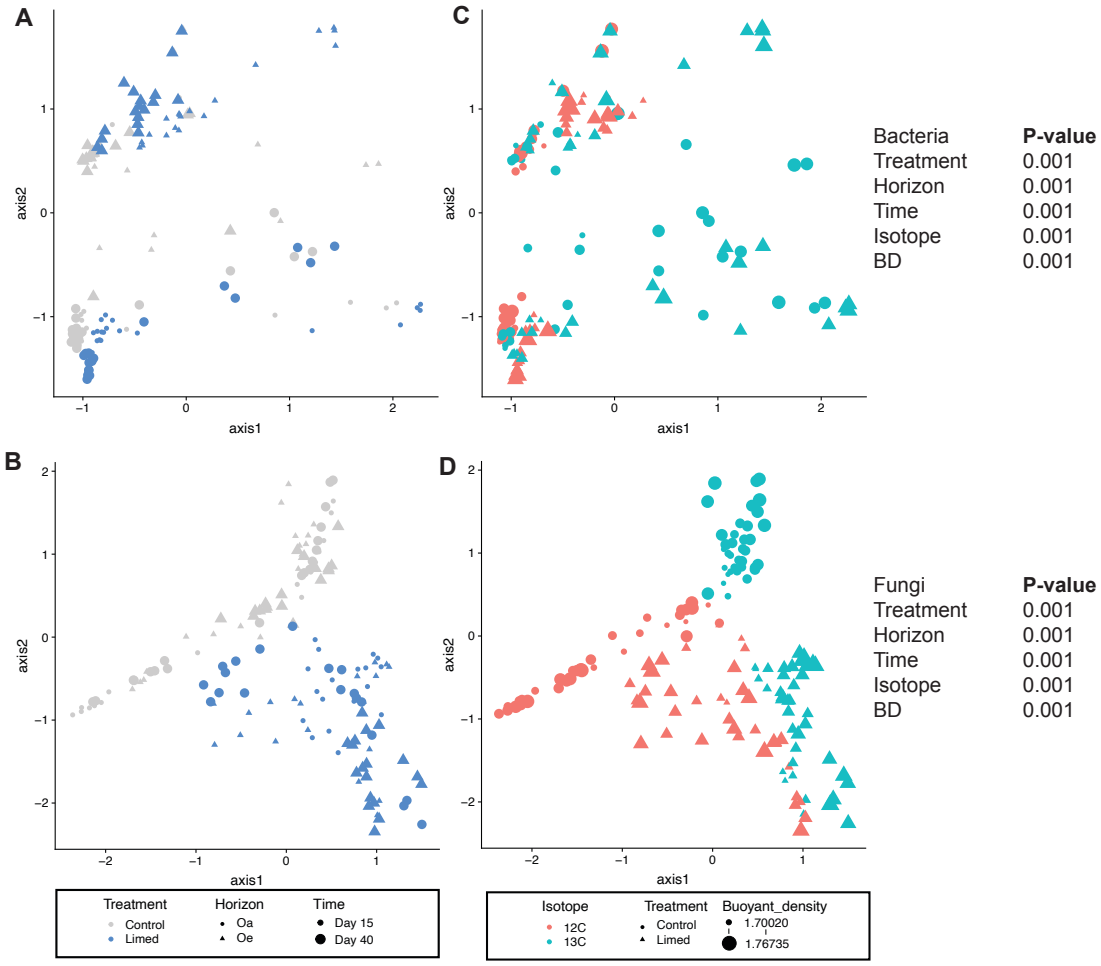

Figure S3 Canonical correspondence analysis ordinations of (A) bacterial (16S) and (B) fungal (ITS) sequence composition in gradient fractions. Dissimilarity in sequence composition was quantified using the Bray-Curtis metric. Sample points are fractions coded by treatment, horizon, time, and isotope. (C) and (D) show the same ordination for bacteria and fungi respectively with sample points colored by isotope instead of treatment

Figure S4 (A) Bacterial and (B) fungal ASVs that showed large changes in differential abundance in limed soils relative to control soils. ASVs with $\log_2$ fold change ≥ 1or ≤ -1 in limed relative to control are shown, with leaf ^{13}C labeled incorporator ASVs highlighted in black. Panels on the right show their relative abundance in the heavy fractions in control and limed soils.

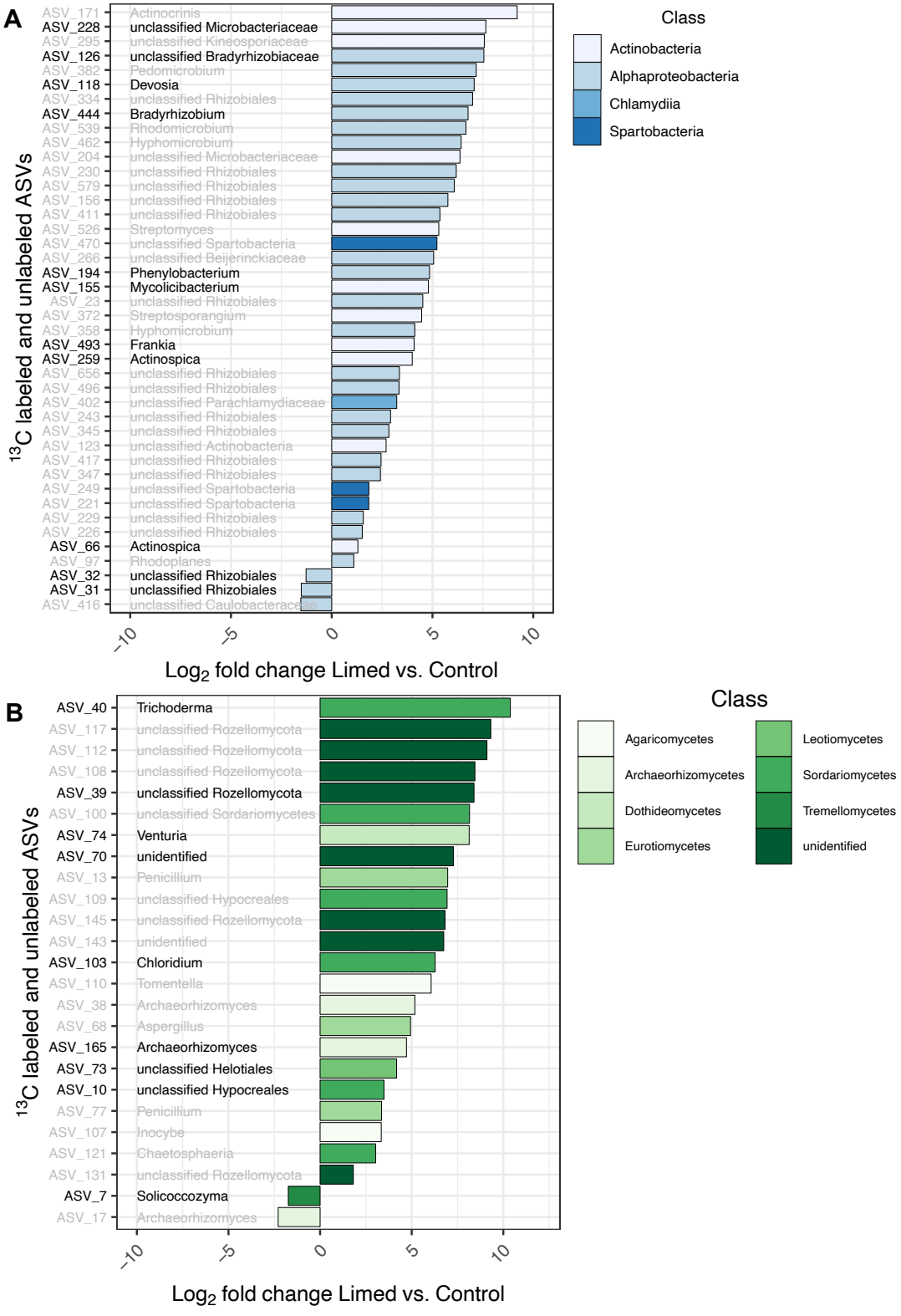
A
ASV_171 Actinocrinis
ASV_228 unclassified Microbacteriaceae
ASV_295 unclassified Kineosporiaceae
ASV_126 unclassified Bradyrhizobiaceae
ASV_382 Pedomicrobium
ASV_118 Devosia
ASV_334 unclassified Rhizobiales
ASV_444 Bradyrhizobium
ASV_539 Rhodomicrobium
ASV_462 Hyphomicrobium
ASV_204 unclassified Microbacteriaceae
ASV_230 unclassified Rhizobiales
ASV_579 unclassified Rhizobiales
ASV_156 unclassified Rhizobiales
ASV_411 unclassified Rhizobiales
ASV_526 Streptomyces
ASV_470 unclassified Spartobacteria
ASV_266 unclassified Beijerinckiaceae
ASV_194 Phenylobacterium
ASV_155 Mycolicibacterium
ASV_23 unclassified Rhizobiales
ASV_372 Streptosporangium
ASV_358 Hyphomicrobium
ASV_493 Frankia
ASV_259 Actinospica
ASV_656 unclassified Rhizobiales
ASV_496 unclassified Rhizobiales
ASV_402 unclassified Parachlamydiaceae
ASV_243 unclassified Rhizobiales
ASV_345 unclassified Rhizobiales
ASV_123 unclassified Actinobacteria
ASV_417 unclassified Rhizobiales
ASV_347 unclassified Rhizobiales
ASV_249 unclassified Spartobacteria
ASV_221 unclassified Spartobacteria
ASV_229 unclassified Rhizobiales
ASV_226 unclassified Rhizobiales
ASV_66 Actinospica
ASV_97 Rhodoplanes
ASV_32 unclassified Rhizobiales
ASV_31 unclassified Rhizobiales
ASV_416 unclassified Caulobacteraceae
−10
−5
0
5
10
^{13}C labeled and unlabeled ASVs
Log$_2$ fold change Limed vs. Control
Class
Actinobacteria
Alphaproteobacteria
Chlamydiia
Spartobacteria
B
ASV_40 Trichoderma
ASV_117 unclassified Rozellomycota
ASV_112 unclassified Rozellomycota
ASV_108 unclassified Rozellomycota
ASV_39 unclassified Rozellomycota
ASV_100 unclassified Sordariomycetes
ASV_74 Venturia
ASV_70 unidentified
ASV_13 Penicillium
ASV_109 unclassified Hypocreales
ASV_145 unclassified Rozellomycota
ASV_143 unidentified
ASV_103 Chloridium
ASV_110 Tomentella
ASV_38 Archaeorhizomyces
ASV_68 Aspergillus
ASV_165 Archaeorhizomyces
ASV_73 unclassified Helotiales
ASV_10 unclassified Hypocreales
ASV_77 Penicillium
ASV_107 Inocybe
ASV_121 Chaetosphaeria
ASV_131 unclassified Rozellomycota
ASV_7 Solicoccozyma
ASV_17 Archaeorhizomyces
−10
−5
0
5
10
^{13}C labeled and unlabeled ASVs
Log$_2$ fold change Limed vs. Control
Class
Agaricomycetes
Archaeorhizomycetes
Dothideomycetes
Eurotiomycetes
Leotiomycetes
Sordariomycetes
Tremellomycetes
unidentified

Figure S5 Degree of ^{13}C incorporation of (A) bacterial and (B) fungal incorporators represented by the increase in their sequence counts in soils amended with ^{13}C-labeled oak leaves compared to that in soils amended with ^{12}C oak leaves. The results of this differential abundance analysis in control soils on the x axis are plotted against the same conducted in limed soils on the y axis, across time points and horizons. Points represent incorporator ASVs, are colored by the class they belong to, and jittered by 1 unit for clarity. The range of ^{13}C leaf incorporation in control soils only is annotated by black ellipse and the range in limed soils only is annotated by a blue ellipse with black bars representing median levels of incorporation. ASVs that incorporated ^{13}C from leaves in both control and limed soils are outside the ellipses.

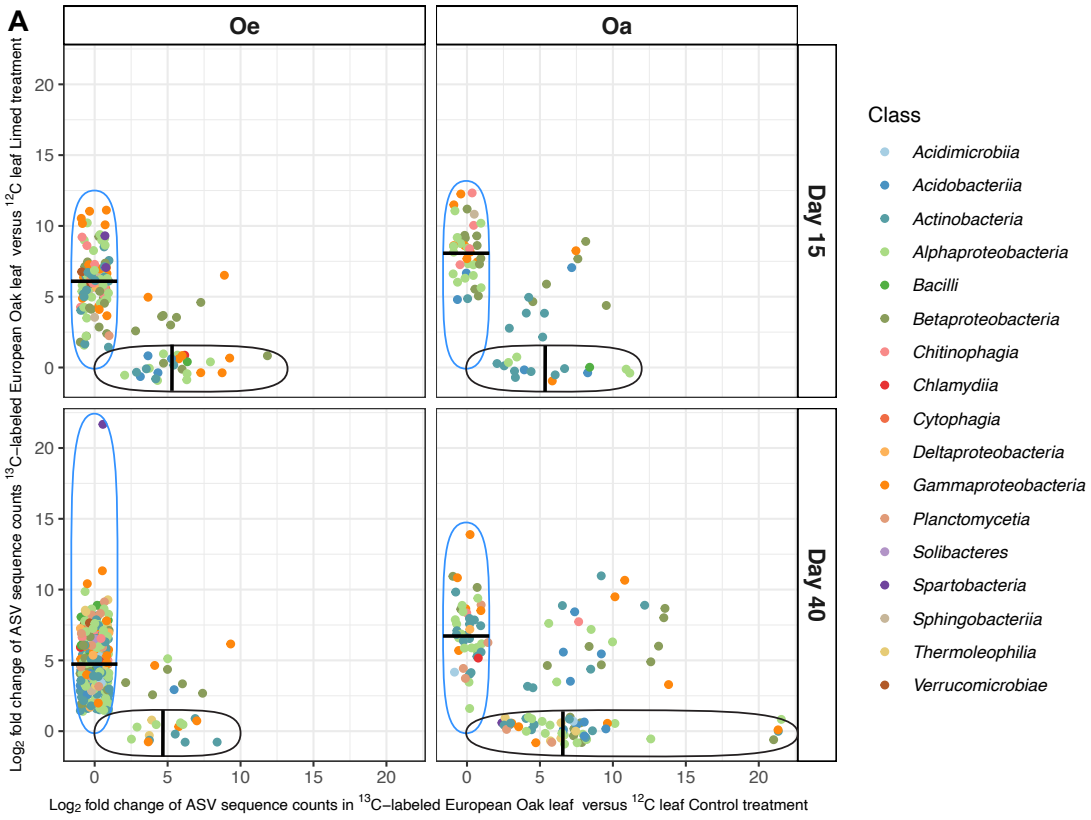
A
Oe
Oa
Day 15
Day 40
Log2 fold change of ASV sequence counts 13C–labeled European Oak leaf versus 12C leaf Limed treatment
Log2 fold change of ASV sequence counts in 13C–labeled European Oak leaf versus 12C leaf Control treatment
0
5
10
15
20
Class
Acidimicrobiia
Acidobacteriia
Actinobacteria
Alphaproteobacteria
Bacilli
Betaproteobacteria
Chitinophagia
Chlamydiia
Cytophagia
Deltaproteobacteria
Gammaproteobacteria
Planctomycetia
Solibacteres
Spartobacteria
Sphingobacteriia
Thermoleophilia
Verrucomicrobiae

Figure S5 (Continued)

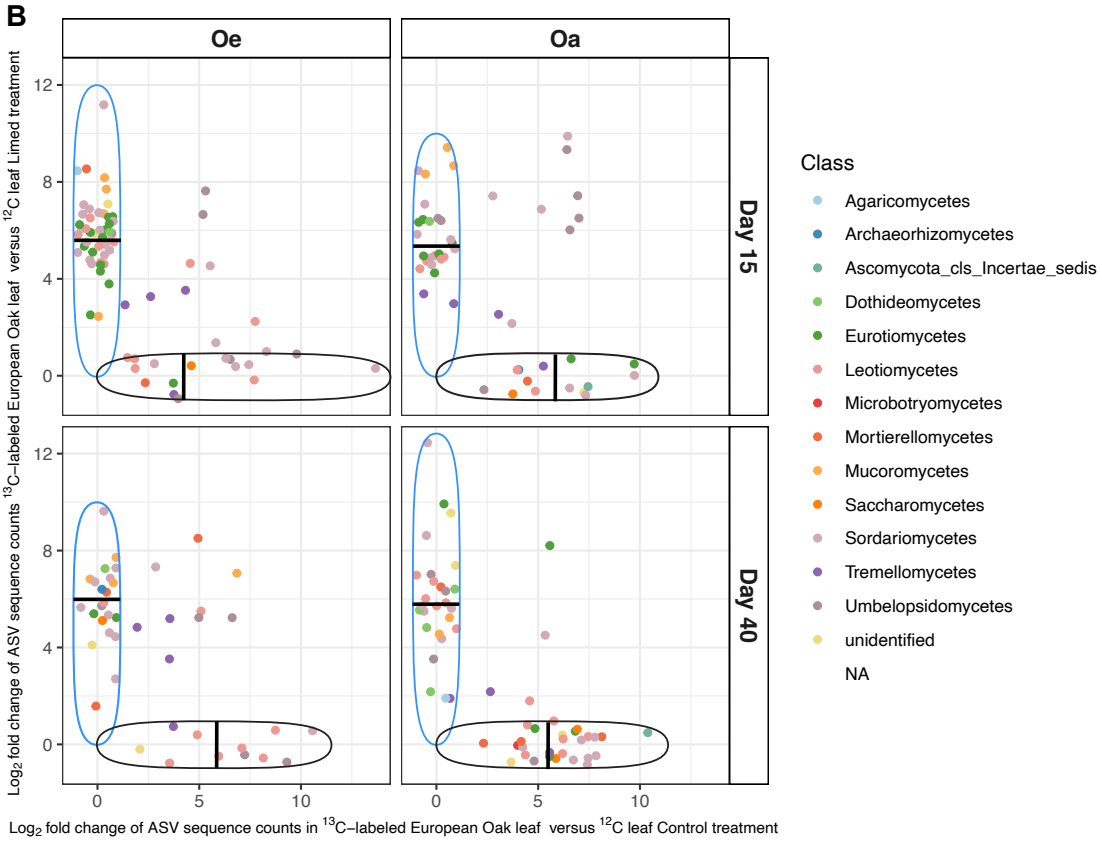

Figure S6 Boxplots showing the degree of ^{13}C leaf incorporation in limed vs control soils across (A) bacterial and (B) fungal classes at early (Day 15) and late (Day 40) time points across both horizons combined. Y-axis shows log_2 fold increase in ASV counts in ^{13}C heavy fractions relative to ^{12}C heavy fractions.

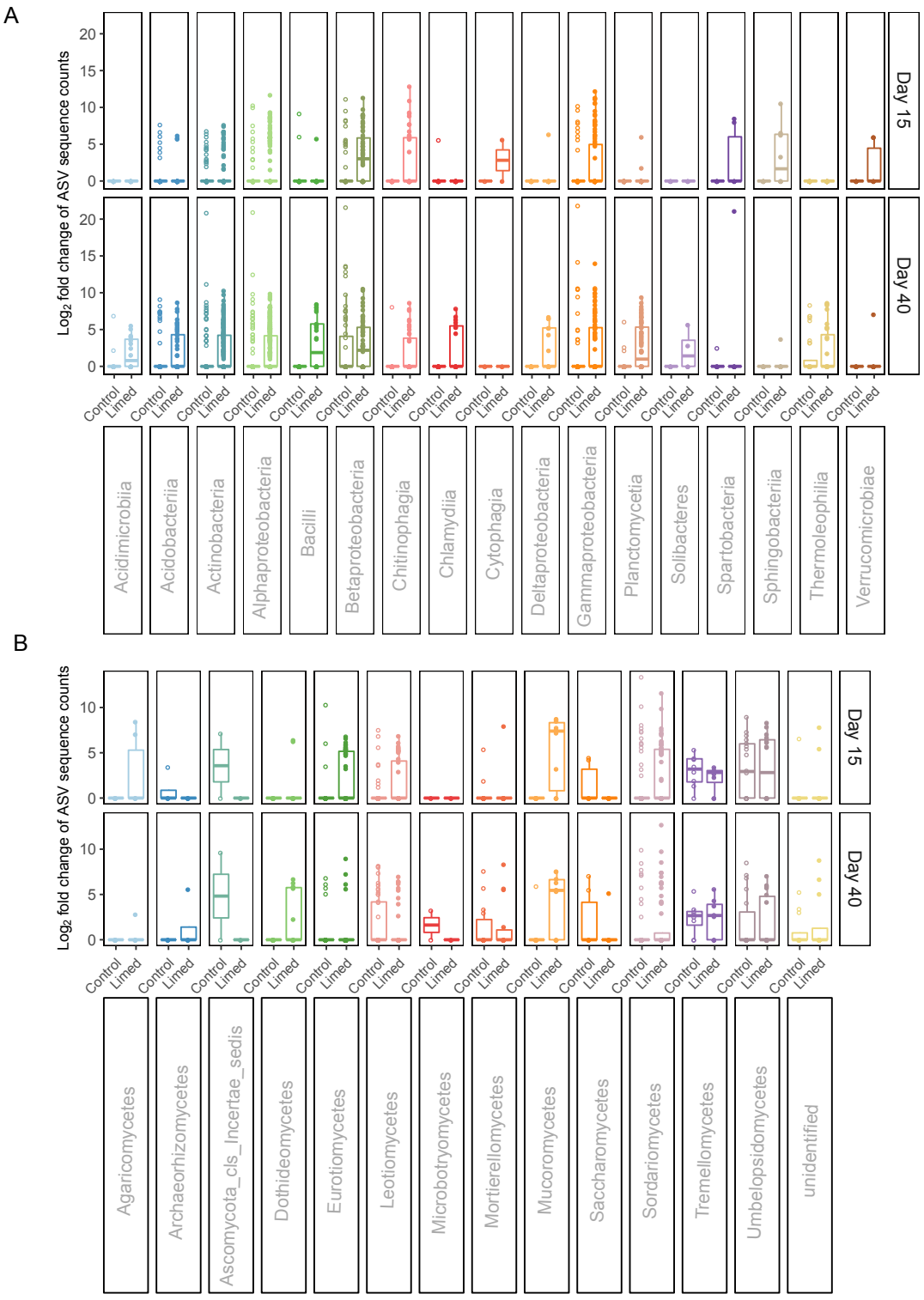
A
Log2 fold change of ASV sequence counts
Day 15
Day 40
Control
Limed
Acidimicrobiia
Acidobacteriia
Actinobacteria
Alphaproteobacteria
Bacilli
Betaproteobacteria
Chitinophagia
Chlamydiia
Cytophagia
Deltaproteobacteria
Gammaproteobacteria
Planctomycetia
Solibacteres
Spartobacteria
Sphingobacteriia
Thermoleophilia
Verrucomicrobiae
B
Log2 fold change of ASV sequence counts
Day 15
Day 40
Control
Limed
Agaricomycetes
Archaeorhizomycetes
Ascomycota_cls_Incertae_sedis
Dothideomycetes
Eurotiomycetes
Leotiomycetes
Microbotryomycetes
Mortierellomycetes
Mucoromycetes
Saccharomycetes
Sordariomycetes
Tremellomycetes
Umbelopsidomycetes
unidentified

Figure S7 Monophyletic clades of incorporators (phylogroups) within order *Streptosporangiales*. Insets show representatives within these phylogroups' phylogenetic placement using distance-based clustering of sequences based on alignment similarity scores relative to the query generated using the BLASTn 16S ribosomal RNA sequence database.

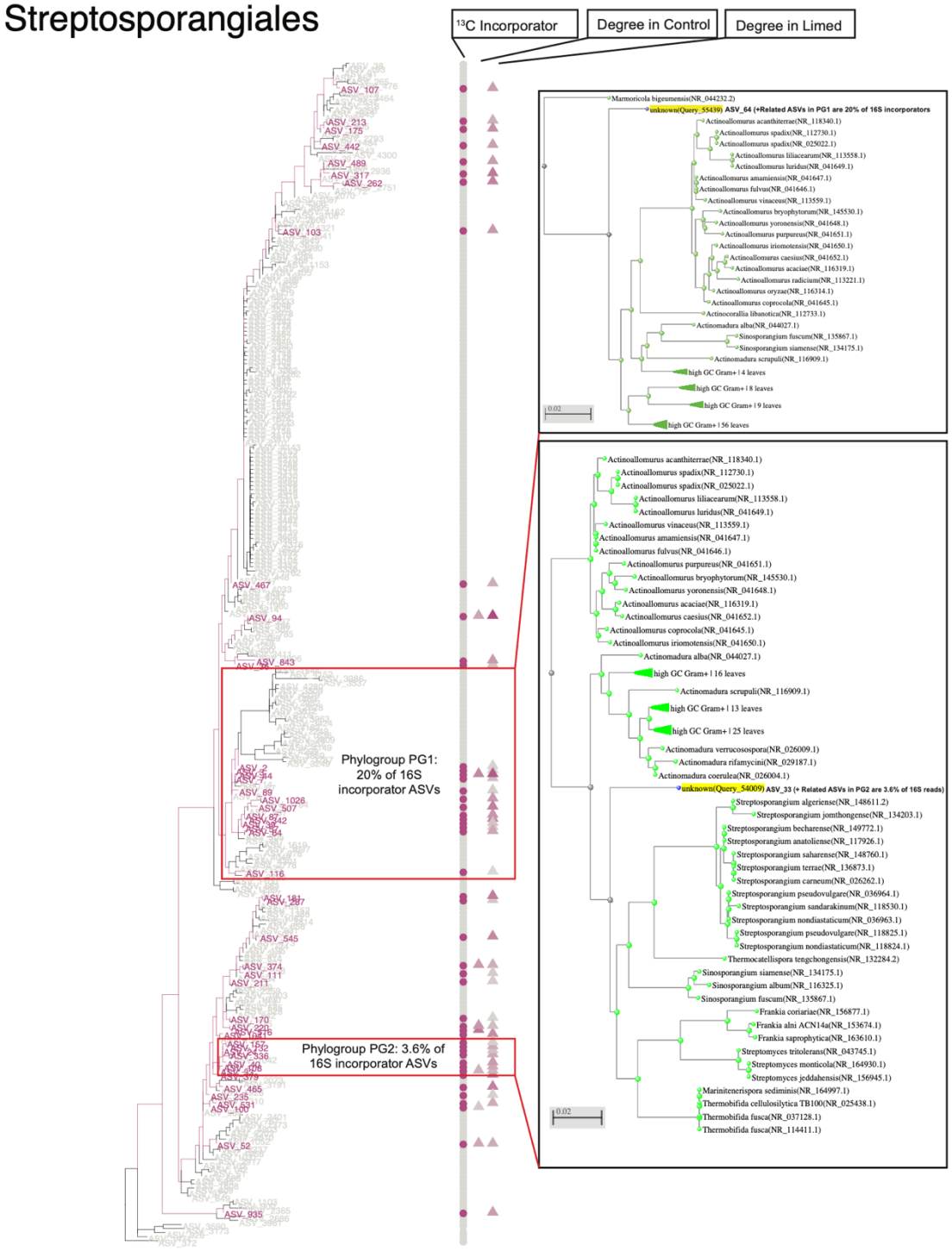
Streptosporangiales
13C Incorporator
Degree in Control
Degree in Limed
Phylogroup PG1: 20% of 16S incorporator ASVs
Phylogroup PG2: 3.6% of 16S incorporator ASVs
Marmoricola bigeumensis(NR_044232.2)
unknown(Query_55439) ASV_64 (+Related ASVs in PG1 are 20% of 16S incorporators
Actinoallomurus acanthiterrae(NR_118340.1)
Actinoallomurus spadix(NR_112730.1)
Actinoallomurus spadix(NR_025022.1)
Actinoallomurus liliacearum(NR_113558.1)
Actinoallomurus luridus(NR_041649.1)
Actinoallomurus amamiensis(NR_041647.1)
Actinoallomurus fulvus(NR_041646.1)
Actinoallomurus vinaceus(NR_113559.1)
Actinoallomurus bryophytorum(NR_145530.1)
Actinoallomurus yoronensis(NR_041648.1)
Actinoallomurus purpureus(NR_041651.1)
Actinoallomurus iriomotensis(NR_041650.1)
Actinoallomurus caesius(NR_041652.1)
Actinoallomurus acaciae(NR_116319.1)
Actinoallomurus radiciam(NR_113221.1)
Actinoallomurus oryzae(NR_116314.1)
Actinoallomurus coprocola(NR_041645.1)
Actinocorallia libanotica(NR_112733.1)
Actinomadura alba(NR_044027.1)
Sinosporangium fuscum(NR_135867.1)
Sinosporangium siamense(NR_134175.1)
Actinomadura scrupuli(NR_116909.1)
high GC Gram+ | 4 leaves
high GC Gram+ | 8 leaves
high GC Gram+ | 9 leaves
high GC Gram+ | 56 leaves
0.02
Actinoallomurus acanthiterrae(NR_118340.1)
Actinoallomurus spadix(NR_112730.1)
Actinoallomurus spadix(NR_025022.1)
Actinoallomurus liliacearum(NR_113558.1)
Actinoallomurus luridus(NR_041649.1)
Actinoallomurus vinaceus(NR_113559.1)
Actinoallomurus amamiensis(NR_041647.1)
Actinoallomurus fulvus(NR_041646.1)
Actinoallomurus purpureus(NR_041651.1)
Actinoallomurus bryophytorum(NR_145530.1)
Actinoallomurus yoronensis(NR_041648.1)
Actinoallomurus acaciae(NR_116319.1)
Actinoallomurus caesius(NR_041652.1)
Actinoallomurus coprocola(NR_041645.1)
Actinoallomurus iriomotensis(NR_041650.1)
Actinomadura alba(NR_044027.1)
high GC Gram+ | 16 leaves
Actinomadura scrupuli(NR_116909.1)
high GC Gram+ | 13 leaves
high GC Gram+ | 25 leaves
Actinomadura verrucosospora(NR_026009.1)
Actinomadura rifamycini(NR_029187.1)
Actinomadura coerulea(NR_026004.1)
unknown(Query_54009) ASV_33 (+ Related ASVs in PG2 are 3.6% of 16S reads)
Streptosporangium algeriense(NR_148611.2)
Streptosporangium jomthongense(NR_134203.1)
Streptosporangium becharense(NR_149772.1)
Streptosporangium anatoliense(NR_117926.1)
Streptosporangium saharense(NR_148760.1)
Streptosporangium terrae(NR_136873.1)
Streptosporangium carneum(NR_026262.1)
Streptosporangium pseudovulgare(NR_036964.1)
Streptosporangium sandarakinum(NR_118530.1)
Streptosporangium nondiastaticum(NR_036963.1)
Streptosporangium pseudovulgare(NR_118825.1)
Streptosporangium nondiastaticum(NR_118824.1)
Thermocatellispora tengchongensis(NR_132284.2)
Sinosporangium siamense(NR_134175.1)
Sinosporangium album(NR_116325.1)
Sinosporangium fuscum(NR_135867.1)
Frankia coriariae(NR_156877.1)
Frankia alni ACN14a(NR_153674.1)
Frankia saprophytica(NR_163610.1)
Streptomyces tritolerans(NR_043745.1)
Streptomyces monticola(NR_164930.1)
Streptomyces jeddahensis(NR_156945.1)
Mariniterenispora sediminis(NR_164997.1)
Thermobifida cellulosilytica TB100(NR_025438.1)
Thermobifida fusca(NR_037128.1)
Thermobifida fusca(NR_114411.1)
0.02

Figure S8 Monophyletic clade of incorporators (phylogroup) within order *Burkholderiales*. Insets show representatives within these phylogroups' phylogenetic placement using distance-based clustering of sequences based on alignment similarity scores relative to the query generated using the BLASTn 16S ribosomal RNA sequence database.

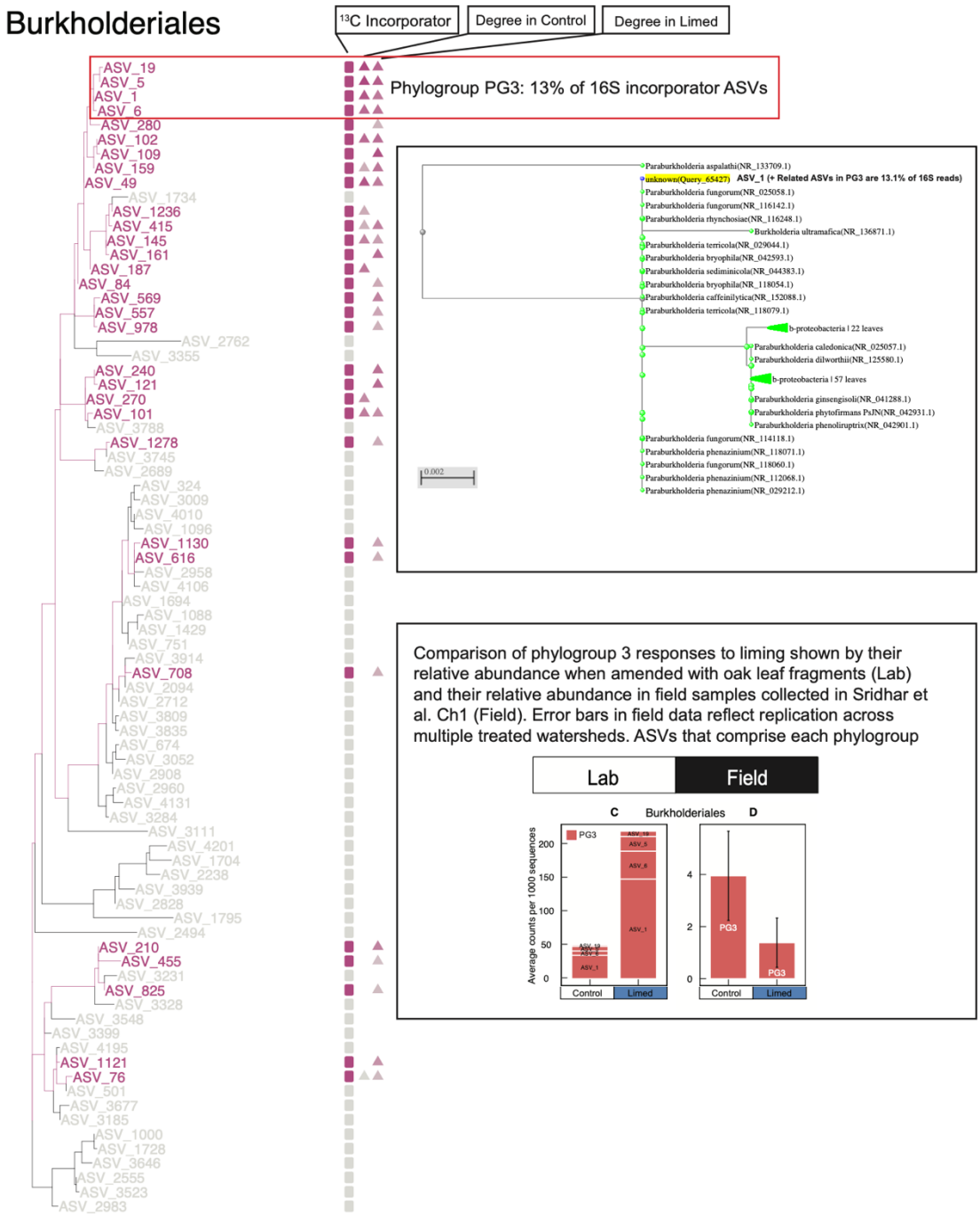
Burkholderiales
13C Incorporator
Degree in Control
Degree in Limed
Phylogroup PG3: 13% of 16S incorporator ASVs
ASV_19
ASV_5
ASV_1
ASV_6
ASV_280
ASV_102
ASV_109
ASV_159
ASV_49
ASV_1734
ASV_1236
ASV_415
ASV_145
ASV_161
ASV_187
ASV_84
ASV_569
ASV_557
ASV_978
ASV_2762
ASV_3355
ASV_240
ASV_121
ASV_270
ASV_101
ASV_3788
ASV_1278
ASV_3745
ASV_2689
ASV_324
ASV_3009
ASV_4010
ASV_1096
ASV_1130
ASV_616
ASV_2958
ASV_4106
ASV_1694
ASV_1088
ASV_1429
ASV_751
ASV_3914
ASV_708
ASV_2094
ASV_2712
ASV_3809
ASV_3835
ASV_674
ASV_3052
ASV_2908
ASV_2960
ASV_4131
ASV_3284
ASV_3111
ASV_4201
ASV_1704
ASV_2238
ASV_3939
ASV_2828
ASV_1795
ASV_2494
ASV_210
ASV_455
ASV_3231
ASV_825
ASV_3328
ASV_3548
ASV_3399
ASV_4195
ASV_1121
ASV_76
ASV_501
ASV_3677
ASV_3185
ASV_1000
ASV_1728
ASV_3646
ASV_2555
ASV_3523
ASV_2983
Paraburkholderia aspalathi(NR_133709.1)
unknown(Query_65427) ASV_1 (+ Related ASVs in PG3 are 13.1% of 16S reads)
Paraburkholderia fungorum(NR_025058.1)
Paraburkholderia fungorum(NR_116142.1)
Paraburkholderia rhynchosiae(NR_116248.1)
Burkholderia ultramafica(NR_136871.1)
Paraburkholderia terricola(NR_029044.1)
Paraburkholderia bryophila(NR_042593.1)
Paraburkholderia sediminicola(NR_044383.1)
Paraburkholderia bryophila(NR_118054.1)
Paraburkholderia caffeinilytica(NR_152088.1)
Paraburkholderia terricola(NR_118079.1)
b-proteobacteria | 22 leaves
Paraburkholderia caledonica(NR_025057.1)
Paraburkholderia dilworthii(NR_125580.1)
b-proteobacteria | 57 leaves
Paraburkholderia ginsengisoli(NR_041288.1)
Paraburkholderia phytofirmans PsJN(NR_042931.1)
Paraburkholderia phenoliruptrix(NR_042901.1)
Paraburkholderia fungorum(NR_114118.1)
Paraburkholderia phenazinium(NR_118071.1)
Paraburkholderia fungorum(NR_118060.1)
Paraburkholderia phenazinium(NR_112068.1)
Paraburkholderia phenazinium(NR_029212.1)
0.002
Comparison of phylogroup 3 responses to liming shown by their relative abundance when amended with oak leaf fragments (Lab) and their relative abundance in field samples collected in Sridhar et al. Ch1 (Field). Error bars in field data reflect replication across multiple treated watersheds. ASVs that comprise each phylogroup
Lab
Field
C
Burkholderiales
D
PG3
Average counts per 1000 sequences
Control
Limed

Figure S9 Monophyletic clade of incorporators (phylogroup) within order *Rhizobiales*. Insets show representatives within these phylogroups' phylogenetic placement using distance-based clustering of sequences based on alignment similarity scores relative to the query generated using the BLASTn 16S ribosomal RNA sequence database

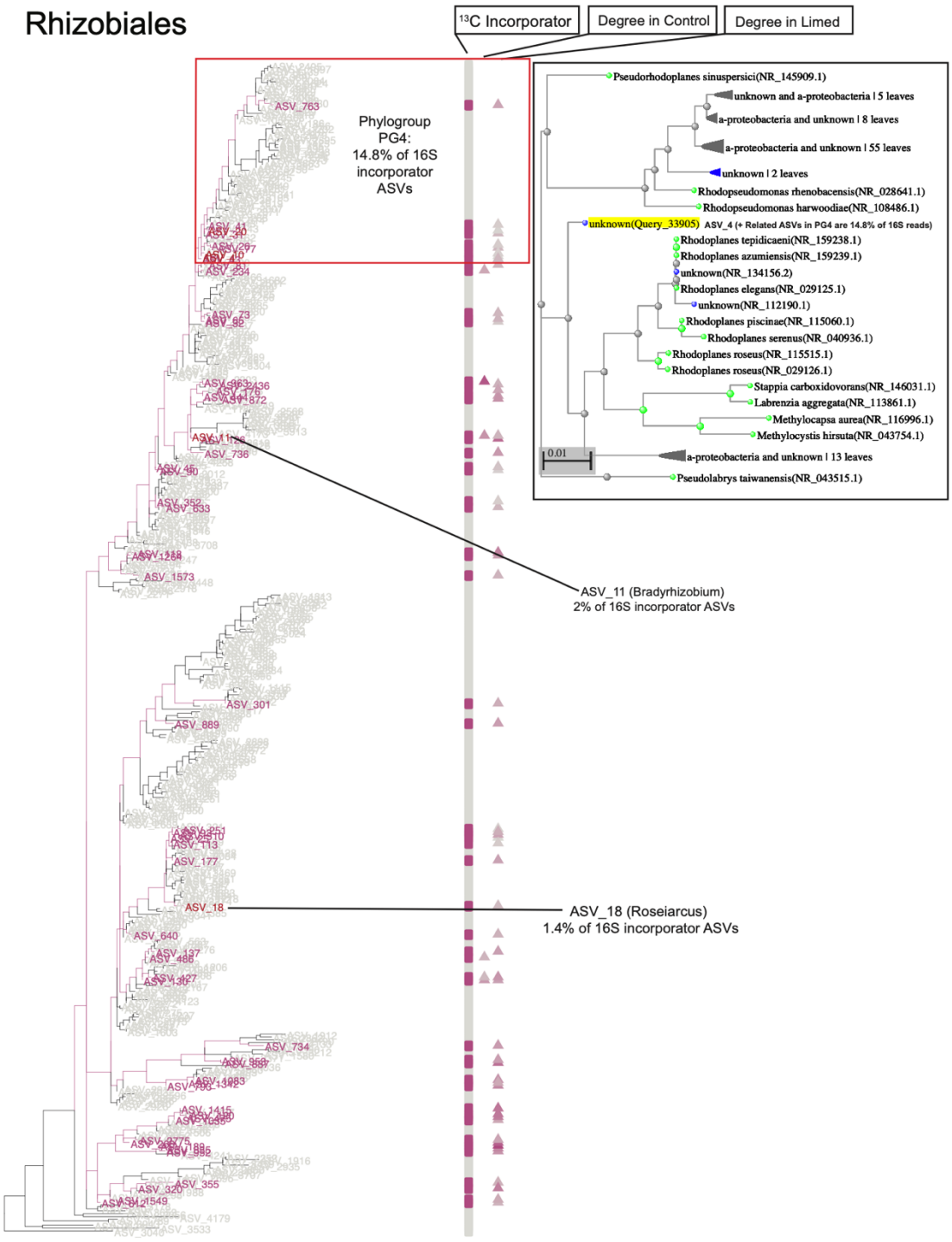
Rhizobiales
13C Incorporator
Degree in Control
Degree in Limed
Phylogroup PG4: 14.8% of 16S incorporator ASVs
Pseudorhodoplanes sinuspersici(NR_145909.1)
unknown and a-proteobacteria | 5 leaves
a-proteobacteria and unknown | 8 leaves
a-proteobacteria and unknown | 55 leaves
unknown | 2 leaves
Rhodopseudomonas rhenobacensis(NR_028641.1)
Rhodopseudomonas harwoodiae(NR_108486.1)
unknown(Query_33905) ASV_4 (+ Related ASVs in PG4 are 14.8% of 16S reads)
Rhodoplanes tepidicaeni(NR_159238.1)
Rhodoplanes azumiensis(NR_159239.1)
unknown(NR_134156.2)
Rhodoplanes elegans(NR_029125.1)
unknown(NR_112190.1)
Rhodoplanes piscinae(NR_115060.1)
Rhodoplanes serenus(NR_040936.1)
Rhodoplanes roseus(NR_115515.1)
Rhodoplanes roseus(NR_029126.1)
Stappia carboxidovorans(NR_146031.1)
Labrenzia aggregata(NR_113861.1)
Methylocapsa aurea(NR_116996.1)
Methylocystis hirsuta(NR_043754.1)
0.01
a-proteobacteria and unknown | 13 leaves
Pseudolabrys taiwanensis(NR_043515.1)
ASV_11 (Bradyrhizobium)
2% of 16S incorporator ASVs
ASV_18 (Roseiarcus)
1.4% of 16S incorporator ASVs

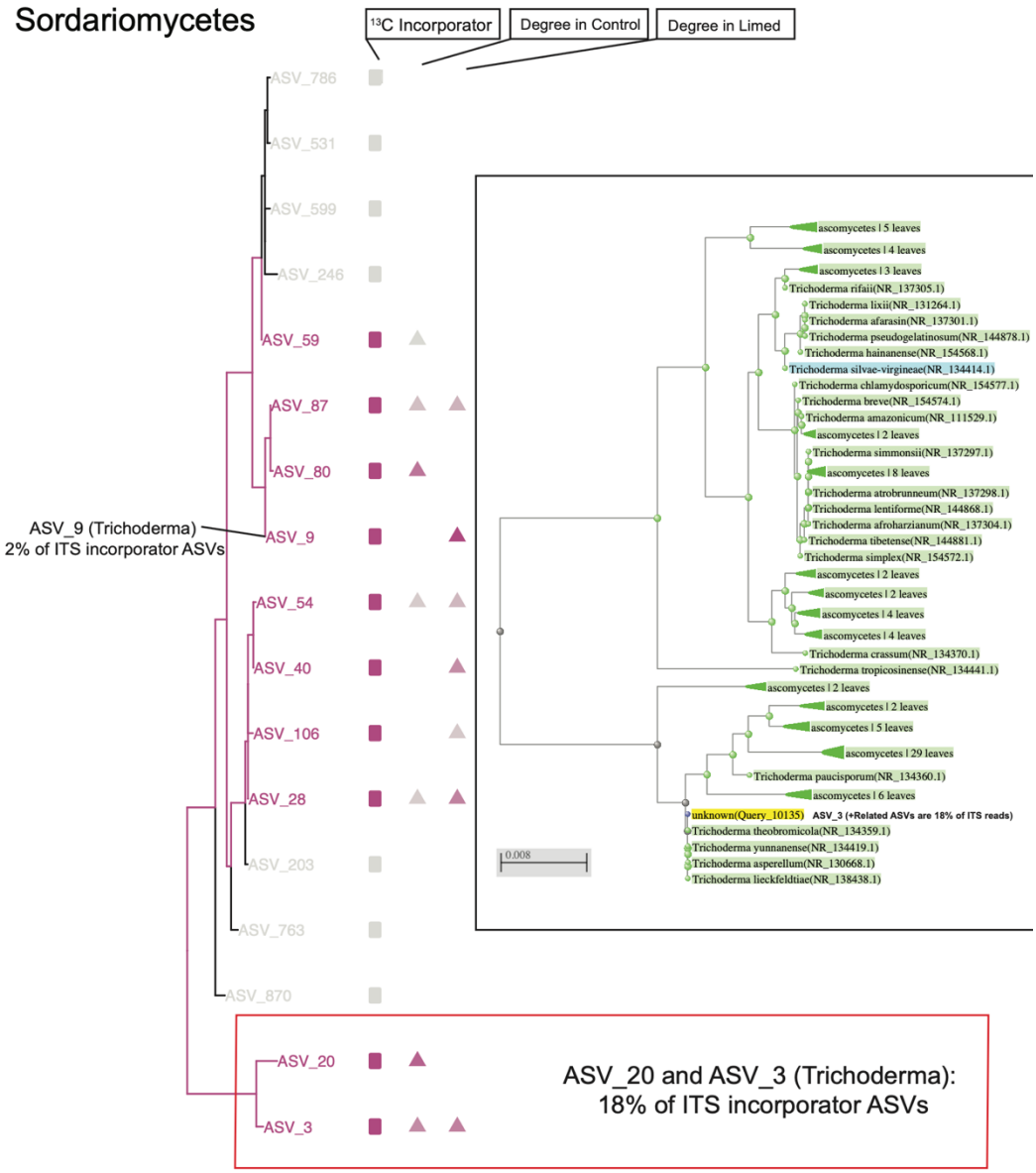

Figure S10 Monophyletic clade of incorporators (phylogroup) within class *Sordariomycetes*. Insets show representatives within these phylogroups' phylogenetic placement using distance-based clustering of sequences based on alignment similarity scores relative to the query generated using the BLASTn ITS from Fungi database.

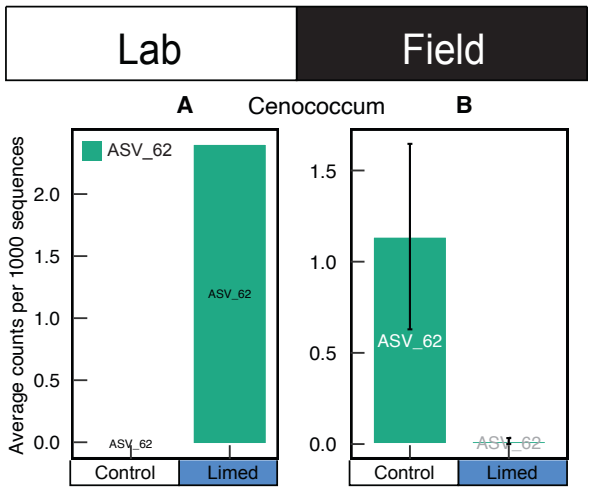

Figure S11 Comparison of the response of an unclassified ectomycorrhizal ASV in genus *Cenococcum* to liming shown by their relative abundance when amended with oak leaf fragments (Lab) and their relative abundance in field samples collected in Sridhar et al. Ch1 (Field). Error bars in field data reflect replication across multiple treated subcatchments

.

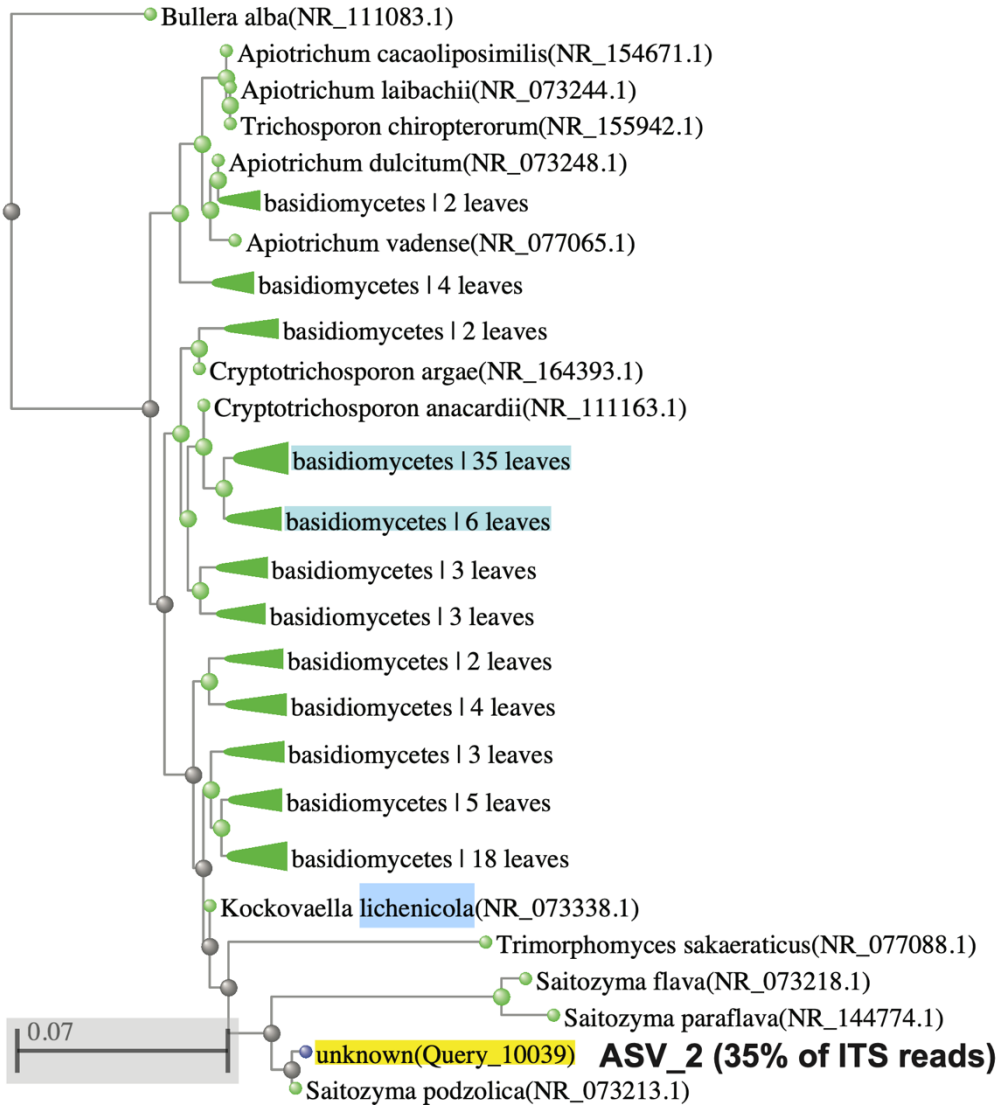

Figure S12 The phylogenetic placement of ASV_2, an unclassified *Tremellomycetes*, using distance-based clustering of sequences based on alignment similarity scores relative to the query generated using the BLASTn ITS from Fungi database.

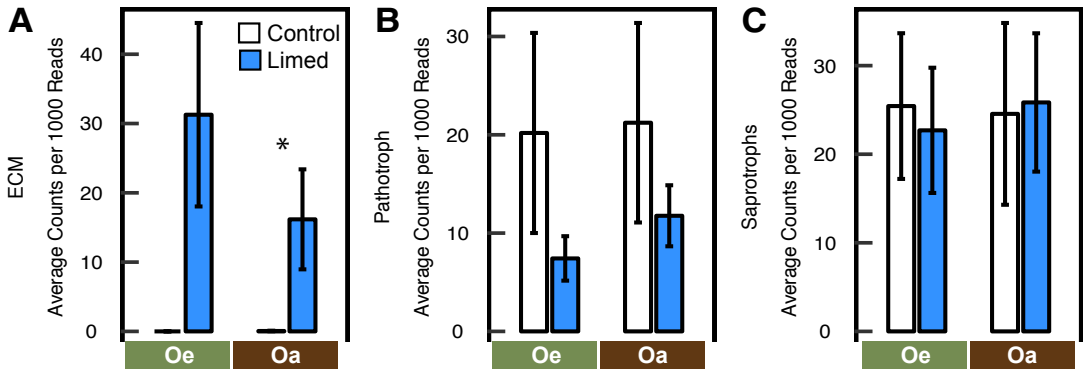

Figure S13 Average relative abundance of ASVs classified into (A) Ectomycorrhizal (ECM), (B) Pathogenic, and (C) Saprotrophic guilds by FUNGuild over treatment and horizon in SIP experiment. Only probable, highly probably, and unambiguous guild classifications were included. Significant within-horizon treatment differences are marked by * ($P < 0.05$).

Table S1 PERMANOVA results for Bray-Curtis distance of gradient fraction compositions

	Df	SumsOfSqs	MeanSqs	F.Model	R2	P	Sig.
(A) PERMANOVA for bacteria							
Treatment	1	3.271	3.2706	23.604	0.09	0.001	***
Horizon	1	5.151	5.1513	37.177	0.147	0.001	***
Time	1	1.093	1.0927	7.886	0.031	0.001	***
Isotope	1	1.584	1.5842	11.433	0.045	0.001	***
Buoyant_density	66	13.136	0.199	1.436	0.376	0.001	***
Residuals	77	10.669	0.1386		0.305		
Total	147	34.904			1		
(B) PERMANOVA for fungi							
Treatment	1	5.248	5.2482	33.725	0.140	0.001	***
Horizon	1	1.907	1.9071	12.255	0.051	0.001	***
Time	1	0.938	0.9382	6.029	0.025	0.001	***
Isotope	1	5.083	5.0827	32.661	0.136	0.001	***
Buoyant_density	66	12.143	0.184	1.182	0.325	0.025	*
Residuals	77	11.983	0.1556		0.321		
Total	147	37.302			1		

Table S2 PERMANOVA results for Bray-Curtis distances of incorporators in pre-fractionated DNA

PERMANOVA for bacteria							
	Df	**SumsOfSqs**	**MeanSqs**	**F.Model**	**R2**	**P**	**Sig.**
Treatment	1	0.44597	0.44597	3.9986	0.18	0.002	**
Horizon	1	0.44941	0.44941	4.0294	0.19	0.001	***
Time	1	0.09378	0.09378	0.8409	0.04	0.55	
Isotope	1	0.20186	0.20186	1.8099	0.08	0.09	.
Residuals	11	1.22685	0.11153	0.50741			
Total	15	2.41788	1				
(B) PERMANOVA for fungi							
Treatment	1	0.6232	0.6232	7.6375	0.23	0.001	***
Horizon	1	0.47849	0.47849	5.864	0.18	0.001	***
Time	1	0.12865	0.12865	1.5766	0.05	0.166	
Isotope	1	0.56454	0.56454	6.9185	0.21	0.001	***
Residuals	11	0.89758	0.0816	0.33337			
Total	15	2.69246	1				

Table S3: Identity of 496 bacteria ^{13}C incorporators and the treatments, horizons, and times in which they took up label. ASVs characterized as "NA" are not matched in the taxonomic database at the specific taxonomic level.

OTU	Treatments	Times	Horizons	Phylum	Family	Class	Order	Genus	Species
ASV_1	Control Limed	Day 15 Day 40	Oa Oe	Proteobacteria	Burkholderiaceae	Betaproteobacteria	Burkholderiales	Paraburkholderia	NA
ASV_10	Limed	Day 40	Oe	Proteobacteria	NA	Alphaproteobacteria	Rhizobiales	NA	NA
ASV_100	Control	Day 15	Oa	Actinobacteria	Thermomonosporaceae	Actinobacteria	Streptosporangiales	NA	NA
ASV_101	Control Limed	Day 15 Day 40	Oe Oa	Proteobacteria	Burkholderiaceae	Betaproteobacteria	Burkholderiales	Paraburkholderia	Paraburkholderia susongensis
ASV_102	Control Limed	Day 40 Day 15	Oa Oe	Proteobacteria	Burkholderiaceae	Betaproteobacteria	Burkholderiales	Paraburkholderia	NA
ASV_1026	Limed	Day 40	Oe	Actinobacteria	NA	Actinobacteria	Streptosporangiales	NA	NA
ASV_103	Limed	Day 40	Oe	Actinobacteria	Thermomonosporaceae	Actinobacteria	Streptosporangiales	Actinoallomurus	NA
ASV_1035	Limed	Day 15	Oe	Proteobacteria	Rhizobiaceae	Alphaproteobacteria	Rhizobiales	NA	NA
ASV_104	Control Limed	Day 15 Day 40	Oa Oe	Actinobacteria	Streptomycetaceae	Actinobacteria	Streptomycetales	NA	NA
ASV_1041	Limed	Day 40	Oe	Actinobacteria	Thermomonosporaceae	Actinobacteria	Streptosporangiales	Actinomadura	NA
ASV_1043	Limed	Day 40	Oe	Proteobacteria	Erythrobacteraceae	Alphaproteobacteria	Sphingomonadales	NA	NA
ASV_1049	Limed	Day 40	Oe	Planctomycetes	Isosphaeraceae	Planctomycetia	Planctomycetales	Aquisphaera	Aquisphaera giovannonii
ASV_1056	Limed	Day 40	Oe	Actinobacteria	Geodermatophilaceae	Actinobacteria	Geodermatophilales	NA	NA
ASV_106	Limed	Day 15 Day 40	Oe	Proteobacteria	Sphingomonadaceae	Alphaproteobacteria	Sphingomonadales	Novosphingobium	NA
ASV_107	Limed	Day 40	Oe	Actinobacteria	Thermomonosporaceae	Actinobacteria	Streptosporangiales	Actinoallomurus	NA
ASV_108	Limed	Day 40	Oe	Actinobacteria	NA	Actinobacteria	Streptosporangiales	NA	NA
ASV_1083	Limed	Day 15	Oa	Proteobacteria	Xanthobacteraceae	Alphaproteobacteria	Rhizobiales	Labrys	NA
ASV_109	Limed	Day 15 Day 40	Oa Oe	Proteobacteria	Burkholderiaceae	Betaproteobacteria	Burkholderiales	Paraburkholderia	NA
ASV_1098	Limed	Day 40	Oe	Bacteroidetes	Chitinophagaceae	Chitinophagia	Chitinophagales	NA	NA
ASV_11	Control Limed	Day 40	Oa Oe	Proteobacteria	Bradyrhizobiaceae	Alphaproteobacteria	Rhizobiales	Bradyrhizobium	NA
ASV_110	Control Limed	Day 40	Oa Oe	Actinobacteria	Mycobacteriaceae	Actinobacteria	Corynebacteriales	Mycobacterium	NA
ASV_1106	Control	Day 40	Oa	Actinobacteria	Dermacoccaceae	Actinobacteria	Micrococcales	NA	NA
ASV_1107	Limed	Day 40	Oa	Proteobacteria	Sinobacteraceae	Gammaproteobacteria	Nevskiales	Nevskia	NA
ASV_111	Limed	Day 40	Oe	Actinobacteria	Thermomonosporaceae	Actinobacteria	Streptosporangiales	Actinomadura	NA
ASV_1121	Limed	Day 15 Day 40	Oe	Proteobacteria	Oxalobacteraceae	Betaproteobacteria	Burkholderiales	NA	NA
ASV_113	Limed	Day 40	Oe	Proteobacteria	Roseiarcaceae	Alphaproteobacteria	Rhizobiales	Roseiarcus	Roseiarcus fermentans
ASV_1130	Limed	Day 15	Oa	Proteobacteria	Comamonadaceae	Betaproteobacteria	Burkholderiales	NA	NA
ASV_1138	Control	Day 40	Oa	Proteobacteria	Coxiellaceae	Gammaproteobacteria	Legionellales	Aquicella	Aquicella siphonis
ASV_1141	Limed	Day 40	Oe	Firmicutes	Paenibacillaceae	Bacilli	Bacillales	Paenibacillus	NA
ASV_1145	Limed	Day 40	Oe	Proteobacteria	NA	Gammaproteobacteria	NA	NA	NA
ASV_1148	Limed	Day 15	Oa	Proteobacteria	Rhodanobacteraceae	Gammaproteobacteria	Xanthomonadales	Dokdonella	Dokdonella ginsengisoli
ASV_115	Control	Day 15 Day 40	Oa	Proteobacteria	Acetobacteraceae	Alphaproteobacteria	Rhodospirillales	NA	NA
ASV_1158	Limed	Day 15	Oe	Bacteroidetes	Sphingobacteriaceae	Sphingobacteriia	Sphingobacteriales	Mucilaginibacter	NA
ASV_116	Limed	Day 40	Oe	Actinobacteria	Thermomonosporaceae	Actinobacteria	Streptosporangiales	Actinoallomurus	NA
ASV_117	Control Limed	Day 15 Day 40	Oa Oe	Proteobacteria	Acetobacteraceae	Alphaproteobacteria	Rhodospirillales	Acidocella	NA
ASV_1177	Limed	Day 40	Oe	Actinobacteria	NA	Actinobacteria	NA	NA	NA
ASV_118	Limed	Day 15 Day 40	Oe Oa	Proteobacteria	Hyphomicrobiaceae	Alphaproteobacteria	Rhizobiales	Devosia	NA
ASV_119	Limed	Day 40	Oe	Planctomycetes	Isosphaeraceae	Planctomycetia	Planctomycetales	NA	NA
ASV_1197	Control	Day 15	Oe	Acidobacteria	Acidobacteriaceae	Acidobacteriia	Acidobacteriales	Terracidiphilus	Terracidiphilus gabretensis
ASV_120	Limed	Day 15 Day 40	Oe	Proteobacteria	Rhizobiaceae	Alphaproteobacteria	Rhizobiales	Rhizobium	NA
ASV_1202	Control	Day 40	Oa	Proteobacteria	Acetobacteraceae	Alphaproteobacteria	Rhodospirillales	NA	NA
ASV_1204	Limed	Day 15	Oe	Proteobacteria	Sinobacteraceae	Gammaproteobacteria	Nevskiales	Nevskia	Nevskia soli
ASV_121	Limed	Day 15 Day 40	Oa Oe	Proteobacteria	Burkholderiaceae	Betaproteobacteria	Burkholderiales	Paraburkholderia	NA
ASV_1210	Limed	Day 15	Oe	Proteobacteria	Sinobacteraceae	Gammaproteobacteria	Nevskiales	NA	NA

ASV_122	Control Limed	Day 40	Oa Oe	Actinobacteria	NA	Acidimicrobiia	Acidimicrobiales	NA	NA
ASV_1236	Control	Day 40	Oa	Proteobacteria	Burkholderiaceae	Betaproteobacteria	Burkholderiales	Burkholderia	Burkholderia alpina
ASV_124	Limed	Day 40	Oe	Planctomycetes	Isosphaeraceae	Planctomycetia	Planctomycetales	Aquisphaera	Aquisphaera giovannonii
ASV_125	Limed	Day 40	Oe	Planctomycetes	Isosphaeraceae	Planctomycetia	Planctomycetales	NA	NA
ASV_126	Limed	Day 15 Day 40	Oe Oa	Proteobacteria	Bradyrhizobiaceae	Alphaproteobacteria	Rhizobiales	NA	NA
ASV_1264	Limed	Day 15	Oe	Proteobacteria	Hyphomicrobiaceae	Alphaproteobacteria	Rhizobiales	Devosia	NA
ASV_1278	Limed	Day 15	Oe	Proteobacteria	Burkholderiaceae	Betaproteobacteria	Burkholderiales	Cupriavidus	NA
ASV_128	Control Limed	Day 15 Day 40	Oa Oe	Acidobacteria	Acidobacteriaceae	Acidobacteriia	Acidobacteriales	NA	NA
ASV_1290	Limed	Day 40	Oe	Bacteroidetes	Chitinophagaceae	Chitinophagia	Chitinophagales	Taibaiella	Taibaiella coffeisoli
ASV_13	Limed	Day 40	Oe	Planctomycetes	Isosphaeraceae	Planctomycetia	Planctomycetales	NA	NA
ASV_130	Control Limed	Day 40	Oa Oe	Proteobacteria	Beijerinckiaceae	Alphaproteobacteria	Rhizobiales	Methylovirgula	Methylovirgula ligni
ASV_1301	Limed	Day 15	Oe	Bacteroidetes	Sphingobacteriaceae	Sphingobacteriia	Sphingobacteriales	Mucilaginibacter	NA
ASV_131	Limed	Day 15 Day 40	Oa Oe	Proteobacteria	Rhodanobacteraceae	Gammaproteobacteria	Xanthomonadales	NA	NA
ASV_132	Limed	Day 40	Oe	Actinobacteria	NA	Actinobacteria	Streptosporangiales	NA	NA
ASV_133	Control Limed	Day 15 Day 40	Oe Oa	Acidobacteria	Acidobacteriaceae	Acidobacteriia	Acidobacteriales	Silvibacterium	Silvibacterium bohemicum
ASV_1332	Control	Day 40	Oe	Actinobacteria	Frankiaceae	Actinobacteria	Frankiales	Jatrophihabitans	NA
ASV_134	Control Limed	Day 40 Day 15	Oa	Acidobacteria	Acidobacteriaceae	Acidobacteriia	Acidobacteriales	NA	NA
ASV_1342	Limed	Day 15	Oe	Proteobacteria	Xanthobacteraceae	Alphaproteobacteria	Rhizobiales	Labrys	NA
ASV_1349	Limed	Day 40	Oe	Proteobacteria	Caulobacteraceae	Alphaproteobacteria	Caulobacterales	Phenylobacterium	NA
ASV_135	Control Limed	Day 15 Day 40	Oe Oa	Acidobacteria	Acidobacteriaceae	Acidobacteriia	Acidobacteriales	Edaphobacter	Edaphobacter dinghuensis
ASV_1351	Limed	Day 40	Oe	Proteobacteria	Sphingomonadaceae	Alphaproteobacteria	Sphingomonadales	Sphingobium	NA
ASV_1352	Limed	Day 40	Oa	Actinobacteria	NA	Actinobacteria	NA	NA	NA
ASV_136	Limed	Day 40	Oe	Proteobacteria	Pasteurellaceae	Gammaproteobacteria	Pasteurellales	Haemophilus	NA
ASV_137	Limed	Day 40	Oe	Proteobacteria	Beijerinckiaceae	Alphaproteobacteria	Rhizobiales	NA	NA
ASV_1378	Limed	Day 40	Oe	Proteobacteria	Caulobacteraceae	Alphaproteobacteria	Caulobacterales	NA	NA
ASV_1393	Limed	Day 15	Oe	Bacteroidetes	Not Available	Cytophagia	Cytophagales	Chryseolinea	Chryseolinea serpens
ASV_1394	Control	Day 15	Oe	Proteobacteria	Acetobacteraceae	Alphaproteobacteria	Rhodospirillales	Acidocella	NA
ASV_141	Limed	Day 15 Day 40	Oe	Bacteroidetes	Chitinophagaceae	Chitinophagia	Chitinophagales	Niastella	NA
ASV_1415	Limed	Day 15 Day 40	Oe	Proteobacteria	Rhizobiaceae	Alphaproteobacteria	Rhizobiales	Rhizobium	NA
ASV_1417	Limed	Day 15	Oa	Acidobacteria	Acidobacteriaceae	Acidobacteriia	Acidobacteriales	NA	NA
ASV_143	Control Limed	Day 15 Day 40	Oe Oa	Proteobacteria	Rhodanobacteraceae	Gammaproteobacteria	Xanthomonadales	Dyella	NA
ASV_1433	Limed	Day 40	Oe	Actinobacteria	NA	Actinobacteria	NA	NA	NA
ASV_144	Limed	Day 40	Oe	Planctomycetes	Isosphaeraceae	Planctomycetia	Planctomycetales	Singulisphaera	Singulisphaera rosea
ASV_145	Control Limed	Day 15 Day 40	Oe Oa	Proteobacteria	Burkholderiaceae	Betaproteobacteria	Burkholderiales	Burkholderia	NA
ASV_1454	Limed	Day 15	Oe	Proteobacteria	NA	Gammaproteobacteria	NA	NA	NA
ASV_1462	Limed	Day 15	Oa	Proteobacteria	Xanthomonadaceae	Gammaproteobacteria	Xanthomonadales	NA	NA
ASV_148	Limed	Day 40	Oe	Actinobacteria	Acidimicrobiaceae	Acidimicrobiia	Acidimicrobiales	NA	NA
ASV_149	Limed	Day 40	Oe	Planctomycetes	Isosphaeraceae	Planctomycetia	Planctomycetales	Aquisphaera	Aquisphaera giovannonii
ASV_1492	Limed	Day 40	Oe	Proteobacteria	Sphingomonadaceae	Alphaproteobacteria	Sphingomonadales	Sphingomonas	NA
ASV_15	Limed	Day 40	Oe	Acidobacteria	Acidobacteriaceae	Acidobacteriia	Acidobacteriales	NA	NA
ASV_150	Limed	Day 40	Oe	Firmicutes	Bacillaceae	Bacilli	Bacillales	Bacillus	NA
ASV_151	Limed	Day 40	Oe	Chlamydiae	Parachlamydiaceae	Chlamydiia	Parachlamydiales	Candidatus Protochlamydia	Candidatus Protochlamydia naegleriophila
ASV_152	Limed	Day 40	Oe	Actinobacteria	Conexibacteraceae	Thermoleophilia	Solirubrobacterales	Conexibacter	Conexibacter woesei
ASV_1522	Limed	Day 40	Oe	Bacteroidetes	Chitinophagaceae	Chitinophagia	Chitinophagales	NA	NA
ASV_153	Limed	Day 40	Oe	Planctomycetes	Isosphaeraceae	Planctomycetia	Planctomycetales	NA	NA
ASV_1549	Limed	Day 40	Oe	Proteobacteria	Phyllobacteriaceae	Alphaproteobacteria	Rhizobiales	Mesorhizobium	NA
ASV_155	Limed	Day 40	Oa Oe	Actinobacteria	Mycobacteriaceae	Actinobacteria	Corynebacteriales	Mycolicibacterium	NA
ASV_157	Limed	Day 40	Oe	Actinobacteria	NA	Actinobacteria	Streptosporangiales	NA	NA

ASV_1570	Control	Day 40	Oa	Proteobacteria	Caulobacteraceae	Alphaproteobacteria	Caulobacterales	Phenylobacterium	NA
ASV_1572	Control	Day 15	Oe	Proteobacteria	NA	Gammaproteobacteria	NA	NA	NA
ASV_1573	Limed	Day 40	Oe	Proteobacteria	Hyphomicrobiaceae	Alphaproteobacteria	Rhizobiales	Devosia	NA
ASV_159	Control Limed	Day 40 Day 15	Oa Oe	Proteobacteria	Burkholderiaceae	Betaproteobacteria	Burkholderiales	NA	NA
ASV_16	Limed	Day 15 Day 40	Oa Oe	Proteobacteria	Rhodanobacteraceae	Gammaproteobacteria	Xanthomonadales	Dyella	Dyella japonica
ASV_160	Limed	Day 40	Oe	Planctomycetes	Isosphaeraceae	Planctomycetia	Planctomycetales	NA	NA
ASV_161	Limed	Day 15 Day 40	Oa Oe	Proteobacteria	Burkholderiaceae	Betaproteobacteria	Burkholderiales	Burkholderia	NA
ASV_1616	Control	Day 40	Oa	Actinobacteria	Conexibacteraceae	Thermoleophilia	Solirubrobacterales	Conexibacter	Conexibacter woesei
ASV_1629	Limed	Day 40	Oa	Actinobacteria	Frankiaceae	Actinobacteria	Frankiales	Jatrophihabitans	NA
ASV_1638	Limed	Day 40	Oe	Proteobacteria	Sphingomonadaceae	Alphaproteobacteria	Sphingomonadales	Sphingomonas	Sphingomonas formosensis
ASV_164	Control Limed	Day 40	Oa Oe	Actinobacteria	Conexibacteraceae	Thermoleophilia	Solirubrobacterales	Conexibacter	Conexibacter woesei
ASV_165	Limed	Day 40	Oe	Actinobacteria	Nocardioidaceae	Actinobacteria	Propionibacteriales	Nocardioides	Nocardioides endophyticus
ASV_166	Limed	Day 40	Oe	Planctomycetes	Isosphaeraceae	Planctomycetia	Planctomycetales	Singulisphaera	Singulisphaera acidiphila
ASV_1663	Limed	Day 40	Oa	Proteobacteria	Sphingomonadaceae	Alphaproteobacteria	Sphingomonadales	Sphingomonas	NA
ASV_167	Limed	Day 40	Oe	Proteobacteria	Pseudomonadaceae	Gammaproteobacteria	Pseudomonadales	Pseudomonas	NA
ASV_168	Limed	Day 40	Oe	Firmicutes	Streptococcaceae	Bacilli	Lactobacillales	Streptococcus	NA
ASV_17	Limed	Day 40	Oa Oe	Firmicutes	Streptococcaceae	Bacilli	Lactobacillales	Streptococcus	NA
ASV_170	Limed	Day 40	Oe	Actinobacteria	NA	Actinobacteria	Streptosporangiales	NA	NA
ASV_1700	Limed	Day 15	Oe	Bacteroidetes	Chitinophagaceae	Chitinophagia	Chitinophagales	Niastella	Niastella koreensis
ASV_172	Limed	Day 40	Oe	Firmicutes	Streptococcaceae	Bacilli	Lactobacillales	Streptococcus	NA
ASV_173	Limed	Day 40	Oe	Acidobacteria	Bryobacteraceae	Solibacteres	Solibacterales	Paludibaculum	Paludibaculum fermentans
ASV_1749	Limed	Day 15	Oe	Bacteroidetes	Chitinophagaceae	Chitinophagia	Chitinophagales	Chitinophaga	NA
ASV_175	Limed	Day 40	Oe	Actinobacteria	Thermomonosporaceae	Actinobacteria	Streptosporangiales	Actinoallomurus	NA
ASV_176	Limed	Day 40	Oe	Proteobacteria	Bradyrhizobiaceae	Alphaproteobacteria	Rhizobiales	Bradyrhizobium	NA
ASV_177	Limed	Day 40	Oe	Proteobacteria	Roseiarcaceae	Alphaproteobacteria	Rhizobiales	Roseiarcus	Roseiarcus fermentans
ASV_1779	Limed	Day 15 Day 40	Oe Oa	Actinobacteria	Streptomycetaceae	Actinobacteria	Streptomycetales	Streptomyces	NA
ASV_178	Control Limed	Day 15 Day 40	Oe	Proteobacteria	Acetobacteraceae	Alphaproteobacteria	Rhodospirillales	NA	NA
ASV_179	Control	Day 15	Oe	Chlamydiae	NA	Chlamydiia	NA	NA	NA
ASV_18	Limed	Day 40	Oe	Proteobacteria	Roseiarcaceae	Alphaproteobacteria	Rhizobiales	Roseiarcus	Roseiarcus fermentans
ASV_180	Limed	Day 40	Oe	Planctomycetes	Isosphaeraceae	Planctomycetia	Planctomycetales	Singulisphaera	NA
ASV_181	Limed	Day 40	Oe	Actinobacteria	Thermomonosporaceae	Actinobacteria	Streptosporangiales	Actinomadura	NA
ASV_1811	Limed	Day 15	Oe	Proteobacteria	NA	Alphaproteobacteria	Sphingomonadales	NA	NA
ASV_1822	Limed	Day 15	Oe	Actinobacteria	Nakamurellaceae	Actinobacteria	Nakamurellales	Nakamurella	Nakamurella flavida
ASV_1824	Limed	Day 15	Oe	Bacteroidetes	Chitinophagaceae	Chitinophagia	Chitinophagales	NA	NA
ASV_183	Control	Day 15	Oe	Firmicutes	Thermoactinomycetaceae	Bacilli	Bacillales	NA	NA
ASV_184	Control Limed	Day 40	Oa Oe	Proteobacteria	Not Available	Gammaproteobacteria	Not Available	Acidibacter	Acidibacter ferrireducens
ASV_185	Control	Day 40	Oa	Actinobacteria	Micromonosporaceae	Actinobacteria	Micromonosporales	NA	NA
ASV_1857	Limed	Day 40	Oe	Proteobacteria	Erythrobacteraceae	Alphaproteobacteria	Sphingomonadales	NA	NA
ASV_187	Control	Day 15 Day 40	Oe Oa	Proteobacteria	Burkholderiaceae	Betaproteobacteria	Burkholderiales	Caballeronia	NA
ASV_188	Limed	Day 40	Oa Oe	Actinobacteria	Mycobacteriaceae	Actinobacteria	Corynebacteriales	NA	NA
ASV_189	Limed	Day 15 Day 40	Oa Oe	Proteobacteria	Rhizobiaceae	Alphaproteobacteria	Rhizobiales	Rhizobium	NA
ASV_19	Control Limed	Day 15 Day 40	Oa Oe	Proteobacteria	Burkholderiaceae	Betaproteobacteria	Burkholderiales	NA	NA
ASV_190	Limed	Day 40	Oe	Acidobacteria	Acidobacteriaceae	Acidobacteriia	Acidobacteriales	NA	NA
ASV_191	Limed	Day 40	Oe	Planctomycetes	Isosphaeraceae	Planctomycetia	Planctomycetales	NA	NA
ASV_192	Control Limed	Day 40	Oa Oe	Actinobacteria	Frankiaceae	Actinobacteria	Frankiales	Jatrophihabitans	NA
ASV_194	Limed	Day 15 Day 40	Oa Oe	Proteobacteria	Caulobacteraceae	Alphaproteobacteria	Caulobacterales	Phenylobacterium	NA
ASV_196	Control Limed	Day 15 Day 40	Oa Oe	Actinobacteria	NA	Actinobacteria	NA	NA	NA
ASV_198	Control Limed	Day 15 Day 40	Oa Oe	Proteobacteria	Acetobacteraceae	Alphaproteobacteria	Rhodospirillales	Acidocella	NA

ASV_2	Limed	Day 40	Oe	Actinobacteria	Thermomonosporaceae	Actinobacteria	Streptosporangiales	Actinoallomurus	NA
ASV_20	Limed	Day 40	Oe	Proteobacteria	NA	Alphaproteobacteria	Rhizobiales	NA	NA
ASV_2009	Limed	Day 15	Oe	Proteobacteria	Sphingomonadaceae	Alphaproteobacteria	Sphingomonadales	Sphingomonas	Sphingomonas wittichii
ASV_201	Limed	Day 40	Oe	Acidobacteria	Acidobacteriaceae	Acidobacteriia	Acidobacteriales	Silvibacterium	Silvibacterium bohemicum
ASV_203	Limed	Day 40	Oe	Actinobacteria	NA	Thermoleophilia	Solirubrobacterales	NA	NA
ASV_205	Limed	Day 40	Oe	Firmicutes	Streptococcaceae	Bacilli	Lactobacillales	Streptococcus	NA
ASV_2057	Limed	Day 40	Oe	Proteobacteria	Labilitrichaceae	Deltaproteobacteria	Myxococcales	Labilithrix	Labilithrix luteola
ASV_208	Control Limed	Day 40	Oa	Actinobacteria	Mycobacteriaceae	Actinobacteria	Corynebacteriales	Mycolicibacterium	NA
ASV_21	Control Limed	Day 15 Day 40	Oa Oe	Proteobacteria	Rhodanobacteraceae	Gammaproteobacteria	Xanthomonadales	Dyella	NA
ASV_210	Limed	Day 15 Day 40	Oe	Proteobacteria	Alcaligenaceae	Betaproteobacteria	Burkholderiales	Bordetella	NA
ASV_211	Limed	Day 40	Oe	Actinobacteria	Thermomonosporaceae	Actinobacteria	Streptosporangiales	Actinomadura	NA
ASV_2111	Limed	Day 40	Oe	Proteobacteria	Sphingomonadaceae	Alphaproteobacteria	Sphingomonadales	NA	NA
ASV_213	Limed	Day 40	Oe	Actinobacteria	Thermomonosporaceae	Actinobacteria	Streptosporangiales	Actinoallomurus	NA
ASV_214	Limed	Day 40	Oa Oe	Planctomycetes	Isosphaeraceae	Planctomycetia	Planctomycetales	NA	NA
ASV_2142	Limed	Day 40	Oa	Proteobacteria	Caulobacteraceae	Alphaproteobacteria	Caulobacterales	NA	NA
ASV_215	Limed	Day 40	Oa	Actinobacteria	NA	Actinobacteria	NA	NA	NA
ASV_216	Control Limed	Day 40	Oa Oe	Proteobacteria	Acetobacteraceae	Alphaproteobacteria	Rhodospirillales	NA	NA
ASV_217	Control Limed	Day 15 Day 40	Oa Oe	Actinobacteria	Streptomycetaceae	Actinobacteria	Streptomycetales	NA	NA
ASV_218	Limed	Day 40	Oe	Firmicutes	NA	Bacilli	Lactobacillales	NA	NA
ASV_219	Limed	Day 40	Oe	Planctomycetes	Isosphaeraceae	Planctomycetia	Planctomycetales	Aquisphaera	Aquisphaera giovannonii
ASV_22	Control Limed	Day 40 Day 15	Oa Oe	Proteobacteria	Rhodanobacteraceae	Gammaproteobacteria	Xanthomonadales	Luteibacter	Luteibacter rhizovicinus
ASV_220	Control Limed	Day 15 Day 40	Oa Oe	Actinobacteria	NA	Actinobacteria	Streptosporangiales	NA	NA
ASV_2204	Limed	Day 15	Oa	Actinobacteria	Nocardioidaceae	Actinobacteria	Propionibacteriales	Nocardioides	NA
ASV_223	Limed	Day 40	Oe	Proteobacteria	Acetobacteraceae	Alphaproteobacteria	Rhodospirillales	NA	NA
ASV_228	Limed	Day 15	Oe	Actinobacteria	Microbacteriaceae	Actinobacteria	Micrococcales	NA	NA
ASV_231	Control	Day 40	Oa	Actinobacteria	Mycobacteriaceae	Actinobacteria	Corynebacteriales	Mycobacterium	NA
ASV_233	Control	Day 40	Oa	Proteobacteria	NA	Alphaproteobacteria	NA	NA	NA
ASV_234	Control	Day 15	Oe	Proteobacteria	NA	Alphaproteobacteria	Rhizobiales	NA	NA
ASV_235	Limed	Day 40	Oe	Actinobacteria	Thermomonosporaceae	Actinobacteria	Streptosporangiales	NA	NA
ASV_2356	Limed	Day 15	Oe	Proteobacteria	Pseudomonadaceae	Gammaproteobacteria	Pseudomonadales	Pseudomonas	Pseudomonas chlororaphis
ASV_236	Control	Day 15	Oe	Acidobacteria	Acidobacteriaceae	Acidobacteriia	Acidobacteriales	NA	NA
ASV_239	Limed	Day 40	Oe	Proteobacteria	Labilitrichaceae	Deltaproteobacteria	Myxococcales	Labilithrix	Labilithrix luteola
ASV_24	Limed	Day 40	Oe	Actinobacteria	NA	Actinobacteria	Streptosporangiales	NA	NA
ASV_240	Limed	Day 15 Day 40	Oa	Proteobacteria	Burkholderiaceae	Betaproteobacteria	Burkholderiales	NA	NA
ASV_241	Control Limed	Day 40	Oa Oe	Actinobacteria	Conexibacteraceae	Thermoleophilia	Solirubrobacterales	Conexibacter	Conexibacter woesei
ASV_242	Limed	Day 40	Oe	Actinobacteria	Corynebacteriaceae	Actinobacteria	Corynebacteriales	Corynebacterium	Corynebacterium durum
ASV_2436	Limed	Day 15	Oe	Proteobacteria	Bradyrhizobiaceae	Alphaproteobacteria	Rhizobiales	Bradyrhizobium	NA
ASV_244	Limed	Day 40	Oe	Proteobacteria	Neisseriaceae	Betaproteobacteria	Neisseriales	NA	NA
ASV_246	Control Limed	Day 40	Oa	Actinobacteria	Mycobacteriaceae	Actinobacteria	Corynebacteriales	Mycolicibacterium	NA
ASV_247	Limed	Day 40	Oe	Firmicutes	Not Available	Bacilli	Bacillales	Gemella	NA
ASV_25	Limed	Day 40	Oe	Proteobacteria	Roseiarcaceae	Alphaproteobacteria	Rhizobiales	Roseiarcus	Roseiarcus fermentans
ASV_251	Limed	Day 40	Oe	Proteobacteria	Roseiarcaceae	Alphaproteobacteria	Rhizobiales	Roseiarcus	Roseiarcus fermentans
ASV_253	Control	Day 15 Day 40	Oe Oa	Proteobacteria	Rhodanobacteraceae	Gammaproteobacteria	Xanthomonadales	NA	NA
ASV_254	Control Limed	Day 40	Oa Oe	Acidobacteria	Acidobacteriaceae	Acidobacteriia	Acidobacteriales	Granulicella	Granulicella sapmiensis
ASV_256	Control	Day 40	Oa	Actinobacteria	Conexibacteraceae	Thermoleophilia	Solirubrobacterales	Conexibacter	NA
ASV_258	Limed	Day 40	Oe	Planctomycetes	Isosphaeraceae	Planctomycetia	Planctomycetales	Aquisphaera	Aquisphaera giovannonii
ASV_259	Control Limed	Day 40	Oa	Actinobacteria	Actinospicaceae	Actinobacteria	Catenulisporales	Actinospica	NA
ASV_2594	Limed	Day 15	Oe	Verrucomicrobia	Verrucomicrobiaceae	Verrucomicrobiae	Verrucomicrobiales	Prosthecobacter	NA

ASV_26	Limed	Day 40	Oe	Proteobacteria	Hyphomicrobiaceae	Alphaproteobacteria	Rhizobiales	Rhodoplanes	NA
ASV_260	Limed	Day 15 Day 40	Oe	Proteobacteria	NA	Alphaproteobacteria	Rhizobiales	NA	NA
ASV_261	Limed	Day 40	Oe	Proteobacteria	Not Available	Gammaproteobacteria	Not Available	Acidibacter	Acidibacter ferrireducens
ASV_262	Limed	Day 40	Oe	Actinobacteria	Thermomonosporaceae	Actinobacteria	Streptosporangiales	NA	NA
ASV_267	Limed	Day 40	Oe	Proteobacteria	Acetobacteraceae	Alphaproteobacteria	Rhodospirillales	NA	NA
ASV_268	Limed	Day 40	Oe	Planctomycetes	Isosphaeraceae	Planctomycetia	Planctomycetales	NA	NA
ASV_27	Control Limed	Day 15 Day 40	Oa Oe	Proteobacteria	Rhodanobacteraceae	Gammaproteobacteria	Xanthomonadales	NA	NA
ASV_270	Control	Day 15 Day 40	Oe Oa	Proteobacteria	Burkholderiaceae	Betaproteobacteria	Burkholderiales	Paraburkholderia	NA
ASV_276	Control Limed	Day 15 Day 40	Oa Oe	Actinobacteria	Streptomycetaceae	Actinobacteria	Streptomycetales	NA	NA
ASV_277	Limed	Day 40	Oe	Acidobacteria	Acidobacteriaceae	Acidobacteriia	Acidobacteriales	NA	NA
ASV_2775	Limed	Day 15	Oe	Proteobacteria	Rhizobiaceae	Alphaproteobacteria	Rhizobiales	Rhizobium	NA
ASV_279	Limed	Day 40	Oe	Bacteroidetes	Chitinophagaceae	Chitinophagia	Chitinophagales	Chitinophaga	Chitinophaga soli
ASV_28	Limed	Day 40	Oe	Actinobacteria	Acidimicrobiaceae	Acidimicrobiia	Acidimicrobiales	NA	NA
ASV_280	Limed	Day 15 Day 40	Oe	Proteobacteria	Burkholderiaceae	Betaproteobacteria	Burkholderiales	Paraburkholderia	NA
ASV_281	Limed	Day 40	Oe	Proteobacteria	Legionellaceae	Gammaproteobacteria	Legionellales	Legionella	NA
ASV_284	Limed	Day 40	Oe	Acidobacteria	Acidobacteriaceae	Acidobacteriia	Acidobacteriales	NA	NA
ASV_2842	Limed	Day 15	Oe	Proteobacteria	NA	Alphaproteobacteria	Rhodobacterales	NA	NA
ASV_2863	Limed	Day 15	Oe	Proteobacteria	Sphingomonadaceae	Alphaproteobacteria	Sphingomonadales	Sphingomonas	NA
ASV_287	Limed	Day 40	Oe	Actinobacteria	Thermomonosporaceae	Actinobacteria	Streptosporangiales	Actinomadura	NA
ASV_290	Control	Day 40	Oa	Proteobacteria	Micropepsaceae	Alphaproteobacteria	Micropepsales	Rhizomicrobium	NA
ASV_291	Limed	Day 40	Oe	Actinobacteria	Micrococcaceae	Actinobacteria	Micrococcales	Rothia	Rothia dentocariosa
ASV_292	Control Limed	Day 40 Day 15	Oa Oe	Actinobacteria	Microbacteriaceae	Actinobacteria	Micrococcales	NA	NA
ASV_293	Limed	Day 15 Day 40	Oe	Proteobacteria	Caulobacteraceae	Alphaproteobacteria	Caulobacterales	Caulobacter	Caulobacter henricii
ASV_294	Limed	Day 40	Oe	Proteobacteria	Acetobacteraceae	Alphaproteobacteria	Rhodospirillales	NA	NA
ASV_296	Limed	Day 40	Oe	Actinobacteria	Micrococcaceae	Actinobacteria	Micrococcales	Rothia	Rothia mucilaginosa
ASV_2998	Limed	Day 15	Oa	Proteobacteria	Sphingomonadaceae	Alphaproteobacteria	Sphingomonadales	Sphingomonas	Sphingomonas formosensis
ASV_3	Limed	Day 40	Oe	Actinobacteria	Thermomonosporaceae	Actinobacteria	Streptosporangiales	Actinoallomurus	NA
ASV_30	Limed	Day 40	Oa	Proteobacteria	Micropepsaceae	Alphaproteobacteria	Micropepsales	Rhizomicrobium	Rhizomicrobium electricum
ASV_301	Limed	Day 40	Oe	Proteobacteria	Hyphomicrobiaceae	Alphaproteobacteria	Rhizobiales	Rhodomicrobium	Rhodomicrobium vannielii
ASV_302	Limed	Day 15 Day 40	Oa	Proteobacteria	Rhodanobacteraceae	Gammaproteobacteria	Xanthomonadales	Dyella	Dyella kyungheensis
ASV_306	Limed	Day 40	Oe	Chlamydiae	Parachlamydiaceae	Chlamydiia	Parachlamydiales	Parachlamydia	Parachlamydia acanthamoebae
ASV_308	Control Limed	Day 40	Oa Oe	Planctomycetes	Isosphaeraceae	Planctomycetia	Planctomycetales	NA	NA
ASV_31	Limed	Day 40	Oa Oe	Proteobacteria	NA	Alphaproteobacteria	Rhizobiales	NA	NA
ASV_311	Limed	Day 40	Oe	Actinobacteria	NA	Actinobacteria	NA	NA	NA
ASV_314	Limed	Day 40	Oe	Acidobacteria	Acidobacteriaceae	Acidobacteriia	Acidobacteriales	NA	NA
ASV_315	Limed	Day 40	Oe	Chlamydiae	Parachlamydiaceae	Chlamydiia	Parachlamydiales	NA	NA
ASV_3169	Limed	Day 15	Oe	Proteobacteria	Myxococcaceae	Deltaproteobacteria	Myxococcales	Myxococcus	NA
ASV_317	Limed	Day 40	Oe	Actinobacteria	Thermomonosporaceae	Actinobacteria	Streptosporangiales	Actinoallomurus	NA
ASV_319	Limed	Day 15	Oe	Proteobacteria	Pseudomonadaceae	Gammaproteobacteria	Pseudomonadales	Pseudomonas	NA
ASV_32	Limed	Day 40	Oe	Proteobacteria	NA	Alphaproteobacteria	Rhizobiales	NA	NA
ASV_320	Limed	Day 40	Oa Oe	Proteobacteria	Phyllobacteriaceae	Alphaproteobacteria	Rhizobiales	NA	NA
ASV_322	Limed	Day 40	Oe	Actinobacteria	NA	Actinobacteria	NA	NA	NA
ASV_323	Control Limed	Day 40	Oa Oe	Verrucomicrobia	Chthoniobacteraceae	Spartobacteria	Chthoniobacterales	Chthoniobacter	Chthoniobacter flavus
ASV_326	Limed	Day 15 Day 40	Oe	Proteobacteria	Sphingomonadaceae	Alphaproteobacteria	Sphingomonadales	NA	NA
ASV_327	Control Limed	Day 15 Day 40	Oa Oe	Acidobacteria	Acidobacteriaceae	Acidobacteriia	Acidobacteriales	Granulicella	NA
ASV_328	Limed	Day 15 Day 40	Oe	Actinobacteria	Nocardioidaceae	Actinobacteria	Propionibacteriales	Nocardioides	NA
ASV_33	Control Limed	Day 15 Day 40	Oa Oe	Actinobacteria	NA	Actinobacteria	Streptosporangiales	NA	NA
ASV_333	Limed	Day 15	Oe	Proteobacteria	Pseudomonadaceae	Gammaproteobacteria	Pseudomonadales	Pseudomonas	NA

ASV_335	Limed	Day 15 Day 40	Oe	Proteobacteria	Rhizobiaceae	Alphaproteobacteria	Rhizobiales	Rhizobium	NA
ASV_336	Limed	Day 40	Oe	Actinobacteria	NA	Actinobacteria	Streptosporangiales	NA	NA
ASV_338	Limed	Day 40	Oe	Proteobacteria	Sphingomonadaceae	Alphaproteobacteria	Sphingomonadales	Sphingopyxis	NA
ASV_339	Limed	Day 40	Oe	Actinobacteria	Actinomycetaceae	Actinobacteria	Actinomycetales	Actinomyces	Actinomyces odontolyticus
ASV_341	Control Limed	Day 40	Oa Oe	Acidobacteria	Acidobacteriaceae	Acidobacteriia	Acidobacteriales	NA	NA
ASV_342	Limed	Day 40	Oe	Actinobacteria	NA	Actinobacteria	Streptosporangiales	NA	NA
ASV_343	Limed	Day 40	Oa	Actinobacteria	Acidimicrobiaceae	Acidimicrobiia	Acidimicrobiales	NA	NA
ASV_346	Limed	Day 15 Day 40	Oa	Proteobacteria	Caulobacteraceae	Alphaproteobacteria	Caulobacterales	NA	NA
ASV_348	Control Limed	Day 40	Oa	Proteobacteria	Acetobacteraceae	Alphaproteobacteria	Rhodospirillales	NA	NA
ASV_35	Limed	Day 40	Oe	Proteobacteria	Legionellaceae	Gammaproteobacteria	Legionellales	Legionella	NA
ASV_352	Limed	Day 40	Oe	Proteobacteria	Bradyrhizobiaceae	Alphaproteobacteria	Rhizobiales	NA	NA
ASV_353	Limed	Day 40	Oe	Proteobacteria	Acetobacteraceae	Alphaproteobacteria	Rhodospirillales	NA	NA
ASV_355	Limed	Day 40	Oe	Proteobacteria	Phyllobacteriaceae	Alphaproteobacteria	Rhizobiales	NA	NA
ASV_357	Limed	Day 15 Day 40	Oa Oe	Proteobacteria	Sphingomonadaceae	Alphaproteobacteria	Sphingomonadales	Sphingomonas	NA
ASV_36	Limed	Day 40	Oe	Actinobacteria	Thermomonosporaceae	Actinobacteria	Streptosporangiales	Actinoallomurus	NA
ASV_360	Limed	Day 15	Oa	Bacteroidetes	Chitinophagaceae	Chitinophagia	Chitinophagales	Chitinophaga	NA
ASV_361	Limed	Day 15	Oe	Actinobacteria	Nocardiaceae	Actinobacteria	Corynebacteriales	Rhodococcus	NA
ASV_362	Limed	Day 40	Oe	Actinobacteria	Actinomycetaceae	Actinobacteria	Actinomycetales	Actinomyces	NA
ASV_363	Limed	Day 15 Day 40	Oe	Proteobacteria	Pseudomonadaceae	Gammaproteobacteria	Pseudomonadales	Pseudomonas	NA
ASV_364	Limed	Day 40	Oe	Acidobacteria	Acidobacteriaceae	Acidobacteriia	Acidobacteriales	NA	NA
ASV_366	Limed	Day 15 Day 40	Oe	Firmicutes	Paenibacillaceae	Bacilli	Bacillales	Cohnella	NA
ASV_37	Limed	Day 40	Oe	Planctomycetes	Isosphaeraceae	Planctomycetia	Planctomycetales	NA	NA
ASV_374	Control Limed	Day 15 Day 40	Oa Oe	Actinobacteria	Thermomonosporaceae	Actinobacteria	Streptosporangiales	Actinomadura	NA
ASV_377	Limed	Day 15 Day 40	Oa Oe	Proteobacteria	Rhodanobacteraceae	Gammaproteobacteria	Xanthomonadales	Rhodanobacter	NA
ASV_379	Limed	Day 40	Oe	Actinobacteria	NA	Actinobacteria	Streptosporangiales	NA	NA
ASV_380	Limed	Day 40	Oe	Proteobacteria	Micropepsaceae	Alphaproteobacteria	Micropepsales	Rhizomicrobium	Rhizomicrobium palustre
ASV_383	Limed	Day 40	Oe	Chlamydiae	Parachlamydiaceae	Chlamydiia	Parachlamydiales	NA	NA
ASV_385	Control Limed	Day 15 Day 40	Oa	Acidobacteria	Acidobacteriaceae	Acidobacteriia	Acidobacteriales	NA	NA
ASV_386	Limed	Day 40	Oe	Actinobacteria	NA	Actinobacteria	NA	NA	NA
ASV_389	Control	Day 40	Oa	Proteobacteria	Coxiellaceae	Gammaproteobacteria	Legionellales	Aquicella	Aquicella siphonis
ASV_39	Limed	Day 40	Oe	Actinobacteria	Thermomonosporaceae	Actinobacteria	Streptosporangiales	Actinoallomurus	NA
ASV_391	Control	Day 40	Oa Oe	Actinobacteria	Conexibacteraceae	Thermoleophilia	Solirubrobacterales	Conexibacter	Conexibacter woesei
ASV_393	Limed	Day 40	Oa	Planctomycetes	Isosphaeraceae	Planctomycetia	Planctomycetales	NA	NA
ASV_397	Limed	Day 40	Oe	Proteobacteria	Labilitrichaceae	Deltaproteobacteria	Myxococcales	Labilithrix	Labilithrix luteola
ASV_398	Control	Day 40	Oa	Acidobacteria	Acidobacteriaceae	Acidobacteriia	Acidobacteriales	NA	NA
ASV_399	Limed	Day 15 Day 40	Oa Oe	Bacteroidetes	Chitinophagaceae	Chitinophagia	Chitinophagales	NA	NA
ASV_4	Limed	Day 40	Oe	Proteobacteria	NA	Alphaproteobacteria	Rhizobiales	NA	NA
ASV_40	Limed	Day 40	Oe	Actinobacteria	NA	Actinobacteria	Streptosporangiales	NA	NA
ASV_405	Limed	Day 15	Oe	Proteobacteria	Pseudomonadaceae	Gammaproteobacteria	Pseudomonadales	Pseudomonas	NA
ASV_408	Control Limed	Day 40	Oa Oe	Proteobacteria	Caulobacteraceae	Alphaproteobacteria	Caulobacterales	NA	NA
ASV_409	Limed	Day 40	Oa	Proteobacteria	Caulobacteraceae	Alphaproteobacteria	Caulobacterales	NA	NA
ASV_41	Limed	Day 40	Oe	Proteobacteria	NA	Alphaproteobacteria	Rhizobiales	NA	NA
ASV_410	Control Limed	Day 40	Oe Oa	Actinobacteria	Microbacteriaceae	Actinobacteria	Micrococcales	NA	NA
ASV_412	Limed	Day 15 Day 40	Oe	Proteobacteria	Rhodanobacteraceae	Gammaproteobacteria	Xanthomonadales	NA	NA
ASV_413	Control Limed	Day 40	Oa	Proteobacteria	Acetobacteraceae	Alphaproteobacteria	Rhodospirillales	Acidocella	Acidocella aluminiidurans
ASV_414	Limed	Day 15 Day 40	Oa Oe	Proteobacteria	Sphingomonadaceae	Alphaproteobacteria	Sphingomonadales	Sphingomonas	NA
ASV_415	Control Limed	Day 40 Day 15	Oa Oe	Proteobacteria	Burkholderiaceae	Betaproteobacteria	Burkholderiales	Burkholderia	Burkholderia alpina
ASV_42	Control Limed	Day 15 Day 40	Oa Oe	Proteobacteria	Acetobacteraceae	Alphaproteobacteria	Rhodospirillales	NA	NA

ASV_421	Limed	Day 40	Oe	Proteobacteria	Rhodospirillaceae	Alphaproteobacteria	Rhodospirillales	NA	NA
ASV_427	Control Limed	Day 40	Oe Oa	Proteobacteria	Beijerinckiaceae	Alphaproteobacteria	Rhizobiales	Methylovirgula	Methylovirgula ligni
ASV_429	Limed	Day 40	Oe	Proteobacteria	Not Available	Gammaproteobacteria	Not Available	Acidibacter	Acidibacter ferrireducens
ASV_43	Limed	Day 40	Oe	Proteobacteria	NA	Alphaproteobacteria	Rhizobiales	NA	NA
ASV_431	Limed	Day 40	Oe	Actinobacteria	Conexibacteraceae	Thermoleophilia	Solirubrobacterales	Conexibacter	Conexibacter woesei
ASV_436	Limed	Day 40	Oe	Acidobacteria	Acidobacteriaceae	Acidobacteriia	Acidobacteriales	NA	NA
ASV_437	Limed	Day 40	Oe	Proteobacteria	Caulobacteraceae	Alphaproteobacteria	Caulobacterales	Phenylobacterium	NA
ASV_438	Limed	Day 40	Oe	Proteobacteria	Labilitrichaceae	Deltaproteobacteria	Myxococcales	Labilithrix	Labilithrix luteola
ASV_44	Control Limed	Day 15 Day 40	Oe Oa	Actinobacteria	Thermomonosporaceae	Actinobacteria	Streptosporangiales	Actinoallomurus	NA
ASV_441	Limed	Day 40	Oe	Actinobacteria	Conexibacteraceae	Thermoleophilia	Solirubrobacterales	Conexibacter	NA
ASV_442	Limed	Day 40	Oe	Actinobacteria	NA	Actinobacteria	Streptosporangiales	NA	NA
ASV_444	Limed	Day 40	Oa	Proteobacteria	Bradyrhizobiaceae	Alphaproteobacteria	Rhizobiales	Bradyrhizobium	NA
ASV_445	Limed	Day 40	Oe	Proteobacteria	Micropepsaceae	Alphaproteobacteria	Micropepsales	Rhizomicrobium	Rhizomicrobium palustre
ASV_45	Limed	Day 40	Oe	Proteobacteria	Bradyrhizobiaceae	Alphaproteobacteria	Rhizobiales	NA	NA
ASV_454	Limed	Day 40	Oe	Acidobacteria	Acidobacteriaceae	Acidobacteriia	Acidobacteriales	NA	NA
ASV_455	Limed	Day 15	Oe	Proteobacteria	Alcaligenaceae	Betaproteobacteria	Burkholderiales	Achromobacter	NA
ASV_458	Limed	Day 40	Oe	Acidobacteria	Acidobacteriaceae	Acidobacteriia	Acidobacteriales	Edaphobacter	NA
ASV_46	Control Limed	Day 15 Day 40	Oe Oa	Proteobacteria	Rhodanobacteraceae	Gammaproteobacteria	Xanthomonadales	NA	NA
ASV_461	Limed	Day 40	Oe	Actinobacteria	Micrococcaceae	Actinobacteria	Micrococcales	Rothia	Rothia mucilaginosa
ASV_463	Limed	Day 15	Oa	Bacteroidetes	Sphingobacteriaceae	Sphingobacteriia	Sphingobacteriales	Pedobacter	NA
ASV_464	Limed	Day 40	Oe	Proteobacteria	Caulobacteraceae	Alphaproteobacteria	Caulobacterales	NA	NA
ASV_465	Limed	Day 40	Oe	Actinobacteria	NA	Actinobacteria	Streptosporangiales	NA	NA
ASV_467	Limed	Day 40	Oe	Actinobacteria	Thermomonosporaceae	Actinobacteria	Streptosporangiales	Actinoallomurus	NA
ASV_47	Control Limed	Day 40	Oa Oe	Actinobacteria	Acidimicrobiaceae	Acidimicrobiia	Acidimicrobiales	NA	NA
ASV_475	Limed	Day 15 Day 40	Oe	Proteobacteria	Rhizobiaceae	Alphaproteobacteria	Rhizobiales	Rhizobium	NA
ASV_477	Limed	Day 40	Oe	Actinobacteria	NA	Actinobacteria	NA	NA	NA
ASV_479	Limed	Day 40	Oe	Planctomycetes	Isosphaeraceae	Planctomycetia	Planctomycetales	NA	NA
ASV_48	Limed	Day 40	Oe	Actinobacteria	Mycobacteriaceae	Actinobacteria	Corynebacteriales	Mycobacterium	NA
ASV_481	Limed	Day 40	Oe	Planctomycetes	Isosphaeraceae	Planctomycetia	Planctomycetales	Aquisphaera	Aquisphaera giovannonii
ASV_482	Limed	Day 40	Oe	Proteobacteria	Coxiellaceae	Gammaproteobacteria	Legionellales	Aquicella	Aquicella siphonis
ASV_483	Limed	Day 40	Oe	Chlamydiae	Parachlamydiaceae	Chlamydiia	Parachlamydiales	NA	NA
ASV_486	Control	Day 40	Oa	Proteobacteria	Beijerinckiaceae	Alphaproteobacteria	Rhizobiales	Methylovirgula	Methylovirgula ligni
ASV_488	Control Limed	Day 15 Day 40	Oa Oe	Firmicutes	Paenibacillaceae	Bacilli	Bacillales	Paenibacillus	NA
ASV_489	Limed	Day 40	Oe	Actinobacteria	Thermomonosporaceae	Actinobacteria	Streptosporangiales	Actinoallomurus	NA
ASV_49	Control Limed	Day 15 Day 40	Oa Oe	Proteobacteria	Burkholderiaceae	Betaproteobacteria	Burkholderiales	Caballeronia	NA
ASV_490	Control	Day 40	Oe	Actinobacteria	Streptomycetaceae	Actinobacteria	Streptomycetales	Streptomyces	NA
ASV_491	Limed	Day 40	Oe	Actinobacteria	NA	Thermoleophilia	Solirubrobacterales	NA	NA
ASV_492	Limed	Day 15 Day 40	Oe	Proteobacteria	Sphingomonadaceae	Alphaproteobacteria	Sphingomonadales	Sphingomonas	Sphingomonas hengshuiensis
ASV_493	Limed	Day 40	Oa	Actinobacteria	Frankiaceae	Actinobacteria	Frankiales	Frankia	NA
ASV_495	Control Limed	Day 40	Oa	Bacteroidetes	Chitinophagaceae	Chitinophagia	Chitinophagales	NA	NA
ASV_498	Limed	Day 40	Oe	Chlamydiae	Parachlamydiaceae	Chlamydiia	Parachlamydiales	Candidatus Protochlamydia	Candidatus Protochlamydia naegleriophila
ASV_5	Control Limed	Day 15 Day 40	Oa Oe	Proteobacteria	Burkholderiaceae	Betaproteobacteria	Burkholderiales	NA	NA
ASV_50	Control Limed	Day 15 Day 40	Oa	Actinobacteria	Actinospicaceae	Actinobacteria	Catenulisporales	Actinospica	NA
ASV_505	Limed	Day 40	Oe	Actinobacteria	NA	Actinobacteria	NA	NA	NA
ASV_506	Control	Day 15	Oe	Proteobacteria	Acetobacteraceae	Alphaproteobacteria	Rhodospirillales	NA	NA
ASV_507	Limed	Day 40	Oe	Actinobacteria	NA	Actinobacteria	Streptosporangiales	NA	NA
ASV_508	Control Limed	Day 15 Day 40	Oe Oa	Proteobacteria	Acetobacteraceae	Alphaproteobacteria	Rhodospirillales	Acidocella	NA
ASV_509	Limed	Day 40	Oe	Bacteroidetes	Chitinophagaceae	Chitinophagia	Chitinophagales	Pseudoflavitalea	Pseudoflavitalea soli

ASV_510	Limed	Day 40	Oe	Proteobacteria	Roseiarcaceae	Alphaproteobacteria	Rhizobiales	Roseiarcus	Roseiarcus fermentans
ASV_512	Limed	Day 15 Day 40	Oe	Bacteroidetes	Sphingobacteriaceae	Sphingobacteriia	Sphingobacteriales	Mucilaginibacter	NA
ASV_514	Limed	Day 40	Oe	Planctomycetes	Isosphaeraceae	Planctomycetia	Planctomycetales	Singulisphaera	Singulisphaera rosea
ASV_515	Limed	Day 15	Oe	Proteobacteria	Pseudomonadaceae	Gammaproteobacteria	Pseudomonadales	Pseudomonas	NA
ASV_516	Control	Day 15	Oa	Actinobacteria	Thermomonosporaceae	Actinobacteria	Streptosporangiales	NA	NA
ASV_52	Control Limed	Day 40	Oa Oe	Actinobacteria	Thermomonosporaceae	Actinobacteria	Streptosporangiales	NA	NA
ASV_522	Limed	Day 40	Oe	Proteobacteria	Caulobacteraceae	Alphaproteobacteria	Caulobacterales	Phenylobacterium	NA
ASV_523	Limed	Day 40	Oe	Actinobacteria	NA	Actinobacteria	NA	NA	NA
ASV_525	Limed	Day 40	Oe	Proteobacteria	Micropepsaceae	Alphaproteobacteria	Micropepsales	Rhizomicrobium	Rhizomicrobium palustre
ASV_529	Limed	Day 40	Oe	Actinobacteria	Acidimicrobiaceae	Acidimicrobiia	Acidimicrobiales	Aciditerrimonas	Aciditerrimonas ferrireducens
ASV_53	Limed	Day 40	Oe	Actinobacteria	Conexibacteraceae	Thermoleophilia	Solirubrobacterales	Conexibacter	Conexibacter woesei
ASV_530	Limed	Day 40	Oa	Proteobacteria	Acetobacteraceae	Alphaproteobacteria	Rhodospirillales	NA	NA
ASV_531	Limed	Day 40	Oe	Actinobacteria	NA	Actinobacteria	Streptosporangiales	NA	NA
ASV_536	Limed	Day 40	Oa	Actinobacteria	NA	Actinobacteria	NA	NA	NA
ASV_538	Limed	Day 15 Day 40	Oe	Proteobacteria	Pseudomonadaceae	Gammaproteobacteria	Pseudomonadales	Pseudomonas	NA
ASV_540	Limed	Day 40	Oe	Actinobacteria	Corynebacteriaceae	Actinobacteria	Corynebacteriales	Corynebacterium	NA
ASV_545	Limed	Day 40	Oe	Actinobacteria	Thermomonosporaceae	Actinobacteria	Streptosporangiales	Actinomadura	NA
ASV_547	Limed	Day 15 Day 40	Oe	Bacteroidetes	Chitinophagaceae	Chitinophagia	Chitinophagales	Taibaiella	NA
ASV_550	Limed	Day 40	Oe	Actinobacteria	Mycobacteriaceae	Actinobacteria	Corynebacteriales	Mycolicibacterium	NA
ASV_552	Limed	Day 40	Oe	Proteobacteria	NA	Gammaproteobacteria	NA	NA	NA
ASV_557	Limed	Day 15 Day 40	Oe	Proteobacteria	Burkholderiaceae	Betaproteobacteria	Burkholderiales	Caballeronia	NA
ASV_559	Limed	Day 15 Day 40	Oa	Proteobacteria	Rhodanobacteraceae	Gammaproteobacteria	Xanthomonadales	NA	NA
ASV_56	Limed	Day 15	Oe	Planctomycetes	Isosphaeraceae	Planctomycetia	Planctomycetales	NA	NA
ASV_561	Limed	Day 15	Oe	Proteobacteria	Pseudomonadaceae	Gammaproteobacteria	Pseudomonadales	Pseudomonas	NA
ASV_566	Limed	Day 40	Oe	Acidobacteria	Acidobacteriaceae	Acidobacteriia	Acidobacteriales	NA	NA
ASV_569	Limed	Day 15 Day 40	Oe	Proteobacteria	Burkholderiaceae	Betaproteobacteria	Burkholderiales	Caballeronia	NA
ASV_57	Limed	Day 40	Oe	Actinobacteria	NA	Actinobacteria	Streptosporangiales	NA	NA
ASV_572	Control	Day 40	Oe	Actinobacteria	Microbacteriaceae	Actinobacteria	Micrococcales	Humibacter	NA
ASV_574	Limed	Day 40	Oe	Actinobacteria	Frankiaceae	Actinobacteria	Frankiales	Jatrophihabitans	NA
ASV_577	Control	Day 40	Oa	Actinobacteria	Conexibacteraceae	Thermoleophilia	Solirubrobacterales	Conexibacter	Conexibacter woesei
ASV_581	Limed	Day 40	Oe	Proteobacteria	Caulobacteraceae	Alphaproteobacteria	Caulobacterales	NA	NA
ASV_588	Limed	Day 40	Oe	Actinobacteria	Conexibacteraceae	Thermoleophilia	Solirubrobacterales	Conexibacter	Conexibacter woesei
ASV_59	Limed	Day 40	Oe	Proteobacteria	Acetobacteraceae	Alphaproteobacteria	Rhodospirillales	NA	NA
ASV_590	Limed	Day 40	Oe	Proteobacteria	Sphingomonadaceae	Alphaproteobacteria	Sphingomonadales	Sphingobium	NA
ASV_592	Limed	Day 15 Day 40	Oa	Proteobacteria	Micropepsaceae	Alphaproteobacteria	Micropepsales	Rhizomicrobium	NA
ASV_595	Limed	Day 40	Oe	Planctomycetes	Isosphaeraceae	Planctomycetia	Planctomycetales	NA	NA
ASV_597	Limed	Day 40	Oa	Proteobacteria	Micropepsaceae	Alphaproteobacteria	Micropepsales	Rhizomicrobium	Rhizomicrobium electricum
ASV_598	Limed	Day 40	Oe	Actinobacteria	Conexibacteraceae	Thermoleophilia	Solirubrobacterales	Conexibacter	Conexibacter woesei
ASV_6	Control Limed	Day 15 Day 40	Oa Oe	Proteobacteria	Burkholderiaceae	Betaproteobacteria	Burkholderiales	Paraburkholderia	NA
ASV_60	Control Limed	Day 40	Oa Oe	Planctomycetes	Isosphaeraceae	Planctomycetia	Planctomycetales	NA	NA
ASV_602	Limed	Day 40	Oe	Proteobacteria	Caulobacteraceae	Alphaproteobacteria	Caulobacterales	Phenylobacterium	NA
ASV_603	Limed	Day 40	Oe	Planctomycetes	Isosphaeraceae	Planctomycetia	Planctomycetales	Singulisphaera	Singulisphaera acidiphila
ASV_606	Limed	Day 40	Oa	Proteobacteria	Labilitrichaceae	Deltaproteobacteria	Myxococcales	Labilithrix	Labilithrix luteola
ASV_609	Limed	Day 40	Oe	Firmicutes	Paenibacillaceae	Bacilli	Bacillales	Paenibacillus	NA
ASV_612	Limed	Day 40	Oe	Proteobacteria	Phyllobacteriaceae	Alphaproteobacteria	Rhizobiales	Mesorhizobium	NA
ASV_616	Limed	Day 15	Oa	Proteobacteria	Comamonadaceae	Betaproteobacteria	Burkholderiales	Variovorax	NA
ASV_62	Limed	Day 40	Oe	Planctomycetes	Isosphaeraceae	Planctomycetia	Planctomycetales	Aquisphaera	Aquisphaera giovannonii
ASV_623	Control	Day 40	Oa	Acidobacteria	Acidobacteriaceae	Acidobacteriia	Acidobacteriales	NA	NA

ASV_624	Limed	Day 40	Oe	Proteobacteria	Legionellaceae	Gammaproteobacteria	Legionellales	Legionella	NA
ASV_625	Control	Day 40	Oe	Actinobacteria	NA	Thermoleophilia	Solirubrobacterales	NA	NA
ASV_630	Limed	Day 40	Oe	Acidobacteria	Bryobacteraceae	Solibacteres	Solibacterales	Paludibaculum	Paludibaculum fermentans
ASV_632	Limed	Day 15	Oe	Verrucomicrobia	Verrucomicrobiaceae	Verrucomicrobiae	Verrucomicrobiales	Luteolibacter	NA
ASV_633	Limed	Day 40	Oe	Proteobacteria	NA	Alphaproteobacteria	Rhizobiales	NA	NA
ASV_635	Limed	Day 15 Day 40	Oe	Actinobacteria	Microbacteriaceae	Actinobacteria	Micrococcales	Leifsonia	NA
ASV_64	Limed	Day 40	Oe	Actinobacteria	NA	Actinobacteria	Streptosporangiales	NA	NA
ASV_640	Limed	Day 40	Oe	Proteobacteria	NA	Alphaproteobacteria	Rhizobiales	NA	NA
ASV_641	Limed	Day 40	Oe	Proteobacteria	Polyangiaceae	Deltaproteobacteria	Myxococcales	NA	NA
ASV_65	Limed	Day 40	Oe	Proteobacteria	NA	Alphaproteobacteria	Rhizobiales	NA	NA
ASV_650	Limed	Day 40	Oa	Actinobacteria	NA	Actinobacteria	NA	NA	NA
ASV_654	Limed	Day 40	Oe	Actinobacteria	NA	Actinobacteria	NA	NA	NA
ASV_657	Limed	Day 15	Oe	Actinobacteria	Nakamurellaceae	Actinobacteria	Nakamurellales	Nakamurella	Nakamurella flavida
ASV_66	Control Limed	Day 15 Day 40	Oa Oe	Actinobacteria	Actinospicaceae	Actinobacteria	Catenulisporales	Actinospica	NA
ASV_660	Control	Day 40	Oe	Proteobacteria	Acetobacteraceae	Alphaproteobacteria	Rhodospirillales	Acidocella	NA
ASV_664	Limed	Day 40	Oe	Proteobacteria	Rhodospirillaceae	Alphaproteobacteria	Rhodospirillales	NA	NA
ASV_670	Limed	Day 40	Oe	Proteobacteria	Rhodospirillaceae	Alphaproteobacteria	Rhodospirillales	NA	NA
ASV_671	Limed	Day 15	Oe	Bacteroidetes	Chitinophagaceae	Chitinophagia	Chitinophagales	NA	NA
ASV_68	Control	Day 15 Day 40	Oe	Proteobacteria	Rhodanobacteraceae	Gammaproteobacteria	Xanthomonadales	Rhodanobacter	NA
ASV_681	Limed	Day 40	Oa	Actinobacteria	NA	Actinobacteria	NA	NA	NA
ASV_682	Limed	Day 40	Oe	Actinobacteria	Microbacteriaceae	Actinobacteria	Micrococcales	NA	NA
ASV_684	Limed	Day 15	Oe	Proteobacteria	Sphingomonadaceae	Alphaproteobacteria	Sphingomonadales	Novosphingobium	NA
ASV_690	Limed	Day 15 Day 40	Oe	Proteobacteria	Sphingomonadaceae	Alphaproteobacteria	Sphingomonadales	NA	NA
ASV_693	Limed	Day 40	Oe	Proteobacteria	Caulobacteraceae	Alphaproteobacteria	Caulobacterales	NA	NA
ASV_696	Limed	Day 15	Oe	Bacteroidetes	Chitinophagaceae	Chitinophagia	Chitinophagales	Niastella	Niastella hibisci
ASV_697	Limed	Day 40	Oe	Planctomycetes	Isosphaeraceae	Planctomycetia	Planctomycetales	Singulisphaera	Singulisphaera acidiphila
ASV_698	Limed	Day 40	Oe	Proteobacteria	Rhodospirillaceae	Alphaproteobacteria	Rhodospirillales	NA	NA
ASV_7	Limed	Day 40	Oe	Actinobacteria	Thermomonosporaceae	Actinobacteria	Streptosporangiales	Actinoallomurus	NA
ASV_70	Limed	Day 40	Oe	Acidobacteria	Acidobacteriaceae	Acidobacteriia	Acidobacteriales	NA	NA
ASV_702	Limed	Day 40	Oe	Proteobacteria	NA	Alphaproteobacteria	Rhodospirillales	NA	NA
ASV_703	Limed	Day 40	Oe	Actinobacteria	Nocardioidaceae	Actinobacteria	Propionibacteriales	Nocardioides	Nocardioides endophyticus
ASV_705	Control	Day 40	Oe	Proteobacteria	Acetobacteraceae	Alphaproteobacteria	Rhodospirillales	NA	NA
ASV_708	Limed	Day 40	Oe	Proteobacteria	Comamonadaceae	Betaproteobacteria	Burkholderiales	NA	NA
ASV_712	Limed	Day 15 Day 40	Oe	Proteobacteria	Sphingomonadaceae	Alphaproteobacteria	Sphingomonadales	Novosphingobium	NA
ASV_719	Limed	Day 40	Oe	Bacteroidetes	Chitinophagaceae	Chitinophagia	Chitinophagales	NA	NA
ASV_721	Control	Day 40	Oa	Acidobacteria	Acidobacteriaceae	Acidobacteriia	Acidobacteriales	NA	NA
ASV_73	Limed	Day 40	Oe	Proteobacteria	Hyphomicrobiaceae	Alphaproteobacteria	Rhizobiales	Rhodoplanes	NA
ASV_733	Limed	Day 40	Oe	Chlamydiae	Parachlamydiaceae	Chlamydiia	Parachlamydiales	NA	NA
ASV_734	Limed	Day 40	Oe	Proteobacteria	Chelatococcaceae	Alphaproteobacteria	Rhizobiales	Chelatococcus	Chelatococcus reniformis
ASV_736	Limed	Day 40	Oe	Proteobacteria	Bradyrhizobiaceae	Alphaproteobacteria	Rhizobiales	Bradyrhizobium	NA
ASV_75	Control Limed	Day 40	Oa Oe	Planctomycetes	Isosphaeraceae	Planctomycetia	Planctomycetales	Singulisphaera	NA
ASV_752	Control	Day 40	Oe	Actinobacteria	Pseudonocardiaceae	Actinobacteria	Pseudonocardiales	NA	NA
ASV_753	Control	Day 40	Oa	Proteobacteria	Caulobacteraceae	Alphaproteobacteria	Caulobacterales	NA	NA
ASV_757	Limed	Day 40	Oe	Actinobacteria	Acidimicrobiaceae	Acidimicrobiia	Acidimicrobiales	Aciditerrimonas	Aciditerrimonas ferrireducens
ASV_758	Limed	Day 15 Day 40	Oe	Proteobacteria	Sinobacteraceae	Gammaproteobacteria	Nevskiales	NA	NA
ASV_76	Control Limed	Day 15 Day 40	Oe	Proteobacteria	Burkholderiaceae	Betaproteobacteria	Burkholderiales	Ralstonia	Ralstonia pickettii
ASV_763	Limed	Day 40	Oe	Proteobacteria	NA	Alphaproteobacteria	Rhizobiales	NA	NA
ASV_769	Limed	Day 15 Day 40	Oe	Actinobacteria	Frankiaceae	Actinobacteria	Frankiales	Jatrophihabitans	NA

ASV_77	Limed	Day 40	Oe	Proteobacteria	Hyphomicrobiaceae	Alphaproteobacteria	Rhizobiales	Rhodoplanes	NA
ASV_775	Limed	Day 40	Oe	Actinobacteria	Nocardiaceae	Actinobacteria	Corynebacteriales	Nocardia	NA
ASV_777	Limed	Day 40	Oa	Planctomycetes	Isosphaeraceae	Planctomycetia	Planctomycetales	Aquisphaera	Aquisphaera giovannonii
ASV_781	Limed	Day 40	Oe	Actinobacteria	Acidimicrobiaceae	Acidimicrobiia	Acidimicrobiales	Aciditerrimonas	Aciditerrimonas ferrireducens
ASV_79	Limed	Day 40	Oe	Proteobacteria	Not Available	Gammaproteobacteria	Not Available	Acidibacter	Acidibacter ferrireducens
ASV_792	Control	Day 15	Oe	Proteobacteria	Acetobacteraceae	Alphaproteobacteria	Rhodospirillales	Acidisoma	NA
ASV_793	Limed	Day 15	Oa	Proteobacteria	Xanthobacteraceae	Alphaproteobacteria	Rhizobiales	Labrys	Labrys methylaminiphilus
ASV_796	Limed	Day 40	Oa	Actinobacteria	Streptomycetaceae	Actinobacteria	Streptomycetales	Streptomyces	NA
ASV_797	Limed	Day 40	Oe	Proteobacteria	Erythrobacteraceae	Alphaproteobacteria	Sphingomonadales	NA	NA
ASV_799	Limed	Day 15	Oe	Planctomycetes	Isosphaeraceae	Planctomycetia	Planctomycetales	Paludisphaera	Paludisphaera borealis
ASV_808	Control	Day 40	Oa	Actinobacteria	NA	Actinobacteria	NA	NA	NA
ASV_81	Limed	Day 40	Oe	Proteobacteria	NA	Alphaproteobacteria	Rhizobiales	NA	NA
ASV_82	Control Limed	Day 15 Day 40	Oa Oe	Actinobacteria	Actinospicaceae	Actinobacteria	Catenulisporales	Actinospica	NA
ASV_820	Limed	Day 15 Day 40	Oe	Actinobacteria	Microbacteriaceae	Actinobacteria	Micrococcales	NA	NA
ASV_823	Limed	Day 15	Oa	Proteobacteria	Caulobacteraceae	Alphaproteobacteria	Caulobacterales	Phenylobacterium	Phenylobacterium koreense
ASV_824	Limed	Day 40	Oe	Verrucomicrobia	Verrucomicrobiaceae	Verrucomicrobiae	Verrucomicrobiales	Luteolibacter	Luteolibacter arcticus
ASV_825	Limed	Day 40	Oe	Proteobacteria	Alcaligenaceae	Betaproteobacteria	Burkholderiales	NA	NA
ASV_827	Limed	Day 40	Oe	Actinobacteria	NA	Actinobacteria	NA	NA	NA
ASV_83	Limed	Day 40	Oe	Proteobacteria	Sphingomonadaceae	Alphaproteobacteria	Sphingomonadales	Sphingomonas	NA
ASV_837	Limed	Day 15	Oa Oe	Proteobacteria	Bradyrhizobiaceae	Alphaproteobacteria	Rhizobiales	Bosea	NA
ASV_84	Limed	Day 15 Day 40	Oe	Proteobacteria	Burkholderiaceae	Betaproteobacteria	Burkholderiales	NA	NA
ASV_843	Limed	Day 40	Oe	Actinobacteria	NA	Actinobacteria	Streptosporangiales	NA	NA
ASV_85	Limed	Day 40	Oe	Planctomycetes	Isosphaeraceae	Planctomycetia	Planctomycetales	Singulisphaera	Singulisphaera rosea
ASV_850	Limed	Day 40	Oe	Proteobacteria	NA	Alphaproteobacteria	NA	NA	NA
ASV_854	Limed	Day 40	Oe	Planctomycetes	Isosphaeraceae	Planctomycetia	Planctomycetales	NA	NA
ASV_855	Control	Day 15	Oe	Proteobacteria	Acetobacteraceae	Alphaproteobacteria	Rhodospirillales	Acidisoma	Acidisoma tundrae
ASV_86	Limed	Day 15 Day 40	Oa Oe	Bacteroidetes	Chitinophagaceae	Chitinophagia	Chitinophagales	Chitinophaga	NA
ASV_863	Limed	Day 15 Day 40	Oe	Proteobacteria	Sphingomonadaceae	Alphaproteobacteria	Sphingomonadales	Sphingobium	NA
ASV_865	Limed	Day 15 Day 40	Oe	Actinobacteria	Microbacteriaceae	Actinobacteria	Micrococcales	Microbacterium	NA
ASV_87	Limed	Day 40	Oe	Actinobacteria	Thermomonosporaceae	Actinobacteria	Streptosporangiales	Actinoallomurus	NA
ASV_872	Limed	Day 15	Oa	Proteobacteria	Bradyrhizobiaceae	Alphaproteobacteria	Rhizobiales	Tardiphaga	Tardiphaga robiniae
ASV_88	Control	Day 15 Day 40	Oe Oa	Proteobacteria	Acetobacteraceae	Alphaproteobacteria	Rhodospirillales	Acidocella	Acidocella aluminiidurans
ASV_881	Limed	Day 40	Oe	Actinobacteria	Microbacteriaceae	Actinobacteria	Micrococcales	NA	NA
ASV_882	Limed	Day 40	Oe	Proteobacteria	Labilitrichaceae	Deltaproteobacteria	Myxococcales	Labilithrix	Labilithrix luteola
ASV_889	Limed	Day 40	Oe	Proteobacteria	Rhizobiaceae	Alphaproteobacteria	Rhizobiales	Kaistia	NA
ASV_89	Limed	Day 40	Oe	Actinobacteria	Thermomonosporaceae	Actinobacteria	Streptosporangiales	Actinoallomurus	NA
ASV_890	Limed	Day 40	Oe	Proteobacteria	Sinobacteraceae	Gammaproteobacteria	Nevskiales	NA	NA
ASV_892	Limed	Day 40	Oe	Proteobacteria	NA	Gammaproteobacteria	NA	NA	NA
ASV_895	Limed	Day 40	Oe	Bacteroidetes	Chitinophagaceae	Chitinophagia	Chitinophagales	NA	NA
ASV_90	Limed	Day 40	Oe	Proteobacteria	Bradyrhizobiaceae	Alphaproteobacteria	Rhizobiales	NA	NA
ASV_902	Limed	Day 40	Oa	Proteobacteria	Micropepsaceae	Alphaproteobacteria	Micropepsales	Rhizomicrobium	NA
ASV_905	Limed	Day 15	Oe	Verrucomicrobia	Not Available	Spartobacteria	Not Available	Terrimicrobium	Terrimicrobium sacchariphilum
ASV_906	Limed	Day 15	Oe	Proteobacteria	Caulobacteraceae	Alphaproteobacteria	Caulobacterales	NA	NA
ASV_908	Control	Day 40	Oa	Proteobacteria	Acetobacteraceae	Alphaproteobacteria	Rhodospirillales	Acidocella	Acidocella aluminiidurans
ASV_916	Limed	Day 15	Oe	Actinobacteria	Nocardioidaceae	Actinobacteria	Propionibacteriales	Marmoricola	NA
ASV_92	Limed	Day 40	Oe	Proteobacteria	Not Available	Gammaproteobacteria	Not Available	Acidibacter	Acidibacter ferrireducens
ASV_921	Limed	Day 40	Oe	Firmicutes	Paenibacillaceae	Bacilli	Bacillales	Paenibacillus	NA
ASV_923	Limed	Day 40	Oe	Proteobacteria	NA	Gammaproteobacteria	NA	NA	NA

ASV_93	Limed	Day 40	Oe	Proteobacteria	Roseiarcaceae	Alphaproteobacteria	Rhizobiales	Roseiarcus	Roseiarcus fermentans
ASV_930	Limed	Day 15	Oe	Bacteroidetes	Chitinophagaceae	Chitinophagia	Chitinophagales	Niastella	NA
ASV_932	Limed	Day 15	Oe	Verrucomicrobia	Not Available	Spartobacteria	Not Available	Terrimicrobium	Terrimicrobium sacchariphilum
ASV_934	Limed	Day 15	Oa	Bacteroidetes	Chitinophagaceae	Chitinophagia	Chitinophagales	Taibaiella	NA
ASV_935	Limed	Day 40	Oe	Actinobacteria	Streptosporangiaceae	Actinobacteria	Streptosporangiales	Herbidospora	NA
ASV_939	Control	Day 40	Oa	Proteobacteria	Acetobacteraceae	Alphaproteobacteria	Rhodospirillales	Acidisoma	NA
ASV_94	Control Limed	Day 15 Day 40	Oe Oa	Actinobacteria	Thermomonosporaceae	Actinobacteria	Streptosporangiales	NA	NA
ASV_942	Limed	Day 15 Day 40	Oe	Actinobacteria	Microbacteriaceae	Actinobacteria	Micrococcales	NA	NA
ASV_95	Limed	Day 40	Oe	Actinobacteria	Conexibacteraceae	Thermoleophilia	Solirubrobacterales	Conexibacter	Conexibacter woesei
ASV_952	Limed	Day 15	Oa	Proteobacteria	Rhizobiaceae	Alphaproteobacteria	Rhizobiales	Rhizobium	NA
ASV_953	Limed	Day 40	Oe	Proteobacteria	Bradyrhizobiaceae	Alphaproteobacteria	Rhizobiales	Bosea	NA
ASV_954	Limed	Day 15	Oe	Proteobacteria	Sphingomonadaceae	Alphaproteobacteria	Sphingomonadales	Sphingomonas	NA
ASV_96	Limed	Day 40	Oe	Planctomycetes	Isosphaeraceae	Planctomycetia	Planctomycetales	NA	NA
ASV_963	Control	Day 40	Oa	Proteobacteria	Bradyrhizobiaceae	Alphaproteobacteria	Rhizobiales	Bradyrhizobium	NA
ASV_978	Limed	Day 40	Oe	Proteobacteria	Burkholderiaceae	Betaproteobacteria	Burkholderiales	Caballeronia	NA
ASV_98	Limed	Day 40	Oa	Chlamydiae	Parachlamydiaceae	Chlamydiia	Parachlamydiales	NA	NA
ASV_983	Limed	Day 15 Day 40	Oe	Actinobacteria	Microbacteriaceae	Actinobacteria	Micrococcales	NA	NA
ASV_989	Limed	Day 40	Oe	Planctomycetes	Isosphaeraceae	Planctomycetia	Planctomycetales	NA	NA
ASV_994	Limed	Day 15	Oa Oe	Proteobacteria	Sphingomonadaceae	Alphaproteobacteria	Sphingomonadales	NA	NA
ASV_995	Limed	Day 40	Oe	Proteobacteria	Micropepsaceae	Alphaproteobacteria	Micropepsales	Rhizomicrobium	Rhizomicrobium palustre

Table S4: Identity of 134 fungal ^{13}C incorporators and the treatments, horizons, and times in which they took up label. ASVs characterized as "NA" are not matched in the taxonomic database at the specific taxonomic level. Suffix "_IS" stands for *Incertae_sedis*.

OTU	Treatments	Times	Horizons	Phylum	Family	Class	Order	Genus	Species
ASV_10	Control Limed	Day 15 Day 40	Oa Oe	Ascomycota	NA	Sordariomycetes	Hypocreales	NA	NA
ASV_101	Control	Day 15	Oe	Ascomycota	Helotiaceae	Leotiomycetes	Helotiales	Cudoniella	Cudoniella_acicularis
ASV_103	Limed	Day 15	Oe	Ascomycota	Chaetosphaeriaceae	Sordariomycetes	Chaetosphaeriales	Chloridium	Chloridium_sp
ASV_105	Control Limed	Day 40 Day 15	Oa Oe	Ascomycota	Herpotrichiellaceae	Eurotiomycetes	Chaetothyriales	Cladophialophora	Cladophialophora_sp
ASV_106	Limed	Day 40	Oa	Ascomycota	Hypocreaceae	Sordariomycetes	Hypocreales	Trichoderma	Trichoderma_piluliferum
ASV_111	Control	Day 15	Oa	Ascomycota	Trichocomaceae	Eurotiomycetes	Eurotiales	Talaromyces	Talaromyces_kendrickii
ASV_113	Limed	Day 15 Day 40	Oa Oe	Mucoromycota	Mucoraceae	Mucoromycetes	Mucorales	Mucor	Mucor_silvaticus
ASV_118	Control	Day 15	Oe	NA	NA	NA	NA	NA	NA
ASV_12	Control Limed	Day 15 Day 40	Oa Oe	NA	unidentified	NA	NA	unidentified	NA
ASV_122	Control Limed	Day 15 Day 40	Oe Oa	Mucoromycota	Umbelopsidaceae	Umbelopsidomycetes	Umbelopsidales	Umbelopsis	NA
ASV_124	Limed	Day 15 Day 40	Oa	Ascomycota	Helotiales_fam_IS	Leotiomycetes	Helotiales	Leptodontidium	Leptodontidium_trabinellum
ASV_125	Limed	Day 15 Day 40	Oe	Mucoromycota	Mucoraceae	Mucoromycetes	Mucorales	Mucor	Mucor_abundans
ASV_128	Limed	Day 15 Day 40	Oe	Mortierellomycota	Mortierellaceae	Mortierellomycetes	Mortierellales	Mortierella	NA
ASV_129	Control Limed	Day 15	Oa	Mucoromycota	Umbelopsidaceae	Umbelopsidomycetes	Umbelopsidales	Umbelopsis	Umbelopsis_angularis
ASV_134	Control Limed	Day 40 Day 15	Oa Oe	Ascomycota	unidentified	Leotiomycetes	Helotiales	unidentified	Helotiales_sp
ASV_135	Control Limed	Day 40 Day 15	Oa	Ascomycota	NA	Leotiomycetes	Helotiales	NA	NA
ASV_136	Limed	Day 40	Oa	Ascomycota	unidentified	Leotiomycetes	Helotiales	unidentified	Helotiales_sp
ASV_139	Control	Day 15	Oe	Ascomycota	Hyaloscyphaceae	Leotiomycetes	Helotiales	Hyaloscypha	Hyaloscypha_fuckelii
ASV_14	Control	Day 15	Oa	Ascomycota	Archaeorhizomycetaceae	Archaeorhizomycetes	Archaeorhizomycetales	Archaeorhizomyces	Archaeorhizomyces_sp
ASV_140	Control Limed	Day 15 Day 40	Oa Oe	Mucoromycota	Umbelopsidaceae	Umbelopsidomycetes	Umbelopsidales	Umbelopsis	NA
ASV_141	Control	Day 40	Oa	Mortierellomycota	Mortierellaceae	Mortierellomycetes	Mortierellales	Mortierella	NA
ASV_142	Limed	Day 15	Oa	Mucoromycota	Umbelopsidaceae	Umbelopsidomycetes	Umbelopsidales	Umbelopsis	NA
ASV_144	Control	Day 40	Oa	Ascomycota	Helotiales_fam_IS	Leotiomycetes	Helotiales	Leptodontidium	Leptodontidium_trabinellum
ASV_146	Control	Day 15	Oa	Mortierellomycota	Mortierellaceae	Mortierellomycetes	Mortierellales	Mortierella	NA
ASV_147	Limed	Day 40	Oe	Ascomycota	Glomerellaceae	Sordariomycetes	Glomerellales	Colletotrichum	NA
ASV_15	Control Limed	Day 15 Day 40	Oe Oa	Ascomycota	Pseudeurotiaceae	Leotiomycetes	Leotiomycetes_ord_IS	Geomyces	Geomyces_auratus
ASV_150	Limed	Day 15	Oe	Ascomycota	Aspergillaceae	Eurotiomycetes	Eurotiales	Penicillium	NA
ASV_152	Limed	Day 15	Oe	Basidiomycota	Hydnodontaceae	Agaricomycetes	Trechisporales	Trechispora	Trechispora_stellulata
ASV_160	Control	Day 15 Day 40	Oe Oa	Ascomycota	Coniochaetaceae	Sordariomycetes	Coniochaetales	Coniochaeta	Coniochaeta_sp
ASV_162	Limed	Day 15	Oe	Ascomycota	Aspergillaceae	Eurotiomycetes	Eurotiales	Penicillium	NA
ASV_165	Limed	Day 40	Oe	Ascomycota	Archaeorhizomycetaceae	Archaeorhizomycetes	Archaeorhizomycetales	Archaeorhizomyces	Archaeorhizomyces_sp
ASV_176	Control	Day 40	Oe	Ascomycota	NA	Leotiomycetes	Helotiales	NA	NA
ASV_177	Control	Day 40	Oa	Ascomycota	unidentified	Saccharomycetes	Saccharomycetales	unidentified	Saccharomycetales_sp
ASV_178	Control	Day 40	Oa	Mortierellomycota	Mortierellaceae	Mortierellomycetes	Mortierellales	Mortierella	Mortierella_longigemmata
ASV_18	Control	Day 40	Oa	Ascomycota	Aspergillaceae	Eurotiomycetes	Eurotiales	Penicillium	NA
ASV_183	Control	Day 15	Oa	Ascomycota	Aspergillaceae	Eurotiomycetes	Eurotiales	Aspergillus	Aspergillus_baeticus
ASV_184	Limed	Day 15 Day 40	Oe	Ascomycota	Nectriaceae	Sordariomycetes	Hypocreales	NA	NA
ASV_190	Limed	Day 15	Oe	Ascomycota	NA	Leotiomycetes	Helotiales	NA	NA
ASV_197	Limed	Day 15	Oa	Mucoromycota	Mucoraceae	Mucoromycetes	Mucorales	Mucor	Mucor_bainieri
ASV_2	Control Limed	Day 15 Day 40	Oa Oe	Basidiomycota	unidentified	Tremellomycetes	Tremellales	unidentified	Tremellales_sp
ASV_20	Control	Day 15 Day 40	Oa Oe	Ascomycota	Hypocreaceae	Sordariomycetes	Hypocreales	Trichoderma	NA

ASV_205	Control	Day 15 Day 40	Oe Oa	Ascomycota	Leotiomycetes_fam_IS	Leotiomycetes	Leotiomycetes_ord_IS	Scytalidium	Scytalidium_lignicola
ASV_21	Control	Day 15 Day 40	Oa	Ascomycota	Chaetosphaeriaceae	Sordariomycetes	Chaetosphaeriales	Chaetosphaeria	Chaetosphaeria_vermicularioides
ASV_210	Limed	Day 15	Oa	Ascomycota	Chaetomiaceae	Sordariomycetes	Sordariales	Humicola	Humicola_nigrescens
ASV_216	Limed	Day 15	Oe	Basidiomycota	Hydnodontaceae	Agaricomycetes	Trechisporales	Trechispora	Trechispora_stellulata
ASV_22	Limed	Day 40	Oa Oe	Ascomycota	Aspergillaceae	Eurotiomycetes	Eurotiales	Penicillium	Penicillium_odoratum
ASV_223	Limed	Day 15	Oe	Ascomycota	Nectriaceae	Sordariomycetes	Hypocreales	NA	NA
ASV_23	Control	Day 40	Oe	Ascomycota	NA	NA	NA	NA	NA
ASV_230	Limed	Day 40	Oe	Ascomycota	Herpotrichiellaceae	Eurotiomycetes	Chaetothyriales	Cladophialophora	Cladophialophora_sp
ASV_232	Control	Day 15 Day 40	Oa	Ascomycota	unidentified	unidentified	unidentified	unidentified	Ascomycota_sp
ASV_235	Limed	Day 15	Oa	Ascomycota	Aspergillaceae	Eurotiomycetes	Eurotiales	Penicillium	NA
ASV_25	Control Limed	Day 15 Day 40	Oe	Mortierellomycota	Mortierellaceae	Mortierellomycetes	Mortierellales	Mortierella	Mortierella_sp
ASV_258	Control	Day 15	Oe	Ascomycota	Chaetosphaeriaceae	Sordariomycetes	Chaetosphaeriales	Chaetosphaeria	Chaetosphaeria_sp
ASV_266	Limed	Day 15	Oe	Ascomycota	unidentified	Leotiomycetes	Helotiales	unidentified	Helotiales_sp
ASV_273	Limed	Day 15	Oa Oe	Ascomycota	Hypocreales_fam_IS	Sordariomycetes	Hypocreales	Acremonium	Acremonium_persicinum
ASV_279	Limed	Day 40	Oa	Rozellomycota	unidentified	unidentified	unidentified	unidentified	Rozellomycota_sp
ASV_28	Control Limed	Day 15 Day 40	Oa Oe	Ascomycota	Hypocreaceae	Sordariomycetes	Hypocreales	Trichoderma	NA
ASV_281	Limed	Day 15	Oe	Mucoromycota	Umbelopsidaceae	Umbelopsidomycetes	Umbelopsidales	Umbelopsis	NA
ASV_283	Limed	Day 15	Oa	Ascomycota	unidentified	Sordariomycetes	Hypocreales	unidentified	Hypocreales_sp
ASV_29	Control	Day 40	Oa	Basidiomycota	unidentified	Microbotryomycetes	Leucosporidiales	unidentified	Leucosporidiales_sp
ASV_290	Limed	Day 40	Oa	Ascomycota	unidentified	Leotiomycetes	Helotiales	unidentified	Helotiales_sp
ASV_299	Limed	Day 40	Oa	Ascomycota	Pleomassariaceae	Dothideomycetes	Pleosporales	unidentified	Pleomassariaceae_sp
ASV_3	Control Limed	Day 15 Day 40	Oa Oe	Ascomycota	Hypocreaceae	Sordariomycetes	Hypocreales	Trichoderma	NA
ASV_30	Control Limed	Day 15 Day 40	Oe Oa	Basidiomycota	Trichosporonaceae	Tremellomycetes	Trichosporonales	NA	NA
ASV_309	Control	Day 40	Oa	Ascomycota	Herpotrichiellaceae	Eurotiomycetes	Chaetothyriales	Cladophialophora	Cladophialophora_sp
ASV_316	Limed	Day 40	Oa	Ascomycota	Cordycipitaceae	Sordariomycetes	Hypocreales	Lecanicillium	Lecanicillium_primulinum
ASV_319	Control	Day 15	Oe	Ascomycota	Sporocadaceae	Sordariomycetes	Xylariales	NA	NA
ASV_32	Control	Day 15 Day 40	Oa Oe	Ascomycota	Sclerotiniaceae	Leotiomycetes	Helotiales	NA	NA
ASV_33	Limed	Day 40	Oa	Mortierellomycota	Mortierellaceae	Mortierellomycetes	Mortierellales	Mortierella	Mortierella_angusta
ASV_332	Limed	Day 15	Oa	Ascomycota	Didymellaceae	Dothideomycetes	Pleosporales	NA	NA
ASV_342	Limed	Day 15 Day 40	Oe	Ascomycota	unidentified	unidentified	unidentified	unidentified	Ascomycota_sp
ASV_352	Limed	Day 15	Oe	Ascomycota	Nectriaceae	Sordariomycetes	Hypocreales	NA	NA
ASV_365	Limed	Day 15	Oa	Ascomycota	Aspergillaceae	Eurotiomycetes	Eurotiales	Penicillium	NA
ASV_369	Control	Day 40	Oa	Ascomycota	Herpotrichiellaceae	Eurotiomycetes	Chaetothyriales	Capronia	Capronia_semi-immersa
ASV_372	Limed	Day 40	Oa	Ascomycota	unidentified	Dothideomycetes	Capnodiales	unidentified	Capnodiales_sp
ASV_383	Control	Day 15	Oa	Ascomycota	NA	Leotiomycetes	Helotiales	NA	NA
ASV_39	Limed	Day 15	Oe	Rozellomycota	unidentified	unidentified	unidentified	unidentified	Rozellomycota_sp
ASV_40	Limed	Day 15 Day 40	Oa Oe	Ascomycota	Hypocreaceae	Sordariomycetes	Hypocreales	Trichoderma	Trichoderma_stellatum
ASV_404	Limed	Day 15	Oe	Ascomycota	Hypocreales_fam_IS	Sordariomycetes	Hypocreales	Acremonium	Acremonium_persicinum
ASV_41	Control Limed	Day 15 Day 40	Oe Oa	Mucoromycota	Umbelopsidaceae	Umbelopsidomycetes	Umbelopsidales	Umbelopsis	Umbelopsis_angularis
ASV_42	Control Limed	Day 15 Day 40	Oe	Ascomycota	Clavicipitaceae	Sordariomycetes	Hypocreales	Pochonia	Pochonia_bulbillosa
ASV_430	Limed	Day 15	Oe	Ascomycota	Hypocreales_fam_IS	Sordariomycetes	Hypocreales	Acremonium	Acremonium_persicinum
ASV_45	Control	Day 15 Day 40	Oa	Mucoromycota	Umbelopsidaceae	Umbelopsidomycetes	Umbelopsidales	Umbelopsis	Umbelopsis_dimorpha
ASV_46	Control	Day 15	Oe	Ascomycota	Helotiaceae	Leotiomycetes	Helotiales	Meliniomyces	Meliniomyces_sp
ASV_47	Control Limed	Day 15 Day 40	Oa Oe	Mucoromycota	Umbelopsidaceae	Umbelopsidomycetes	Umbelopsidales	Umbelopsis	Umbelopsis_angularis
ASV_477	Limed	Day 15	Oe	Ascomycota	Aspergillaceae	Eurotiomycetes	Eurotiales	Penicillium	NA
ASV_49	Control Limed	Day 40 Day 15	Oa Oe	Ascomycota	Clavicipitaceae	Sordariomycetes	Hypocreales	Pochonia	Pochonia_bulbillosa
ASV_5	Control	Day 15	Oe	Ascomycota	Aspergillaceae	Eurotiomycetes	Eurotiales	Penicillium	Penicillium_herquei
ASV_506	Limed	Day 15	Oe	Ascomycota	Hypocreales_fam_IS	Sordariomycetes	Hypocreales	Acremonium	Acremonium_persicinum
ASV_523	Limed	Day 15	Oe	Ascomycota	Aspergillaceae	Eurotiomycetes	Eurotiales	Penicillium	NA

ASV_530	Limed	Day 15	Oe	Ascomycota	Hypocreales_fam_IS	Sordariomycetes	Hypocreales	Acremonium	Acremonium_persicinum
ASV_535	Limed	Day 15	Oe	Ascomycota	Hypocreales_fam_IS	Sordariomycetes	Hypocreales	Acremonium	Acremonium_persicinum
ASV_54	Control Limed	Day 40 Day 15	Oa Oe	Ascomycota	Hypocreaceae	Sordariomycetes	Hypocreales	Trichoderma	Trichoderma_stellatum
ASV_547	Limed	Day 15	Oe	Ascomycota	NA	NA	NA	unidentified	NA
ASV_57	Control	Day 15 Day 40	Oa Oe	Basidiomycota	Trichosporonaceae	Tremellomycetes	Trichosporonales	Trichosporon	Trichosporon_wieringae
ASV_576	Limed	Day 15	Oe	Ascomycota	Hypocreales_fam_IS	Sordariomycetes	Hypocreales	Acremonium	Acremonium_persicinum
ASV_59	Control	Day 40	Oa	Ascomycota	Hypocreaceae	Sordariomycetes	Hypocreales	Trichoderma	NA
ASV_595	Limed	Day 15	Oe	Ascomycota	Aspergillaceae	Eurotiomycetes	Eurotiales	Penicillium	NA
ASV_596	Limed	Day 15	Oe	Ascomycota	Aspergillaceae	Eurotiomycetes	Eurotiales	Penicillium	NA
ASV_597	Limed	Day 15	Oe	Ascomycota	Hypocreales_fam_IS	Sordariomycetes	Hypocreales	Acremonium	Acremonium_persicinum
ASV_6	Limed	Day 15	Oa	Ascomycota	Aspergillaceae	Eurotiomycetes	Eurotiales	Penicillium	Penicillium_malachiteum
ASV_62	Limed	Day 40	Oa	Ascomycota	Gloniaceae	Dothideomycetes	Dothideomycetes_ord_I	Cenococcum	NA
ASV_63	Limed	Day 15 Day 40	Oa Oe	Ascomycota	NA	Leotiomycetes	Helotiales	NA	NA
ASV_651	Limed	Day 15	Oe	Ascomycota	Aspergillaceae	Eurotiomycetes	Eurotiales	Penicillium	NA
ASV_66	Control	Day 15	Oe	Ascomycota	unidentified	Saccharomycetes	Saccharomycetales	unidentified	Saccharomycetales_sp
ASV_681	Limed	Day 15	Oe	Ascomycota	Aspergillaceae	Eurotiomycetes	Eurotiales	Penicillium	NA
ASV_692	Limed	Day 15	Oe	Ascomycota	Aspergillaceae	Eurotiomycetes	Eurotiales	Penicillium	NA
ASV_694	Limed	Day 15	Oe	Ascomycota	Hypocreales_fam_IS	Sordariomycetes	Hypocreales	Acremonium	Acremonium_persicinum
ASV_7	Control Limed	Day 15 Day 40	Oa Oe	Basidiomycota	Piskurozymaceae	Tremellomycetes	Filobasidiales	Solicoccozyma	Solicoccozyma_terricola
ASV_70	Limed	Day 40	Oa	unidentified	unidentified	unidentified	unidentified	unidentified	Fungi_sp
ASV_71	Control Limed	Day 40	Oa Oe	Mortierellomycota	Mortierellaceae	Mortierellomycetes	Mortierellales	Mortierella	Mortierella_longigemmata
ASV_72	Control Limed	Day 40 Day 15	Oe	Mucoromycota	Mucoraceae	Mucoromycetes	Mucorales	Mucor	Mucor_abundans
ASV_73	Limed	Day 15	Oe	Ascomycota	NA	Leotiomycetes	Helotiales	NA	NA
ASV_735	Limed	Day 15	Oa	Ascomycota	Aspergillaceae	Eurotiomycetes	Eurotiales	Penicillium	NA
ASV_74	Limed	Day 15 Day 40	Oe Oa	Ascomycota	Venturiaceae	Dothideomycetes	Venturiales	Venturia	Venturia_sp
ASV_75	Limed	Day 15 Day 40	Oa Oe	Mucoromycota	Mucoraceae	Mucoromycetes	Mucorales	Mucor	Mucor_silvaticus
ASV_752	Limed	Day 15	Oe	Ascomycota	Aspergillaceae	Eurotiomycetes	Eurotiales	Penicillium	NA
ASV_76	Control Limed	Day 40 Day 15	Oa	Ascomycota	unidentified	Leotiomycetes	Helotiales	unidentified	Helotiales_sp
ASV_771	Limed	Day 15	Oa Oe	Ascomycota	Aspergillaceae	Eurotiomycetes	Eurotiales	Penicillium	NA
ASV_795	Limed	Day 15	Oe	Ascomycota	Aspergillaceae	Eurotiomycetes	Eurotiales	Penicillium	NA
ASV_80	Control	Day 15 Day 40	Oa Oe	Ascomycota	Hypocreaceae	Sordariomycetes	Hypocreales	Trichoderma	NA
ASV_81	Control	Day 40	Oa Oe	unidentified	unidentified	unidentified	unidentified	unidentified	Fungi_sp
ASV_82	Limed	Day 15 Day 40	Oe Oa	Ascomycota	Helotiaceae	Leotiomycetes	Helotiales	Meliniomyces	Meliniomyces_sp
ASV_84	Control Limed	Day 15 Day 40	Oe Oa	Ascomycota	unidentified	Leotiomycetes	Helotiales	unidentified	Helotiales_sp
ASV_86	Limed	Day 15	Oe	Ascomycota	Hyaloscyphaceae	Leotiomycetes	Helotiales	unidentified	Hyaloscyphaceae_sp
ASV_87	Control Limed	Day 15	Oa	Ascomycota	Hypocreaceae	Sordariomycetes	Hypocreales	Trichoderma	NA
ASV_9	Limed	Day 15 Day 40	Oa Oe	Ascomycota	Hypocreaceae	Sordariomycetes	Hypocreales	Trichoderma	NA
ASV_90	Control Limed	Day 15 Day 40	Oa Oe	Ascomycota	unidentified	Saccharomycetes	unidentified	unidentified	Saccharomycetes_sp
ASV_92	Limed	Day 40	Oa	Basidiomycota	Hydnodontaceae	Agaricomycetes	Trechisporales	Trechispora	Trechispora_sp
ASV_924	Limed	Day 40	Oa	Ascomycota	unidentified	Leotiomycetes	Helotiales	unidentified	Helotiales_sp
ASV_96	Control	Day 15 Day 40	Oa	Ascomycota	Ascomycota_fam_IS	Ascomycota_cls_IS	Ascomycota_ord_IS	Trichocladium	Trichocladium_opacum
ASV_97	Control Limed	Day 15 Day 40	Oa Oe	Mucoromycota	Umbelopsidaceae	Umbelopsidomycetes	Umbelopsidales	Umbelopsis	Umbelopsis_isabellina
ASV_98	Control	Day 40	Oe	Ascomycota	unidentified	Leotiomycetes	Helotiales	unidentified	Helotiales_sp
ASV_99	Limed	Day 40	Oe	Ascomycota	Melanommataceae	Dothideomycetes	Pleosporales	Herpotrichia	Herpotrichia_juniperi